STUDIES

UNITED STATES DEPARTMENT OF THE INTERIOR

GEOLOGICAL SURVEY

ENVIRONMENTAL GEOLOGIC STUDIES ON THE SOUTHEASTERN ATLANTIC OUTER CONTINENTAL SHELF, 1977-1978

Edited by

Peter Popenoe

Final report submitted to the
U.S. BUREAU OF LAND MANAGEMENT
under Memorandum of Understanding
AA551-MU8-13

U.S. Geological Survey
Open-File Report 81-582-A

This report is preliminary and has not been reviewed for conformity with U.S. Geological Survey editorial standards. Any use of trade names is for descriptive purposes only and does not imply endorsement by the USGS.

1981

UNITED STATES DEPARTMENT OF THE INTERIOR

GEOLOGICAL SURVEY

ENVIRONMENTAL GEOLOGIC STUDIES ON THE SOUTHEASTERN ATLANTIC OUTER CONTINENTAL SHELF, 1977-1978

Edited by

Peter Popenoe

Final report submitted to the
U.S. BUREAU OF LAND MANAGEMENT
under Memorandum of Understanding
AA551-MU8-13

U.S. Geological Survey
Open-File Report 81-582-A

This report is preliminary and has not been reviewed for conformity with U.S. Geological Survey editorial standards. Any use of trade names is for descriptive purposes only and does not imply endorsement by the USGS.

1981

TABLE OF CONTENTS

CHAPTER 1. INTRODUCTION by Peter Popenoe

CHAPTER 2. COMPONENTS AND PATHWAYS OF SESTON FLUX OF THE GEORGIA EMBAYMENT by L. J. Doyle, P. R. Betzer, Zack Clayton, and M. A. Peacock

CHAPTER 3. ^{210}PB IN SEDIMENT CORES FROM THE ATLANTIC CONTINENTAL SHELF: ESTIMATES OF RATES OF SEDIMENT MIXING by Michael H. Bothner and Peter P. Johnson

CHAPTER 4. SEDIMENTS AND SEDIMENTARY PROCESSES AS INTERPRETED FROM PISTON CORES AND GRAB SAMPLES FROM THE CONTINENTAL SLOPE OF THE SOUTHEASTERN UNITED STATES by Larry J. Doyle, Frederick M. Wall, and Paul Schroeder

CHAPTER 5. PISTON CORE AND SURFICIAL SEDIMENT INVESTIGATIONS OF THE FLORIDA-HATTERAS SLOPE AND INNER BLAKE PLATEAU by Mark W. Ayers and Orrin H. Pilkey

CHAPTER 6. OCEAN BOTTOM SURVEY OF THE GEORGIA BIGHT by Vernon J. Henry, Jr., Charles J. McCreery, Francis D. Foley, and David R. Kendall

CHAPTER 7. SEISMIC STRATIGRAPHY OF THE NORTHERN AND CENTRAL BLAKE PLATEAU by Paul R. Pinet, Peter Popenoe, Susan M. McCarthy, and Marshall L. Otter

CHAPTER 8. AN ASSESSMENT OF POTENTIAL GEOLOGIC HAZARDS OF THE NORTHERN AND CENTRAL BLAKE PLATEAU by Paul R. Pinet, Peter Popenoe, Marshall L. Otter, and Susan M. McCarthy

APPENDIX 1. CRUISE REPORTS (microfiche in pocket in back cover)

APPENDIX 2. THROUGH 5. (To accompany Chapters 2 through 5 respectively) (microfiche in pocket in back cover)

CHAPTER 1

INTRODUCTION

Peter Popenoe

This report is a summary of the second year of marine environmental research activities by the U.S. Geological Survey (USGS) on the southeastern U.S. Atlantic Continental Margin, in accordance with Memorandum of Understanding (MOU) AA551-MU8-13 between the USGS and the Bureau of Land Management (BLM). The report covers studies whose fieldwork was conducted during the period from 1 October 1977 to 30 September 1978. The results of the first year of study are reported in Popenoe (1978a and b) and as U.S. Department of Commerce NTIS report PB 300-820.

The purpose of these investigations is to provide basic geologic and oceanographic data to the BLM Outer Continental Shelf (OCS) Marine Environmental Studies Program in support of management decisions which relate to possible development of oil and gas resources of the continental shelf. The objectives of the USGS-BLM geologic research program for fiscal year 1978 (FY-78) were 1) to determine the sedimentation rates and processes on the upper slope and inner Blake Plateau; 2) to determine the distribution, areal extent, and vertical characteristics of geological features supportive of biological communities; 3) to monitor the transport of bottom sediment across the OCS, evaluate its possible effect on pollutant transfer along the seabed and the potential of sediment as a pollutant sink, determine the implications of erosion/deposition on pipeline emplacement, and aid the interpretation of chemical, biological, and physical data; 4) to determine the concentration levels of chosen trace metals and silica in

three chemically defined fractions of the suspended particulate matter (seston); 5) to study the shelf edge and slope near areas of oil and gas interest, and the northern portion of the Blake Plateau for evidence of slope instability and other geologic hazards, and 6) to determine the depth and rate of sediment mixing caused by large storms and/or by benthic organisms and where possible to estimate the rate of active sediment accumulation.

A description of the methods, techniques, and instrumentation used to accomplish these tasks is reported herein. Not included, however, is the report on task 3, the results of the tripod and current-meter study of sediment transport. Fieldwork for this task continued into FY-79 under MOU AA551-MU9-8 and it was deemed desirable to combine the analyses from these two periods of observation into one data synthesis based on the longer period of observation. Accordingly, results of these studies will be reported in the final report under MOU AA551-MU9-8.

Studies in this report have been ordered within the volume from the water column to the deep stratigraphy. Thus, chapter 2 discusses chemical variations in particulate matter within the water column, chapters 3 to 5 discuss results of sampling of bottom sediments, chapter 6 discusses the reefs and hard grounds of the Georgia Bight, and chapters 7 and 8 the stratigraphy and geologic hazards as defined by seismic-reflection surveys.

Eight large maps showing the distribution of reefs, hard grounds, benthic organisms, and bed forms, six plates showing line drawings of seismic stratigraphy, and one large map defining the distribution of geologic hazards to petroleum exploration and development are included in a pocket in the rear of this volume. Also included on microfiche

film are appendices for chapters 2, 3, 4, and 5.

REFERENCES CITED

Popenoe, Peter, 1980a, Final executive summary report--Environmental studies, southeastern United States Atlantic Outer Continental Shelf, 1977, geology: U.S. Geological Survey Open-File Report 80-147, 52 p.

Popenoe, Peter, ed., 1980b, Final Report--Environmental studies, southeastern United States Atlantic Outer Continental Shelf, 1977, geology: U.S. Geological Survey Open-File Report 80-146, 651 p., 3 sheets, 5 microfiche.

U.S. Geological Survey, 1979, South Atlantic OCS Geological Studies, FY-76 to 77, U.S. Department of Commerce National Technical Information Service Report PB300-820, 562 p.

CHAPTER 2

COMPONENTS AND PATHWAYS OF SESTON FLUX OF THE GEORGIA EMBAYMENT

L. J. Doyle[1], P. R. Betzer[1], Zack Clayton[1], and M. A. Peacock[1]

[1]University of South Florida, Department of Marine Science, St. Petersburg, Florida 33701

CHAPTER 2

Table of Contents

Page

Introduction. 2- 1

Thrust of the study 2- 1

Previous work 2- 6

Approach. 2- 7

Results and Discussion. 2- 8

Seasonal aspects of partitioning among the major, suspended sedimentary components. 2- 8

Sedimentation potential 2-10

Trace-metal distribution. 2-13

Conclusions 2-14

References. 2-16

CHAPTER 2

COMPONENTS AND PATHWAYS OF SESTON FLUX OF THE GEORGIA EMBAYMENT

L. J. Doyle, P. R. Betzer, Zack Clayton, and M. A. Peacock

ABSTRACT

Investigation of the partitioning of total suspended load into its major and trace-metal components showed a seaward decrease in aluminum silicates, amorphous silica, weak acid soluble cadmium, copper, iron, lead, and refractory iron. Trends suggest that material is escaping the estuaries onto at least the inner shelf although the estuaries are obviously a major sink. Seaward decrease of amorphous silica, which is chiefly in the form of diatom frustules, is probably due to mixing of relatively high nutrient shelf water with progressively lower nutrient laden waters offshore. Organic content and calcium carbonate show a trend inverse to the aforementioned components although calcium carbonate distribution is patchy.

INTRODUCTION

Thrust of the Study

Investigation of the suspended sediment of the southeastern United States Continental Margin was undertaken in order to assess seston flux, provenance, pathways, and sinks of the region. The grid of stations shown in figure 2-1 was chosen from a larger group of 50 set up to cover the area. All stations in figure 2-1 were occupied during cruises in February-March, May, August, and November 1977. Shallow stations were sampled top and near-bottom and deeper stations were sampled top, middle and near-bottom.

During the first year, we investigated the total suspended load, particulate organic carbon content, particulate organic nitrogen,

Figure 2-1. Station location. Map For Suspended Load, 1977.

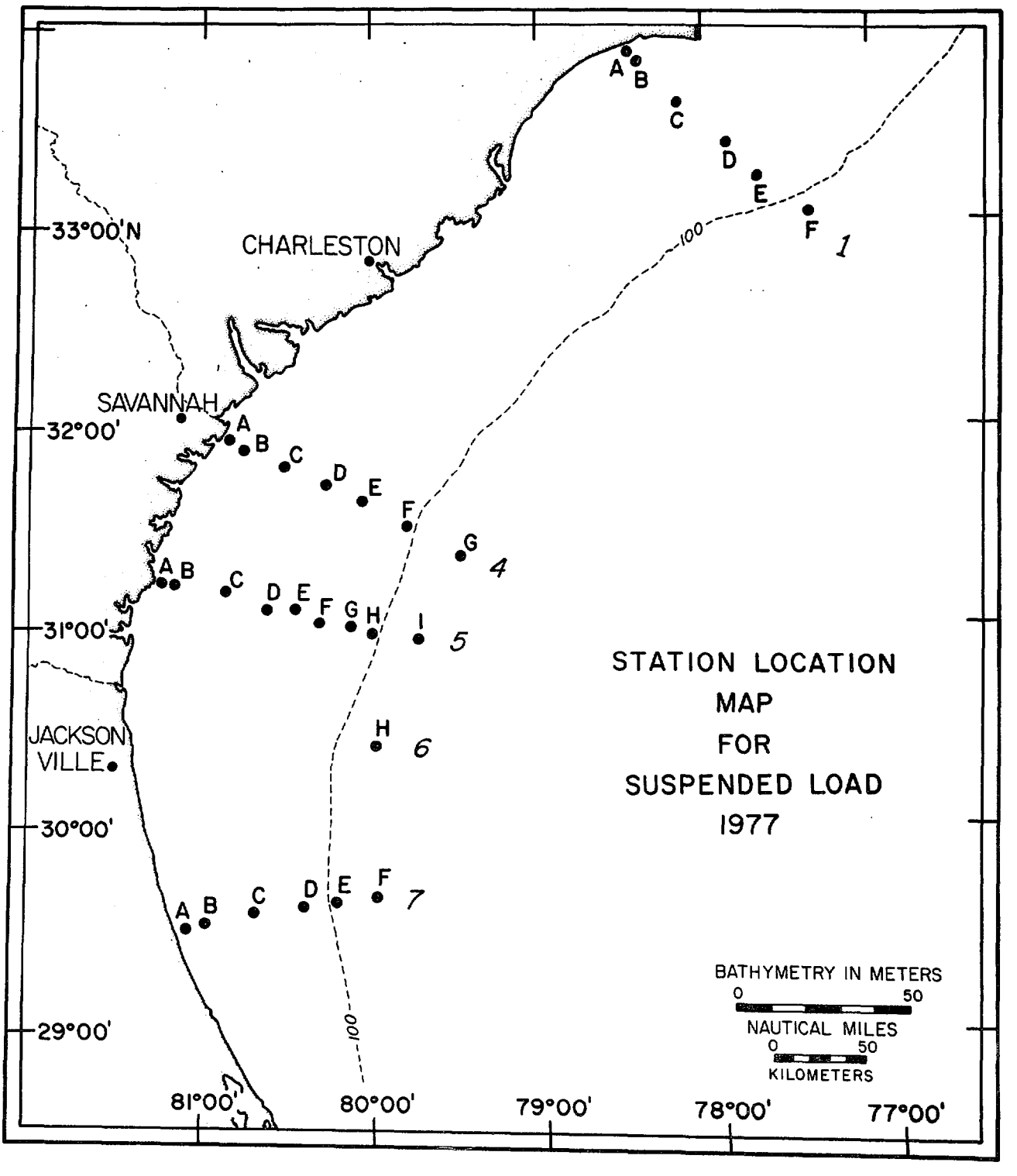
STATION LOCATION
MAP
FOR
SUSPENDED LOAD
1977
CHARLESTON
SAVANNAH
JACKSON
VILLE
33°00'N
32°00'
31°00'
30°00'
29°00'
81°00'
80°00'
79°00'
78°00'
77°00'
100
1
4
5
6
7
BATHYMETRY IN METERS
0
50
NAUTICAL MILES
0
50
KILOMETERS

calcium carbonate, mineralogy, and magnesium content at the larger grid of 50 stations. In addition, in order to characterize the nature of the particles making up the seston, we examined many of the filters with a scanning electron microscope. From the resulting data, we concluded that:

1. Total suspended load values in all seasons decrease seaward. Highest values are associated with low salinity water (less than 33%). During February-March higher suspended particulate loads extend farther out onto the shelf than at other seasons, probably because of winter storms combined with relatively high runoff.
2. During summer and fall high salinity water which was low in suspended particulates extended over large portions of the shelf. Total suspended load estimates for the whole region were highest during the winter (1.77×10^6 metric tons), slightly lower during the summer (1.71×10^6 metric tons), and considerably lower during spring (0.72×10^6 metric tons) and fall (0.83×10^6 metric tons). Some of the disparity may be due to the fact that fewer inshore stations, expected to be relatively high in suspended load, were sampled in the spring and fall. However, similar seasonal trends hold for slope waters as well as shelf waters.
3. Despite the fact that the continental margin had been subjected to an extreme winter, suspended particulate values for the February-March and August cruises were about the same. Similarity may result from quick relaxation and return to normal loads after storms in combination with small amounts of fines available in bottom sediments for resuspension.

4. Calcium carbonate percentages were lowest inshore, where they were masked by high terrigenous content, and were higher in more saline shelf and Florida Current waters.

5. Estimates of standing crop of calcium carbonate were highest during the February-March cruise (17.3×10^4 metric tons), compared to 5.9×10^4 metric tons in May, 9.5×10^4 metric tons in August, and 8.5×10^4 metric tons in November. A large portion of the total calcium carbonate in the winter was found in shelf waters (12.0×10^4 metric tons). This high value indicates that resuspension of calcium carbonate from shelf bottom sediment may have been occurring.

6. Other than the winter values, the calcium carbonate crop remained relatively stable over the southeastern margin throughout the seasons.

7. Coccoliths appear to be most abundant during the May period.

8. Because of the thick overlying water column combined with a relatively small surface area, the continental slope has a higher sedimentation potential than does the adjacent shelf.

9. Kaolinite and illite dominate the clay mineral suite of the suspended sediments and of rivers rising in the Piedmont, while smectite is more important in shelf and Coastal Plain sediments. A mixed suite is found in slope sediments. These relationships suggest that some riverborne fines are escaping from the estuaries, are passing over the shelf, and reaching the slope system.

10. The continental slope is a potential sink for pollutants on some margins. On the southeastern U.S. Continental Margin, a significant amount of any potential fines and therefore a like

amount of any potential particulate pollutants carried over the shelf will become entrained in the Florida Current.

For at least two hundred years, it has been known that the Florida Current affects the outer portions of the continental margin of the region. Meanders and eddies periodically intrude upon portions of the shelf and there appears to be a consistent deflection of the mainstream seaward at the Charleston Bump (Pietrafesa and others, 1978; Rooney and others, 1978; Pietrafesa, in press). It is a given fact that at times the Florida Current and its perturbations act to resuspend shelf sediments and play a major role in the distribution and ultimate fate of the suspended sediment of the study area. The Florida Current factor should be kept in mind throughout the discussion which follows.

Previous Work

Little in the way of three-dimensional or seasonally synoptic investigations of suspended sediment over the area of the southeast U.S. Atlantic Margin have been undertaken. These are summarized in Emery and Uchupi (1972). Using data from bucket samples, Manheim and others (1970) found that surface suspended sediment concentrations decrease rapidly away from shore during a May-June 1965 cruise. Rodolfo and Buss (1971) found that strong wave action associated with the 1969 hurricane Gerda resuspended significant amounts of bottom sediment but that relaxation time was relatively short. Atkinson and Stefansson (1969) found aluminum and iron concentrations in the area ranged, respectively, from 0.4 $\mu g \cdot l^{-1}$ to 70 $\mu g \cdot l^{-1}$ and 0.0 to 2.9 $\mu g \cdot l^{-1}$ and that concentrations were inversely related to salinity. They further pointed out that concentrations were significantly lower than would be expected

from simple mixing, suggesting sedimentation of clays had removed aluminum and iron from the system. Feely (1975), Helz (1976), Krishnaswami and Sarin (1976), Patterson and others (1976), Wallace and others (1977) have described the concentrations of various trace metals in parts of the Atlantic Ocean and Gulf of Mexico not contiguous with the southeastern Atlantic United States Bight.

A considerable amount of trace-metal work is being carried out by Windom and Atkinson at the Skidaway Institute for Oceanography. Much remains in preparation (see 1978 Final Report of Texas Instruments, Inc. to the Bureau of Land Management on Benchmark Studies of the Georgia Embayment for a complete reference list).

Approach

In this second year, we have carried out extensive particulate trace-metal analysis on the samples which were collected during 1977. Our program included analysis for amorphous silica and also for weak acid soluble Cd, Cu, Fe, and Pb. In addition, we have analyzed these samples of suspended material for refractory Al, Cd, Cu, Fe, Pb, and Si. Based on X-ray diffraction studies carried out in the first year, we made use of the ideal formula for kaolinite to account for refractory aluminum and silica which allowed us to estimate total inorganic content and, from that, organic content without the vicissitudes of POC methodology caused by the glass fiber and silver filters (Doyle and others, 1978). Data resulting from these analyses are shown in Appendix 2-1 (microfiche in pocket in back cover) which also contains pertinent data from last year's study for completeness.

First, to remove carbonates and other nonrefractory metal

hydroxides (Chester and Hughes, 1967; Betzer and others, 1977), the samples of suspended material on Nuclepore[1] filters were leached with 25% v/v acetic acid. Following the weak acid leach, biologically precipitated silica was determined for samples from transects 1, 4, 5, and 7 using doubly chelexed, 2.0 M Na_2CO_3 (Eggimann and others, 1980). Finally, the remaining refractory material was brought into solution following the technique of Eggimann and Betzer (1976). The weak acid leach was, of course, performed during the first year's study when Ca and Mg were determined. All samples and solutions were stored in air-tight, acid-leached, snap-top polyethylene vials in which the pH had been reduced to avoid adsorption and precipitation losses (Robertson, 1972). The concentrations of aluminum, cadmium, copper, iron, and lead were determined by atomic absorption spectrometry and silicon by spectrophotometry. Data are tabulated in Appendix 2-1.

Bovine liver and orchard leaves obtained from NBS, as well as the common standards P.C. 1, P.C. 2, and P.C. 3, were run in the trace-metal laboratory in order to check accuracy of analyses. Results are shown in Appendix 2-1A (microfiche in pocket in back cover).

RESULTS AND DISCUSSION

Seasonal Aspects of Partitioning Among the Major, Suspended Sedimentary Components

Appendices 2-2 to 2-5 (microfiche in pocket in back cover) show seasonal distribution of aluminum silicates, amorphous silicates, and organic content in near-surface and near-bottom waters of the study

---

[1]Use of trade names in this report is for descriptive purposes only and does not constitute endorsement by the U.S. Geological Survey.

area.

Percentages of aluminum silicates in surface waters decrease regularly away from shore in all seasons. During the February-March period, the May period, and the November period, surface water percentages of aluminum silicates decrease to between 2.5% to 5% by the 100 m isobath. During the August period, contours were displaced landward with the 2.5% contour lying at about midshelf reflecting the low runoff and relatively quiet weather of that time. During the late winter period of February-March 1977, up to 20% of the total suspended load was composed of aluminum silcates in near-surface waters as far seaward as midshelf, especially in the region north of Charleston.

Distribution of aluminum silicates in bottom waters is somewhat more complicated. Generally, the overriding trend is still one of decrease in the seaward direction, with higher value contours displaced seaward relative to the surface distribution. For example, in bottom samples 5% to 10% aluminum silicates are the norm over the 100 m isobath.

Amorphous silica, chiefly derived from diatom tests, generally follows the trend of aluminum silicate values and decreases with increasing distance from shore. Patterns are more irregular, however, with considerable patchiness, especially in winter and summer periods. Values range from a high of over 60% downward. Organic content ranges from over 90% to under 40% with lowest values nearshore. Patches of low organic content are generally associated with high aluminum silicate values.

Calcium carbonate, the remaining major component, was discussed in the report for BLM contract AA550-MU6-56. Values are generally more patchy than any other major component. SEM photographs (Doyle and

others, 1978) showed that coccolith plates were the major carbonate constituent with a good deal of fragmented material tied up in aggregates and fecal pellets. In most cases, there is an overall trend of lowered carbonate percentages nearshore and also in samples where there is an abundance of aluminum silicates. Values range from a few percent to over 40%. Some of the patchiness may be the result of resuspension of bottom materials caused by storm waves or incursions of the Florida Current. Lack of similar patchiness in the distribution of aluminum silicates suggests that the fine clays have been winnowed from shelf deposits long ago and that what is being contributed now moves relatively quickly across the margin.

Sedimentation Potential

In last year's report, we established the concept of sedimentation potential. We estimated the volume of shelf water lying between 0 and 100 m and slope water lying between 100 and 400 m by calculating surface area using a polar planimeter and multiplying the results by weighted average depths arrived at from bathymetric cross sections. Water volume between 0 and 100 m is estimated at 3.3×10^3 km^3 with a surface area of 67,400 km^2. Water volume between 100 and 400 m depth was calculated to be approximately 6.6×10^3 km^3 with an area of only 22,300 km^2. Using these values, the total suspended loads and the major sedimentary components of the suspended matter, we estimated the standing crop of particulate matter, carbonates, amorphous silica, clays and total inorganic matter for each of the four sampling periods. The results are presented as table 2-1. Since no A stations, those closest inshore, were sampled in the spring and fall, for consistency we have dropped them from the winter and summer calculations as well. In addition, only transects shown in figure 2-1 were used in calculations, not the entire

Table 2-1. Sedimentary loads (m.t.) and potentials ($mg.cm^{-2}$) for the various components of the total suspended load of the Georgia Embayment.

		TSL	$CaCO_3$	$SiO_2.H_2O$ (amorphous)	Alumino-silicates	Total inorganic content	Organic content by difference
February-March 1977	Shelf loads	1.09E 06 ±1.93E 05	9.30E 04 ±3.33E 04	3.68E 05 ±8.12E 04	1.59E 05 ±5.07E 04	6.20E 05 ±1.44E 05	4.71E 05 ±6.15E 04
	Shelf potentials	1.62 ±0.29	0.14 ±0.05	0.55 ±0.12	0.24 ±0.08	0.92 ±0.21	0.70 ±0.09
	Slope loads	4.72E 05 ±1.52E 05	5.01E 04 ±2.07E 04	1.07E 05 ±4.66E 04	1.38E 04 ±7.38E 03	1.71E 05 ±7.17E 04	3.01E 05 ±8.23E 04
	Slope potentials	2.12 ±0.68	0.22 ±0.09	0.48 ±0.21	0.06 ±0.03	0.77 ±0.32	1.35 ±0.37
May 1977	Shelf loads	4.29E 05 ±1.05E 05	3.46E 04 ±1.50E 04	9.04E 04 ±3.59E 04	2.69E 04 ±2.30E 04	1.52E 05 ±5.93E 04	2.77E 05 ±5.50E 04
	Shelf potentials	0.64 ±0.16	0.05 ±0.02	0.13 ±0.05	0.04 ±0.03	0.23 ±0.09	0.41 ±0.08
	Slope loads	2.76E 05 ±1.01E 05	1.80E 04 ±8.20E 03	4.35E 04 ±2.29E 04	6.04E 03 ±1.80E 03	6.76E 04 ±3.16E 04	2.08E 05 ±7.62E 04
	Slope potentials	1.24 ±0.45	0.08 ±0.04	0.20 ±0.10	0.03 ±0.01	0.30 ±0.14	0.93 ±0.34
August 1977	Shelf loads	7.38E 05 ±1.86E 05	3.86E 04 ±1.96E 04	1.30E 05 ±6.14E 04	4.84E 04 ±2.61E 04	2.17E 05 ±1.03E 05	5.21E 05 ±1.03E 05
	Shelf potentials	1.09 ±0.28	0.06 ±0.03	0.19 ±0.09	0.07 ±0.04	0.32 ±0.15	0.77 ±0.15
	Slope loads	4.97E 05 ±2.41E 05	3.54E 04 ±1.87E 04	3.03E 04 ±1.11E 04	1.82E 04 ±8.67E 03	8.39E 04 ±3.56E 04	4.13E 05 ±2.47E 05
	Slope potentials	2.23 ±1.08	0.16 ±0.08	0.14 ±0.05	0.08 ±0.04	0.38 ±0.16	1.85 ±1.11
November 1977	Shelf loads	6.09E 05 ±1.63E 05	6.47E 04 ±2.26E 04	1.03E 05 ±3.13E 04	4.07E 04 ±1.35E 04	2.08E 05 ±6.04E 04	4.01E 05 ±1.16E 05
	Shelf potentials	0.90 ±0.24	0.10 ±0.03	0.15 ±0.05	0.06 ±0.02	0.31 ±0.09	0.59 ±0.17
	Slope loads	3.30E 05 ±8.78E 04	4.88E 04 ±2.17E 04	2.10E 04 ±9.99E 03	1.80E 04 ±9.72E 03	8.79E 04 ±3.19E 04	2.42E 05 ±6.53E 04
	Slope potentials	1.48 ±0.39	0.22 ±0.10	0.09 ±0.04	0.08 ±0.04	0.39 ±0.18	1.09 ±0.29

50 sampled in year 1977. For these reasons, values for total suspended load and calcium carbonate differ slightly from those reported last year.

Also presented in table 2-1 is the sedimentation potential of each of the major components for the shelf and the slope. Sedimentation potential is the amount of material in mg that would be deposited on one square cm if all the material in the water column were sedimented out at once. Obviously, this never occurs in nature but the measurement is of value in illustrating the contrast between the amount of material in suspension over the shelf and over the slope.

Perusal of table 2-1 shows that shelf total suspended loads and inorganic components of that load were highest during the winter period. In addition, the total mass of organic matter over the shelf during the winter was quite high, only being exceeded during the summer sampling. During the spring sampling, shelf waters contained the least amount of particulates. Summer and fall shelf suspended loads were similar in both amounts and in the distribution of major sedimentary components, with the exception of calcium carbonate which was enriched by a factor of two in the suspended fraction of the fall sampling relative to the summer.

The situation on the continental slope is more complex. The total mass of suspended load, of calcium carbonate, and of amorphous silica are all highest during the winter period. However, the mass of aluminum silicates and of organics suspended in slope waters is highest during the summer period. Aluminum silicate loads in slope waters were also higher in the fall sampling than in the winter period.

Values of total suspended load for aluminum silicates shown in table 2-1 are lower by two or three orders of magnitude than the amount

of material estimated to be carried by southeast Atlantic rivers to the sea, about 18.7×10^6 metric $tons \cdot yr^{-1}$. Most must be trapped in estuaries or be present in the innermost shelf zone which we have not adequately sampled. However, it is apparent from the gradients for aluminum silicates and refractory iron over the shelf that some of the riverborne material does escape.

Trace-Metal Distribution

The distribution of trace metals between weak acid soluble and refractory fractions is shown in Appendices 2-6 to 2-9 (microfiche in pocket in back cover). Weak acid soluble cadmium ranges from a high of $0.01\ \mu g \cdot l^{-1}$ to a low of less than $0.0005\ \mu g \cdot l^{-1}$. Values are generally high nearshore and decrease offshore. Highest values were measured during high winter runoff periods. Anomalously, highest values during this period were observed at some offshore stations, notably south of Jacksonville and seaward of the 100 m isobath east of Savannah. Spikes of up to $0.006\ \mu g \cdot l^{-1}$ were present in surface waters near the Savannah area in winter, summer and fall periods. They did not show up during the spring measurements, when concentrations were lowest overall. Bottom values conform, in the main, with surface patterns.

Weak acid soluble copper concentrations range from over $0.1\ \mu g \cdot l^{-1}$ to less than $0.005\ \mu g \cdot l^{-1}$. As with cadmium, the most complex pattern was observed during the winter period. In general, values are regionally highest nearshore and decrease seaward in both surface and in bottom waters. There are several exceptions. During the spring sampling, a relatively high concentration is present in surface waters, but not in bottom waters, over the shelf edge northeast of Jacksonville, Florida, during the summer and a high concentration patch that dominates the whole pattern of distribution like a bull's-eye was present in both

surface and bottom waters of the inner shelf, just seaward of Savannah during the fall.

Weak acid soluble lead ranges in value from over 0.1 $\mu g \cdot l^{-1}$ to less than 0.005 $\mu g \cdot l^{-1}$. Like most of the other trace metals, concentrations are usually highest nearshore and decrease seaward. Lead shows an added trend of high values near the northernmost part of the study area at Cape Fear decreasing to the southeast. This trend is evident in all seasons. It may indicate a source in Pamlico Sound, or that Virginia shelf water, which sometimes invades the Carolinian province, is enriched in lead relative to shelf waters south of Cape Fear. Copper shows a subdued but similar trend of increasing concentration near Cape Fear in the winter and spring measurments.

Both weak acid soluble and refractory iron show the most regular distributions of any variables measured. They decrease from relatively high concentrations nearshore to relatively low concentrations offshore. Only in the November sampling period is there a break in this pattern, a relatively high patch on the inner central shelf about midway between Jacksonville and Savannah. As expected, highest overall concentrations were measured during the high runoff period of late winter.

CONCLUSIONS

Partitioning of the total suspended load into its major components and characterization of its trace-metal load results in the following conclusions and modifications to the conclusions arrived at last year.

1. Total suspended load values in all seasons decrease seaward. This pattern is also evident for the standing crops of aluminum silicates and amorphous silica (chiefly diatoms) as well as for, weak acid soluble cadmium, copper, iron, and lead, and

refractory iron. These relationships suggest that trace metal and refractory iron distributions are governed by aluminum silicates brought down by the rivers and escaping from the estuaries. The trend of decreasing percentage amorphous silica offshore is probably due to the mixing of relatively high nutrient shelf waters with progressively lower and lower nutrient waters offshore as well as an increase in the percentage of organic material and calcium carbonate offshore.

2. Organic content and calcium carbonate show a trend inverse to the aluminum silicates, trace metals, and amorphous silicates although the latter shows the most patchy distribution of any component.

3. The amount of aluminum silicate material in suspension over the margin at any one time is two or three orders of magnitude less than estimates for that brought down by rivers each year. This suggests that most terrigenous material is trapped in estuaries or deposited on the inner shelf. Some leakage to the margin is indicated, especially in the winter, and may be significant in the long term.

4. Patchiness in the distribution of calcium carbonate may in part be the result of resuspension of carbonates by storm waves and incursions of the Florida Current. Lack of patchiness in the alumino-silicate and iron distributions on the other hand suggests that both the river-contributed sediment escaping the estuaries and also inner shelf clastics move rapidly across the shelf.

5. There is a great weight of data in the literature which points out that the continental shelf of the eastern United States is

an area of winnowing and nondeposition. This means that sediment which gets into the system from the continent may be deposited and resuspended on the continental shelf many times by storms, currents, and near the shelf break, perhaps by breaking internal waves. Once it has moved over the shelf break, however, on a normal slope system, the sediment settles out and the water is deep enough to preclude the operation of processes of resuspension and winnowing, which are so important on the shelf. Therefore, sediment builds up and the slope is generally a depositional area relative to the continental shelf. This is the situation that applies to continental margins in general, but is not necessarily specific to that in the study area, where a significant amount of fines and therefore a proportionate amount of any potential particulate pollutants carried over the shelf will become entrained in the Florida Current.

REFERENCES

Atkinson, L.P., and Stefannson, U., 1969, Particulate aluminum and iron in sea water of southeastern coast of the United States: Geochim. et Cosmochim. Acta, v. 33, no. 11, p. 1449-1453.

Betzer, P.R., Eggimann, D.W., Carder, K.L., Kester, D.R., and Betzer, S.B., 1977, Seasonal patterns in suspended calcium carbonate concentrations during dry and wet seasons in the eastern Caribbean, in Anderson, N.R., and Malahoff, A., eds., The Fate of Fossil Fuel CO_2 in the Oceans: New York, Plenum Press, p. 63-79.

Chester, R., and Hughes, M.J., 1967, A chemical technique for the separation of ferromanganese minerals, carbonate minerals and

adsorbed trace metals from pelagic sediments: Chem. Geol., v. 2, p. 249-262.

Doyle, L.J., Betzer, P.R., Peacock, M.A., and Wall, F., 1978, Seston of the southeast Georgia Embayment: Final Report to U.S. Geological Survey, Contract 14-08-0001-15681, 72 p.

Eggimann, D.W., and Betzer, P.R., 1976, Decomposition and analysis of refractory oceanic suspended materials: Anal. Chem., v. 48, p. 886-890.

Eggimann, D.W., Manheim, F.T., and Betzer, P.R., 1980, Dissolution and analysis of amorphous silica in marine sediments: J. Sed. Petrol., v. p. .

Emery, K.O., and Uchupi, E., 1972, Western North Atlantic Ocean: Topography, rocks, structure, water, life, and sediments: Am. Assoc. Petroleum Geol. Memoir 17, 532 p.

Feely, R.A., 1975, Major-element composition of the particulate matter in the near-bottom nepheloid layer of the Gulf of Mexico: Mar. Chem., v. 3, p. 121-156.

Helz, G.R., 1976, Trace element inventory for the northern Chesapeake Bay with emphasis on the influence of man: Geochim. et Cosmochim. Acta, v. 40, p. 573-580.

Krishnaswami, S., and Sarin, M.M., 1976, Atlantic surface particulates: composition, settling rates and dissolution in the deep sea: Earth Planet Sci. Lett., v. 32, p. 430-440.

Manheim, F.T., Meade, R.H., and Bond, G.C., 1970, Suspended matter in surface waters of the Atlantic continental margin from Cape Cod to the Florida Keys: Science, v. 167, p. 371.

Patterson, C., Settle, D., and Glover, B., 1976, Analysis of lead in polluted coastal seawater: Mar. Chem., v. 4, p. 305-319.

Pietrafesa, L.J., in press, On the characterization of the Gulf Stream frontal meanders and filaments in the Carolina Capes: J. of Phys. Ocean.

Pietrafesa, L.J., Blanton, J.O., and Atkinson, L.P., 1978, Evidence for deflection of the Gulf Stream at the Charleston Rise: Gulfstream, v. IV, no. 9, p. 2-7.

Robertson, D.W., 1972, Ultrapurity methods and techniques, Zeif, M., and Speights, R., eds.: New York, Marcel Dekker, p. 207-253.

Rodolfo, K.S., and Buss, B.A., 1971, Suspended sediment increase due to Hurricane Gerda in continental shelf waters off Cape Lookout, North Carolina: J. Sed. Petrol., v. 41, no. 4, p. 1121-1125.

Rooney, D.M., Janowitz, G.S., and Pietrafesa, L.J., 1978, A simple model of the deflection of the Gulf Stream by the Charleston Rise: Gulfstream, v. IV, no. 11, p. 2-7.

Texas Instruments, Inc., 1978, Final report on the South Atlantic OCS Benchmark Program FY 77, BLM Contract AA550-CT7-2.

Wallace, G.T., Jr., Hoffman, G.L., and Duce, R.A., 1977, The influence of organic matter and atmospheric deposition on the particulate trace metal concentration of northwest Atlantic surface seawater: Mar. Chem., v. 5, p. 143-170.

CHAPTER 3

^{210}PB IN SEDIMENT CORES FROM THE ATLANTIC CONTINENTAL SHELF: ESTIMATES OF RATES OF SEDIMENT MIXING

Michael H. Bothner[1] and Peter P. Johnson[1]

[1]U.S. Geological Survey, Woods Hole, Massachusetts 02543

CHAPTER 3

Table of Contents

	Page
Abstract	3- 1
Introduction	3- 2
Methods	3- 6
Results	3-12
Inventories of excess ^{210}Pb in sediments	3-12
^{210}Pb profiles	3-20
The mixing model	3-31
Conclusions and recommendations	3-34
Literature cited	3-38

CHAPTER 3

^{210}Pb IN SEDIMENT CORES FROM THE ATLANTIC CONTINENTAL SHELF: ESTIMATES OF RATES OF SEDIMENT MIXING

Michael H. Bothner and Peter P. Johnson

ABSTRACT

^{210}Pb profiles in sediment cores from the Atlantic Continental Shelf show that this short-lived isotope ($T_{1/2}$ = 22.3 yrs) is being mixed into the surficial layer of relict shelf sediments. Depths of mixing are typically between 20 and 28 cm, except at one location on Georges Bank where the ^{210}Pb profile suggests erosion. A simple model allows an estimate of the mixing coefficient and predicts the depth distribution of a pollutant added to the seafloor with time due to biological reworking. This model may help predict the fate of contaminants added to continental shelf sediments.

^{210}Pb inventories and ^{14}C measurements suggest that the area of fine-grained sediments (8,000 km^2) on the continental shelf south of Martha's Vineyard constitutes a modern sedimentary feature, in contrast to earlier descriptions of the area. To our knowledge, this is the only site of present-day natural deposition on the continental shelf off the eastern United States, exclusive of the Gulf of Maine. This sink for modern fine-grained sediments would also be a sink for modern sediment-related pollutants. Because the net currents on this part of the shelf flow from northeast to southwest, the fine-grained sediments depositing south of Martha's Vineyard may be resuspended from Nantucket Shoals and Georges Bank regions.

INTRODUCTION

The continental shelf environment off the eastern United States provides for a wide range of commercial activities. Fishing and shipping have been important since the early development of this country. More recently other uses or potential uses include waste disposal, hard mineral mining, and petroleum resource development. In order to assess compatibility among all the proposed activities on the continental shelf a basic understanding is required of the natural processes acting in this environment.

This study examines the process of sediment mixing which effects the upper 20-40 cm of sediment and is caused by benthic organisms and/or currents. To monitor the mixing process we have collected sediment cores and determined the distribution of ^{210}Pb, a naturally occurring radioisotope with a half-life of 22.3 yrs.

The specific goals of this study were to: 1) estimate the rates and depths of sediment mixing from ^{210}Pb profiles in sediments; and 2) use the total inventories of ^{210}Pb to define areas likely to be sinks for those pollutants which have a geochemical behavior similar to that of ^{210}Pb. This information is important in predicting the fate of contaminants added to the continental shelf environment. Knowledge of sediment-mixing dynamics permits an estimate of how fast and to what depth a pollutant will be mixed into the sediments. The identification of areas where pollutants accumulate and areas where they do not accumulate is a valuable aid in assessing the impact of any pollutant discharge.

^{210}Pb has a unique geochemical cycle (fig. 3-1). Some of the noble gas ^{222}Rn generated from ^{226}Ra in rocks and sediments near the earth's

Figure 3-1. Geochemical pathways of ^{210}Pb leading to unsupported ^{210}Pb in coastal marine sediments.

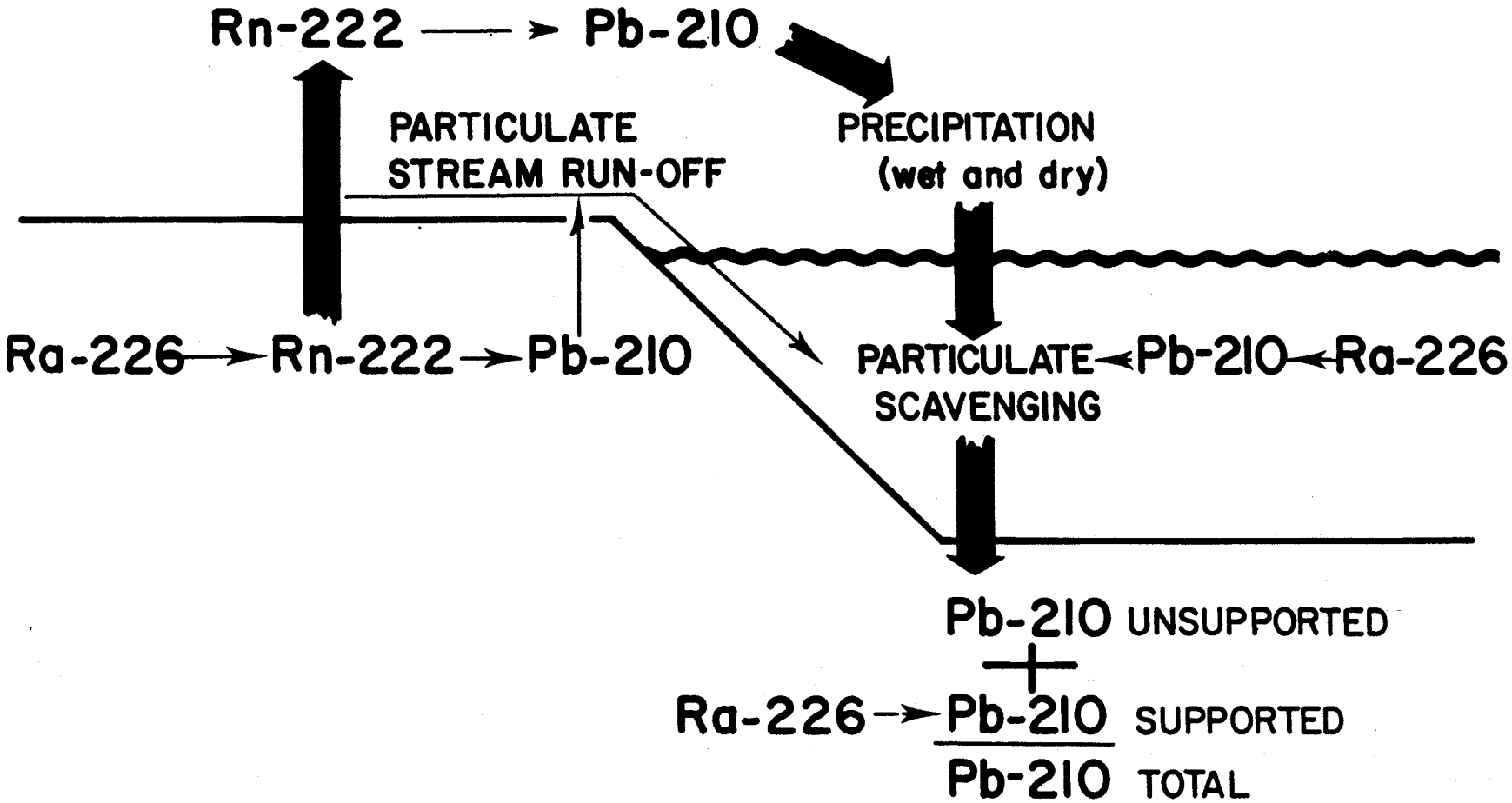
Rn-222 → Pb-210
PARTICULATE
STREAM RUN-OFF
PRECIPITATION
(wet and dry)
Ra-226 → Rn-222 → Pb-210
PARTICULATE
SCAVENGING
Pb-210 ← Ra-226
Pb-210 UNSUPPORTED
+
Ra-226 → Pb-210 SUPPORTED
Pb-210 TOTAL

Figure 3-1

surface diffuses and mixes into the atmosphere. The ^{222}Rn decays to short-lived intermediaries and then to ^{210}Pb which has an atmospheric residence time of about five days (Turekian and others, 1977). ^{210}Pb introduced to coastal waters off the northeastern United States from the atmosphere has a residence time of about two years (Thomson and Turekian, 1973) before being deposited in bottom sediments. The atmospheric flux of ^{210}Pb to the surface waters of the continental shelf off the northeastern United States is about 1 disintergration per minute per square centimetre per year ($dpm \cdot cm^{-2} \cdot yr^{-1}$)(Benninger, 1976). This represents the major source of excess ^{210}Pb. Excess ^{210}Pb is defined as the activity above the level supported by parent isotopes in the sediment. An additional source of excess ^{210}Pb results from the decay of ^{226}Ra dissolved in seawater; however, this contribution is less than 10% of the atmospheric flux for water column depths over the continental shelf (Benninger, 1976). ^{210}Pb is also produced in sediment following the decay of <u>in situ</u> ^{226}Ra; this contribution represents the parent-supported ^{210}Pb activity. The supported ^{210}Pb is subtracted from the total ^{210}Pb to determine the level of excess ^{210}Pb.

The most suitable environments for use of excess ^{210}Pb to determine sedimentation rates are areas with anoxic sediments, little biological or physical mixing, and accumulation rates of millimetres to a few centimetres per year. Bruland (1974) has obtained excellent agreement between the sedimentation rates obtained from ^{210}Pb and from counting annual varves in sediments from the Santa Barbara Basin. The ^{210}Pb technique has also been used to determine the rates of accumulation on the continental shelf off the Columbia River (Nittrouer and others, 1979) and off the Mississippi River (Shoaks, 1976). Application of this technique for determining rates of sediment accumulation is complicated

by bioturbation and other sediment mixing mechanisms, particularly in areas of low sediment accumulation. The use of ^{210}Pb to estimate rates of mixing or rates of accumulation in any environment requires the following assumptions: 1) that the flux of ^{210}Pb to an area is constant with time; and 2) that there is no loss of ^{210}Pb after deposition except by radioactive decay.

In general, the sediments of the continental shelf off the eastern United States have been classified as relict (Emery and Uchupi, 1972). There are no large sources of new sediment to the continental shelf at present. In fact, the large drowned estuaries at the mouths of major rivers on the East Coast are thought to be sinks for continental shelf material transported landward (Meade, 1969). Thus, the profiles of excess ^{210}Pb in sediment cores in most areas may be due primarily to mixing of the sediments by organisms and currents.

METHODS

The sediment cores were collected at the locations shown in figure 3-2 with a hydraulically damped gravity corer which has features similar to those described by Pamatmat (1971). This apparatus (fig. 3-3) is designed to minimize disturbance of material at the water-sediment interface. The sediments are collected in a thin-walled fiberglass core tube which is held vertically within a pyramid structure. Once the structure reaches bottom, the core tube penetrates the sediment at a rate which is slowed by a water-filled piston. Maximum sediment penetration is 70 cm, although in sandy shelf sediments, cores less than 40 cm in length are most common.

The sediment cores were frozen after collection. Prior to analysis, the cores were extruded from the core barrels, allowed to

Figure 3-2. Locations of hydraulically damped gravity cores, vibracores, and piston cores analyzed in this study. Dashed contours south of Cape Cod outline area of anomalous fine-grained sediment called the "mud patch" (Schlee, 1973): --- muddy sand; ——•—— •silt.

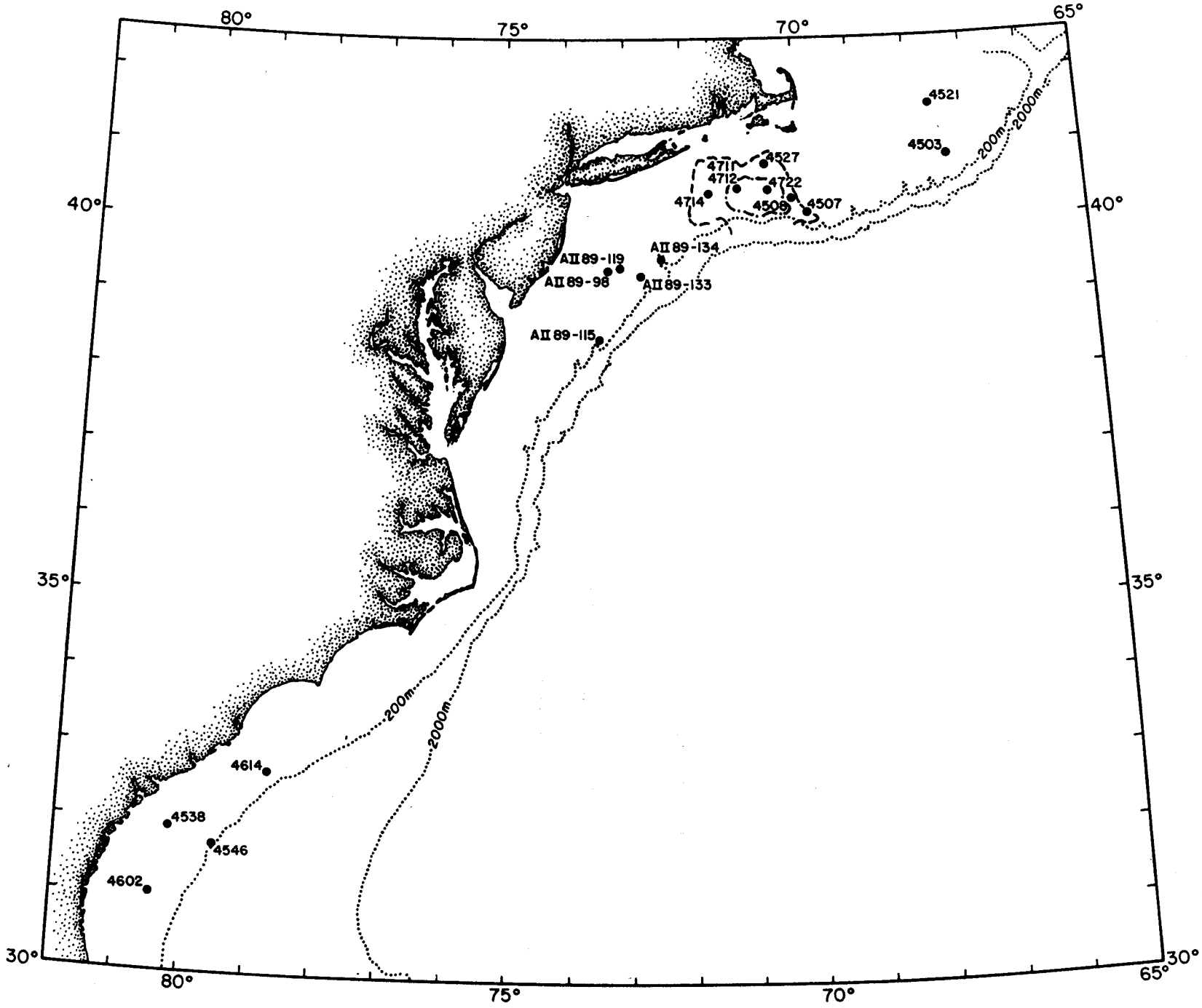
80°
75°
70°
65°
40°
35°
30°
4521
4503
4527
4711
4712
4722
4714
4508
4507
AII 89-134
AII 89-119
AII 89-98
AII 89-133
AII 89-115
200m
2000m
4614
4538
4546
4602

Figure 3-2

Figure 3-3. Hydraulically damped gravity corer: designed to take undisturbed cores of near-surface sediment up to 70 cm in length. A water-filled piston regulates the speed at which the core barrel penetrates the sediment. Width 2 m, overall height 3 m, core diameter (I.D.) 8.4 cm.

Figure 3-3

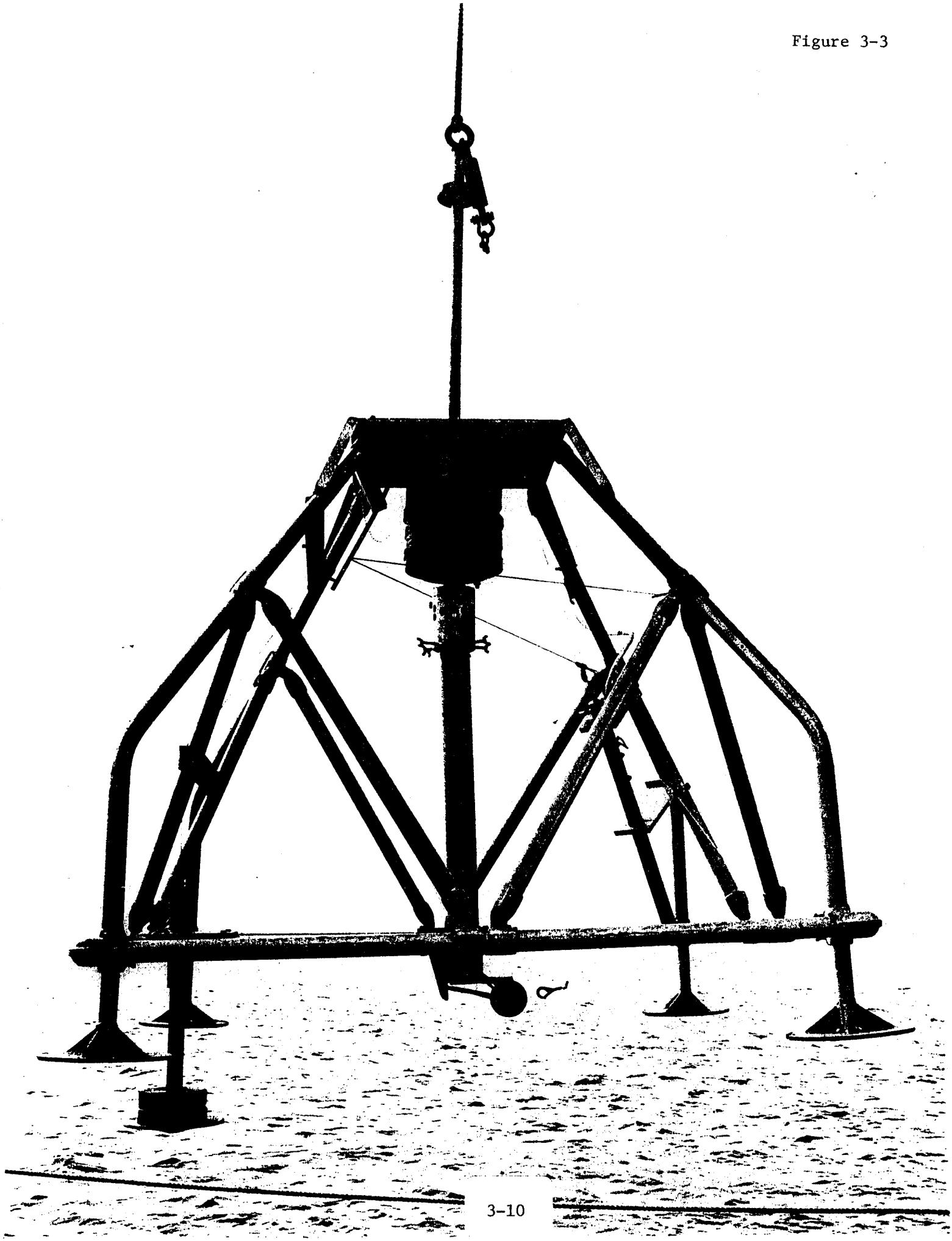

thaw, and cut into 1- or 2-cm intervals. Water contents were determined by ovendrying a known weight of sediment at 70°C for 48 hours. In sediments containing more than 80% sand or coarser material, the water contents are minimum values. Water was observed to drain through these very porous unconsolidated sediments both at the time of sample collection and during subsampling.

Determination of ^{210}Pb activity was carried out by analysis of the granddaughter ^{210}Po which is assumed to be in secular equilibrium with ^{210}Pb as is found in other coastal areas (Nittrouer and others, 1979). Approximately 2 g of dried sediment were wet-oxidized in covered beakers at 130°C for 20 hrs with 20 ml of concentrated nitric acid in the presence of a ^{208}Po spike of known activity. The beakers were then uncovered and the solution evaporated nearly to dryness. Sample temperature was maintained below 150°C to avoid volatilizing the Po isotopes. Because nitric acid interferes with a subsequent step, nitrates were volatilized by adding about 10 ml of 6N HCl and evaporating nearly to dryness. This operation was repeated four times. ^{210}Po and the ^{208}Po spike were spontaneously plated onto silver discs under chemical conditions described by Flynn (1968).

The alpha activity of the Po isotopes on the silver discs was determined by counting with silicon-surface barrier detectors connected to a multichannel analyzer. The activity of the ^{208}Po spike was calibrated against a ^{210}Po standard solution obtained from the Nuclear Regulatory Commission, Health and Safety Laboratory, New York, New York. Standard radioactive decay equations were used to calculate the activity of each sample in the core on the date of sample collection. The level of ^{210}Pb supported by ^{226}Ra activity in the sediments was estimated from the deeper sections of hydraulically damped gravity cores or vibracores

presumably below the influence of modern sedimentary processes. A few sediment samples from the southeast Georgia Embayment were analyzed for ^{226}Ra directly to determine the level of supported ^{210}Pb. Inventories of excess ^{210}Pb were calculated from the ^{210}Pb profiles after correcting for water content in the cores and by assuming a grain density of 2.6 $g \cdot cc^{-1}$. Tabulated data on total ^{210}Pb activity, texture, water content, and estimated supported ^{210}Pb is presented in Appendix tables 3-1, 3-2, 3-3 (microfiche in pocket in back cover).

RESULTS

Inventories of Excess ^{210}Pb in Sediments

The atmospheric ^{210}Pb flux to surface waters of the continental shelf is assumed to be about 1 $dpm \cdot cm^{-2} \cdot yr^{-1}$; the same as that measured for coastal land areas (Turekian and others, 1977). If this same flux reaches the bottom sediment under steady-state conditions, the total inventory of excess ^{210}Pb in sediments would be 32 $dpm \cdot cm^{-2}$. Areas having higher inventories suggest preferential accumulation of ^{210}Pb, perhaps by advection of particulates carrying ^{210}Pb from other areas. Lower inventories imply nondeposition of ^{210}Pb or erosion of sediment. Inventories at the locations sampled are presented in figure 3-4.

Core 4521B, from the central region of Georges Bank, has a ^{210}Pb inventory near zero, suggesting that this area is nondepositional or erosional. This interpretation is consistent with the high energy conditions characteristic of this area (Butman and Folger, 1979). Except for the area south of Martha's Vineyard, cores from the mid-Atlantic Shelf are either below or approximately equal to the level in equilibrium with the atmospheric flux.

South of Martha's Vineyard, the higher ^{210}Pb inventories occur in

Figure 3-4. ^{210}Pb inventories: measure of the total amount of excess ^{210}Pb in disintegrations per minute per cm^2 integrated through the sediment.

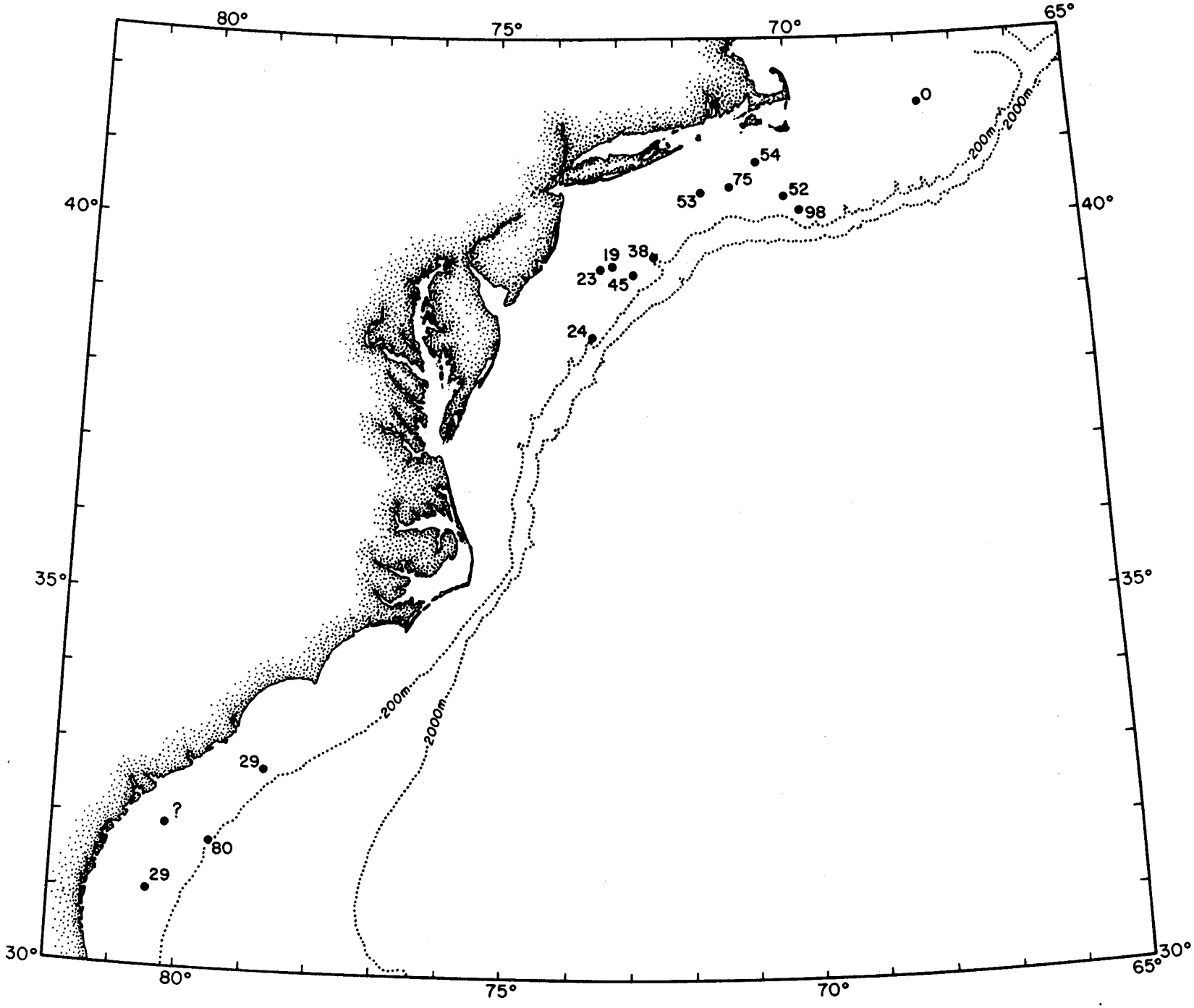
80°
75°
70°
65°
40°
35°
30°
0
54
75
52
53
98
19
38
23
45
24
29
?
80
29
200m
2000m

Figure 3-4

sediments representing a deposit which is finer than the surrounding area. This feature, known as the "mud patch", occupies an area of about 8,000 km^2 and has up to 14 m of fine sediments (Twichell and others, 1979). These higher ^{210}Pb inventories suggest that this feature is a modern sink for pollutants in the water column. ^{14}C profiles support this suggestion.

Four cores approximately 6 m in length were recovered from this sedimentary deposit with piston and vibracorers at locations shown in figure 3-2. ^{14}C analyses were performed on the organic carbon fraction of the sediment by Elliott Spiker, U.S. Geological Survey, Reston, Virginia. The two cores at the east end of the feature have ^{14}C ages increasing uniformly with depth, indicating a uniform rate of sedimentation of approximately 50 cm.1,000 yrs^{-1} (fig. 3-5). Surface ages of about 1,000 yrs extrapolated from this ^{14}C data are expected because: 1) organisms mix older carbon from deeper sediments into surface sediments; 2) the sediments contain older terrestrial carbon and detrital coal and graphite having an infinite ^{14}C age; and 3) the rate of exchange between atmospheric and oceanic carbon is slow.

In the finer sediments characteristic of the central area of the "mud patch", a slower accumulation rate was measured at the tops of cores compared to the bottoms (fig. 3-6). In the upper sediments, the rates are about 30 cm.1,000 yrs^{-1} compared to 125 cm.1,000 yrs^{-1} at the bottom of the cores. The slower rates suggest a decreasing source of fine-grained sediments with time. Because the net currents on this area of the shelf flow from northeast to southwest, parallel to depth contours (Bumpus, 1973), the source of sediments is probably the Nantucket Shoals and Georges Bank regions. A decreasing supply of fine sediments is expected from these sources because the fine sediments

Figure 3-5. ^{14}C age determined on total organic carbon in sediment cores from the eastern edge of the "mud patch" south of Martha's Vineyard. Vertical bars represent the thickness of the sediment sequence sampled. Horizontal bars represent the estimated error (1 σ) from counting statistics plus variable laboratory factors. Least squares regression lines through the data points suggest accumulation for core 4507 of 45 cm$\cdot$1,000^{-1} yrs and for core 4508 of 55 cm$\cdot$1,000^{-1} yrs. Analyses performed by Elliott Spiker, USGS Radiocarbon Laboratory, Reston, Virginia.

Figure 3-5

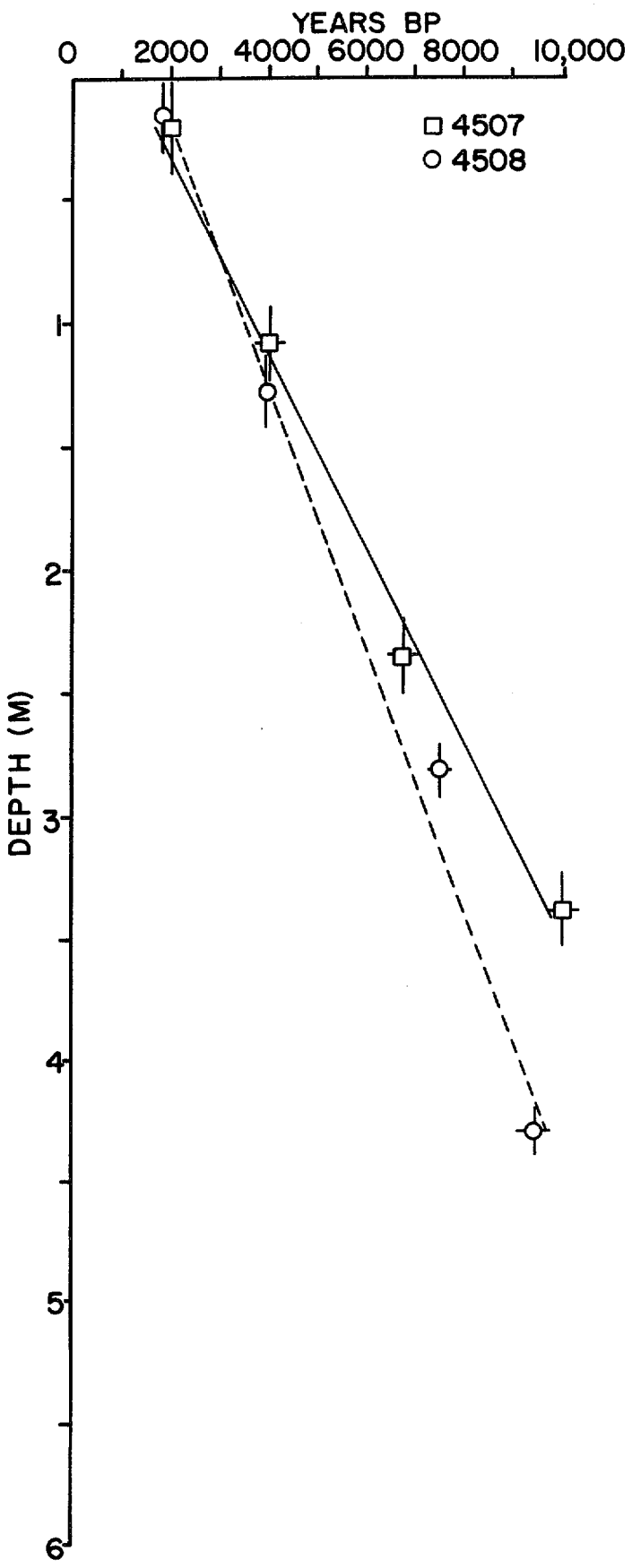

Figure 3-6. ^{14}C age determined on total organic carbon in sediment cores from the central area of the "mud patch" south of Martha's Vineyard. Vertical bars represent the thickness of the sediment sequence sampled. Horizontal bars represent the estimated error (1 σ) from counting statistics plus variable laboratory factors. Least squares regression lines through the data points suggest accumulation for core 4711 of 80 cm•1,000^{-1} yrs and for core 4722 of 130 cm•1,000^{-1} yrs. Analyses performed by Elliott Spiker, USGS Radiocarbon Laboratory, Reston, Virginia.

Figure 3-6

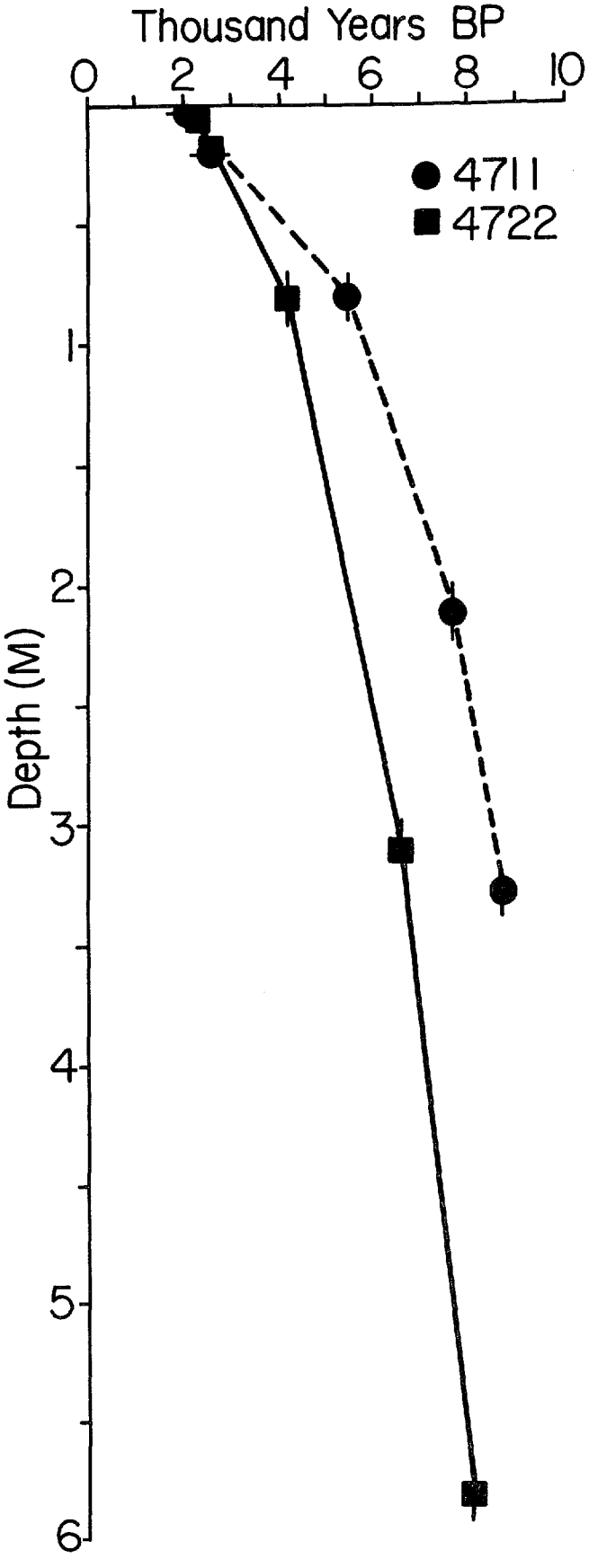

originally deposited in glacial tills and outwash are continuously being eroded away leaving behind an increasingly thick cover of residual sand and gravel.

The increasing ^{14}C ages with sediment depth and the higher ^{210}Pb inventories imply that this area is a modern sink for fine-grained sediments and for pollutants associated with particulates in the water column. Some preliminary data show that zinc and stable isotopes of lead have consistently higher concentrations (up to two times) in surface sediments than in sediments below the mixed zone, implying accumulation of modern contaminants. To our knowledge, this is the only site of present-day natural deposition for fine sediments and sediment-related pollutants on the continental shelf off the eastern United States, exclusive of the Gulf of Maine.

^{210}Pb Profiles

The ^{210}Pb inventories in sandy sediments off the New Jersey coast are variable but average about 30 $dpm \cdot cm^{-2}$. Because there is no modern source for the sand making up the surface sediments we interpret these inventories to be a result of adsorption of excess ^{210}Pb at the water-sediment interface or by incorporation of ^{210}Pb into the sediments with a small amount of fine-grained sediment or organic matter.

In two cores from the southeast Georgia Embayment, the inventories of excess ^{210}Pb are similar to those found on the Middle Atlantic Shelf (29 $dpm \cdot cm^{-2}$). One core on the shelf edge has higher inventories (80 $dpm \cdot cm^{-2}$) and may suggest some preferential accumulation of ^{210}Pb. Estimates of inventories are more uncertain in this study area however, because most cores show a variable level of supported ^{210}Pb in the lower section. One core (4538) had variable texture and erratic ^{210}Pb values throughout its length and no inventory could be calculated. To estimate

the supported ^{210}Pb, we sent a number of samples from the southeast Georgia Embayment to Environmental Analysis Laboratories for determination of ^{226}Ra activity, the parent of ^{210}Pb. The results (Appendix table 3-3) are variable with depth, perhaps because of variation in the carbonate content of the cores. Carbonates have been shown to concentrate ^{226}Ra in some cases (Turekian and Cochran, 1978). We have made an estimate of the average supported ^{210}Pb, but the inventories calculated should be considered preliminary.

The major features of a classical ^{210}Pb profile can be seen in a core collected near the mouth of the Columbia River in an area of active sediment accumulation (fig. 3-7; Nittrouer and others, 1979). The uniform activity in the upper 9 cm is thought to be due to rapid mixing by organisms and currents. The region of semilogarithmic decrease of ^{210}Pb with depth is interpreted to be free of mixing and the rate of sediment accumulation is calculated from the slope of the excess ^{210}Pb decrease. Below about 30 cm, the ^{210}Pb is constant, reflecting the level of ^{210}Pb supported by ^{226}Ra in the sediments.

The profiles of ^{210}Pb obtained in this study are arranged in geographic order from north to south. Most of the cores have at least part of the features present in the classical profile described. Core 4521B (fig. 3-8a) from Georges Bank has uniform and low activities with depth. This sample appears to contain only supported ^{210}Pb activity. Both the uniform profile and the estimated zero inventory of excess ^{210}Pb suggest that the sediments in this area are eroding.

In the "mud patch" south of Martha's Vineyard and Nantucket Island, the ^{210}Pb profiles are similar to the classical profile. The semilogarithmic decrease of ^{210}Pb in this part of the shelf may be due in part to modern sediment accumulation. However, as seen in core 4508A

Figure 3-7. Ideal ^{210}Pb curve (after Nittrouer and others, 1979): 0-9 cm, vertical profile due to sediment mixing; 9-22 cm, semilogarithmic decrease in ^{210}Pb activity due to sediment accumulation; 22-45 cm activity of background ^{210}Pb supported by ^{226}Ra in the sediments.

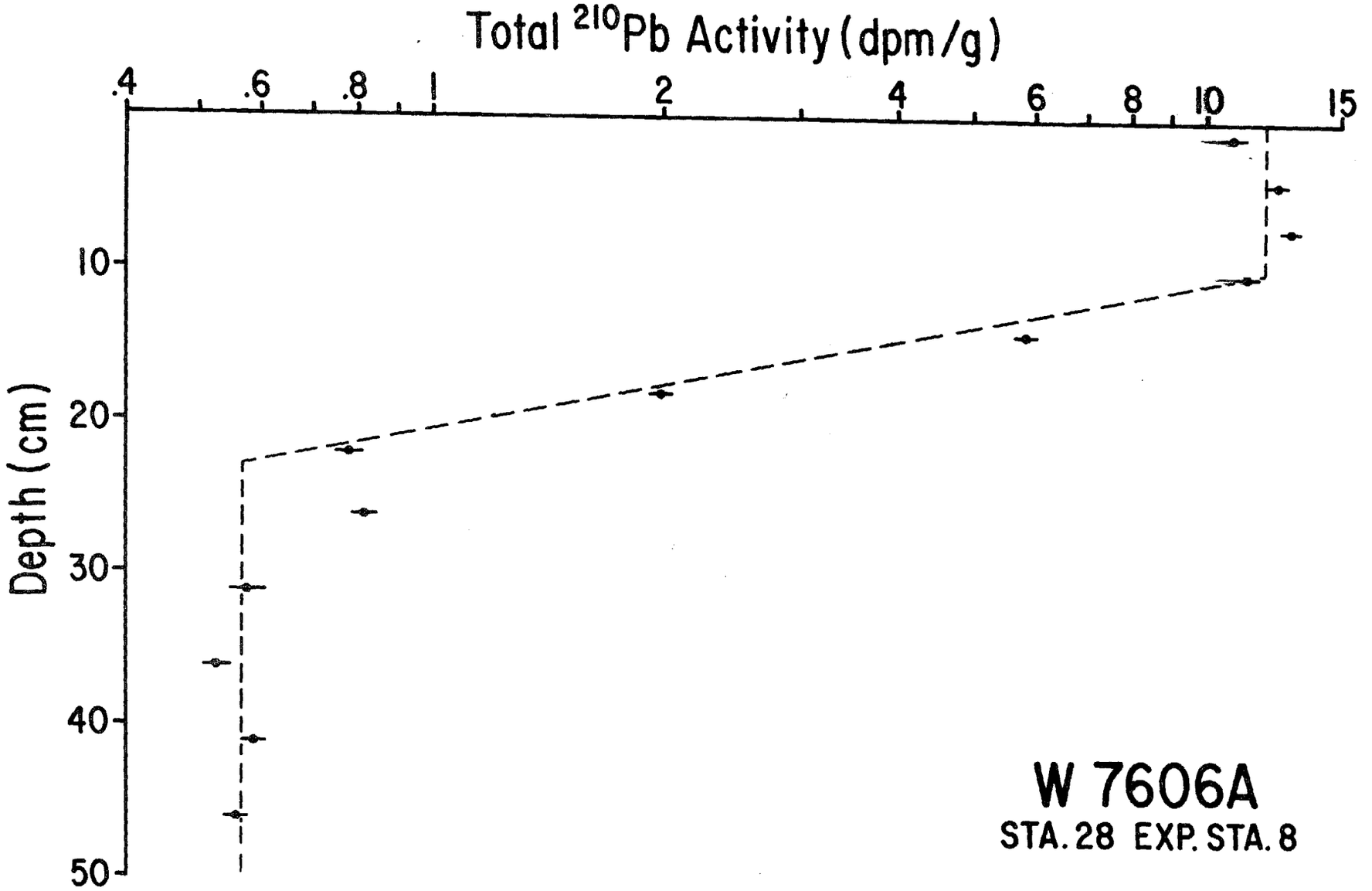
Total ^{210}Pb Activity (dpm/g)
.4
.6
.8
1
2
4
6
8
10
15
Depth (cm)
10
20
30
40
50
W 7606A
STA. 28 EXP. STA. 8

Figure 3-7

Figure 3-8a-8p Profiles of ^{210}Pb activity (-o- excess, -•-total) and texture in hydraulically damped gravity cores. Error bars reflect 1 standard deviation due to counting statistics. Samples having no excess ^{210}Pb indicated by X. Dashed lines represent our best estimate of the ^{210}Pb (excess) trend by excluding points presumably affected by inhomogeneous mixing. Slope of dashed lines are used to estimate mixing rates.

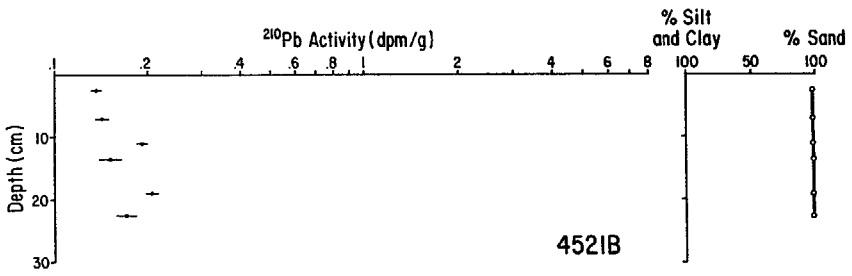

Figure 3-8a

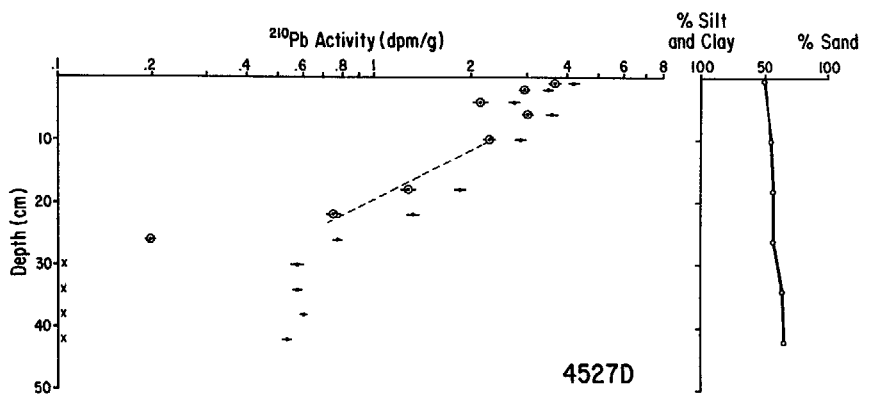

Figure 3-8b

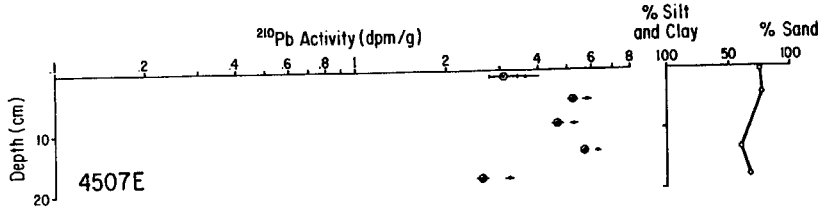

Figure 3-8c

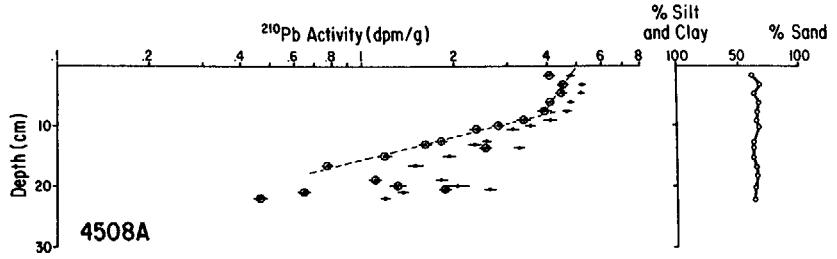

Figure 3-8d

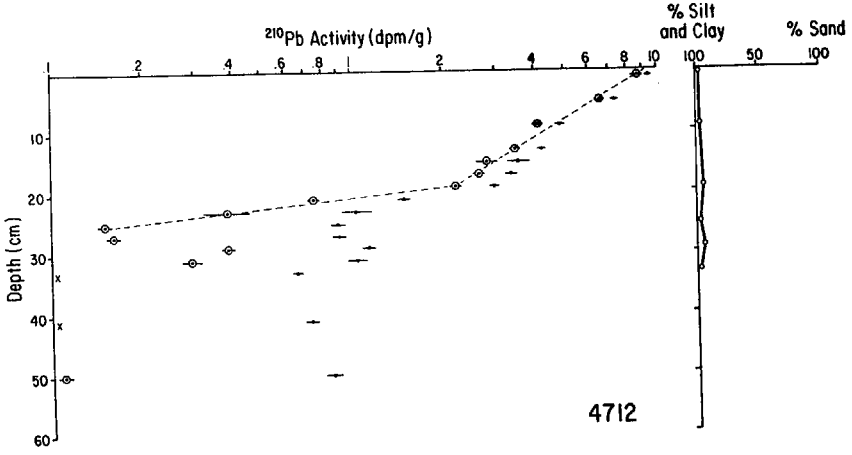

Figure 3-8e

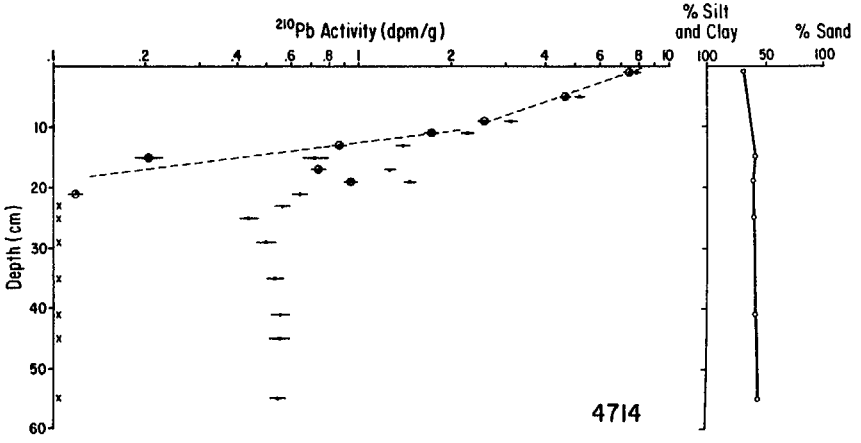

Figure 3-8f

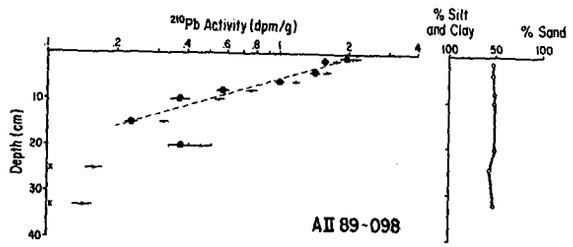

Figure 3-8g

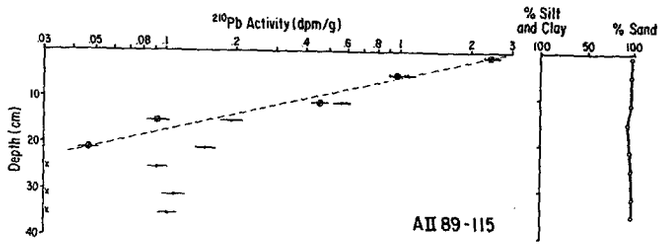

Figure 3-8h

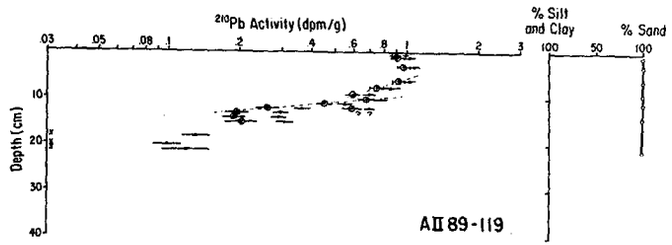

Figure 3-8i

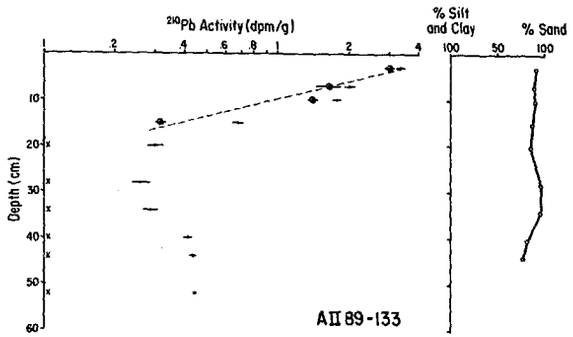

Figure 3-8j

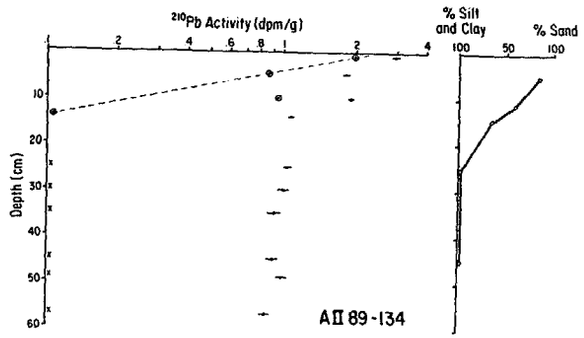

Figure 3-8k

Figure 3-81

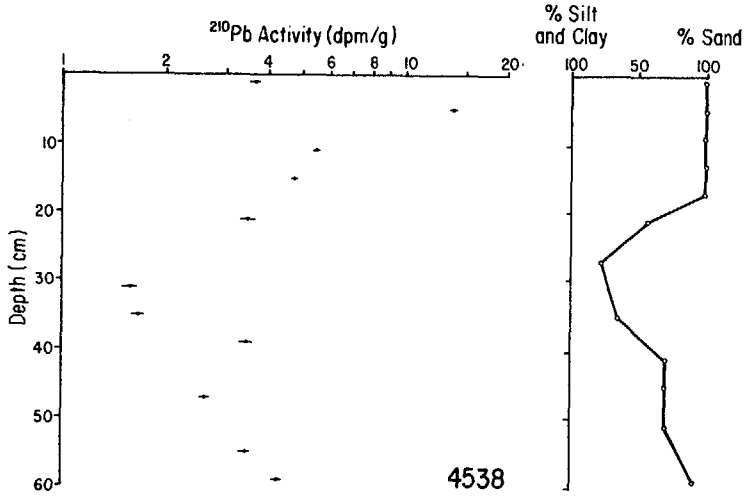

Figure 3-8m

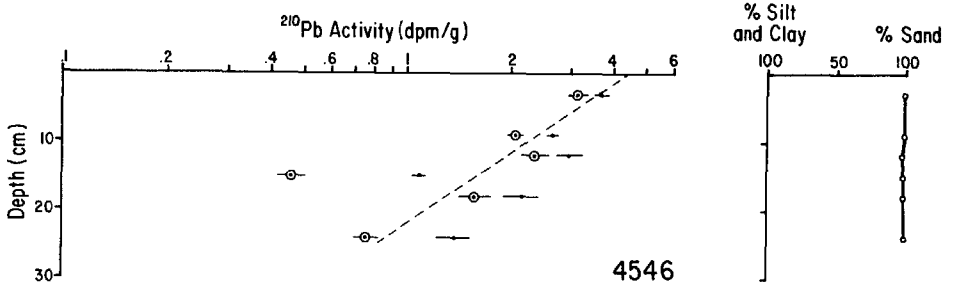

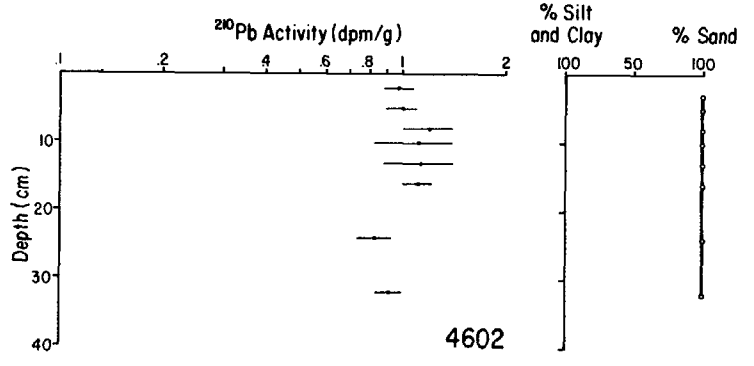

Figure 3-8n

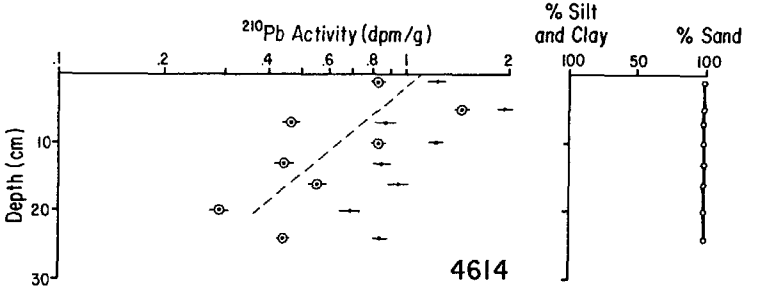

Figure 3-8p

from the eastern edge of the "mud patch" (fig. 3-8d), there are subsurface peaks in the ^{210}Pb activity (for example, at 14 and 21 cm) which are probably due to the transport of surface material downward by organisms. The sedimentation rate calculated from the slope of points which fall close to a straight line is 170 cm.1,000 yrs^{-1}, more than three times higher than the rate determined with ^{14}C. The higher rate is probably a result of mixing the entire 22 cm of sediment recovered with more efficient mixing in the top 10 cm.

The cores from areas of finest sediment in this deposit (4712, 4714) (figs. 3-8e and f) also have subsurface peaks in the ^{210}Pb profile. Sedimentation rates obtained from points approximating a straight line are almost three times faster than those determined with ^{14}C. The noise in the data makes selection of the "best" slope somewhat arbitrary, but clearly, the mixing in these sediments precludes the use of ^{210}Pb as an independent indication of sedimentation rates.

Off the coast of New Jersey at location AII 89-115 (fig. 3-8h) there is evidence that the sediments are not accumulating. Horizontal planes identified with high-resolution seismic reflection are truncated where they outcrop on the flanks of a small ridge (H.J. Knebel, U.S. Geological Survey, personal communication, 1979). In addition, the heavy minerals in surface sediments in this area are concentrated (Knebel and Twichell, 1978) which suggests winnowing.

The ^{210}Pb profiles in these relict sediments (Emery and Uchupi, 1972) must be due to sediment mixing by organisms and currents. Organisms are likely to be the most important mixing agents in those cores which have a logarithmic decrease in ^{210}Pb starting at the water-sediment interface. Storm resuspension and deposition would probably leave a uniform ^{210}Pb distribution over the depth interval

affected. These ^{210}Pb profiles are used to estimate rates of mixing with a simple mixing model, which is discussed in a later section.

The ^{210}Pb profiles in cores from the southeast Georgia Embayment, do not show the features of the idealized curve. Cores 4546 and 4614 (figs. 3-8m and p) show a general decrease in ^{210}Pb activity with depth but the cores did not penetrate to a depth of constant low ^{210}Pb activity as was observed in many cores from the "mud patch" area. The scatter in the data from these two cores may be due to difficulties in selecting homogeneous small subsamples from coarse-grained sediments. A second explanation may be the variable content of ^{226}Ra with depth in these sediments contributed by carbonate minerals. Since ^{226}Ra is the grandparent of ^{210}Pb, variations in ^{226}Ra would account for variations in the level of supported ^{210}Pb. We interpret the general decrease of ^{210}Pb activity in these two cores to result from adsorption of excess ^{210}Pb at the water-sediment interface with subsequent biological reworking which apparently extends to at least 25 cm.

Core 4602 (fig. 3-8n) has a nearly uniform ^{210}Pb activity throughout the 32 cm of penetration. The ^{226}Ra levels are very low (0.04 $dpm \cdot g^{-1}$)(Appendix table 3-3) suggesting that the entire sediment column contains about 1 $dpm \cdot g^{-1}$ of excess ^{210}Pb. Our interpretation of this profile is that very rapid mixing affects the entire sediment core.

The process responsible may be physical mixing by currents in addition to biological mixing. A core on the leading edge of an active sand ripple with amplitude in excess of 32 cm would be expected to have a ^{210}Pb profile similar to the one observed at this station.

The ^{210}Pb profile of core 4538 (fig. 3-81) is unusual because the activity is lowest at 30 cm and then increases with depth to 60 cm. Texturally this core is complicated by a zone of finer material at about

20-40 cm depth with coarse material above and below. The carbonate fragments in the upper and lower section of this core were the size of gravel and so samples were ground to assure that small subsamples were representative of the cored sediment.

The ^{226}Ra values from this core are highly variable with depth. In the coarser sediments at 15 and 60 cm, the ^{226}Ra and total ^{210}Pb activity are nearly the same, suggesting no excess ^{210}Pb. At 5 cm and 31 cm, however, the low ^{226}Ra activity suggests that excess ^{210}Pb is present. The presence of excess ^{210}Pb is expected in the upper parts of the core due to mixing. It's difficult to interpret excess ^{210}Pb at 31 cm below a layer where no excess ^{210}Pb exists. Either this sample has been affected by deep-mixing organisms or the isotopic data is in error.

Our experience with this core suggests that ^{210}Pb analysis should be restricted to cores having uniform texture and mineralogy throughout their length.

The Mixing Model

The mechanism of incorporating ^{210}Pb into a relict sediment column which is mixed by biological or physical processes requires adsorption at the water-sediment interface. Resuspension of bottom sediment, a common phenomenon on the continental shelf during storms (Butman and Folger, 1979), could present additional adsorption surfaces to dissolved ^{210}Pb. This mechanism has been cited to explain the horizontal concentration gradient of dissolved ^{210}Pb in the deep sea (Bacon and others, 1976). Once associated with the bottom, the new ^{210}Pb is carried with sediment during the mixing process. In addition, organisms which draw overlying seawater into the sediments could enhance the exposure of dissolved ^{210}Pb to sedimentary particles.

The framework for the model is the conservation of mass equation for a radioactive tracer, and treats mixing as a diffusive process:

$$\frac{\partial A}{\partial t} = K \frac{\partial^2 A}{\partial Z^2} - S \frac{\partial A}{\partial Z} - \lambda A \qquad (1)$$

A = the mass of element A, t = time in seconds, K is a diffusion or mixing coefficient ($cm^2.s^{-1}$), Z is sediment depth in core, S is a sedimentation rate, and λ is the decay constant for ^{210}Pb (s^{-1}). If we assume steady state and no sediment accumulation, the equation reduces to a balance of mixing and radioactive decay.

$$K \frac{\partial^2 A}{\partial Z^2} = \lambda A \qquad (2)$$

The solution of this equation is:

$$A = A_o e^{-(\lambda/K)^{\frac{1}{2}} \cdot Z} \qquad (3)$$

The mixing coefficient K is the only unknown in the equation and can be evaluated from the slope of the line relating excess ^{210}Pb activity and depth. For core AII 89-115, the mixing coefficient is 2.5×10^{-8} $cm^2.s^{-1}$. This is within the range measured by others using more elaborate mixing models in the coastal zone (Guinasso and Schink, 1975). Mixing coefficients calculated with this model are reported for all the cores in table 3-1.

The mixing depth, also reported in table 3-1, is defined as the maximum penetration of excess ^{210}Pb into sediments that are not accumulating. This depth is estimated directly from the profile of excess ^{210}Pb in the sediment cores. In the area of the "mud patch" both

Table 3-1. Estimated mixing coefficient and maximum depth of mixing

Core	Mixing coefficient cm^2/s	Depth interval considered (cm)	Mixing depth (cm)
4507	too few samples		>18
4508	3×10^{-8}	(8 - 16)	21
4521	No excess ^{210}Pb		0 (apparent erosion)
4527	1.3×10^{-7}	(10 - 20)	28
4712	1.7×10^{-7}	(0 - 19)	22
	6.7×10^{-9}	(19 - 25)	
4714	5.8×10^{-8}	(1 - 10)	20
	8.3×10^{-9}	(10 - 15)	
AII 89-098	3.2×10^{-8}	(0 - 15)	19
AII 89-115	2.5×10^{-8}	(0 - 15)	21
AII 89-119	5.0×10^{-8}	(6 - 11)	18
	4.4×10^{-9}	(11 - 14)	
AII 89-133	4.3×10^{-8}	(3 - 15)	19
AII 89-134	1.9×10^{-8}	(1 - 14)	12
4538	profile too erratic for estimate of mixing rate		
4546	2.1×10^{-7}	(0 - 25)	>25
4602	mixing homogeneous, too fast for estimate by this method		>32
4614	3.5×10^{-7}	(0 - 25)	>25

the mixing coefficient and mixing depth are maximum values because the effect of sedimentation has not been included.

We have used the mixing coefficient and the estimated mixing depth to calculate the expected distribution of contaminant in sediment as a function of time. The hypothetical example requires that the contaminant be added in a single pulse to the surface of the sediments and that it behave chemically and physically like Pb. Assuming that the contaminant is stable and that it is redistributed only by continuous biological mixing, its distribution with time may be described by:

$$\frac{\partial A}{\partial T} = K \frac{\partial^2 A}{\partial Z^2} \qquad (4)$$

The solution to this equation is:

$$A = \frac{Q}{\pi K t} e^{-Z^2/4Kt} \qquad (5)$$

where Q = the amount of material.cm^{-2} (Csanady, 1973).

Figure 3-9 shows the calculated depth profiles of the contaminant at 5, 10, 50 and 100 yrs after initial deposition using the mixing coefficient and the depth of maximum mixing predicted from the ^{210}Pb data at location AII 89-115. Mixing by biological processes alone accounts for 5 cm penetration in 5 yrs. The effect of storms could increase the rate of pollutant penetration considerably.

CONCLUSIONS AND RECOMMENDATIONS

One of the most interesting findings of this study is that ^{210}Pb is mixed into relict continental shelf sediments. Pollutants having a similar affinity for sediments may be incorporated into sediments by the

Figure 3-9. Hypothetical distribution of a pollutant in sediments 5, 10, 50, and 100 years after instantaneous deposition on the seafloor. Redistribution is due to diffusive mixing. The mathematical model uses a mixing coefficient of 2.5×10^{-8} cm $/s^{-1}$.

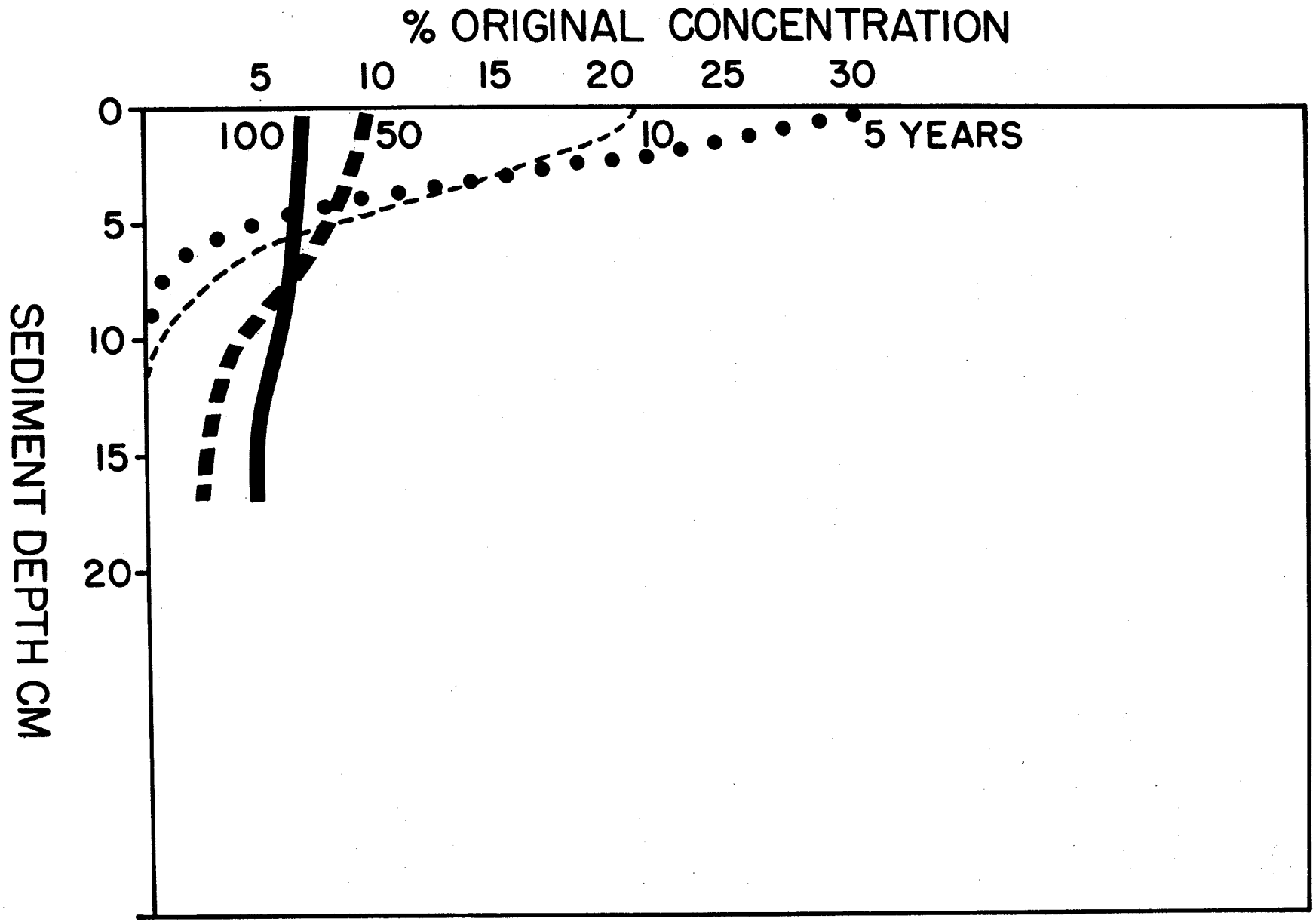
% ORIGINAL CONCENTRATION
5
10
15
20
25
30
0
5
10
15
20
SEDIMENT DEPTH CM
100
50
10
5 YEARS

Figure 3-9

same mechanism, which is thought to involve adsorption at the water-sediment interface followed by mixing into the sediment by organisms and currents. The surface 10 cm is often mixed very rapidly relative to the 22.3 yr half-life of ^{210}Pb, resulting in a uniform ^{210}Pb activity. Below 10 cm in relict sediments, a slower rate of mixing is generally observed with mixing coefficients ranging from 9×10^{-7} to 4×10^{9} $cm^2.s^{-1}$. The depth of active sediment mixing estimated from the ^{210}Pb profiles typically extends to 20 cm and occasionally to 28 cm. This data is useful in predicting the rates and depth of mixing for other pollutants which behave chemically like Pb.

The inventories of excess ^{210}Pb suggest sediment erosion on Georges Bank, in agreement with the high energy of tidal and storm currents known to characterize this area. High ^{210}Pb inventories in the fine-grained sediments south of Martha's Vineyard support the evidence from ^{14}C data that the sediments in this area are presently accumulating. This area is thus identified as a modern sink for fine-grained sediments and for pollutants associated with particulates in the water column. To our knowledge, this is the only site of present-day natural deposition on the continental shelf off the eastern United States, exclusive of the Gulf of Maine. Because the net currents on this area of the shelf flow from northeast to southwest, this area may receive its sediments and possible contaminants from the Nantucket Shoals and Georges Bank regions.

Any future work to refine the estimates of mixing rates and sedimentation rates should incorporate the use of more than one isotope. This approach would be helpful in sorting out the processes of sediment mixing and local accumulation. Analysis of ^{226}Ra in sediments is needed for a more accurate determination of supported ^{210}Pb activity,

particularly in sediments of the southeast Georgia Embayment where coarse carbonate-rich sediments have variable levels of ^{226}Ra with depth. In such areas ^{226}Ra analyses may be required for each sample analyzed for ^{210}Pb. This is also important for short cores which do not collect a lower section of uniform ^{210}Pb activity. Collection of larger diameter cores (box cores) in key locations would also be advantageous because sufficient material would be available for study of sediment structures with X-ray techniques as well as for isotope determinations over closely spaced intervals.

LITERATURE CITED

Bacon, M.P., Spencer, D.W., and Brewer, P.G., 1976, $^{210}Pb/^{226}Ra$ and $^{210}Po/^{210}Pb$ disequilibria in seawater and suspended particulate matter: Earth and Planetary Science Letters, v. 32, p. 277-296.

Benninger, L.K., 1976, The uranium-series radionuclides as tracers of geochemical processes in Long Island Sound: Ph.D. Thesis, Yale University, 151 p.

Bruland, K., 1974, Pb-210 geochronology in the coastal marine environment: Ph.D. Thesis, University of Southern California, 106 p.

Bumpus, D.F., 1973, A description of the circulation on the continental shelf of the East Coast of the United States: Progress in Oceanography, v. 6, p. 111-156.

Butman, B., and Folger, D.W., 1979, An instrument system for long-term sediment transport studies on the Continental Shelf: Journal of Geophysical Research, v. 84, p. 1215-1220.

Csanady, G.T., 1973, Turbulent diffusion in the environment: Dordrecht, Holland, D. Reidel Publishing Company, 249 p.

Emery, K.O., and Uchupi, E., 1972, Western North Atlantic Ocean: Topography, rocks, structure, water, life, and sediment: American Association of Petroleum Geologists Memoir 17, 532 p.

Guinasso, N.C., Jr., and Schink, D.R., 1975, Quantitative estimates of biological mixing rates in abyssal sediments: Journal of Geophysical Research, v. 80, p. 3032-3043.

Knebel, H.J., and Twichell, D.C., 1978, Heavy mineral variability in the Baltimore Canyon Trough area: Journal Research U.S. Geological Survey, v. 6, no. 2, p. 215-219.

Flynn, W.W., 1968, The determination of low levels of polonium-210 in environmental materials: Anal. Chim. Acta., v. 43, p. 221-227.

Meade, R.H., 1969, Landward transport of bottom sediments in estuaries of the Atlantic Coastal Plain: Journal of Sedimentary Petrology, v. 39, p. 222-234.

Nittrouer, C.A., Sternberg, R.W., Carpenter, R., and Bennett, J.T., 1979, The use of Pb-210 geochronology as a sedimentological tool: application to the Washington Continental Shelf: Marine Geology, v. 31, no. 3/4, p. 297-316.

Pamatmat, M.M., 1971, Oxygen consumption by the seabed. IV. Shipboard and laboratory experiments: Limnology and Oceanography, v. 16, p. 536-550.

Schlee, J., 1973, Atlantic Continental Shelf and Slope of the Eastern United States - sediment texture of the northeast part: U.S. Geological Survey Professional Paper 529-L, 64 p.

Skokes, R.F., 1976, Rate-dependent distributions of lead-210 and interstitial sulfate in sediments of the Mississippi River Delta: Ph.D. Thesis, Technical Report 76-1-T, Texas A & M University, 122 p.

Thomson, J., and Turekian, K.K., 1973, ^{210}Pb in coastal waters of the eastern United States, in Turekian, K.K., ed., Uranium and Thorium Decay Series Nuclide Abundances in Marine Plankton: Department of Geology and Geophysics, Yale University, Advanced Research Projects Agency Order No. 1793.

Turekian, K.K., and Cochran, J.K., 1978, Determination of marine chronologies using natural radionuclides, in Riley, J.P., and Chester, R., eds., Chemical Oceanography: London, Academic Press, v. 7, p. 313-360.

Turekian, K.K., Nozaki, Y., and Benninger, L.K., 1977, Geochemistry of atmospheric radon and radon products: Annual Review of Earth and Planetary Science Letters, v. 5, p. 227-255.

Twichell, D.C., McLennen, C.E., and Butman, B., 1980, Morphology and processes asssociated with the accumulation of the fine-grained sediment deposit on the southern New England Shelf: Journal of Sedimentary Petrology, in press.

CHAPTER 4

SEDIMENTS AND SEDIMENTARY PROCESSES AS INTERPRETED FROM PISTON CORES AND GRAB SAMPLES FROM THE CONTINENTAL SLOPE OF THE SOUTHEASTERN UNITED STATES

Larry J. Doyle[1], Frederick M. Wall[1], and Paul Schroeder[1]

[1]University of South Florida, Department of Marine Science, St. Petersburg, Florida 33701

CHAPTER 4

Table of Contents

Page

Page

Abstract. 4- 1

Introduction. 4- 1

Thrust of the study 4- 1

Acknowledgements. 4- 2

Setting 4- 5

Approach. 4- 6

Results 4- 7

General description 4- 7

Texture 4-13

Composition 4-20

Discussion. 4-36

Summary conclusions 4-41

References cited. 4-43

CHAPTER 4

SEDIMENTS AND SEDIMENTARY PROCESSES AS INTERPRETED FROM PISTON CORES AND GRAB SAMPLES FROM THE CONTINENTAL SLOPE OF THE SOUTHEASTERN UNITED STATES

Larry J. Doyle, Frederick M. Wall, and Paul Schroeder

ABSTRACT

Study of 44 piston cores up to 6 metres in length along with 17 grab samples on the continental slope between the continental shelf of the southeastern United States and the Blake Plateau has shown that there is a major sedimentological break at Cape Hatteras which mirrors that which has long been recognized on the adjacent shelf. South of Cape Hatteras sand and calcium carbonate content increase dramatically relative to the slope north of the Cape. There is also a break in heavy mineral suite. Some upper slope cores contained gas, probably methane.

Sedimentary processes active on the slope include a significant amount of sand sized bed load spillover across the shelf break, resuspension, and winnowing of shelf fines. Incursions of the Florida Current onto the shelf may be important in resuspending shelf sediments and in sweeping them over the shelf break. Fines, probably as fecal pellets, combine with planktonic foraminifera to add to hemipelagic component to the slope sediments. The unaggregated fines must be swept away by the Florida Current. The slope is a potential pollutant sink.

INTRODUCTION

Thrust of the Study

Increasingly the search for hydrocarbons on the world's continental margins is being pushed into ever deeper water. Upper continental slopes are already undergoing active exploration in many areas; yet

little is known about the sediments or processes which affect them. The Atlantic continental slope of the southeastern United States (fig. 4-1) is doubly interesting since it lies between a continental shelf undergoing active exploration and the Blake Plateau which is also beginning to attract exploratory interest. As a zone of sediment flux, study of the slope in this region may disclose a great deal about the whole margin dynamical system in which the Florida current plays a major role.

Key questions which we have set out to investigate are:

1. What are the characteristics of southeastern United States Atlantic slope sediments?
2. What are the principal sedimentary processes which operate on the slope?
3. What is the role and relationship of the adjacent continental shelf in furnishing sediment to the slope?
4. Is the slope a potential pollutant sink?

Our data base is a collection of piston cores up to six metres in length and grab samples whose locations are shown in figure 4-1 which were arranged in transects perpendicular to the isobaths. These cores were collected in cooperation with George Keller, AOML and NOAA, in Miami.

Acknowledgements

We have worked in close conjunction with O.H. Pilkey, Duke University, and C.C. Woo of the U.S. Geological Survey (USGS), Woods Hole branch. The latter has provided a wealth of heavy mineral data on the slope coring project. Steve Sczydlik provided additional information and analyses for this report, some of which will also be used as part of his Master's thesis at the Department of Marine Science, University of South Florida.

Figure 4-1. Station locations. Those stations in each treatment (22, for example) closest to the beach are station 22A; those next deepest 22B; and so on.

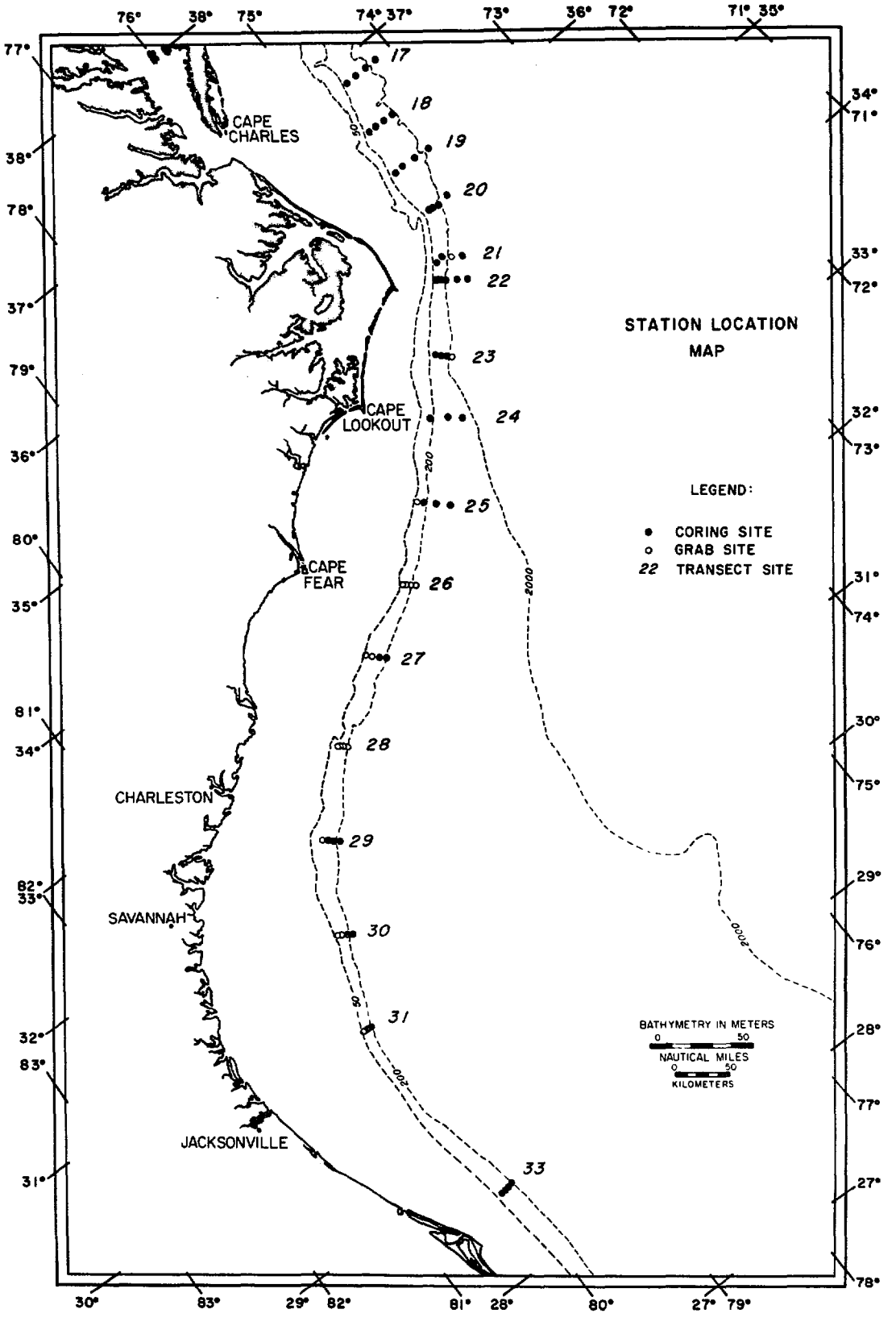
STATION LOCATION MAP
LEGEND:
CORING SITE
GRAB SITE
22 TRANSECT SITE
CAPE CHARLES
CAPE LOOKOUT
CAPE FEAR
CHARLESTON
SAVANNAH
JACKSONVILLE
BATHYMETRY IN METERS
NAUTICAL MILES
KILOMETERS
17
18
19
20
21
22
23
24
25
26
27
28
29
30
31
33

Setting

The continental slope of the eastern United States can be physiographically divided into two major parts with the boundary being Cape Hatteras. Emery and Uchupi (1972) point out that north of Cape Hatteras the slope is cut by numerous submarine canyons. In the environs of Cape Hatteras lies the southernmost of these, the Hatteras Canyon system of which Pamlico Canyon is a branch. South of the Cape the continental slope bifurcates into the Blake Escarpment, with which we are not concerned in this study, and the slope between the continental shelf whose break is at about 75 m and bottom depth 200 m. A minirise, which we have also sampled, more gentle than the slope above then falls away to the surface of the Blake Plateau at 600 to 700 m depth. Only a few surface samples from the upper slope south of Hatteras have been described by Gorsline (1963), Emery and Uchupi (1972), and Milliman and others (1972). It has generally been considered that slope sediments, south of Hatteras were dominated by a sand sized fraction chiefly composed of planktonic foraminifera tests.

The adjacent shelf and the Hatteras Canyon system are well studied. Most of the pertinent literature is reviewed and summarized in Emery and Uchupi (1972) and Milliman and others (1972). Clay mineralogy of the region is discussed by Hathaway (1973). The shelf of the southeastern United States is a palimpsest veneered with a Holocene quartz-carbonate sand sheet. Calcium carbonate, chiefly in the form of molluscan shell hash, makes up an average of about 18% of the sediment. This is in sharp contrast to the shelf north of Hatteras where calcium carbonate makes up only an average of about 2.5% (Emery and Uchupi, 1972). Carbonate content generally increases to the south. Heavy mineral provinces, too, are different north and south of Cape Hatteras with the

suite of the latter containing considerably more epidote and less garnet than the suite of the former (Milliman and others, 1972).

Clay mineralogy of shelf sediments, as well as sediments of the adjacent Coastal Plain and the rivers which rise in it, is dominated by smectite (Pevear, 1972) while the Piedmont is dominated by kaolinite. Rivers which rise in the Piedmont likewise carry predominantly kaolinite. Almost all sediment brought to the sea in the southeastern United States is carried by Piedmont-rising rivers. In an investigation of suspended sediments companion to this study, Pierce and others (1972) and Doyle and others (1979a, b) found that kaolinite and illite are the only clays in the water column indicating that some fine sediments are escaping nearshore estuarine traps and are moving across the shelf.

Approach

Cores were X-rayed, split, described, and then subsampled for textural, percent calcium carbonate constitutents, total organic carbon, and clay mineralogic analysis. A multiple sampling scheme was utilized. All cores were sampled top, middle, and bottom and were also channel sampled in order to obtain an integration of the sedimentary parameters over the top few metres. Cores 24B, 24C, and 24D were sampled in detail, 2 cm every 10 cm down their entire length. Since sedimentary layers are not traceable from core to core, the cores in one transect are from a variety of bathymetric positions, and funds have not been sufficient for an extensive radiometric dating program, stratigraphic correlation among cores has not been possible, and channel samples have provided the most usable data. Grab samples were split, subsampled, and analyzed in the same way as the core channel samples. All figures showing distribution of average sedimentary parameters incorporate channel and grab sample data.

Standard procedures were used throughout as described in Carver (1971). Total organic carbon was determined using an Angstrom model 7000[1] carbon analyzer in combination with calcium carbonate determination by acid leaching, gas displacement technique. Clay mineralogy was determined by X-ray diffraction on carbonate-free, organic-free samples. Identification of the major clay minerals, smectite, illite, and kaolinite was carried out using the examination techniques of Griffin (1962) and Grim (1968). Relative percentages of clay minerals present were estimated by comparing basal (001) peak areas. Data are presented as Appendices 4-1 through 4-6 (microfiche in pocket in back cover) and in tables 4-1a and b.

RESULTS

General Description

Slope sediments of the southeastern United States are predominantly some shade of gray or olive gray in color although various shades of olive, green, brown, and even yellow are also found, especially in the middle area in transects 22 and 27. Most cores are burrowed and mottled but not sufficiently disturbed to destroy bedding on the magnitude of a few centimetres in thickness. Very thin sand layers only a few millimetres thick remain intact. Several of the thicker sand layers on the upper slope exhibit graded bedding typical of what is commonly interpreted as a turbidite in rise or deep-sea deposits. An additional interesting aspect of cores in transects 20, 21, and 23, specifically cores 20B, 20C, 21A, 23A, and 23B, is that sediments in them showed

---

[1]Use of brand names in this report is for descriptive purposes only and does not constitute endorsement by the U.S. Geological Survey.

TABLE 4-1a
Cores

Sample #	PHI MOMENT MEASURES				GRAPHIC PHI PARAMETER									
					Mean		Standard Deviation		Skewness (1)		Skewness (2)		Kurtosis	
	Mean	Standard Deviation	Skewness	Kurtosis	a	b	a	b	a	b	a	b	a	b
18A	3.000	0.888	-1.100	4.907	3.023	3.100	0.739	0.840	-0.313	-0.440	-1.192	------	1.102	1.320
B	2.074	1.239	-0.262	-0.587	2.064	2.115	1.390	1.310	-0.110	-0.157	-0.299	------	0.459	0.846
C	2.487	1.114	-0.394	-0.402	2.428	2.546	1.217	1.155	-0.290	-0.338	-0.571	------	0.481	0.821
D	2.414	0.878	-0.261	-0.066	2.426	2.441	0.995	0.939	-0.047	-0.062	-0.111	------	0.464	0.921
19A	2.786	1.158	-0.854	2.241	2.684	2.861	1.064	1.101	-0.498	-0.560	-1.097	------	0.762	1.203
B	2.186	1.184	-0.377	-0.006	2.181	2.245	1.274	1.214	-0.151	-0.193	-0.352	------	0.495	0.884
C	2.283	1.168	-0.331	-0.511	2.279	2.344	1.266	1.210	-0.152	-0.212	-0.408	------	0.503	0.843
D	2.753	1.131	-0.672	0.643	2.574	2.783	1.171	1.142	-0.536	-0.573	-0.956	------	0.570	1.021
20A	2.790	0.981	-0.679	1.098	2.749	2.870	0.967	0.989	-0.377	-0.449	-0.899	------	0.724	1.057
B	3.284	0.624	-1.680	11.890	3.422	3.422	0.393	0.514	-0.000	-0.251	-1.336	------	1.660	1.482
C	2.675	1.220	-0.678	0.766	2.486	2.714	1.249	1.211	-0.548	-0.581	-0.952	------	0.551	1.041
D	2.981	1.017	-1.037	3.585	2.956	3.077	0.826	0.939	-0.438	-0.542	-1.358	------	1.101	1.783
21A	3.073	0.805	-1.053	4.272	3.050	3.136	0.728	0.777	-0.353	-0.448	-1.015	------	0.871	1.370
B	2.415	1.239	-0.561	0.253	2.340	2.468	1.267	1.283	-0.304	-0.383	-0.783	------	0.692	1.231
D	3.038	0.878	-1.114	4.642	3.056	3.135	0.718	0.841	-0.331	-0.465	-1.329	------	1.215	1.518
22A	3.174	0.637	-1.012	3.665	3.153	3.215	0.635	0.662	-0.292	-0.384	-0.852	------	0.789	1.409
B	2.408	1.262	-0.511	-0.075	2.264	2.431	1.364	1.324	-0.366	-0.418	-0.730	------	0.552	1.039
C	3.224	0.669	-1.238	5.316	3.337	3.357	0.470	0.610	-0.127	-0.344	-1.477	------	1.633	1.681
D	3.222	0.692	-1.271	5.573	3.374	3.383	0.434	0.604	-0.063	-0.320	-1.696	------	1.936	1.746
E	2.964	0.823	-0.712	1.082	2.916	3.018	0.836	0.840	-0.367	-0.433	-0.831	------	0.669	1.029
F	2.981	0.787	-0.766	1.735	2.967	3.047	0.779	0.805	-0.306	-0.393	-0.845	------	0.763	1.054
23A	3.139	0.638	-1.190	8.203	3.115	3.172	0.656	0.614	-0.258	-0.289	-0.459	------	0.441	0.924
B	2.871	0.799	-0.711	2.260	2.914	2.958	0.781	0.801	-0.170	-0.268	-0.636	------	0.734	0.971
C	2.929	0.979	-0.869	2.196	2.878	3.006	0.886	0.947	-0.435	-0.518	-1.129	------	0.877	1.267

a. Inman (1952)
b. Folk and Ward (1957)

TABLE 4-1a (Cont.)

Sample #	PHI MOMENT MEASURES				GRAPHIC PHI PARAMETER									
					Mean		Standard Deviation		Skewness (1)		Skewness (2)		Kurtosis	
	Mean	Standard Deviation	Skewness	Kurtosis	a	b	a	b	a	b	a	b	a	b
24A	0.567	1.095	-0.311	-0.684	0.435	0.560	1.249	1.166	-0.300	-0.332	-0.520	------	0.431	0.899
B	2.885	0.880	-0.804	3.007	2.869	2.963	0.860	0.848	-0.328	-0.387	-0.718	------	0.608	0.935
C	3.133	0.706	-0.949	2.757	3.093	3.173	0.693	0.731	-0.346	-0.436	-0.962	------	0.827	1.557
D	2.904	0.953	-0.805	1.966	2.814	2.953	0.940	0.924	-0.443	-0.490	-0.858	------	0.595	1.033
25B	2.607	0.967	-0.694	2.782	2.637	2.673	0.966	0.917	-0.112	-0.162	-0.315	------	0.485	0.914
C	2.096	0.736	0.271	-0.608	2.104	2.055	0.820	0.798	0.177	0.239	0.472	------	0.561	0.874
D	2.227	0.852	-0.206	0.416	2.224	2.235	0.896	0.860	-0.037	0.021	0.121	------	0.517	0.892
27C	1.715	1.326	-0.485	0.587	1.784	1.819	1.141	1.328	-0.093	-0.199	-0.667	------	1.193	1.405
28C	1.770	1.175	-0.208	-0.731	1.644	1.805	1.259	1.168	-0.384	-0.285	-0.263	------	0.412	0.724
D	2.887	0.848	-0.868	3.474	2.933	2.987	0.778	0.810	-0.210	-0.312	-0.741	------	0.787	1.010
29B	2.410	1.116	-0.581	1.102	2.423	2.483	1.116	1.136	-0.161	-0.252	-0.587	------	0.709	1.122
C	2.921	1.124	-1.138	4.797	2.956	3.067	0.817	0.972	-0.408	-0.532	-1.495	------	1.278	1.625
D	2.739	1.383	-1.035	3.299	2.885	3.000	0.868	1.207	-0.395	-0.561	-2.139	------	1.940	1.840
30C	2.649	0.998	-0.820	3.407	2.746	2.770	0.880	0.931	-0.082	-0.212	-0.630	------	0.841	1.082
D	1.873	0.894	-0.384	1.215	1.934	1.936	0.832	0.885	-0.007	-0.092	-0.331	------	0.861	1.037
31C	2.399	0.753	-0.419	1.628	2.369	2.399	0.724	0.768	-0.125	-0.093	-0.113	------	0.848	1.314
D	1.287	1.811	-0.297	-1.211	0.778	1.206	2.136	1.886	-0.601	-0.515	-0.543	------	0.265	0.605
33A	1.729	1.879	-0.382	-0.959	1.179	1.591	2.342	2.018	-0.528	-0.508	-0.581	------	0.193	0.758
B	2.138	1.653	-0.482	-0.399	1.802	2.140	1.856	1.718	-0.545	-0.566	-0.823	------	0.405	0.917
C	2.980	1.156	-1.230	5.338	3.039	3.143	0.753	0.970	-0.413	-0.557	-1.825	------	1.601	2.471
D	2.757	0.987	-0.518	-0.212	2.625	2.789	1.094	1.046	-0.452	-0.486	-0.782	------	0.507	0.925

a. Inman (1952)
b. Folk and Ward (1957)

TABLE 4-1b
Grabs

Sample #	PHI MOMENT MEASURES				GRAPHIC PHI PARAMETER									
					Mean		Standard Deviation		Skewness (1)		Skewness (2)		Kurtosis	
	Mean	Standard Deviation	Skewness	Kurtosis	a	b	a	b	a	b	a	b	a	b
22A	3.310	0.482	-1.386	8.037	3.409	3.409	0.402	0.472	-0.000	-0.203	-0.904	------	1.228	1.242
23A	2.934	0.890	-1.220	7.899	2.976	3.036	0.754	0.778	-0.238	-0.332	-0.748	------	0.757	1.011
D	2.983	0.874	-0.731	0.833	2.823	2.977	0.949	0.907	-0.488	-0.519	-0.827	------	0.504	1.115
25A	-0.231	0.770	0.411	1.145	-0.155	-0.217	0.757	0.813	0.246	0.206	0.314	------	0.892	1.214
D	2.082	0.723	0.311	-0.573	2.093	2.041	0.810	0.789	0.193	0.255	0.497	------	0.565	0.879
26A	0.944	0.806	-0.432	0.633	0.940	0.995	0.817	0.817	-0.200	-0.280	-0.593	------	0.651	0.933
B	0.839	1.245	-0.121	-0.923	0.803	0.860	1.416	1.342	-0.122	-0.131	-0.206	------	0.477	0.860
C	2.077	0.677	-0.553	4.691	2.062	2.086	0.717	0.648	-0.101	-0.104	-0.143	------	0.332	0.750
D	1.955	0.577	-0.071	0.714	1.977	1.958	0.699	0.631	0.081	0.083	0.111	------	0.327	0.743
27A	0.737	1.129	-0.186	-0.912	0.602	0.760	1.236	1.180	-0.385	-0.326	-0.400	------	0.501	0.796
B	2.590	1.055	-0.207	-1.472	2.515	2.714	1.201	1.035	-0.498	-0.471	-0.530	------	0.195	0.583
28A	0.452	1.312	0.187	-0.881	0.587	0.458	1.450	1.382	0.267	0.229	0.286	------	0.496	0.838
B	1.029	1.315	-0.150	-0.952	0.988	1.045	1.508	1.395	-0.114	-0.149	-0.257	------	0.404	0.796
C	2.603	0.987	-0.847	3.944	2.733	2.732	0.845	0.904	0.003	-0.141	-0.534	------	0.880	1.114
D	2.232	0.997	-0.473	1.009	2.223	2.274	0.986	1.031	-0.157	-0.192	-0.408	------	0.803	1.182
29A	1.356	0.966	0.156	1.089	1.183	1.239	0.763	0.939	-0.221	-0.031	0.384	------	1.411	1.518
B	2.528	0.810	-1.000	7.468	2.671	2.639	0.623	0.711	0.153	0.033	-0.184	------	1.116	1.392
30A	0.677	1.068	0.143	-0.469	0.807	0.723	1.228	1.168	0.205	0.190	0.261	------	0.491	1.109
B	1.841	1.051	-0.261	-1.162	1.633	1.836	1.194	1.062	-0.510	-0.457	-0.518	------	0.285	0.646
C	2.420	0.907	-0.563	1.861	2.458	2.477	0.896	0.938	-0.065	-0.136	-0.372	------	0.802	1.380
D	1.905	1.081	-0.014	0.032	2.212	2.038	1.127	1.121	0.463	0.303	0.234	------	0.632	0.909
31A	0.902	1.146	-0.329	-0.399	0.721	0.878	1.207	1.219	-0.391	-0.345	-0.503	------	0.682	1.038
B	1.039	0.696	0.239	-0.020	1.046	1.010	0.772	0.750	0.139	0.203	0.414	------	0.555	0.871

a. Inman (1952)
b. Folk and Ward (1957)

Figure 4-2. Number of sand layers in transects 19 through 33, modified after Doyle and others (1979b).

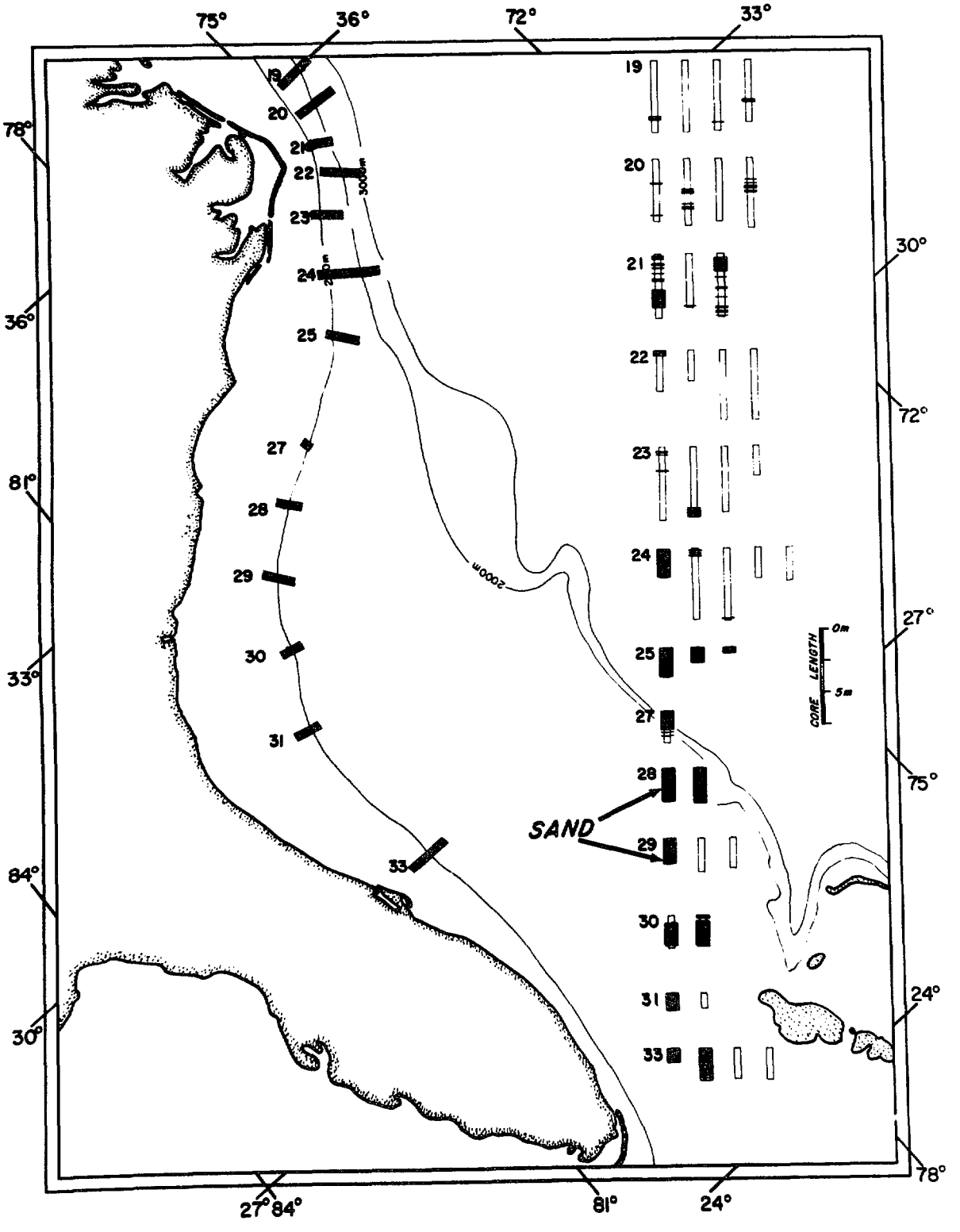
75°
36°
72°
33°
78°
36°
81°
33°
84°
30°
30°
72°
27°
75°
24°
78°
27°
84°
81°
24°
19
20
21
22
23
24
25
27
28
29
30
31
33
300m
2000m
SAND
CORE LENGTH
0m
5m

numerous gas cracks, probably indicating presence of methane, since sediments did not smell of H_2S.

South of Cape Hatteras sand layers, as shown in fig. 4-2 (modified after Doyle and others, 1979b), increase dramatically relative to cores taken north of the Cape. This change at the Cape is reflected in many of the parameters discussed below as well as in shelf sediments.

Texture

Figure 4-3 shows the distribution of the average sand content of the samples in the study area. South of Cape Hatteras sand content can be seen to increase dramatically, paralleling the increase in sand layers shown in fig. 4-2. South of Hatteras sand content also decreases regularly downslope although it remains as high as 30% on the minirise on the Blake Plateau. Tables 4-1a and 4-1b show the standard statistical measures of the sand size fraction for 44 cores and 20 grabs from the study area. Several different sets of statistical measures are presented for comparison. Perusal of the tables shows that mean grain size ranges from coarse to very fine sand with most samples lying in the fine to very fine sand range. Standard deviations are such that most samples are moderately sorted to poorly sorted with a few being moderately well sorted.

Figures 4-4 and 4-5 show the average percentage of silt and clay within the cores. Comparison with figure 4-3 shows that as sand regularly decreases seaward south of the Cape, silt and clay increase in about equal proportions. Off the Charleston-Savannah area silt increases somewhat faster than clay content. The relatively large amount of finer than sand-sized material is surprising since the Florida Current sweeps the slope/minirise in this region and is thought to keep large portions of the surface of the Blake Plateau free of clastic and

Figure 4-3. Distribution of percent sand. Contour interval 20%. Data from channel samples of cores and from grab samples.

Figure 4-3

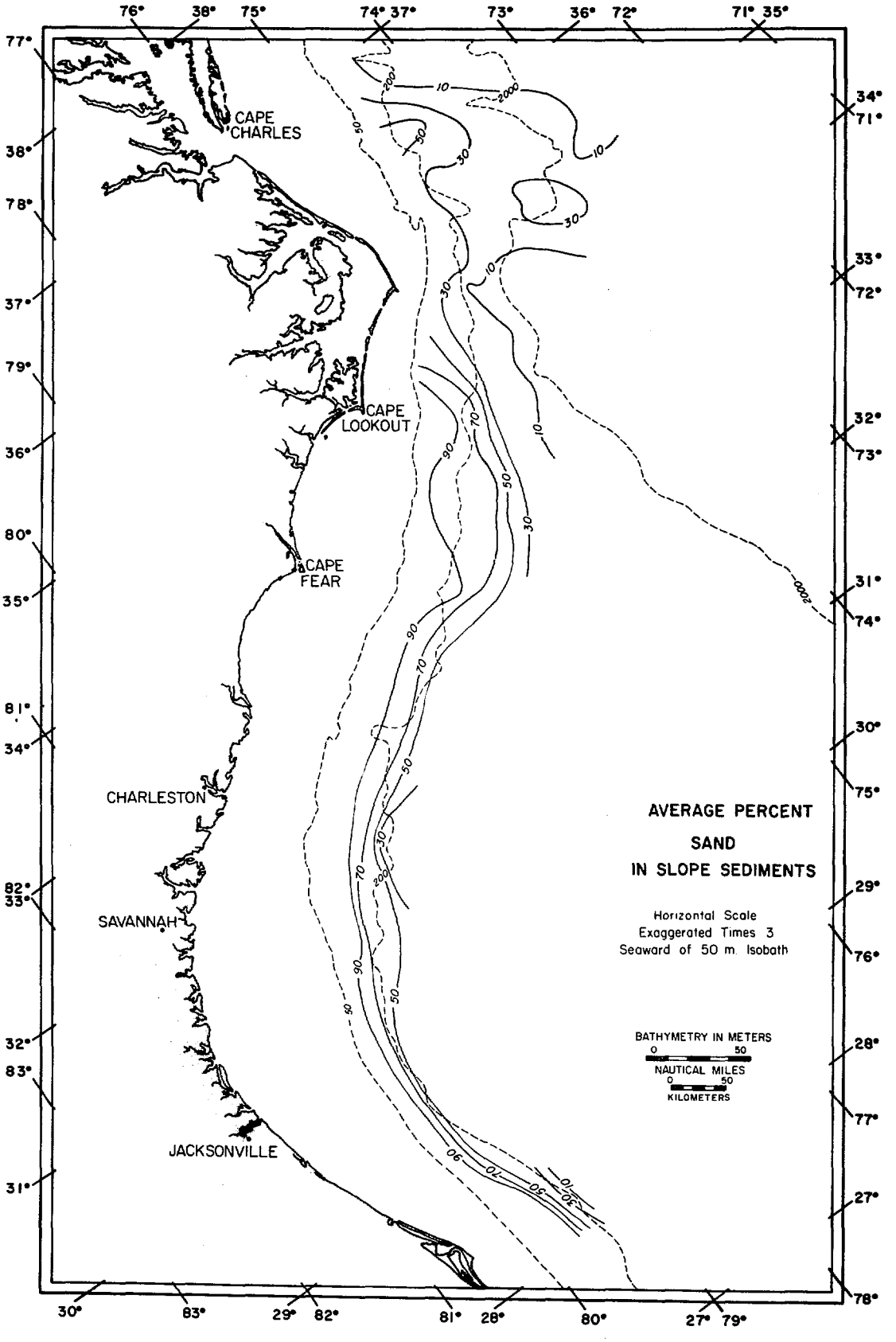
CAPE CHARLES
CAPE LOOKOUT
CAPE FEAR
CHARLESTON
SAVANNAH
JACKSONVILLE
AVERAGE PERCENT SAND IN SLOPE SEDIMENTS
Horizontal Scale Exaggerated Times 3 Seaward of 50 m. Isobath
BATHYMETRY IN METERS
NAUTICAL MILES
KILOMETERS

Figure 4-4. Distribution of percent silt. Contour interval 10%. Data from channel samples of cores and from grab samples.

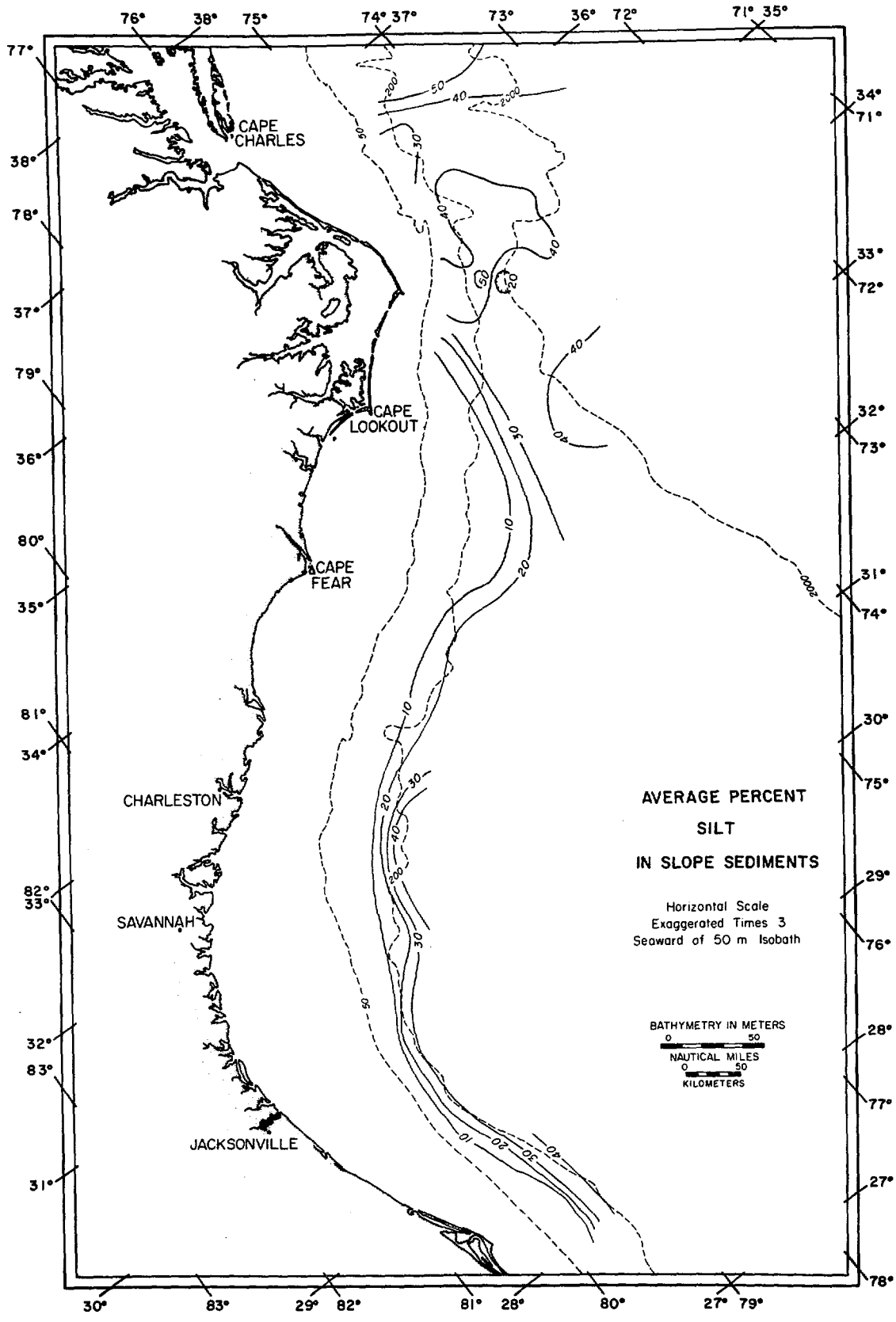
CAPE CHARLES
CAPE LOOKOUT
CAPE FEAR
CHARLESTON
SAVANNAH
JACKSONVILLE
AVERAGE PERCENT
SILT
IN SLOPE SEDIMENTS
Horizontal Scale
Exaggerated Times 3
Seaward of 50 m Isobath
BATHYMETRY IN METERS
0 50
NAUTICAL MILES
0 50
KILOMETERS

Figure 4-5. Distribution of percent clay. Contour interval 10%. Data from channel samples of cores and from grab samples.

Figure 4-5

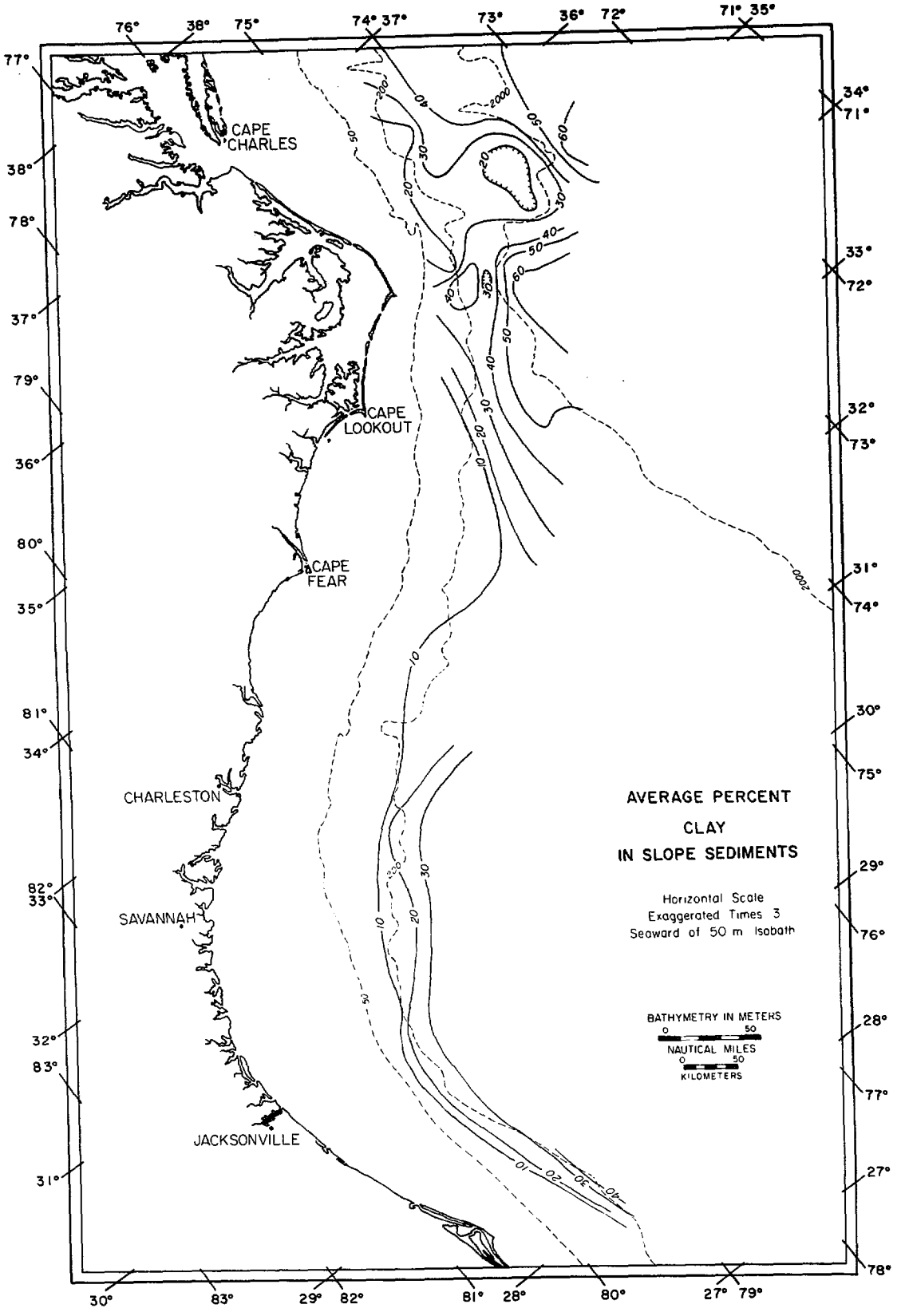
CAPE CHARLES
CAPE LOOKOUT
CAPE FEAR
CHARLESTON
SAVANNAH
JACKSONVILLE
AVERAGE PERCENT
CLAY
IN SLOPE SEDIMENTS
Horizontal Scale
Exaggerated Times 3
Seaward of 50 m Isobath
BATHYMETRY IN METERS
NAUTICAL MILES
KILOMETERS

biogenic sediments. North of Cape Hatteras fine grain sizes increase dramatically with a lobe of dominantly fine sediments extending as far south as the minirise off Cape Lookout.

Composition

Figure 4-6 shows the average distribution of percent calcium carbonate in the slope/minirise sediments of the area. Perusal of figure 4-6 clearly reveals an aburpt increase in calcium carbonate content south of Cape Hatteras. Carbonate content is high, between 50% and 80%. About halfway between Jacksonville, Florida, and Savannah, Georgia, the trend of the calcium carbonate distribution changes again. North of that line calcium carbonate percentages increase slowly downslope while south of that line they show a slow decrease seaward, paralleling the sand distribution.

Total organic carbon values shown in Appendix 4-1 generally decrease down core from a high value of as much as 1.5% near the top. Core 23A, with visible gas cracks, and 24C, 27C, and 29D maintain levels of over 1% total organic carbon over their whole length.

The sand fraction of the upper slope resembles that of the adjacent shelf. Carbonates are mostly shell hash with planktonic foraminifera becoming more important the farther downslope one progresses. Shelf-derived quartz sand is also an important component of the sand fraction. Even the heavy minerals are like those of the shelf with epidote predominant and phosphate and glauconite being present in some samples (Doyle and others, 1979b).

Distribution of the major groups of clay minerals, illite/mica, kaolinite, and smectite are shown in figures 4-7 through 4-12. These figures are paired, 4-7/4-8, 4-9/4-10, etc., with the first showing the relative percentage of the clay mineral in the topmost layer undisturbed

Figure 4-6. Distribution of percent $CaCO_3$. Contour interval 10%. Data from channel samples of cores and from grab samples.

Figure 4-6

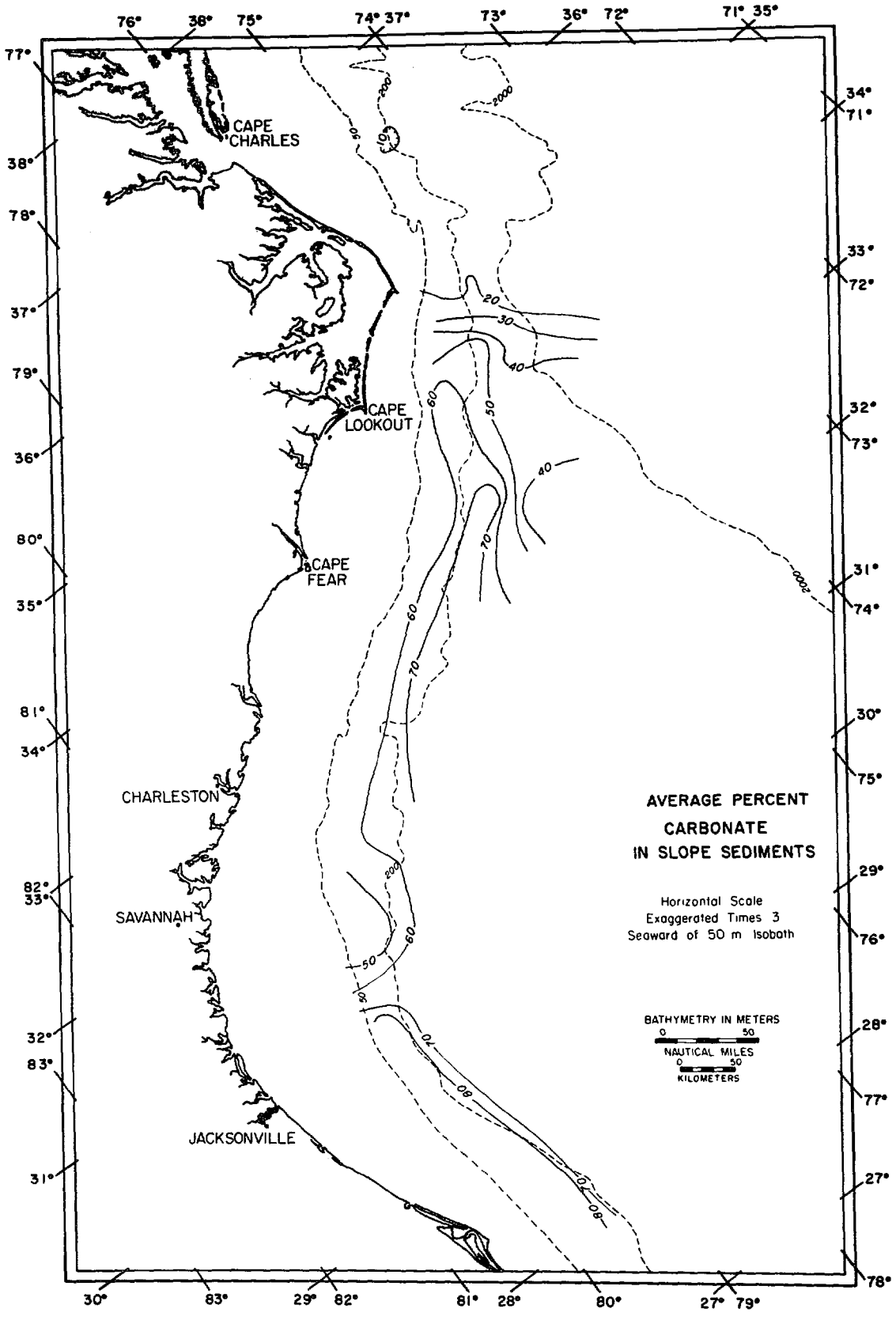
CAPE CHARLES
CAPE LOOKOUT
CAPE FEAR
CHARLESTON
SAVANNAH
JACKSONVILLE
AVERAGE PERCENT CARBONATE IN SLOPE SEDIMENTS
Horizontal Scale Exaggerated Times 3 Seaward of 50 m Isobath
BATHYMETRY IN METERS
0 50
NAUTICAL MILES
0 50
KILOMETERS

by the coring process and the second showing the average percentage of that clay mineral. The top layer should be representative of late Holocene deposition while the average should integrate depositional patterns over the past several thousand years.

Figure 4-7 shows the distribution of illite/mica in the top layers. South of an imaginary line about midway between Cape Fear and Charleston, percentages of illite regularly increase seaward. North of that line the reverse is true. Illite increases toward the north and west reaching a high off Cape Lookout of 70%. Average illite/mica distribution (fig. 4-8) shows a similar pattern although the imaginary boundary is farther to the south, lying between Charleston and Savannah. The pattern of increasing illite/mica to the north is clearer but more subdued in the form of a lobe decreasing to the south. A decrease from the center of the lobe of relatively high illite/mica seaward is also suggested. Both figures 4-7 and 4-8 show that illite is most significant on the slope north of Cape Hatteras.

Figures 4-9 and 4-10, the top layer and average kaolinite distributions are generally similar to each other in most particulars. Both show over 50% kaolinite on the slope between Cape Lookout and Charleston decreasing offshore, a bulge of relatively low kaolinite values of around 30% increasing seaward of Savannah, and a relatively high area with over 60% kaolinite decreasing rapidly offshore, northeast of Jacksonville.

Smectite values for top and core averages shown in figures 4-11 and 4-12 generally are inversely related to kaolinite values. Both show a bulge of relatively high percentages off Savannah decreasing seaward, relatively low values on the northern portion of the slope increasing seaward, and a relatively low bulge in percentage northeast of

Figure 4-7. Distribution of illite/mica in tops of cores. Contour interval 10%.

Figure 4-7

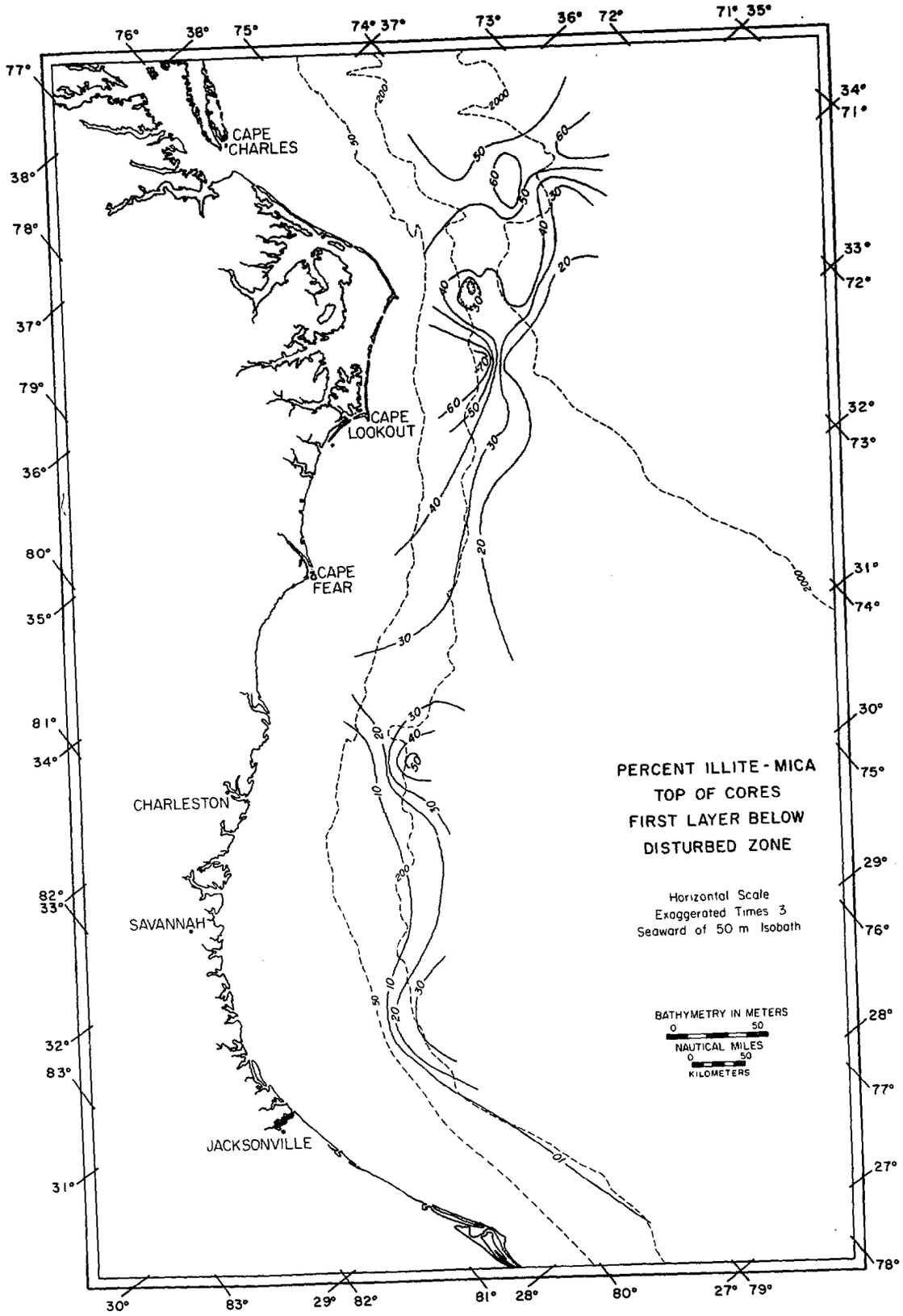
CAPE CHARLES
CAPE LOOKOUT
CAPE FEAR
CHARLESTON
SAVANNAH
JACKSONVILLE
PERCENT ILLITE-MICA
TOP OF CORES
FIRST LAYER BELOW
DISTURBED ZONE
Horizontal Scale
Exaggerated Times 3
Seaward of 50 m Isobath
BATHYMETRY IN METERS
0 50
NAUTICAL MILES
0 50
KILOMETERS

Figure 4-8. Distribution of average percent illite/mica averaged over the whole core. Contour interval 10%.

Figure 4-8

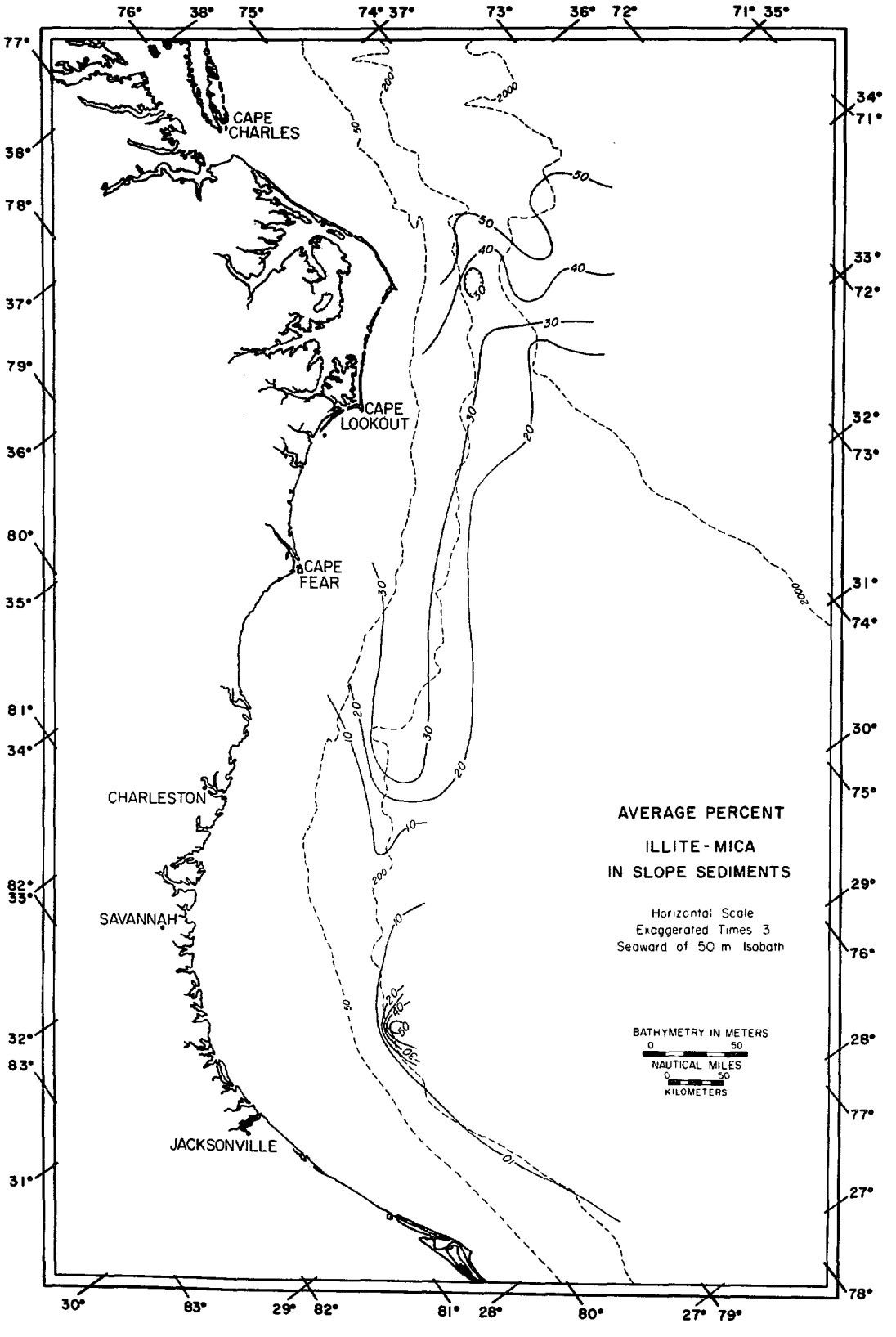
CAPE CHARLES
CAPE LOOKOUT
CAPE FEAR
CHARLESTON
SAVANNAH
JACKSONVILLE
AVERAGE PERCENT
ILLITE-MICA
IN SLOPE SEDIMENTS
Horizontal Scale
Exaggerated Times 3
Seaward of 50 m Isobath
BATHYMETRY IN METERS
0 50
NAUTICAL MILES
0 50
KILOMETERS

Figure 4-9. Distribution of percent kaolinite in tops of cores. Contour interval 10%.

Figure 4-9

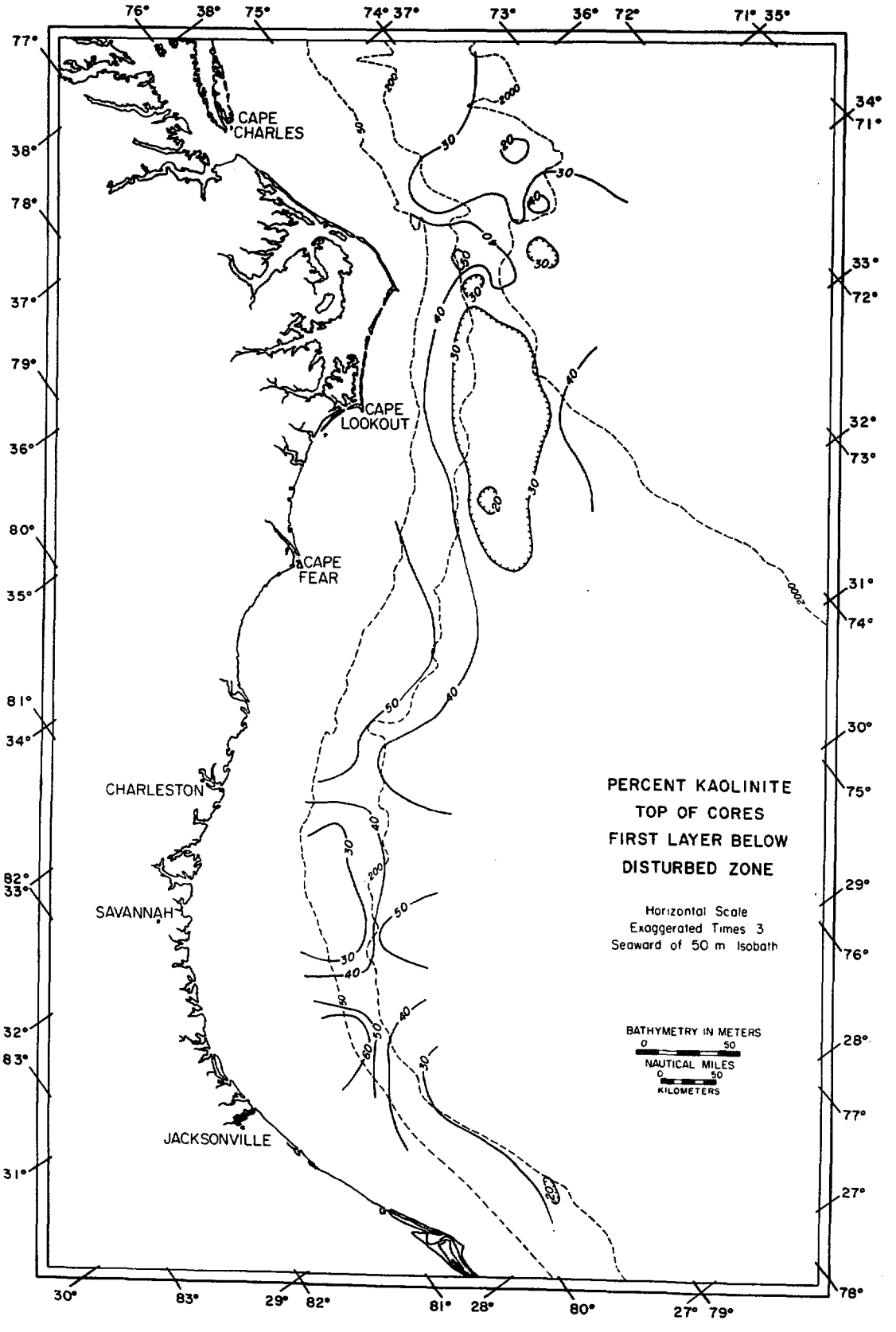
CAPE CHARLES
CAPE LOOKOUT
CAPE FEAR
CHARLESTON
SAVANNAH
JACKSONVILLE
PERCENT KAOLINITE
TOP OF CORES
FIRST LAYER BELOW
DISTURBED ZONE
Horizontal Scale
Exaggerated Times 3
Seaward of 50 m Isobath
BATHYMETRY IN METERS
0 50
NAUTICAL MILES
0 50
KILOMETERS

Figure 4-10. Distribution of averaged over the whole core percent kaolinite. Contour interval 10%.

Figure 4-10

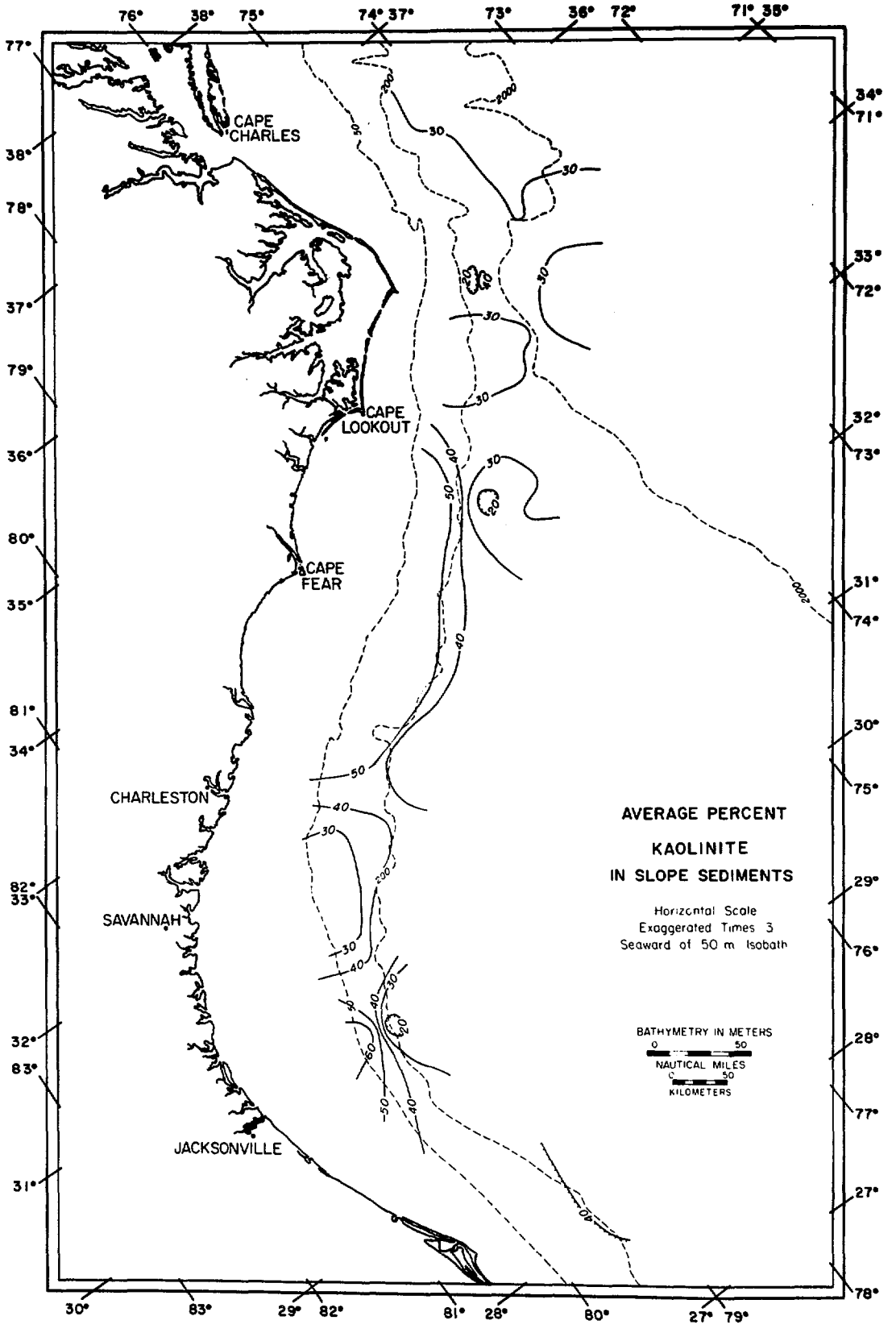
CAPE CHARLES
CAPE LOOKOUT
CAPE FEAR
CHARLESTON
SAVANNAH
JACKSONVILLE
AVERAGE PERCENT
KAOLINITE
IN SLOPE SEDIMENTS
Horizontal Scale
Exaggerated Times 3
Seaward of 50 m Isobath
BATHYMETRY IN METERS
0 50
NAUTICAL MILES
0 50
KILOMETERS

Figure 4-11. Distribution of percent smectite in tops of cores. Contour interval 10%.

Figure 4-11

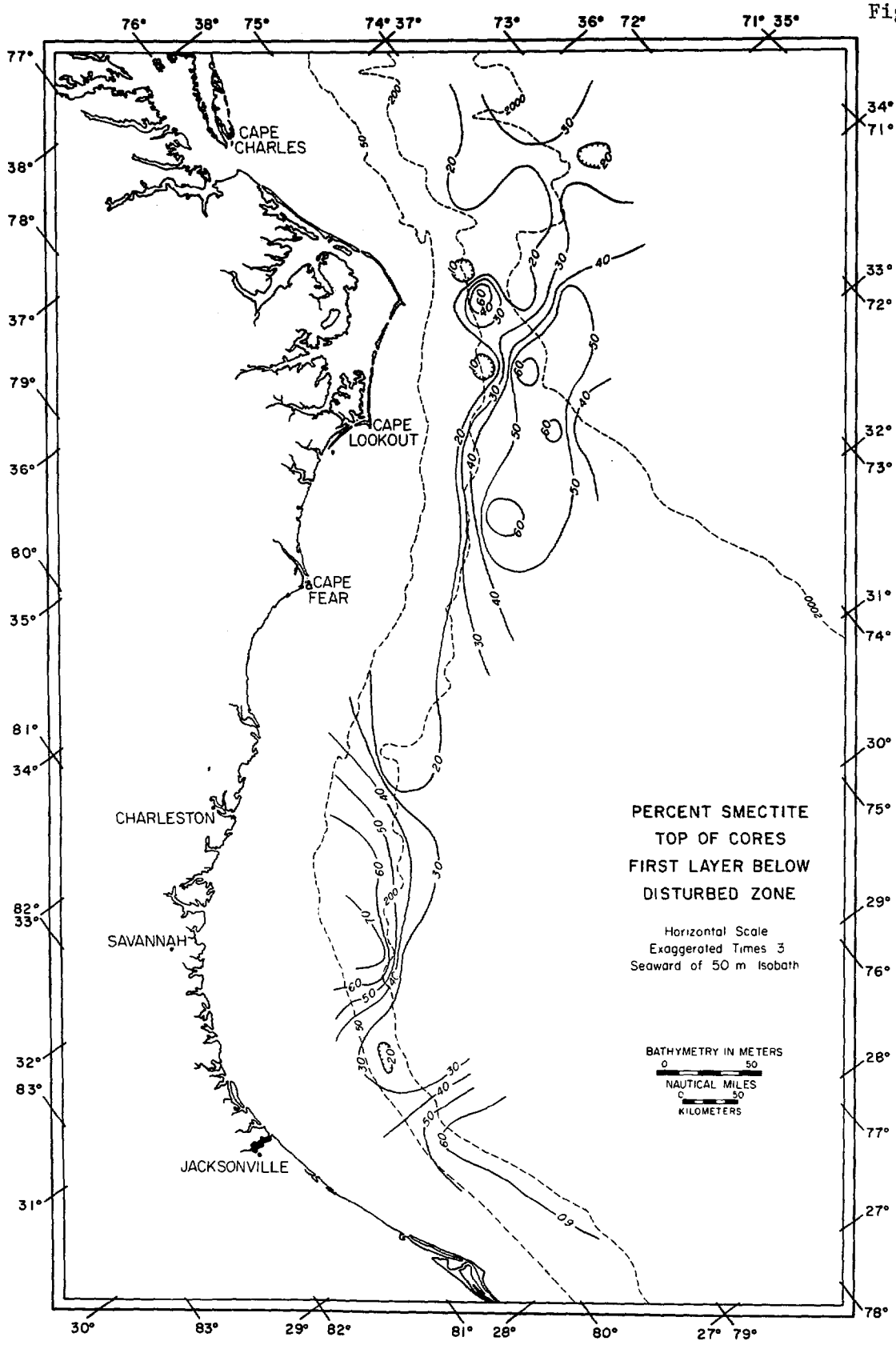
CAPE CHARLES
CAPE LOOKOUT
CAPE FEAR
CHARLESTON
SAVANNAH
JACKSONVILLE
PERCENT SMECTITE
TOP OF CORES
FIRST LAYER BELOW
DISTURBED ZONE
Horizontal Scale
Exaggerated Times 3
Seaward of 50 m Isobath
BATHYMETRY IN METERS
0 50
NAUTICAL MILES
0 50
KILOMETERS

Figure 4-12. Distribution of averaged over the whole core percent smectite. Contour interval 10%.

Figure 4-12

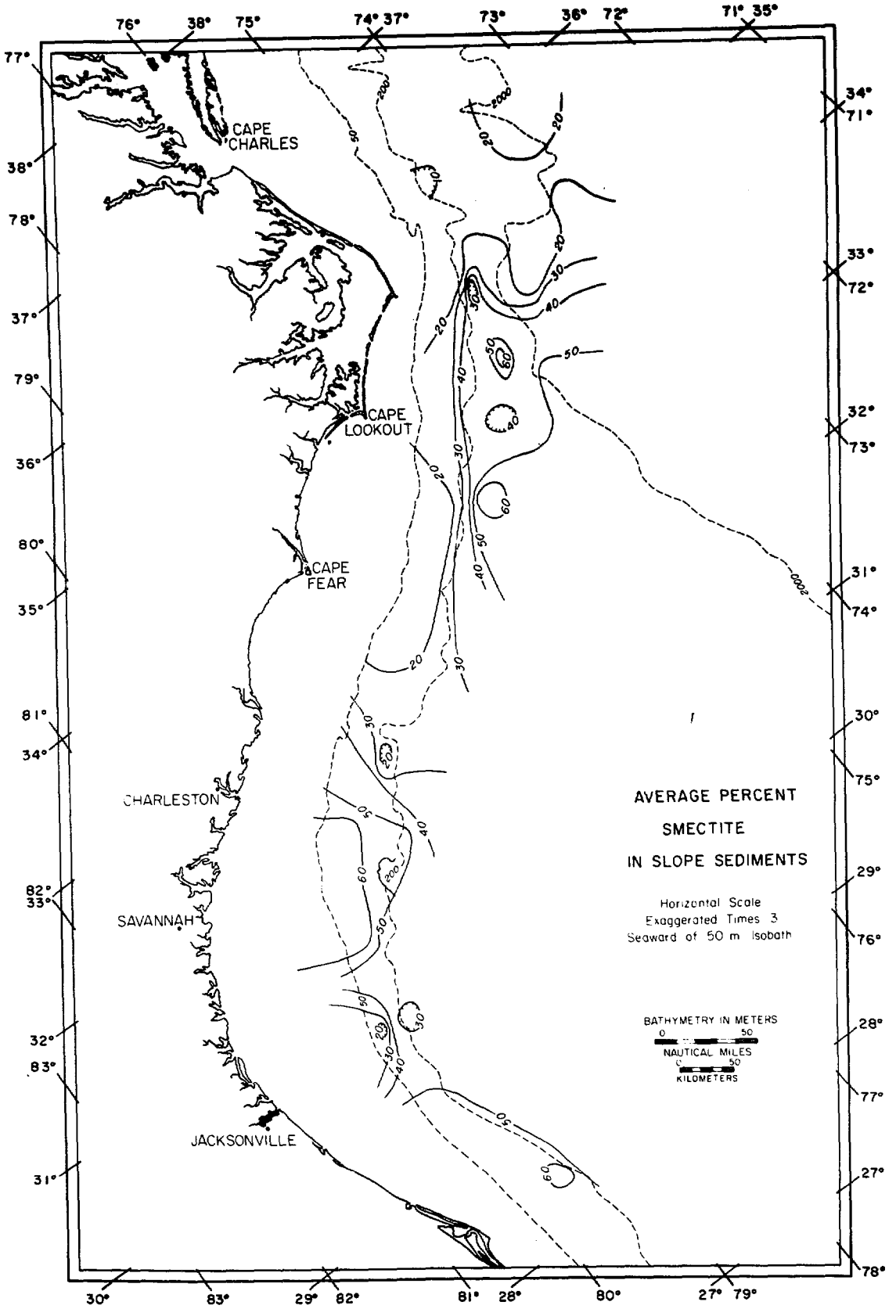
CAPE CHARLES
CAPE LOOKOUT
CAPE FEAR
CHARLESTON
SAVANNAH
JACKSONVILLE
AVERAGE PERCENT
SMECTITE
IN SLOPE SEDIMENTS
Horizontal Scale
Exaggerated Times 3
Seaward of 50 m Isobath
BATHYMETRY IN METERS
0 50
NAUTICAL MILES
0 50
KILOMETERS

Jacksonville corresponding to the high in kaolinite values. Figure 4-12 shows this low increasing seaward and then decreasing again. It further shows a seaward decrease from a high of 60% to a low of 30% in the area south of Jacksonville. Figure 4-11, on the other hand, shows a different pattern, with the low off Jacksonville decreasing to still lower values offshore, while the area to the south of Jacksonville reverses the trend in figure 4-12 and increases from 50% to 60% offshore.

Figure 4-13 shows the detailed distribution of clay minerals and calcium carbonate in cores 24B, 24C, and 24D. In core 24B both illite and calcium carbonate percentages vary little down core with the exception of one low carbonate spike at 190 cm depth. Spikes of kaolinite and smectite mirror each other down core. Down core in 24C carbonate percentages are much more variable than in 24B. All three clay mineral groups also vary considerably. In core 24D, carbonate percentage reduces gradually down core to about 190 cm at which point it increases from 40% to 70% to the end of the core. The three clay mineral groups again all show considerable variation with respect to each other.

DISCUSSION

The break in sedimentary pattern which has been long recognized on the shelf is also present and in some cases even magnified on the slope. Texture, carbonate content, heavy mineralogy, and even clay mineral distribution all reflect this change in sedimentary regime.

While the increase in sand content and in discrete sand layers on the slope south of the Cape is significant, a surprising amount of fine-grained sediment is present on the lower portion of the slope and

Figure 4-13. Detailed distribution of percentages of clay minerals and calcium carbonate in cores 24B, 24C, and 24D.

Figure 4-13

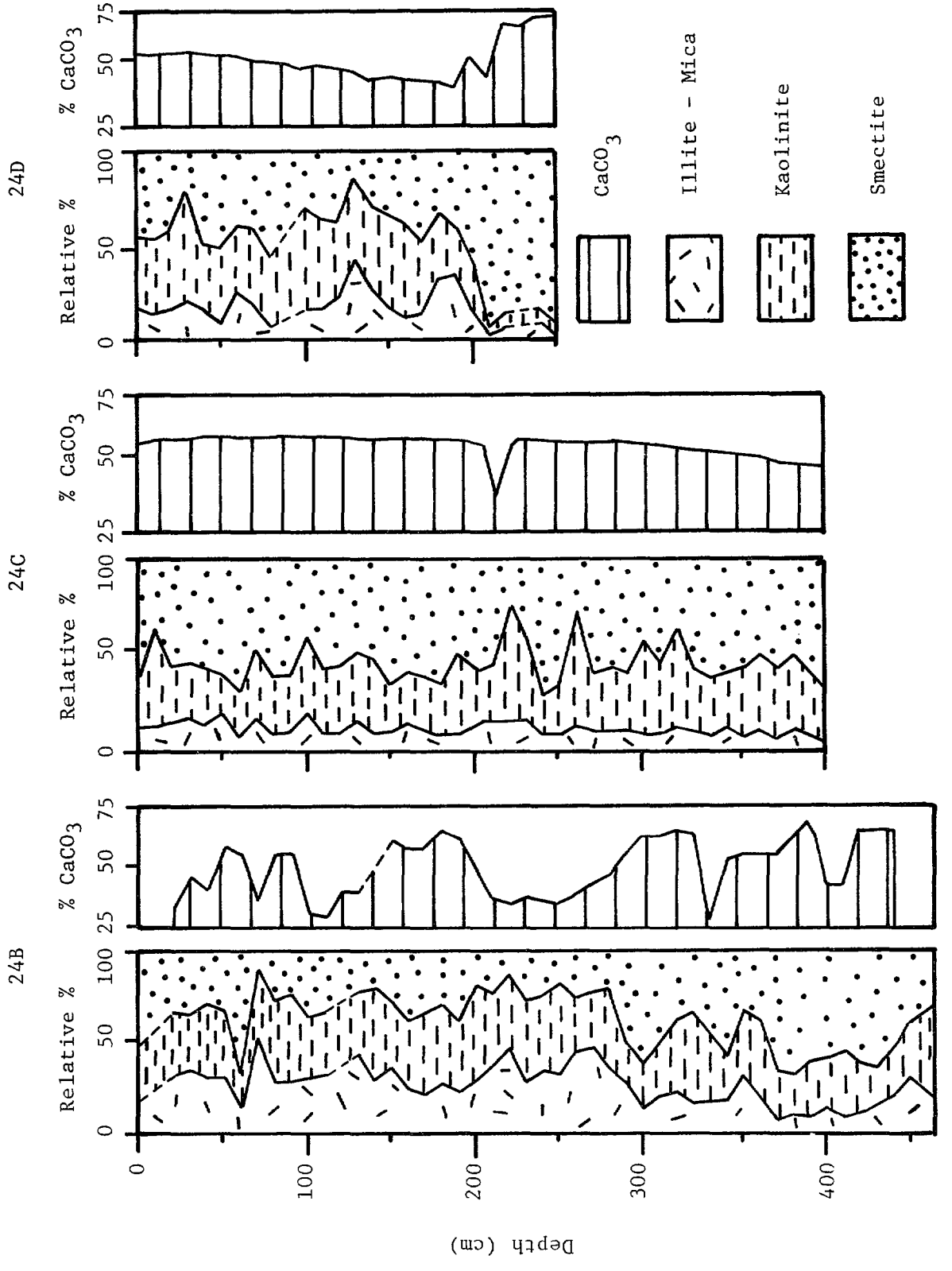
24B
24C
24D
Relative %
% $CaCO_3$
0
50
100
25
50
75
0
100
200
300
400
Depth (cm)
$CaCO_3$
Illite - Mica
Kaolinite
Smectite

on the minirise, considering the vigorous current regime postulated by Bartlett (1883) and finally demonstrated by Pratt (1963) which is sufficiently strong to sweep the surface clean of unconsolidated sediment over deeper portions of the Blake Plateau. Fine sediments probably are sedimented as fecal pellets of much larger size than the individual minerals which make them up. Several fecal pellets are shown in the scanning electron micrographs of suspended sediments of the area (Doyle and others, 1978).

Some sand on the open slope is found in discrete layers with the graded characteristics typical of tubidites. This despite the fact that open continental slopes are commonly thought of as turbidity current generating areas not turbidite depositional areas. While not as common as turbidites in rise and abyssal plain sediments, their presence on the upper slope is a warning that another depositional environment need be considered when turbidites are found in the ancient rock record.

Most of the sand on the southeastern slope is not found in graded sequences; indeed, these are relatively rare. Most, rather, appear to be disseminated throughout the upper few metres of the sediment column. Of particular significance is the abundant shelf-derived component, composed of quartz, an epidote rich heavy mineral suite also containing phosphorite and glauconite, and typical shelf carbonte constituents such as molluscan shell fragments. Distribution of this component combined with the regular decline in sand sizes downslope suggest a relatively steady spillover of sediment from the shelf through time. A much more subdued shelf contribution is suggested for the slope north of Cape Hatteras (Doyle and others, 1979b). Sand may spill over the shelf as the result of storms on the shelf. This process should work both north and south of the Cape. Probably of much more importance on the

southeastern Atlantic margin is the incursion of the Gulf Stream onto the continental shelf. Doyle and others (1979a) in a companion report on the suspended sediments of the region have found evidence that considerable resuspension of bottom sediment occurs at the front between Gulf Stream incursions onto the shelf and shelf water. Some of this resuspension is undoubtedly swept over the shelf break and downslope probably with a concomitant bed load factored in. Spillover and cascading down slope may be relatively more important south of the Cape because, even though fine sediments make up a significant portion of slope and minirise sediments, an appreciable amount must be swept away in the Florida Current.

Pevear (1972) points out that clay mineral suites derived from the Piedmont are dominated by kaolinite, while those derived from the Coastal Plain and continental shelf are dominated by smectite. Biscaye (1965) and Griffin and others (1968) point out that North Atlantic bottom sediments are dominated by illite. Doyle and others (1979b) have pointed out that Piedmont-rising rivers carry most of the sediment brought to the sea in the study area and that Coastal Plain-rising rivers are relatively insignificant in the amount of sediment they carry. The ability to identify provenance by clay mineral suite, especially to distinguish between Piedmont and Coastal Plain/shelf sources is important. Doyle and others (1978) were able to find only kaolinite and illite in the clay mineral suites of suspended sediments in the shelf and slope waters. Pierce and others (1972) found that Virginian Coastal Water covering the shelf north of Cape Hatteras contained chlorite, illite, and traces of kaolinite, that Carolinian Coastal Water covering most of the shelf off North Carolina contained mixtures of smectite, illite, and kaolinite, that the Florida Current

carried very little sediment but that little was mostly kaolinite, and that Carolinian Slope Water carried illite and kaolinite.

Smectite distributions shown in figures 4-11 and 4-12 reinforce the contention that the shelf has supplied a considerable amount of sediment to the slope/minirise and that this system is a potential sink for pollutants, especially if they pass through the food chain and become involved as fecal particles. Shelf winnowing seems to have been particularly effective in the area between Charleston and Savannah. Kaolinite distribution shown in figures 4-9 and 4-10 reinforces the contention of Doyle and others (1979b) that significant amounts of fine sediments brought down by Piedmont rivers are escaping the estuaries and are being deposited on the slope-rise system. Illite as shown in figures 4-7 and 4-8 is an important constituent in the sediments north of Hatteras and of a southern lobe, possibly deposited from Virginian coastal water which occasionally makes incursions around the Cape. The origin of the pocket of high illite/mica content on the slope between Jacksonville and Savannah is not clear, but some illite/mica is brought to the sea by Piedmont-rising rivers as well.

Spikes of kaolinite and smectite shown in figure 4-13 may indicate ascendancy of either a shelf source or Piedmont source back through the past few thousand years. Radio dating needs to be done in order to test this concept.

SUMMARY CONCLUSIONS

Let us review the results of our study to date by examining what we can conclude about the four problems we set out to investigate.

1. What are the characteristics of southeastern United States Atlantic slope sediments?

The upper few metres of sediments in this region are sands to muds, the latter having significant proportions of sand, silt, and clay even on the lower portions of the minirise. Sands are similar in most respects to those on the adjacent shelf, with a component of planktonic foraminifera added and becoming increasingly important downslope. Some turbiditelike sand layers are present. Total organic carbon content is high near the surface, over 1.5%, and normally decreases to about 0.5% at 400 cm down core. Some sediments are gassy, probably with methane the chief contributor, and in these sediments, total organic carbon content remains above 1% all the way down the core. There is a major break in sand content, carbonate content, and mineralogy around Cape Hatteras which parallels that which has been long recognized on the adjacent shelf.

2. What are the principal sedimentary processes which operate on the slope?

It is clear from the amount and composition of the sand in the cores that a significant amount of bed load spillover from the shelf occurs, probably as a result of storms and interaction between Gulf Stream incursions with shelf water. In addition these processes resuspend fine sediment which through fecal pellet formation combine with a rain of planktonic foraminifera to form a hemipelagic component of sedimentation. The Florida Current must act to winnow away unconsolidated fines, especially those brought into it from the shelf.

3. What is the role and relationship of the adjacent continental shelf in furnishing sediment to the slope?

The shelf is and has been an important source for fine and sand-sized sediments to the continental slope. It also acts as a zone of flux over which passes a sedimentary complement ultimately derived

from Piedmont-rising rivers.

4. Is the slope a potential pollutant sink?

In short, yes. The presence of a significant fine fraction in southeastern slope sediments and the fact that they are derived from shelf winnowing and bypassing from the nearshore suggest that pollutants which become involved with them will also be deposited. Fecal pellet formation and resultant rapid sedimentation may serve to magnify the process.

REFERENCES CITED

Bartlett, J.R., 1883, Deep-sea soundings and temperatures in the Gulf Stream off the Atlantic coast: Proc. Amer. Ass. Adv. Sci., v. 31, p. 1-4.

Biscaye, P.E., 1965, Mineralogy and sedimentation of recent deep-sea clay in the Atlantic Ocean and adjacent seas and oceans: Geol. Soc. Am. Bull., v. 76, p. 803-832.

Carver, Robert E., ed., Proceedings in sedimentary petrology: New York, Wylie, Interscience, 653 p.

Doyle, L.J., Betzer, P.R., Peacock, M.A., and Wall, F., 1978, Seston of the southeast Georgia Embayment: Final Report to USGS, Contract No. 14-08-0001-15681, 72 p.

Doyle, L.J., Betzer, P.R., Clayton, Z., and Peacock, M.A., 1979a, Seston composition, pathways, and flux in the Georgia Embayment: Final Report to USGS, Contract No. 14-08-0001-15681.

Doyle, L.J., Pilkey, O.H., and Woo, C.C., 1979b, Sedimentation on the eastern United States continental slope, in Doyle, L.J., and Pilkey, O.H., eds., Geology of Continental Slopes: SEPM Spec. Pub. 27, 365 p.

Emery, K.O., and Uchupi, E., 1972, Western North Atlantic Ocean: Topography, rocks, structure, water, life, and sediments: Am. Assoc. Petroleum Geol. Memoir 17, 532 p.

Folk, R., and Ward, W.C., 1957, Brazos river bar, a study in the significance of grain size parameters: Jour. Sed. Petrology, v. 27, p. 3-27.

Gorsline, D.S., 1963, Bottom sediments of the Atlantic shelf and slope off the southern United States: Jour. Geology, v. 71, p. 422-440.

Griffin, G.M., 1962, Regional clay-mineral facies-products of weathering intensity and current distribution in the northeastern Gulf of Mexico: Geol. Soc. Am. Bull. v. 73, p. 737-768.

Griffin, J.J., Windom, H., and Goldberg, E.D., 1968, The distribution of clay minerals in the world ocean: Deep-Sea Res., v. 11, p. 433-439.

Grim, R.E., 1968, Clay Mineralogy: New York, McGraw-Hill, 596 p.

Hathaway, J.C., 1973, Regional clay mineral facies in estuaries and the continental margin of the United States east coast, in Nelson, B.W., ed., Environmental Framework of Coastal Plain Estuaries: Geol. Soc. Am. Memoir 133, p. 293-317.

Inman, D.L., 1952, Measures for describing the size distribution of sediments: Jour. Sed. Petrology, v. 22, p. 125-145.

Milliman, J.D., Pilkey, O.H., and Ross, D.A., 1972, Sediments of the continental margin off the eastern United States: Geol. Soc. Am. Bull., v. 53, p. 1315-1334.

Pevear, D.R., 1972, Source of recent nearshore marine clays, southeastern United States, in Nelson, B.W., ed., Environmental Framework of Coastal Plain Estuaries: Geol. Soc. Am. Memoir 133, p. 317-335.

Pierce, J.W., Nelson, D.D., and Colquhoun, D.J., 1972, Mineralogy of

suspended sediment off the southeastern United States, in Swift, D.J.P., Duane, D.B., and Pilkey, O.H., eds., Shelf Sediment Transport Process and Pattern: Stroudsburg, Pennsylvania, Dowden, Hutchinson & Ross, p. 282-306.

Pratt, R.M., 1963, Bottom currents on the Blake Plateau: Deep-Sea Res. v. 10, p. 245-249.

CHAPTER 5

PISTON CORE AND SURFICIAL SEDIMENT INVESTIGATIONS OF THE FLORIDA-HATTERAS SLOPE AND INNER BLAKE PLATEAU

Mark W. Ayers[1] and Orrin H. Pilkey[1]

[1]U.S. Geological Survey, Woods Hole, Massachusetts 02543 and Duke University, Durham, North Carolina 20776

CHAPTER 5

Table of Contents

Page

Abstract. 5- 1

Introduction. 5- 2

Background. 5- 2

Origin and stratigraphy of the Florida-Hatteras Slope 5- 2

Oceanic currents. 5- 9

Methods 5-10

Results 5-17

Sediment texture. 5-17

Calcium carbonate content 5-17

Sedimentary structures. 5-24

Shallow core stratigraphy 5-36

Surficial sediments of the Florida-Hatteras Slope and inner Blake Plateau 5-42

Corals on the Blake Plateau 5-55

Slump mass on the lower Florida-Hatteras Slope. 5-63

Discussion. 5-76

Origin of the coral banks on the Blake Plateau. 5-76

Sedimentation on the Florida-Hatteras Slope and inner Blake Plateau 5-79

Conclusions: Potential hazards implied by this study 5-84

References cited. 5-86

CHAPTER 5

PISTON CORE AND SURFICIAL SEDIMENT INVESTIGATIONS OF THE FLORIDA-HATTERAS SLOPE AND INNER BLAKE PLATEAU

Mark W. Ayers and Orrin H. Pilkey

ABSTRACT

Forty-two piston cores ranging from two to six metres in length and 200 surficial sediment samples have been recovered from the Florida-Hatteras Slope and inner Blake Plateau. A study of sediment composition and texture in these cores and samples reveals the nature of deposition in the upper few metres of sediment cover on the slope and the inner plateau. Slumping and density current deposition both occur on the slope. The dominant source of slope sediment is shelf-edge spillover which is an active present-day process. This spillover is initiated by high wave energy during storms and, more importantly, by erosion generated at the front between incursions of the Florida Current and Carolinian Shelf Water.

Only one slump mass has been observed on the Florida-Hatteras Slope. It covers an area of 135 km^2, has a volume of 1.3×10^8 m^3 and is located at the base of the slope between the 400 and 500 metre isobaths. Radiometric ages suggest slumping occurred since late Pleistocene time.

In contrast to the Florida-Hatteras Slope, sediments being deposited on the inner plateau today are mainly residual or biogenic. The residual sediments are derived from pre-Holocene units that outcrop or subcrop on the inner plateau. Biogenic sediments are derived by normal pelagic processes or from the extensive coral banks that cover the plateau.

INTRODUCTION

On Eastward cruise E-2E-78, a suite of piston cores and rock dredges was recovered from the Florida-Hatteras Slope and inner Blake Plateau (fig. 5-1). The suite of 43 cores was studied in order to determine sedimentary structures, textures, and composition. Additionally, radiocarbon dates of corals and foraminifera in the cores were obtained to determine the ages and rates of deposition of the sediment. To our knowledge, this is the first comprehensive piston core coverage of the region. These cores present an excellent opportunity to better understand the recent history of sedimentation on the lower slope and inner plateau.

The areal distribution of surficial sediment types on the outer shelf, slope, and inner plateau was also determined by the study of over 200 surface samples (fig. 5-2) from a preexisting collection at Duke University. Texture, color, and composition of the surface samples were studied. The objective of this part of the investigation was to assess the sources of the sediment presently being deposited in the study area.

BACKGROUND

Origin and Stratigraphy of the Florida-Hatteras Slope

Extensive coverage of the Florida-Hatteras Slope and inner Blake Plateau with single-channel air-gun seismic-reflection data (Paull and Dillon, 1979) and high-resolution sparker data (Edsall, 1979) have made it possible to establish the regional stratigraphy. Cretaceous and Paleocene strata here are flat, indicating that the slope did not exist before Late Paleocene time (Paull and Dillon, 1979). With initiation of the Gulf Stream into the region during the Late Paleocene, a regional

Figure 5-1. Location map of rock dredge (circles) and piston core (dots) sites in the study area. The base map is a compilation of a geologic map from Edsall (1979) and a series of N.O.S. bathymetric charts of the Blake Plateau (contoured in metres). The pre-Holocene units which appear to outcrop in the seismic profiles may actually be blanketed by an acoustically transparent cover of Holocene sediment.

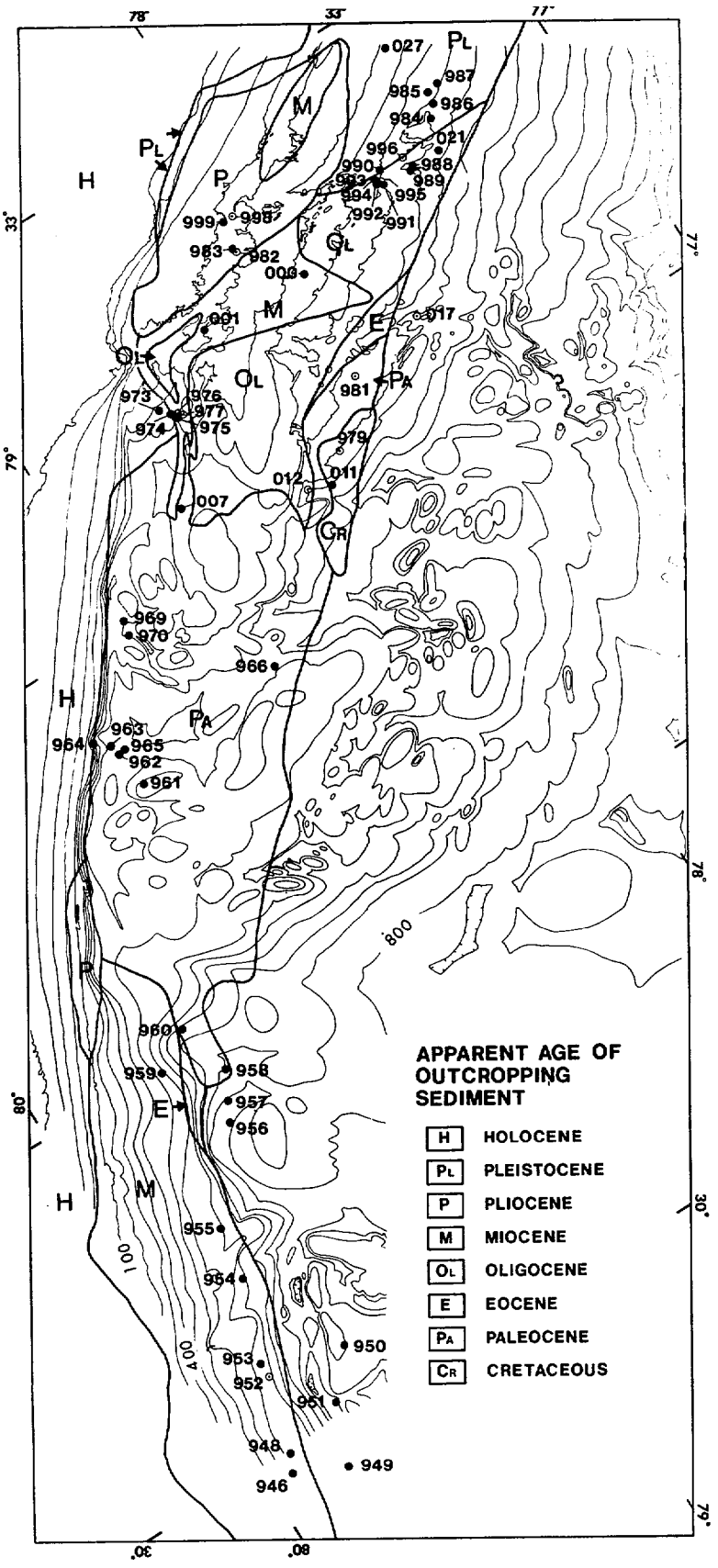
APPARENT AGE OF OUTCROPPING SEDIMENT
H HOLOCENE
PL PLEISTOCENE
P PLIOCENE
M MIOCENE
OL OLIGOCENE
E EOCENE
PA PALEOCENE
CR CRETACEOUS
800
100
400

Figure 5-2. Locations of surficial samples used in this study are shown by black dots. The shelf break and base of slope are from Edsall (1979). Arrows indicate the main courses of major oceanic currents that flow over the study area (from Hollister, 1973; Uchupi, 1967).

Figure 5-2

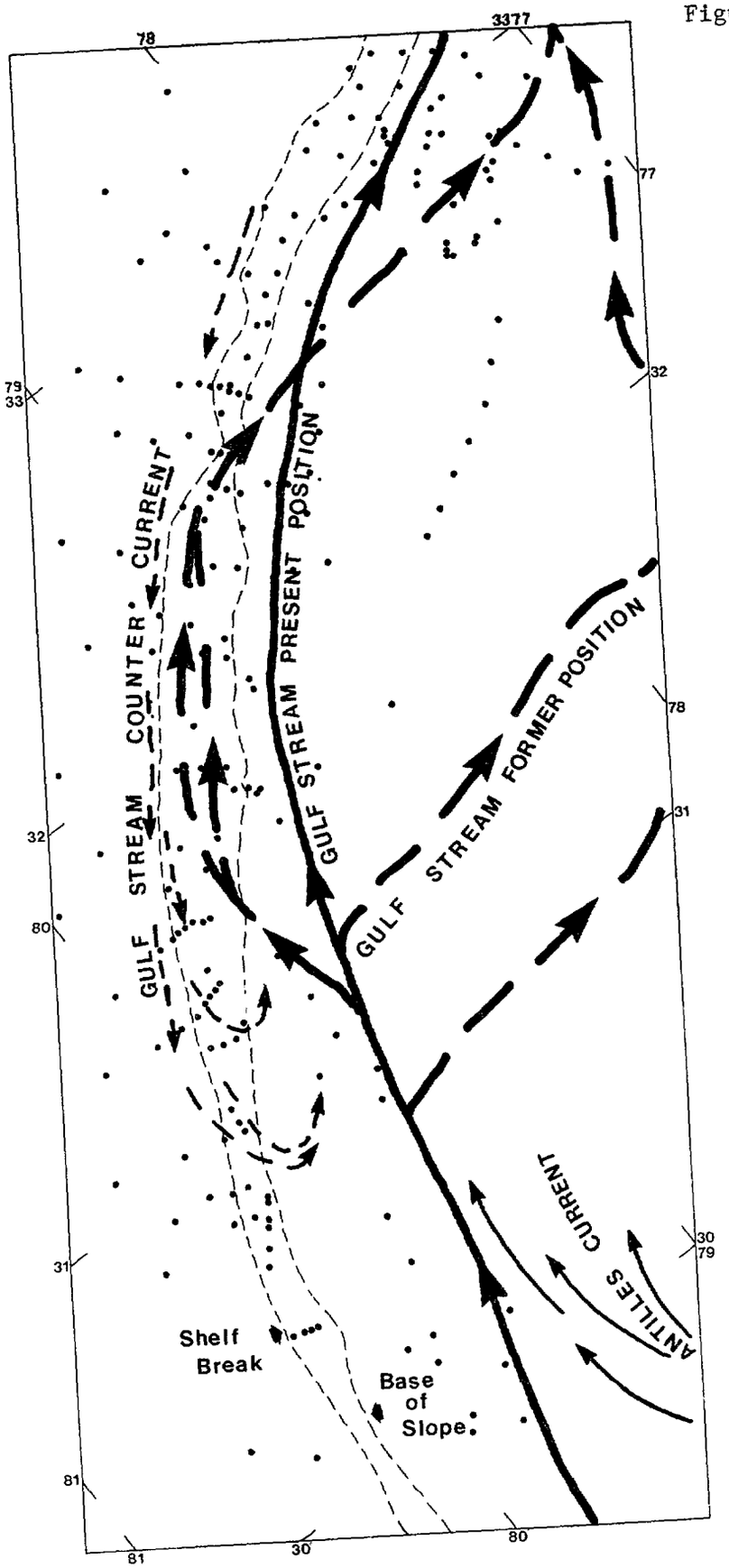
GULF STREAM COUNTER CURRENT
GULF STREAM PRESENT POSITION
GULF STREAM FORMER POSITION
ANTILLES CURRENT
Shelf Break
Base of Slope
78
3377
77
79
33
32
78
31
32
80
31
30
79
81
81
30
80

unconformity developed on the flat plateau along the present position of the Florida-Hatteras Slope. A large seaward progradational wedge buried much of this Paleocene unconformity. Progradation stopped at the end of the Oligocene as a result of renewed Gulf Stream erosion. This Oligocene erosional surface has in turn been buried by progradation of the shelf-slope system from Miocene to recent times. Post-Miocene erosion has selectively eroded and modified parts of the latest progradation wedge even though progradation has continued along many parts of the slope (Edsall, 1979).

Using high-resolution sparker profiles, Edsall (1979) has mapped sedimentary strata of the Florida-Hatteras Slope and inner Blake Plateau. Figure 5-1 shows his interpretation of the ages of strata that outcrop on the lower slope and inner plateau. In order to have some idea of the age of the major acoustic units, the seismic lines were tied into JOIDES and AMCOR drill holes on the continental shelf, the Florida-Hatteras Slope, and the Blake Plateau (Edsall, 1979; Paull and Dillon, 1979). These drill holes also provide some knowledge of the lithologic character of the outcropping units on the lower slope and inner plateau.

Poag (1978) has reviewed the lithologies of strata recovered from drill holes on the plateau and slope. The oldest rocks recovered from the Blake Plateau are Lower Cretaceous. Cretaceous sediments in the study area are composed mainly of chalky calcilutites, oolitic calcarenites, and calcarenites containing abundant foraminifera and algal fragments. Paleocene strata in the study area range from calcareous clays and limestones to greenish-gray, calcareous clays and shales. On the slope the Eocene-age deposits are primarily gray calcareous clays while the Eocene deposits recovered from the plateau

are light gray calcilutites. Oligocene strata under the shelf and plateau consist of olive-green to gray calcilutites and silty clays. The Miocene strata in the study area are composed of olive-gray to pale tan clays and foraminiferal calcarenites and calcilutites. Pliocene strata here consist of light olive-gray calcarenites and homogeneous, tan, foraminiferal calcilutites. On the slope Pleistocene sediments are yellowish or olive-gray calcarenites composed of foraminiferal and molluscan fragments with smaller amounts of silty clay. Pleistocene sediments on the plateau are bathyally derived grayish-yellow or brownish foraminiferal calcarenites and calcilutites.

Detailed sediment analyses of JOIDES cores (Charm and others, 1969) taken in the study area give an idea of the sedimentary petrology of these various strata. Holocene, Pleistocene, and Pliocene sections of the JOIDES cores were undifferentiated and lumped together into a post-Miocene section. Samples from this section contained from 5 to 50% coarse material (>63 m). The coarse fraction is mainly composed of foraminiferal sand (up to 90%). The remainder of the coarse fraction is composed of phosphate pellets (<1%), glauconite (<1-10%), nonforaminiferal biogenic debris (10-15%), and quartz (>0-60%). Quartz contents are highly variable but they usually comprise less than 30% of the coarse fraction. Glauconite content increases toward the base of the section.

JOIDES (J-5, J-6) drill holes on the Florida-Hatteras Slope and inner Blake Plateau contained no Miocene sediments. In order to determine the petrology of the Miocene strata, we must examine a hole drilled on the outer shelf which recovered 230 metre thick Miocene section. Bioclastic debris in the Miocene occurs in lower percentages than in the overlying and underlying strata occasionally comprising <5%

of the total coarse fraction. Quartz in the coarse fraction ranges from 5% to >60%, although it frequently occurs in quantities >60%. Phosphorite pellets comprise >60% of the coarse fractions from the early Miocene section. These phosphorite pellets occur throughout the section but in the upper section they comprise <1% of the coarse fraction. Phosphorite gravels were not recovered from this JOIDES hole. However, evidence suggests phosphorite gravels on the Blake Plateau are Miocene in age (Manheim and others, 1979). Glauconite in the Miocene section occurs in quantities of 5% or less.

Oligocene and Eocene strata on the slope and plateau consist of intercalated gray foraminiferal muds and consolidated limestone beds. Beds range from one-third to 1 metre in thickness. The limestone is massive and recrystallized containing broken shell fragments. The foraminiferal muds contain from 1-10% coarse material (>63μm) that is comprised of foraminifera, echinoderm plates and spines, ostracods, and siliceous sponge spicules. In the Oligocene and upper Eocene section, the terrigenous components are more abundant. Quartz, mica, and heavy minerals occur in quantities as great as 30%. Phosphorite pellets and glauconite are not generally abundant in this section (usually <1%) although in a few samples these two comprise from 5-10% of the coarse fraction.

Oceanic Currents

By far the most important factor affecting sedimentation on the inner Blake Plateau is the Gulf Stream. Surface velocities of the Gulf Stream have been measured at more than 180 $cm.s^{-1}$ (Edsall, 1979). Pratt (1966) has shown that because of the influence of the Gulf Stream analogies can be drawn between the surface of the Blake Plateau and the bed of a graded river system. Uchupi (1967) and Stetson and others

(1969) describe the erosive role the Gulf Stream has played shaping the surface of the Blake Plateau. The Gulf Stream Counter Current and the Antilles Current also influence deposition on the slope and plateau (Hollister, 1973)(fig. 5-2).

Directions and velocities of bottom currents on the Blake Plateau and Florida-Hatteras Slope have been measured directly with instruments (Pratt, 1963; Hawkins, 1969) and indirectly by the study of current lineations in seafloor photographs (Heezen and Hollister, 1971). Forty $cm.s^{-1}$ is the highest bottom current velocity measured on the Blake Plateau (Pratt, 1963).

The first observable effects of the Gulf Stream on the inner Blake Plateau and Florida-Hatteras Slope occurred in the late Paleocene (Paull and Dillon, 1979). Since that time the main course of the Gulf Stream has shifted across the plateau a number of times (Uchupi, 1967). Much more ephemeral changes in the course of the Gulf Stream occur today. Observations of the stream's main course show it meanders constantly (Iselin, 1940). Incursions of the Gulf Stream onto the continental shelf have been documented (Hunt and others, 1975). Large eddy currents form along the eastern margin of the Gulf Stream (Iselin, 1940). Warren (1967) observed one of these eddy currents that became detached and flowed away from the main course of the Gulf Stream in a counterclockwise, circular motion with internal velocities as high as 200 $cm.s^{-1}$.

METHODS

During a 10-day Eastward cruise (E-2E-78) 32 unlined and 10 lined piston cores were recovered from the Florida-Hatteras Slope and inner Blake Plateau. The cores were taken with a modified Ewing piston

corer.[1] At some sites coral and phosphorite gravels prevented successful coring with a 20 foot core pipe. In those circumstances a 10 foot core pipe was substituted. Even with the shorter pipe, coring was occasionally unsuccessful. Upon recovery the unlined cores were split, described, and subsampled. After recovery lined cores were capped and stored for later analysis in shore-based laboratories. Both lined and unlined cores were subsampled at five foot intervals immediately after recovery to determine their light hydrocarbon content and to extract interstitial fluids.

Once back in the shore-based laboratory, the lined cores were split, described, and subsampled. Slabs 1 to 2 cm thick and 20 cm long were cut from select sections in both the lined and unlined cores. These slabs were X-rayed to determine the sedimentary structures. Suitable subsamples of coral gravel and foraminiferal sands were taken from the cores and sent to the University of Miami Geochronology Laboratory for radiocarbon dating (table 5-1). Select subsamples were also age-dated by their foraminiferal assemblages (table 5-2).

Select subsamples from the cores were analyzed to determine texture and composition. The subsamples were first dispersed in a 10% solution of Calgon. Muds were removed from the dispersed sediment by wet sieving with a 63μm diameter sieve. The percentages of silt and clay in the mud fractions were determined by pipette using a technique described in Folk (1974). Textures of the coarse fractions of the piston core subsamples were determined by sieving. The results of the sieve and pipette analyses were plotted on probability paper and Folk's (1974) graphic

---

[1]Use of brand names in this report is for descriptive purposes only and does not constitute endorsement by the U.S. Geological Survey.

Table 5-1. Radiocarbon dates of sediment from the Florida-Hatteras Slope.

Sample #	Radiocarbon Age Years B.P.	Material Dated
949, 30-50 cm	$16,180^{+420}_{-400}$	coral
949, 400 cm	$26,000^{+1,750}_{-1,440}$	coral
950, 20-40 cm	$17,255 \pm 170$	coral
950, 100 cm	$26,170^{+430}_{-410}$	coral
952, surface	$4,740 \pm 80$	coral (Mn? stained)
952, surface	$27,810^{+440}_{-420}$	coral
959, 0-5 cm	$37,140^{+2,060}_{-1,640}$	coral
959, 25-30 cm	$37,430^{+2,800}_{-2,070}$	coral
959, 100-105 cm	$38,970^{+2,460}_{-1,880}$	coral
959, 200-258 cm	$37,900^{+2,830}_{-2,090}$	coral
959, 414-433 cm	$35,170^{+1,200}_{-1,040}$	coral
959, 460-475 cm	$35,400^{+840}_{-760}$	coral
959, 531-540 cm	$44,040^{+3,700}_{-2,500}$	coral
969, 10-15 cm	$31,290^{+870}_{-790}$	calcareous mud with foraminifera
970, 20 cm	$20,225^{+2,000}_{-1,600}$	calcareous mud with foraminifera
987, 25-40 cm	$28,770^{+860}_{-775}$	foram sand
989, 20-40 cm	$38,965^{+1,940}_{-1,560}$	foram sand
16154*, surface	680 ± 65	living *Lophelia prolifera* (coral), collected 1886

*Smithsonian sample from location 29°24′N., 79°43′W.

Table 5-2. Foraminiferal assemblages used to determine the ages of selected Florida-Hatteras Slope samples. Identifications and age determinations by C. Wiley Poag.

Sample #	Age	Assemblage
34953, 190-200 cm	Late Pliocene	*Globorotalia miocenica* *Globorotalia pertenuis* *Globoquadrina altispira* *Globigerinoides obliquus extremus*
34960, 473-478 cm	Late Pleistocene?	*Globigerinoides ruber* (pink) "*Globigerina*" *rubescens* (pink) *Globorotalia ungulata* (abundant) abundant pteropods
34975, 248-245 cm	Middle Miocene	*Globigerinoides sicanus* *Globorotalia sialensis* *Globoquadrina dehiscens advena* *Globoquadrina altispira* *Globigerinoides glomerosa* group

statistics were calculated (Appendix 5-1, pocket in back cover). Three repetitive sieve analyses of a single subsample were performed in order to estimate the precision of the analytical technique (table 5-3). Textures of the surficial subsamples were determined by examination and comparison with known samples using a binocular microscope.

Dried splits of the select subsamples were treated with a 10% HCl acid solution to determine the weight percentage of $CaCO_3$. The weight percent $CaCO_3$ was calculated as the percentage of weight loss by dissolution.

Constituent compositions of the sand fractions from select piston core subsamples and surficial samples were determined by grain counts. The sand fractions were split and mounted on micropaleontological slides for counting. Three hundred grains from each sample were counted and identified using reflected light and a binocular microscope. Three replicate constituent analyses of a single coarse fraction were performed to evaluate the precision of the technique (table 5-4). Because of difficulty in distinguishing dark glauconite from phosphorite, any suspect grains were treated with a molybdic solution (Charlot, 1965). A yellow precipitate forms when the molybdic solution is applied to phosphorite. X-ray diffraction techniques were used to determine the mineral composition of 20 select mud fractions. The samples were mounted in unoriented backpacked powder slides and X-rayed from 3 to 76 degrees two theta. The results of the analyses indicate the mud fractions are mineralogically very similar. Two samples contained small amounts of kaolinite. With those exceptions the samples contained only the minerals quartz, calcite, and aragonite.

Seismic profiles were taken using a 10 in^3 air gun in order to obtain high resolution. Bottom profiles were taken continuously along

Table 5-3. Results of three replicate textural analyses of a single sample. Results are shown in phi-values. The purpose of this table is to demonstrate the precision of the analytical technique.

Textural Parameters	Analysis		
	A	B	C
Median	2.0	2.0	2.0
Mean	3.5	3.4	3.3
Standard Deviation (sorting)	4.9	5.0	5.0

Table 5-4. Replicate grain counts of the sand fraction (63 μm-2 mm) from a single sample made to illustrate the precision of the analytical technique. Three hundred grains were counted in each analysis. The results are expressed here as percent constituents.

Constituent	Percentage		
	Count 1	Count 2	Count 3
Quartz	3	3	5
Spicules	2	1	1
Planktonic Foraminifera	73	75	75
Benthonic Foraminifera	3	5	2
Phosphorite	1	1	1
Glauconite	3	2	3
Pteropods	2	1	2
Gastropods	3	3	2
Indeterminates	3	4	2
Coral	3	3	2
Echinoids	<1	<1	0
Undifferentiated Shell fragments	4	2	4

the entire ship's track using a 12-kHz transducer as a sound source. Loran-C and satellite navigation were used for positioning.

RESULTS

Sediment Texture

Sieve and pipette techniques were used to determine the texture of select piston core subsamples. Results of these analyses are shown in Appendix 5-1. Cores recovered from coral banks contained the most poorly sorted sediment (fig. 5-3). Plateau sediments were the coarsest and best sorted reflecting the influence of strong bottom currents on the plateau. The lower slope sediments were sorted to varying degrees but were typically finer than plateau and coral bank deposits.

It is important to note the highly variable textures of the sediments in individual cores (fig. 5-4). This variability can best be explained by dramatic changes in the bottom current regime throughout the time span represented in the cores. In figure 5-4 this marked degree of variability is illustrated by comparing the textures of sediment in the inner plateau cores with the textures in surficial sediments being deposited today under various prevailing bottom current regimes (Hollister, 1973).

Calcium Carbonate Content

The weight percentage of calcium carbonate was determined in select subsamples from ten cores recovered from the inner Blake Plateau. Downcore trends in the percentage of calcium carbonate often reflect regional changes in the relative contribution of terrigenous sediment and biogenic pelagic debris. A lack of downcore trends in the percent calcium carbonate in the inner plateau cores (fig. 5-5) indicates that no detectable regional change in the relative contribution of biogenic

Figure 5-3. Mean grain size vs. sorting in select piston core subsamples. Cores were recovered from the coral banks on the Blake Plateau (I), from the inner Blake Plateau (II), and from the lowermost Florida-Hatteras Slope (III).

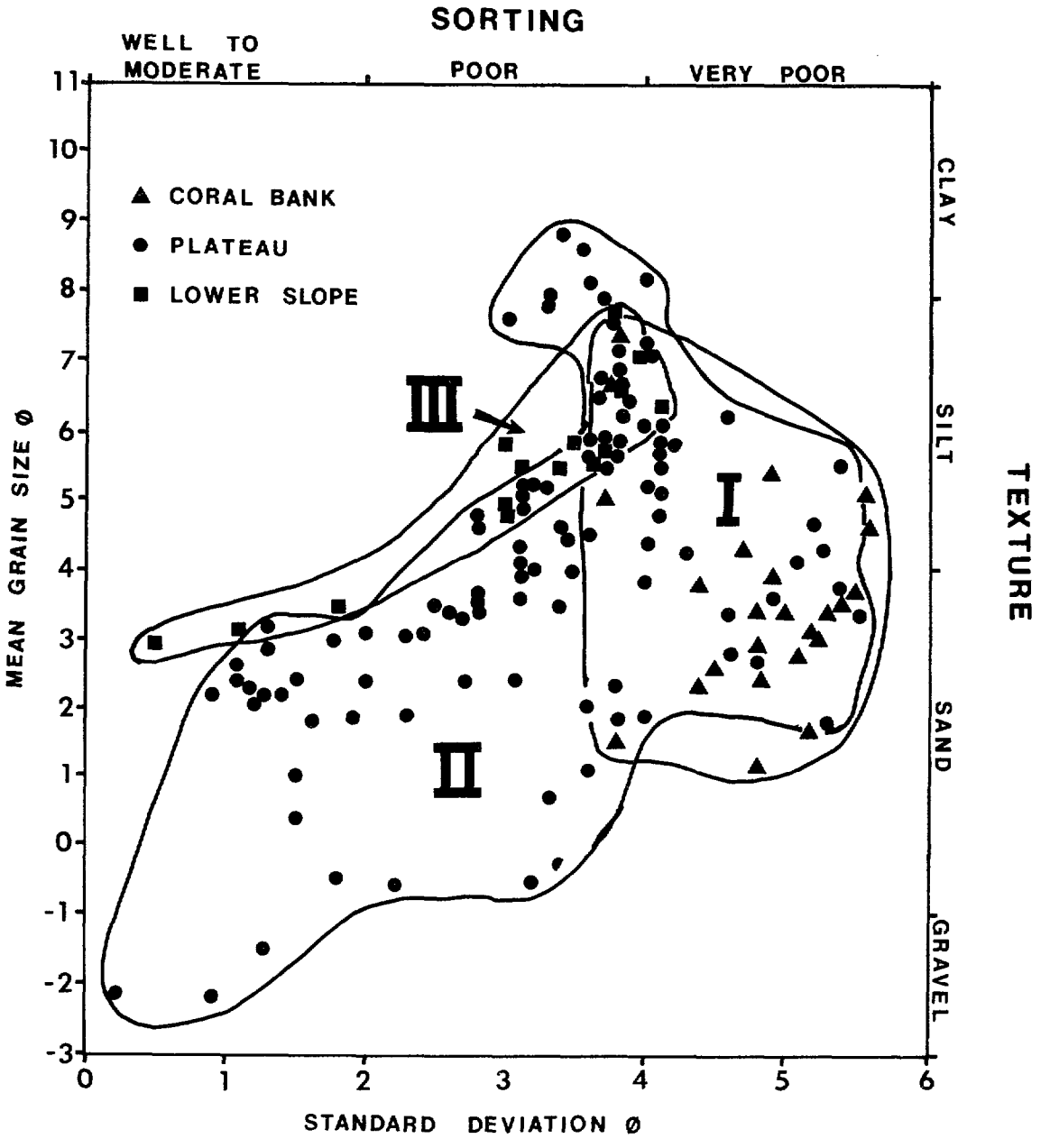
SORTING
WELL TO MODERATE
POOR
VERY POOR
CORAL BANK
PLATEAU
LOWER SLOPE
III
I
II
MEAN GRAIN SIZE Ø
STANDARD DEVIATION Ø
CLAY
SILT
SAND
GRAVEL
TEXTURE
11
10
9
8
7
6
5
4
3
2
1
0
-1
-2
-3
0
1
2
3
4
5
6

Figure 5-4. Mean grain size vs. sorting of select subsamples from six individual piston cores. The square outlines show the range in textures of surficial sediments on the eastern U.S. continental margin that are influenced by different bottom current regimes (as determined by Hollister, 1973).

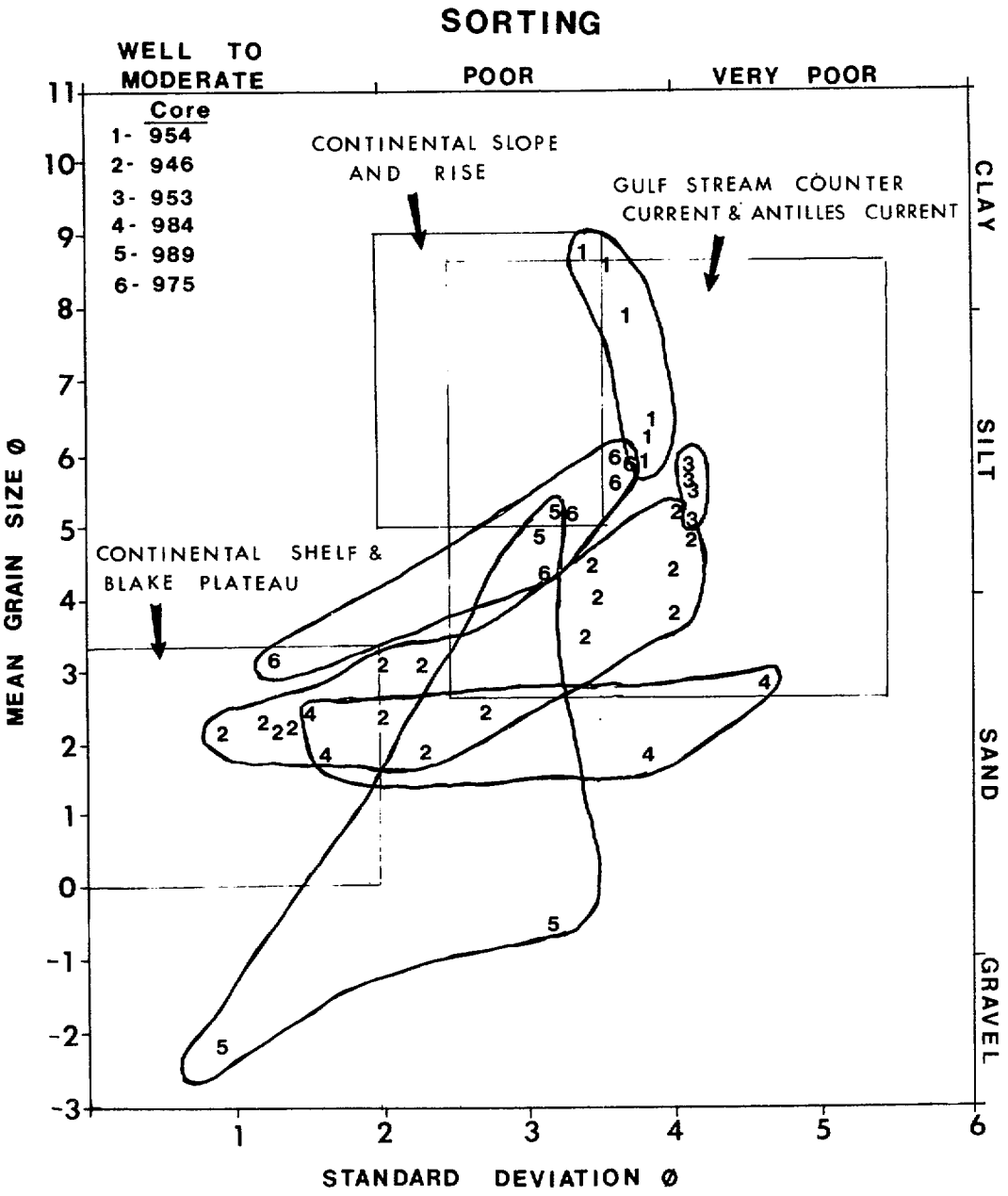
SORTING
WELL TO MODERATE
POOR
VERY POOR
Core
1- 954
2- 946
3- 953
4- 984
5- 989
6- 975
CONTINENTAL SLOPE AND RISE
GULF STREAM COUNTER CURRENT & ANTILLES CURRENT
CONTINENTAL SHELF & BLAKE PLATEAU
MEAN GRAIN SIZE Ø
STANDARD DEVIATION Ø
CLAY
SILT
SAND
GRAVEL

Figure 5-5. Percent calcium carbonate in select subsamples from 10 inner Blake Plateau piston cores.

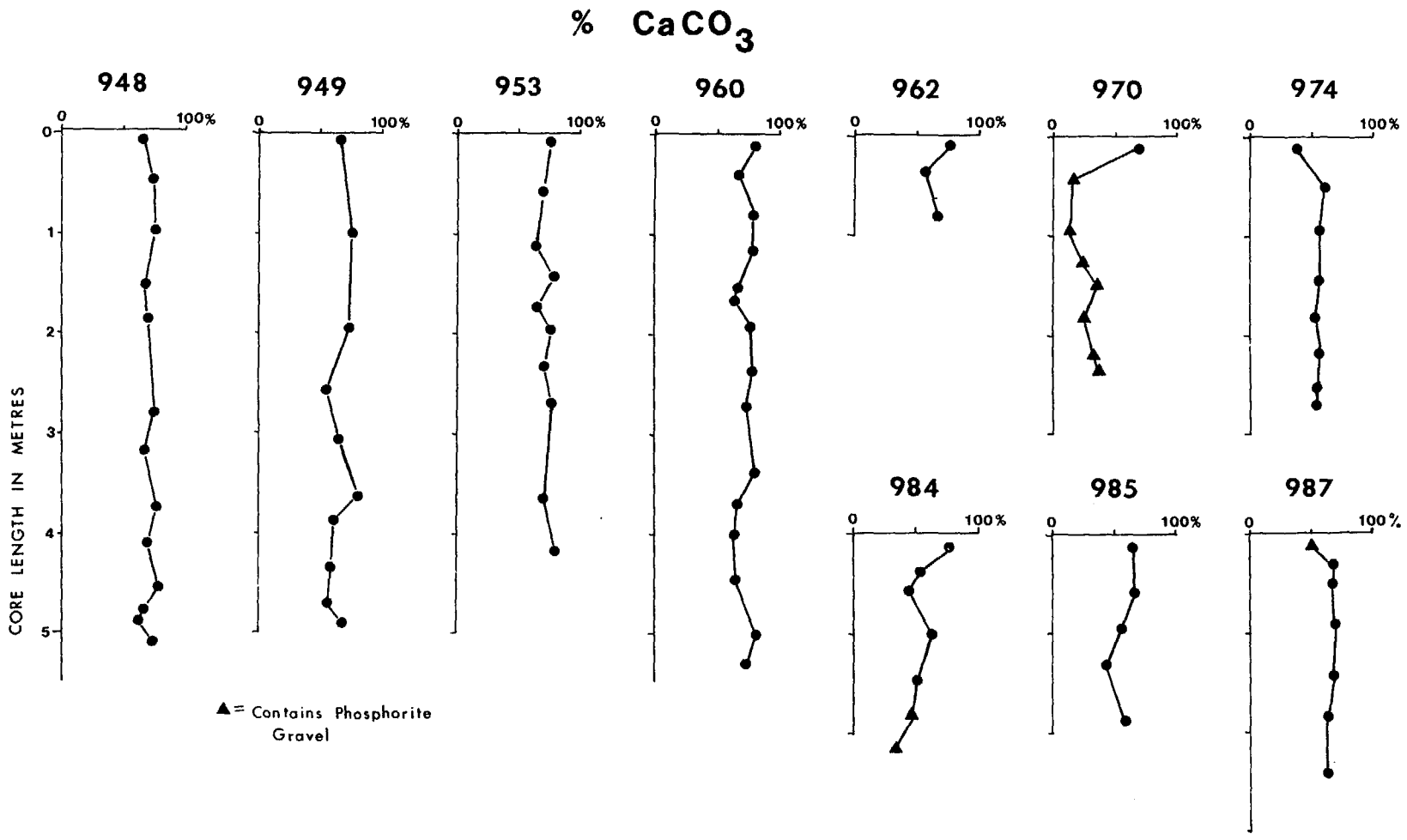
% CaCO3
948
949
953
960
962
970
974
984
985
987
0
100%
CORE LENGTH IN METRES
0
1
2
3
4
5
▲= Contains Phosphorite Gravel

Figure 5-5

relative to terrigenous sediment has occured in the time span represented by the cores.

Percentage of calcium carbonate in the cores averages 70%. Variations from this average generally occur as a result of dilution by phosphorite. In a few subsamples lower percentages of calcium carbonate reflect small increases (<5%) in the percentage of quartz in the coarse fractions. Table 5-5 shows the weight percentage of calcium carbonate in various sediment types from the plateau. Phosphorite gravels contain a much lower average percentage of calcium carbonate. Lutite, sandy lutites, muddy sand, and coral gravels all contain similar percentages of calcium carbonate.

Sedimentary Structures

Sedimentary structures were determined by visual description and also by core X-radiography. Structures observed in the cores are shown in figs. 5-6A to 5-6D. Sedimentary structures were useful in determining modes of deposition as well as the degree of biogenic reworking in the cores. The most striking feature in the cores is occurrence of homogeneous and unstructured sections that are often separated by sections of current indicative structures. It is likely that these unstructured and homogeneous sediments have undergone a high degree of biogenic reworking. Such reworking destroys primary sedimentary structures. Partially mottled sediments and burrows observed in the cores indicate that the biogenic reworking of the sediment is indeed an important process. Two types of burrows occur in the cores. The most common type is a horizontal burrow that ranges from 0.5 to 1 cm in diameter (fig. 5-7). Vertical burrows that range from 0.1 to 0.2 cm in diameter occur less frequently (fig. 5-7). Numerous types of current indicative structures occur intermittently throughout

Table 5-5. Calcium carbonate content in various sediment types.

Sediment Types	No. of Measurements	Hi → Lo	Mean	Standard Deviation
Lutite	7	76 → 60	68	5
Sandy Lutite	9	78 → 70	70	7
Muddy Sand	40	76 → 65	63	7
Gravels (Phosphorite)	14	69 → 19	42	17
Gravels (Coral)	19	84 → 62	72	9

Figure 5-6A. Core stratigraphy of all lined and unlined cores recovered in the study area that were greater than 1 metre in length. See table 5-1 for a description of the material used for radiocarbon dating and table 5-2 for a description of the foraminiferal assemblage used to determine the age of the sediment.

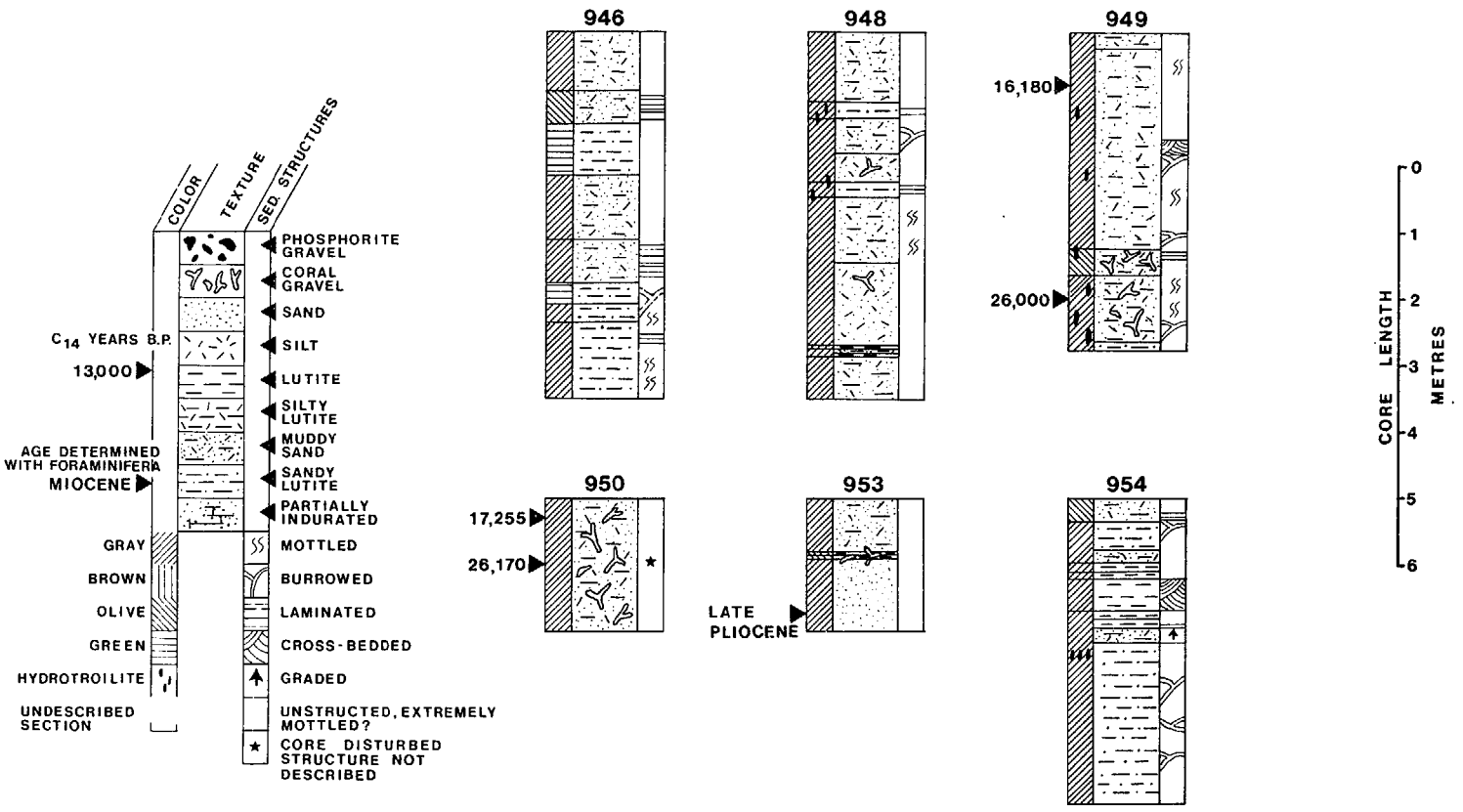
COLOR
TEXTURE
SED. STRUCTURES
PHOSPHORITE GRAVEL
CORAL GRAVEL
SAND
SILT
LUTITE
SILTY LUTITE
MUDDY SAND
SANDY LUTITE
PARTIALLY INDURATED
MOTTLED
BURROWED
LAMINATED
CROSS-BEDDED
GRADED
UNSTRUCTED, EXTREMELY MOTTLED?
CORE DISTURBED STRUCTURE NOT DESCRIBED
C_{14} YEARS B.P.
13,000
AGE DETERMINED WITH FORAMINIFERA
MIOCENE
GRAY
BROWN
OLIVE
GREEN
HYDROTROILITE
UNDESCRIBED SECTION
946
948
949
950
953
954
16,180
26,000
17,255
26,170
LATE PLIOCENE
CORE LENGTH
METRES
0
1
2
3
4
5
6

Figure 5-6A

Figure 5-6B. Core stratigraphy of all lined and unlined cores recovered in the study area that were greater than 1 metre in length. See table 5-1 for a description of the material used for radiocarbon dating and table 5-2 for a description of the foraminiferal assemblages used to determine the age of the sediment. See figure 5-6A for an explanation of the symbols.

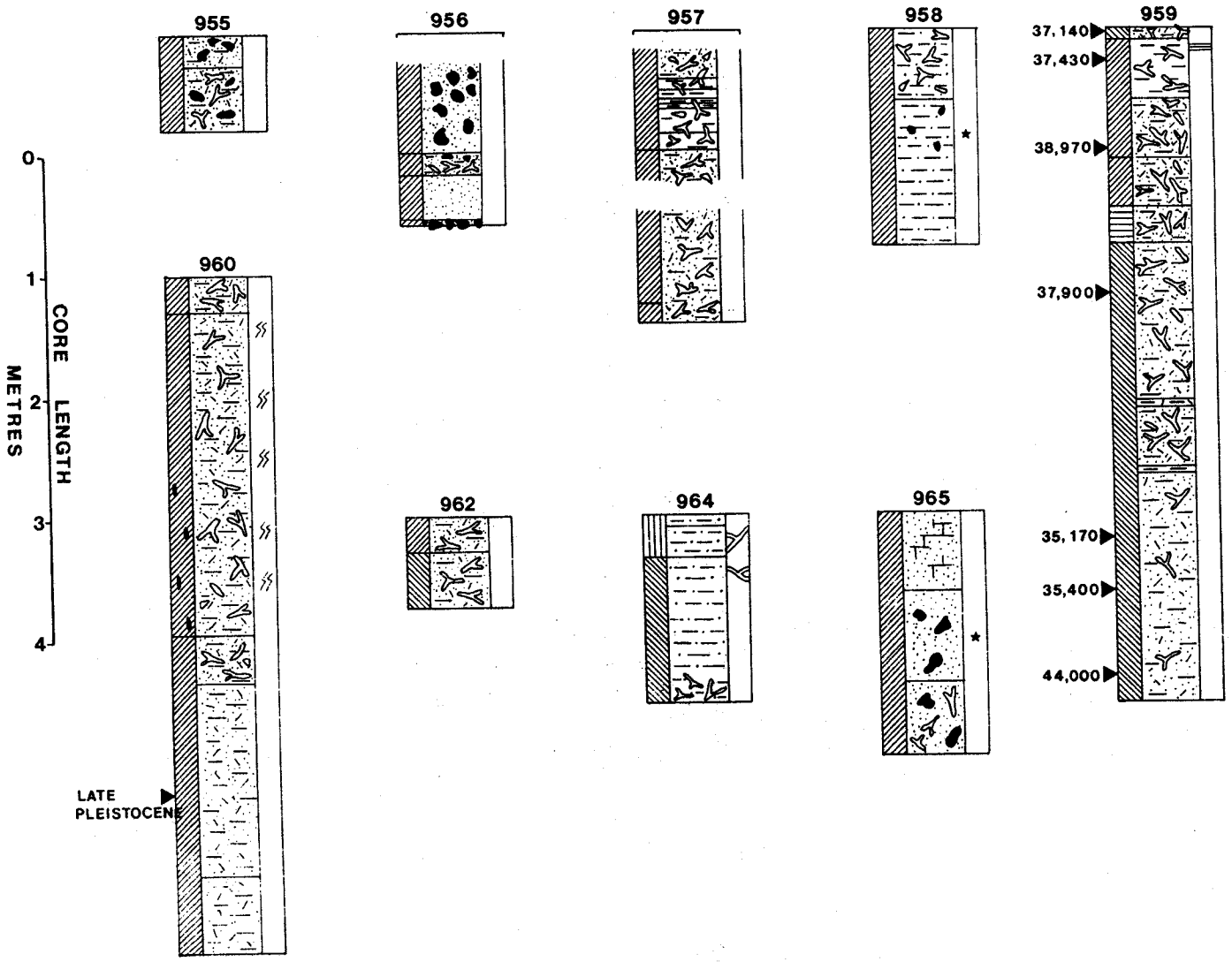
955
956
957
958
959
960
962
964
965
37,140
37,430
38,970
37,900
35,170
35,400
44,000
0
1
2
3
4
METRES
CORE LENGTH
LATE PLEISTOCENE

Figure 5-6B

Figure 5-6C. Core stratigraphy of all lined and unlined cores recovered in the study area that were greater than 1 metre in length. See table 5-1 for a description of the material used for radiocarbon dating and table 5-2 for a description of the foraminiferal assemblages used to determine the age of the sediment. See figure 5-6A for an explanation of the symbols.

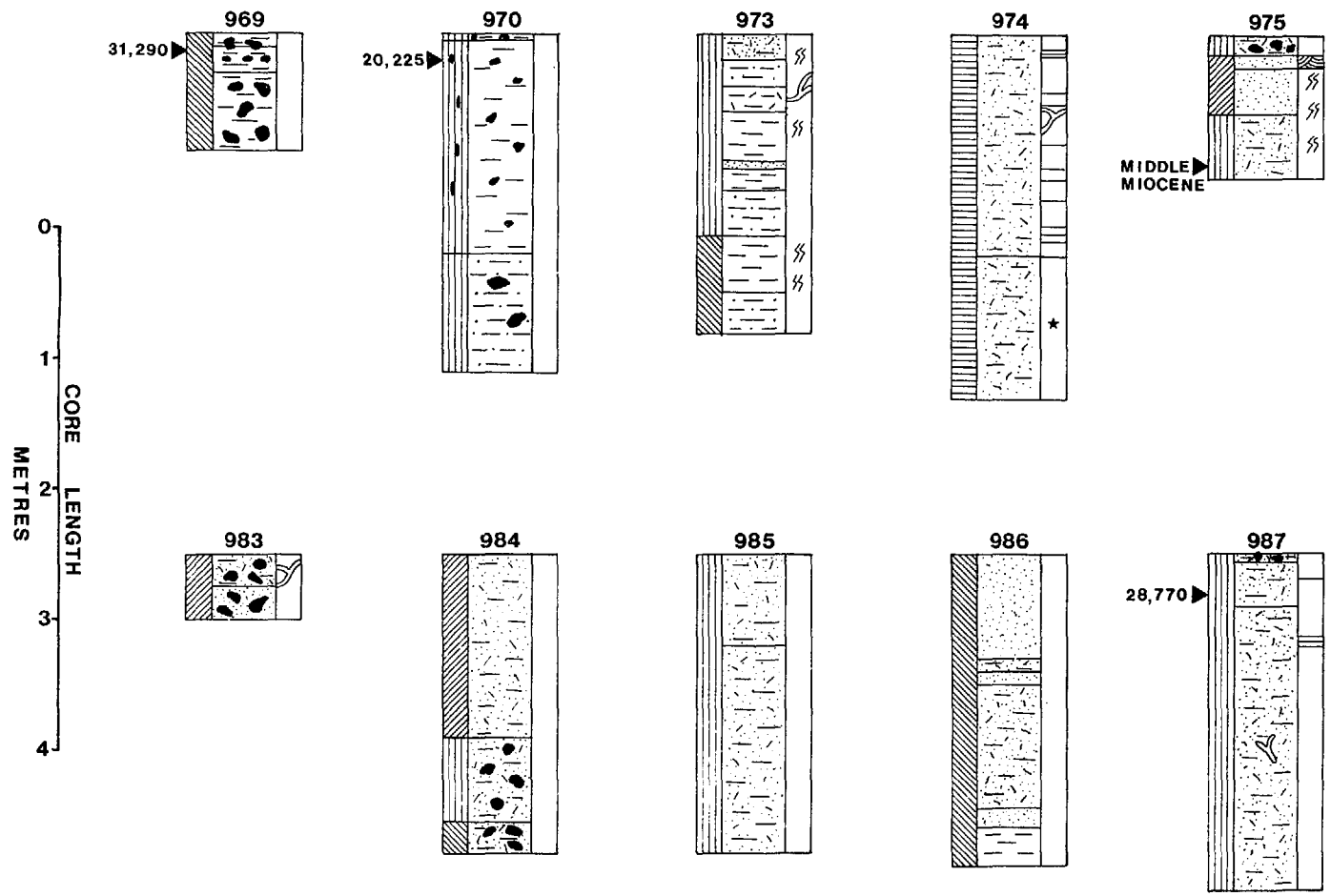
969
970
973
974
975
983
984
985
986
987
31,290
20,225
MIDDLE MIOCENE
28,770
0
1
2
3
4
METRES
CORE LENGTH

Figure 5-6C

Figure 5-6D. Core stratigraphy of all lined and unlined cores recovered in the study area that were greater than 1 metre in length. See table 5-1 for a description of the material used for radiocarbon dating and table 5-2 for a description of the foraminiferal assemblages used to determine the age of the sediment. See figure 5-6A for an explanation of the symbols.

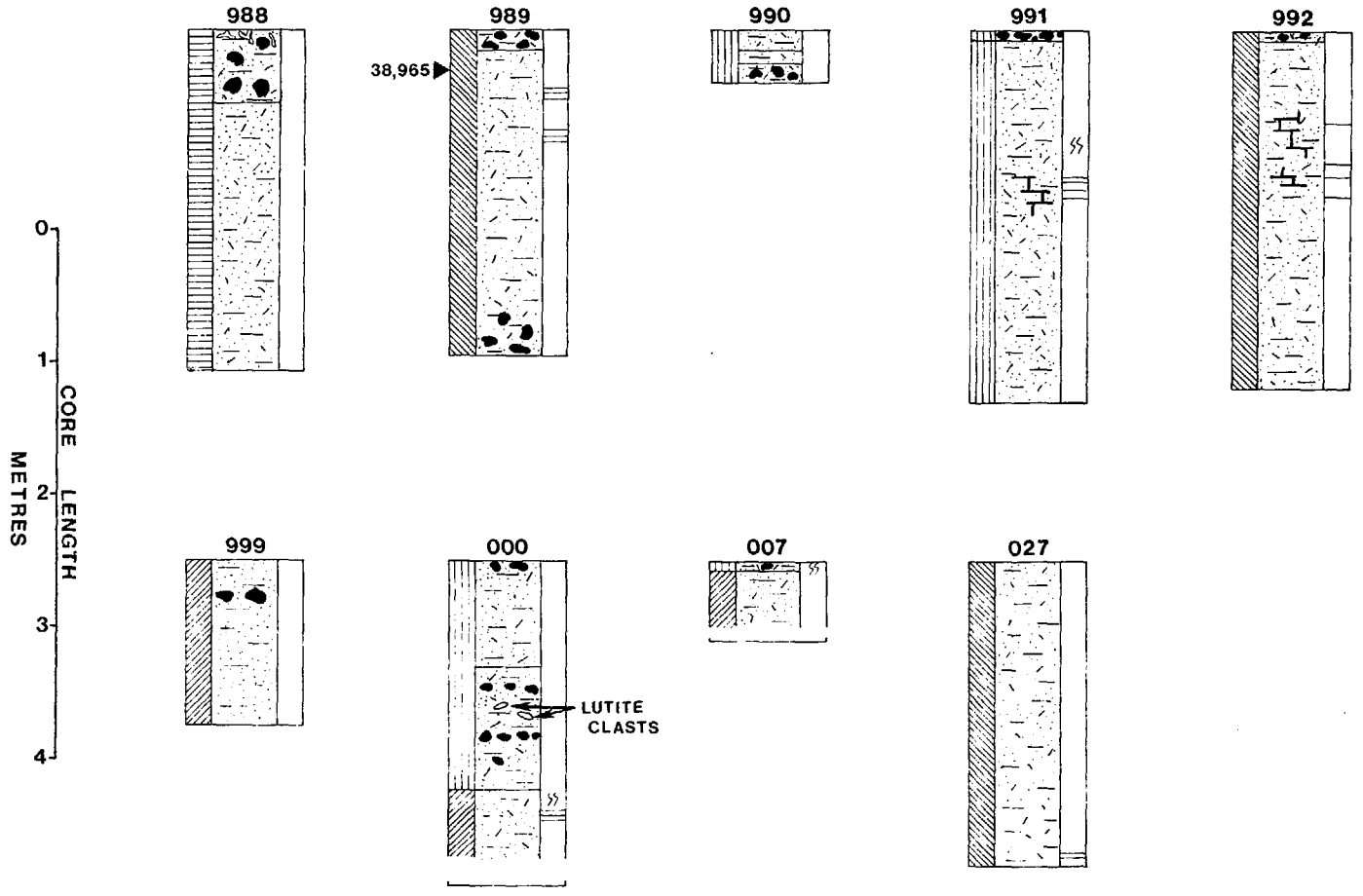
988
989
990
991
992
38,965
999
000
007
027
LUTITE
CLASTS
0
1
2
3
4
CORE LENGTH
METRES

Figure 5-6D

Figure 5-7. Core X-radiographs that illustrate the two types of burrows most commonly observed on the Blake Plateau. Core 954 contains horizontal burrows (arrow), core 964 contains vertical burrows (arrows).

954

338cm

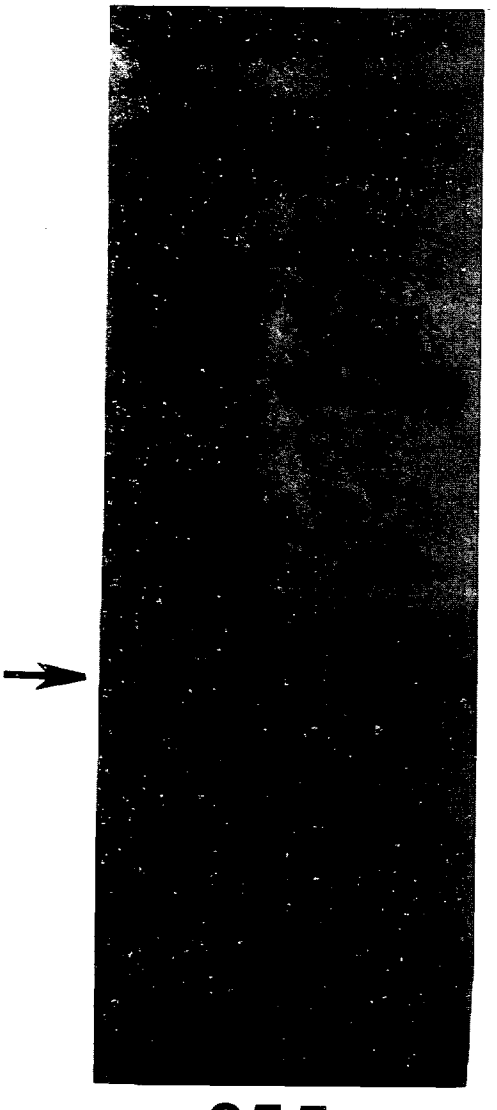

355cm

964

53cm

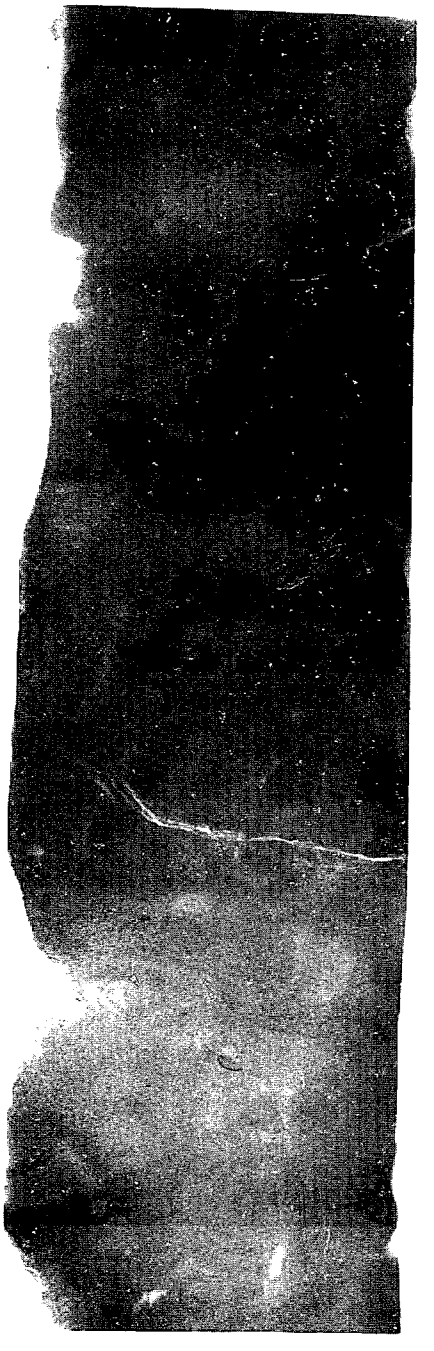

70cm

the cores. Thin horizontal laminations are the most common (fig. 5-8). The density of laminations per metre of core is variable, ranging from 60 to 560. Cross-bedding was observed in cores 949, 954, and 975. The cross-bedded units range in thickness from 0.3 to 0.7 metres in length. Current-laid beds of phosphorite gravel were common in the northernmost cores. Many of these phosphorite gravel units are undoubtedly Miocene lag deposits as suggested by Manheim and others (1979). However, late Quaternary radiocarbon dates were obtained from sediment below two gravel beds (987 and 989), indicating these gravels must have been reworked and deposited during the late Quaternary.

Based on the observed sedimentary structures, gravity-induced flows are not common in the cores. Cores 969 and 970 do, however, contain a debris flow deposit. Radiographs of these cores reveal unoriented, poorly sorted phosphorite gravels suspended in a muddy matrix. Bouma has observed similar structures in slump deposits in the Gulf of Mexico (Krinitzsky, 1970). The proximity of the debris flow near a slump (fig. 5-19) suggests it may have been initiated by the slumping. The phosphorite gravels in the debris flows contrast with those in the current-laid beds (fig. 5-9). Phosphorite gravels in the current-laid beds are better sorted, are packed in grain to grain contact, and have a much lower matrix content.

Shallow Core Stratigraphy

The texture and composition of the inner Blake Plateau and lower Florida-Hatteras Slope cores vary dramatically from site to site. This variation must in part reflect the large variety of depositional environments that coexist in the study area (i.e., "gullies," coral banks, and plateau "highs"). Greenish grays, light olive grays, yellowish grays, and pale olives were the dominant sediment colors on

Figure 5-8. X-radiographs from a single core. In the X-radiograph on the right, the sediment is highly mottled. In the other X-radiograph, the sediment is composed of alternating foraminiferal sand and glauconitic sand laminations.

Figure 5-8

the plateau. On the lower slope moderate and olive browns were dominant. Unit contacts in the cores were typically sharp. Hydrotroilite banding occurred infrequently in a few inner plateau cores. Partial induration of the sediment was noted in cores 965, 991, and 992.

Of the sediment units described on the inner plateau, muddy sands were the most abundant. Muddy sands comprise 47% of the totaled core lengths. Texturally, the muddy sands have an average mean grain size of 4.1 Ø and are very poorly sorted. The muddy sands were typically the thickest units ranging from 0.2 to 2.5 metres in length.

Units containing coral and phosphorite gravel also occur frequently on the inner plateau and comprise 36% of the totaled core lengths. Coral gravels were typically recovered from coral banks (cores 957, 958, 959, 960, 962). Coral gravels also occur as reworked detritus deposited by currents away from the banks (cores 949, 950, 953, 955, 956, 964, 965, 987, and 988). Phosphorite gravels were recovered at a number of core stations (955, 956, 965, 969, 970, 975, 983, 984, 987, 988, 989, 990, 991, 992, 999, 000, 007). The phosphorite gravels are thought to be Miocene in age (Manheim and others, 1979) and, therefore, must be residual sediment. Units containing coral gravel range in thickness from 0.2 to 3 metres and on the average were thicker than the units containing phosphorite gravel which range from 0.2 to 1 metre in length. Units containing coral gravels have an average mean grain size of 3.3 Ø and are extremely poorly sorted (4.4 Ø). Units with phosphorite gravels are typically coarser with an average mean grain size of 2.5 Ø and are also better sorted (standard deviation = 3.2 Ø).

Lutites, sandy lutites, and sands are not abundant on the inner plateau and lower slope, comprising only 17% of the totaled core

lengths. Textural parameters of these sediment types are shown in table 5-6.

Even though the composition of the coarse fractions in the subsamples are variable (table 5-7), some generalized observations can be made. Typically, the sands are composed entirely of foraminifera, quartz, sponge spicules, phosphorite, glauconite, pteropods, gastropods, and coral detritus. Gravel fractions were exclusively composed of phosphorite and coral. Cores recovered from areas that according to seismic data are outcropping Pleistocene, Oligocene, Miocene, and Pliocene deposits on the average contain more glauconite and phosphorite (table 5-7). Cores from the Holocene and Paleocene age deposits generally contained a higher abundance of biogenic debris (i.e., foraminifera, pteropods, and gastropods). The observed differences in the compositions of cores recovered from the various age outcrops apparently reflect the importance of pre-Holocene residual sediment in the near-surface (<5 m deep) sediments. Radiocarbon and foraminiferal dates, however, indicate that many of the cores do not in fact penetrate into the pre-Quaternary units even though the units appear to be outcropping on the surface. Apparently, an acoustically transparent blanket of Holocene sediment covers many of the pre-Holocene units. Edsall (1979) in his study of the seismic stratigraphy of the region suggests that an acoustically transparent cover might blanket units that appear in the seismic records to outcrop.

Surficial Sediments of the Florida-Hatteras Slope and Inner Blake Plateau

The texture of surficial sediment on the Florida-Hatteras Slope and inner Blake Plateau is highly variable (fig. 5-10). This high degree of variability is undoubtedly the result of the varying strengths of the

Table 5-6. Textural statistics of selected piston core subsamples.

Sediment Size	No. of Measure-ments	% Gravel $\bar{x}$	% Gravel sd	% Sand $\bar{x}$	% Sand sd	% Mud $\bar{x}$	% Mud sd	Mean Grain Size Φ $\bar{x}$	Mean Grain Size Φ sd	Sorting Φ $\bar{x}$	Sorting Φ sd
Lutite	7	0	0	30	20	70	20	7.3	1.3	3.5	0.3
Sandy Lutite	15	0	0	45	15	55	15	6.1	1.2	3.8	0.3
Muddy Sand	56	0	0	66	21	39	53	4.1	1.6	2.8	1.0
Sand	7	4	8	49	11	47	19	5.6	0.6	3.9	0.5
Gravels (Phosphorite)	28	39	29	31	23	34	31	2.5	3.1	3.2	1.5
Gravels (Coral)	24	25	17	40	22	35	18	3.3	1.7	4.4	1.1

Table 5-7. Average composition of selected sand fractions analyzed from cores recovered from outcrops of various ages.

Number/Epoch subsamples analyzed	Statistics	Quartz	Spicules	Phosphorite	Forams	Glauconite	Pteropods	Gastropods	Coral
11	$\bar{x}$	7	2	0	61	3	7	12	0
Holocene	s.d.	5	1	0	8	2	3	6	0
	range hi←lo	18-0	4-0	-	78-50	6-0	12-3	20-4	2-0
22	$\bar{x}$	3	1	0	74	9	4	3	0
Pleistocene	s.d.	5	1	0	18	8	8	6	0
	range hi←lo	19-0	4-0	-	96-43	30-0	26-0	22-0	-
4	$\bar{x}$	4	0	1	59	20	2	0	0
Pliocene	s.d.	3	0	1	33	23	2	0	0
	range hi←lo	8-2	-	3-0	89-20	52-2	4-0	1-0	1-0
42	$\bar{x}$	1	1	1	66	7	3	3	2
Miocene	s.d.	1	4	3	18	12	3	4	2
	range hi←lo	5-0	23-0	12-0	91-27	49-0	12-0	16-0	11-0
21	$\bar{x}$	5	0	0	66	16	1	1	0
Oligocene	s.d.	3	0	0	12	9	1	1	0
	range hi←lo	11-0	3-0	2-0	87-39	42-5	5-0	5-0	6-0
6	$\bar{x}$	1	1	0	72	4	6	3	3
Paleocene	s.d.	2	2	0	10	3	8	2	4
	range hi←lo	4-0	5-0	1-0	87-62	9-0	18-0	5-0	8-0

Figure 5-10. Texture of surficial sediments in the study area. See figure 5-2 for locations of the surficial samples.

Figure 5-10

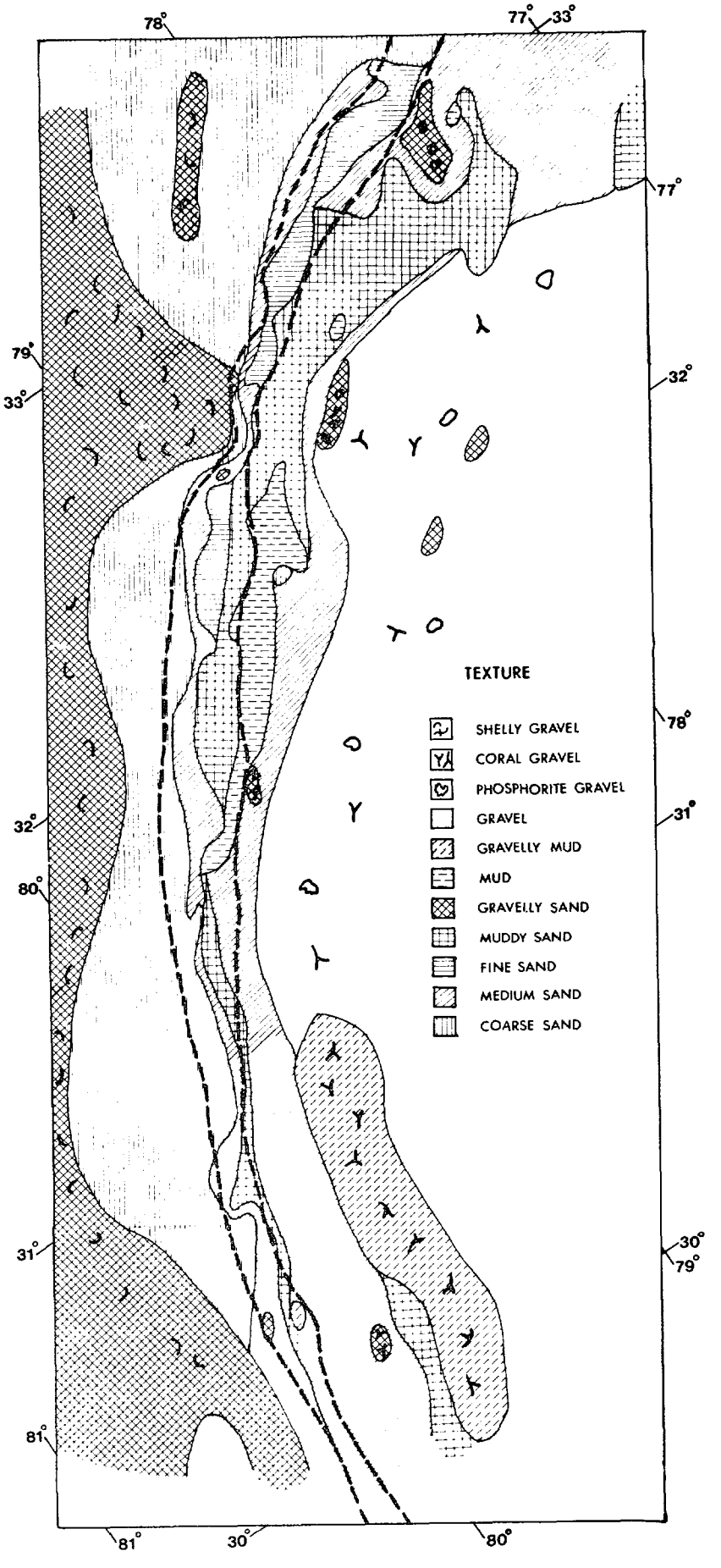
78°
77°
33°
77°
79°
33°
32°
32°
80°
78°
31°
31°
30°
79°
81°
81°
30°
80°
TEXTURE
SHELLY GRAVEL
CORAL GRAVEL
PHOSPHORITE GRAVEL
GRAVEL
GRAVELLY MUD
MUD
GRAVELLY SAND
MUDDY SAND
FINE SAND
MEDIUM SAND
COARSE SAND

prevailing bottom current energy regimes within the study area. Surficial sediment on the continental shelf adjacent to the Florida-Hatteras Slope consists of gravelly sands and coarse sands. The Florida-Hatteras Slope sediment consists of coarse, medium, fine, and less frequently, muddy sands. Muds are present on the Florida-Hatteras Slope but, unlike the slope north of Cape Hatteras, they occur infrequently (Doyle and others, 1979). Coarse, medium, and fine sands occur in linear bands parallel to the regional contours of the slope. The fact that these sands get finer downslope suggests they were derived from the continental shelf.

Muds, gravels, medium sands, muddy sands, muddy gravels, and gravelly sands all are found on the plateau. The gravelly sands and muds were recovered primarily from coral bank deposits. On the plateau, gravelly sands, muddy sands, and occasionally medium sands occur as residual sediments although the medium sands are primarily pelagic foraminiferal oozes. Gravels were recovered from the plateau in an area covered by Miocene phosphorite lag gravels and pavements (Manheim and others, 1979).

The colors and gross compositions of the surficial sediments on the Florida-Hatteras Slope, the adjacent continental shelf, and the Blake Plateau were determined (fig. 5-11, table 5-8). The composition of the continental shelf, Florida-Hatteras Slope and inner Blake Plateau sediment attests to their origin. The quartz plus feldspar content gradationally decreases downslope while the foraminifera content increases (fig. 5-12). Quartz plus feldspar comprise less than 5% of the sand fraction of samples from the Blake Plateau. Foraminifera comprise less than 5% of the sand fraction on the shelf and some parts of the Florida-Hatteras Slope (fig. 5-13).

Figure 5-11. Color and gross composition of the surficial sediments in the study area. See figure 5-2 for locations of the surficial samples.

Figure 5-11

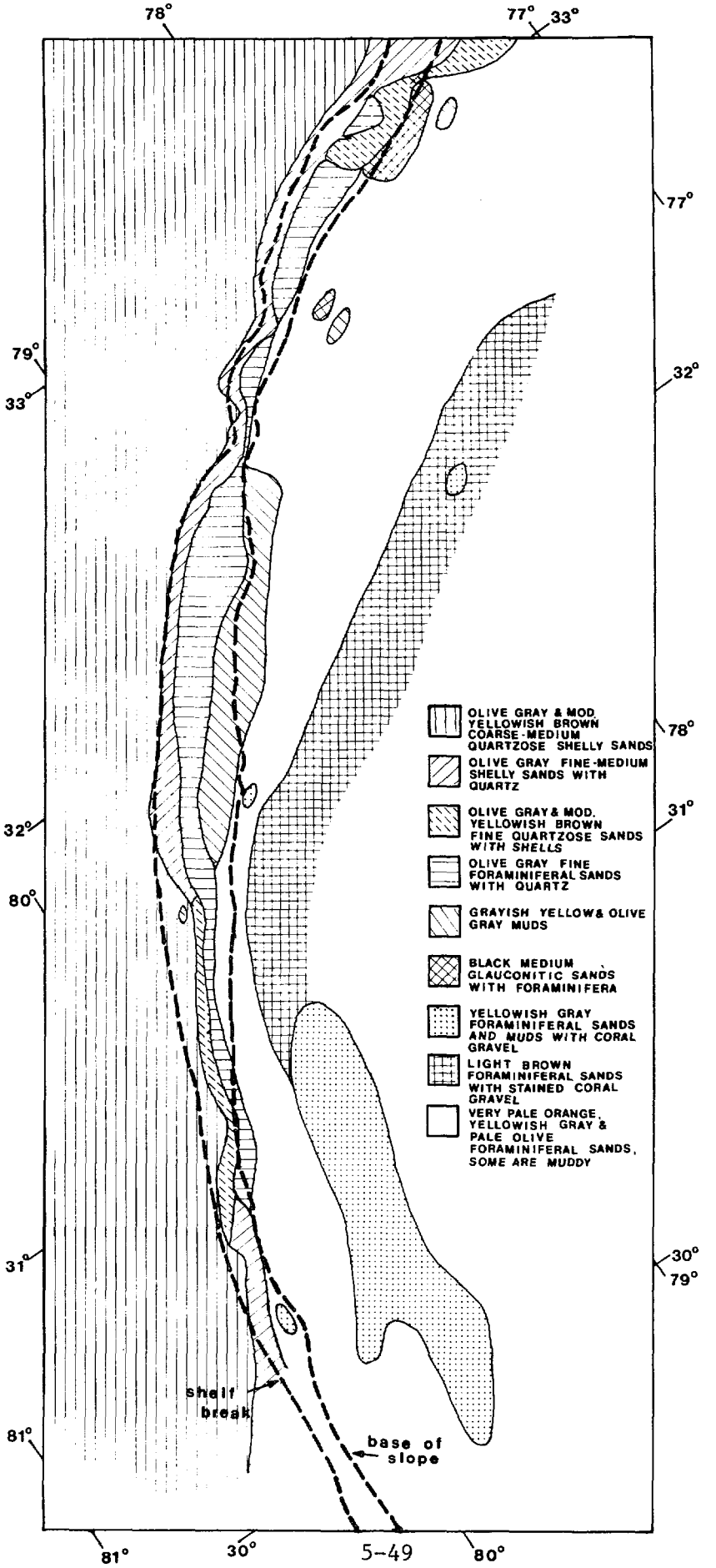
78°
77°
33°
77°
79°
33°
32°
78°
31°
32°
80°
31°
30°
79°
81°
81°
30°
80°
shelf break
base of slope
OLIVE GRAY & MOD. YELLOWISH BROWN COARSE-MEDIUM QUARTZOSE SHELLY SANDS
OLIVE GRAY FINE-MEDIUM SHELLY SANDS WITH QUARTZ
OLIVE GRAY & MOD. YELLOWISH BROWN FINE QUARTZOSE SANDS WITH SHELLS
OLIVE GRAY FINE FORAMINIFERAL SANDS WITH QUARTZ
GRAYISH YELLOW & OLIVE GRAY MUDS
BLACK MEDIUM GLAUCONITIC SANDS WITH FORAMINIFERA
YELLOWISH GRAY FORAMINIFERAL SANDS AND MUDS WITH CORAL GRAVEL
LIGHT BROWN FORAMINIFERAL SANDS WITH STAINED CORAL GRAVEL
VERY PALE ORANGE, YELLOWISH GRAY & PALE OLIVE FORAMINIFERAL SANDS, SOME ARE MUDDY

Table 5-8. Average composition of sand fractions in the surficial sediment types (fig. 5-11) from the Florida-Hatteras Slope, continental shelf, and inner Blake Plateau.

	Quartz	Spicules	Phosphorite	Foraminifera	Glauconite	Pteropods	Gastropods	Pelecypods	Coral	Echinoids	Undifferentiated Shell Fragments
OLIVE GRAY AND MODERATE YELLOWISH BROWN COARSE-MEDIUM QUARTZOSE SHELLY SANDS (50 SAMPLES)											
$\bar{x}$	78	---	2	2	9	< 1	< 1	< 1	2	< 1	4
sd.	11	---	3	4	6	1	< 1	2	2	< 1	4
Range Hi-Lo	96-43	---	15-0	27-0	28-1	5-0	3-0	2-0	8-0	4-0	16-0
OLIVE GRAY FINE-MEDIUM SHELLY SANDS WITH QUARTZ (22 SAMPLES)											
$\bar{x}$	48	< 1	1	8	9	< 1	1	<1	10	< 1	14
sd.	18	< 1	2	8	8	< 1	1	1	8	< 1	9
Range Hi-Lo	75-11	1-0	7-0	35-1	22-1	1-0	3-0	1-0	34-0	1-0	24-3
OLIVE GRAY AND MODERATE YELLOWISH BROWN FINE QUARTZOSE SANDS WITH SHELLS (13 SAMPLES)											
$\bar{x}$	68	< 1	1	7	9	1	2	1	2	1	5
sd.	11	< 1	2	5	5	1	2	2	4	1	3
Range Hi-Lo	86-48	2-0	7-0	17-0	17-2	3-0	6-0	6-0	14-0	2-0	10-0
OLIVE GRAY FINE FORAMINIFERA SAND WITH QUARTZ (28 SAMPLES)											
$\bar{x}$	31	1	< 1	29	13	2	3	2	3	3	9
sd.	15	2	< 1	15	9	2	2	3	3	2	5
Range Hi-Lo	67-5	7-0	1-0	61-7	29-0	11-0	6-0	16-0	10-0	9-0	25-2
GRAYISH YELLOW AND OLIVE GRAY MUDS (13 SAMPLES)											
$\bar{x}$	6	1	1	70	7	2	2	1	2	3	2
sd.	4	2	2	13	13	2	2	2	4	2	2
Range Hi-Lo	14-0	5-0	7-0	88-1	48-1	4-0	6-0	5-0	13-0	6-0	5-0
BLACK MEDIUM GLAUCONITIC SANDS WITH FORAMINIFERA (11 SAMPLES)											
$\bar{x}$	3	< 1	24	18	48	< 1	< 1	1	2	< 1	2
sd.	3	< 1	29	10	33	< 1	< 1	2	3	< 1	1
Range Hi-Lo	8-0	1-0	82-0	43-8	81-4	1-0	2-0	7-0	9-0	1-0	3-1
YELLOWISH GRAY FORAMINIFERAL SANDS AND MUDS WITH CORAL GRAVEL (7 SAMPLES)											
$\bar{x}$	7	3	1	64	2	8	3	1	7	---	1
sd.	18	4	2	11	1	8	2	1	5	---	1
Range Hi-Lo	49-0	9-0	4-0	78-42	3-0	18-0	4-0	2-0	15-0	---	3-0
LIGHT BROWN FORAMINIFERAL SANDS WITH STAINED CORAL GRAVEL (13 SAMPLES)											
$\bar{x}$	< 1	< 1	5	62	3	2	3	< 1	14	1	3
sd.	< 1	< 1	6	12	5	2	2	1	13	4	2
Range Hi-Lo	2-0	2-0	19-0	78-28	16-0	7-0	8-0	3-0	50-3	4-0	8-0
VERY PALE ORANGE, YELLOWISH GRAY, AND PALE OLIVE FORAMINIFERAL SANDS, SOME ARE MUDDY (61 SAMPLES)											
$\bar{x}$	5	1	4	57	16	2	2	1	5	1	3
sd.	7	3	7	19	16	3	2	1	9	1	3
Range Hi-Lo	28-0	23-0	33-0	88-5	56-0	13-0	19-0	6-0	58-0	2-0	11-0

Figure 5-12. The percentage of quartz plus feldspar as determined by grain counts. See figure 5-2 for locations of the surficial samples.

Figure 5-12

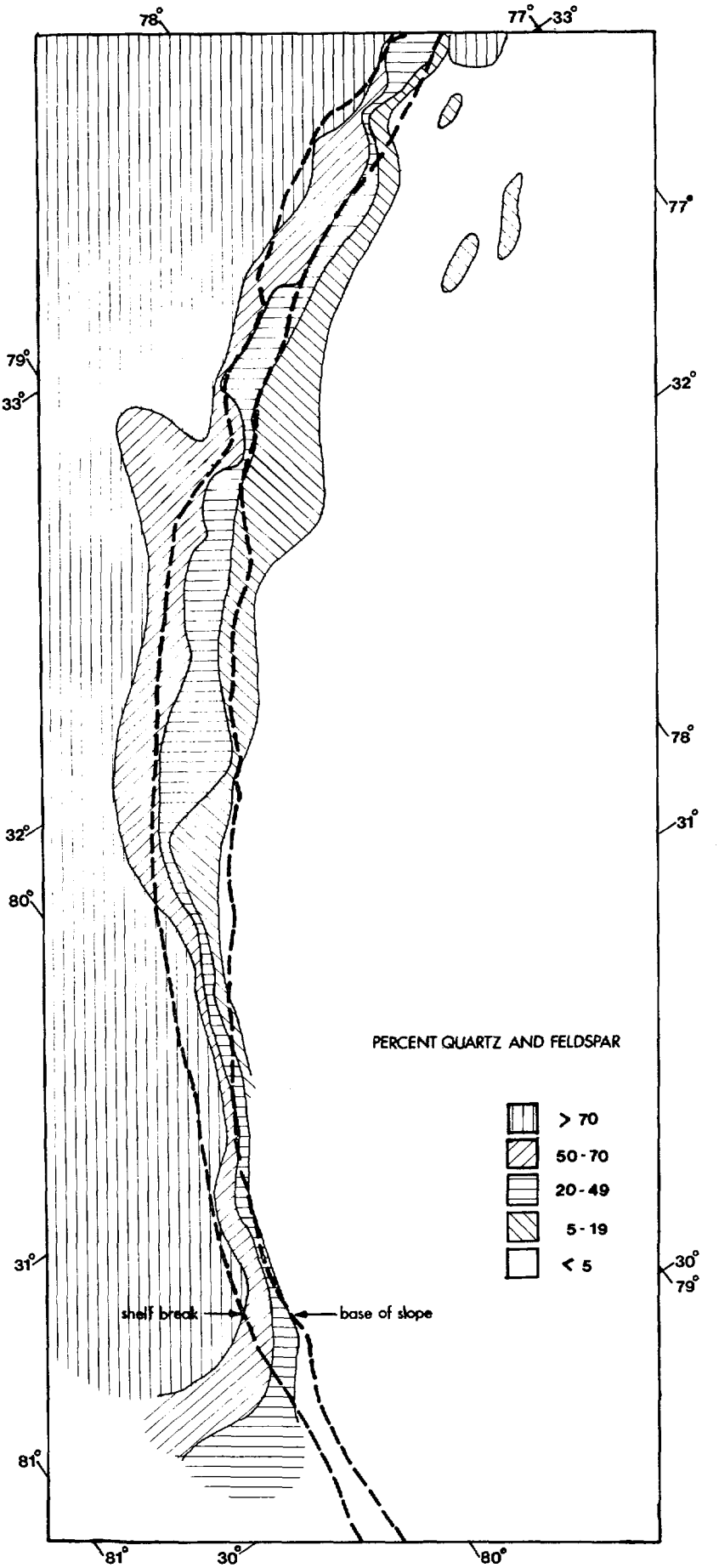
78°
77°
33°
77°
79°
33°
32°
78°
32°
31°
80°
PERCENT QUARTZ AND FELDSPAR
> 70
50 - 70
20 - 49
5 - 19
< 5
31°
30°
79°
shelf break
base of slope
81°
81°
30°
80°

Figure 5-13. Percentage of formainifera in the surficial sediments as determined by grain counts. Locations of the surficial samples are shown in figure 5-2.

Figure 5-13

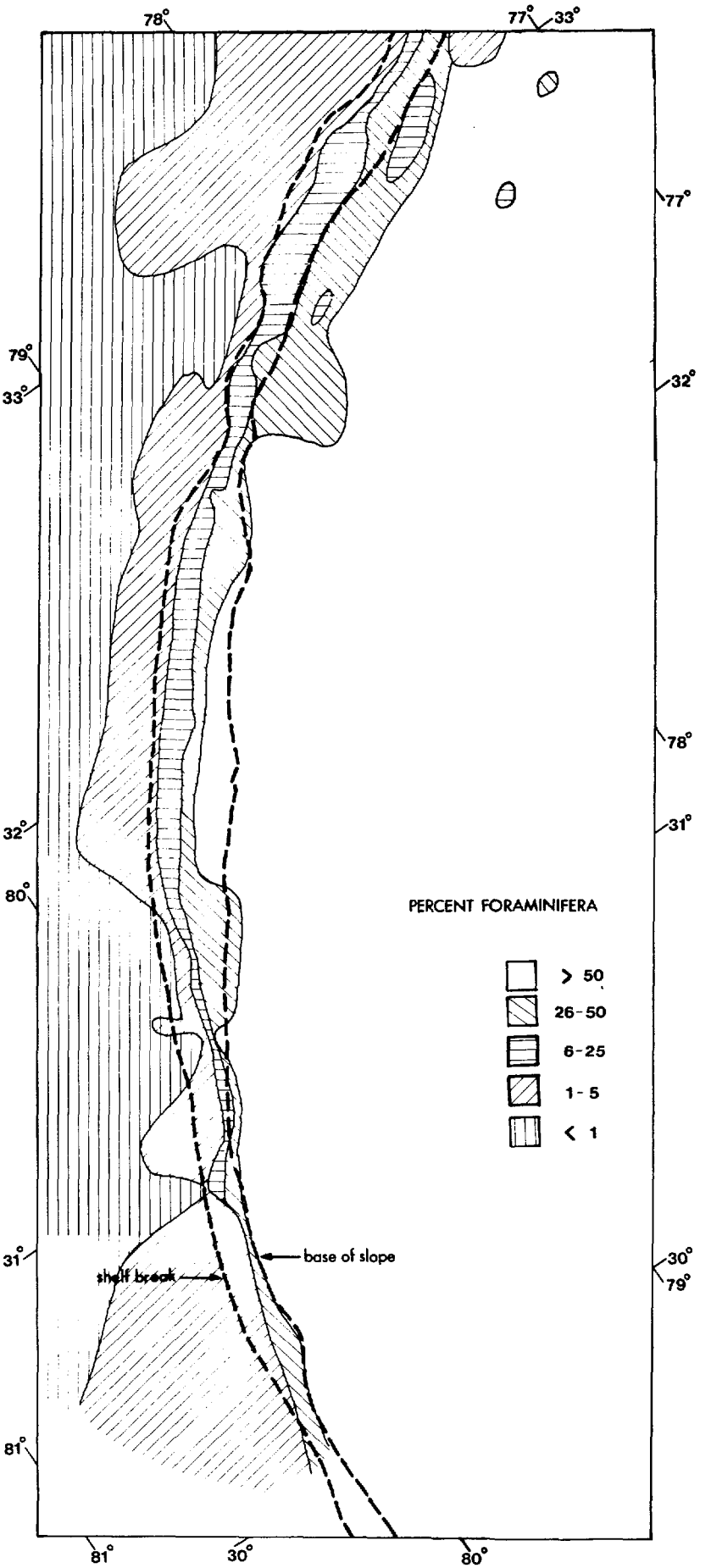
78°
77°
33°
77°
79°
33°
32°
78°
32°
31°
80°
PERCENT FORAMINIFERA
> 50
26-50
6-25
1-5
< 1
base of slope
shelf break
31°
30°
79°
81°
81°
30°
80°

Glauconite on the slope and inner plateau occurs primarily as black polished pellets. Glauconite is found in greatest abundance near outcrops (fig. 5-14) of pre-Holocene age sediments. This distribution of glauconite indicates it is primarily a residual sediment. Milliman (1972) has previously suggested that dark colored glauconite grains on the Florida-Hatteras Slope are residual.

Corals on the Blake Plateau

The distribution of coral banks on the Blake Plateau was determined on the basis of the distinctive hyperbolic character of bottom profiles taken across the banks (fig. 5-15). This distinctive type of bottom return has previously been used to map the distribution of coral banks in the deep sea (Stetson and others, 1962; Wilson, 1979). Coral laden dredges recovered from bottoms with the distinctive hyperbolic returns confirm the existence of the coral banks. Figure 5-16 shows the locations of the hyperbolic bottom reflections, of bottom samples collected in this study that recovered coral, and of bottom samples from the Smithsonian collection which recovered large amounts of colonial corals (fig. 5-16). *Lophelia prolifera* and *Enallopsammia profunda* are the only two species of colonial coral recovered from the plateau. Cairns (1979) has identified the colonial and solitary coral species in select subsamples from the plateau (table 5-9). In addition to the colonial species of coral, the solitary species *Bathypsammia fallosocialis*, *Thecopsammia socialis*, *Bathypsammia tintinnabulum*, and *Concentrotheca laevigata* were also identified in subsamples from the plateau. Not all corals on the plateau were associated with coral banks. Many living corals were recovered from the northern end of the study area attached to large phosphorite gravels and pavements (Appendix 5-2, pocket in back cover).

Figure 5-14. Percentage of glauconite in the surficial sediments as determined by grain counts. Locations of the surficial samples are shown in figure 5-2.

Figure 5-14

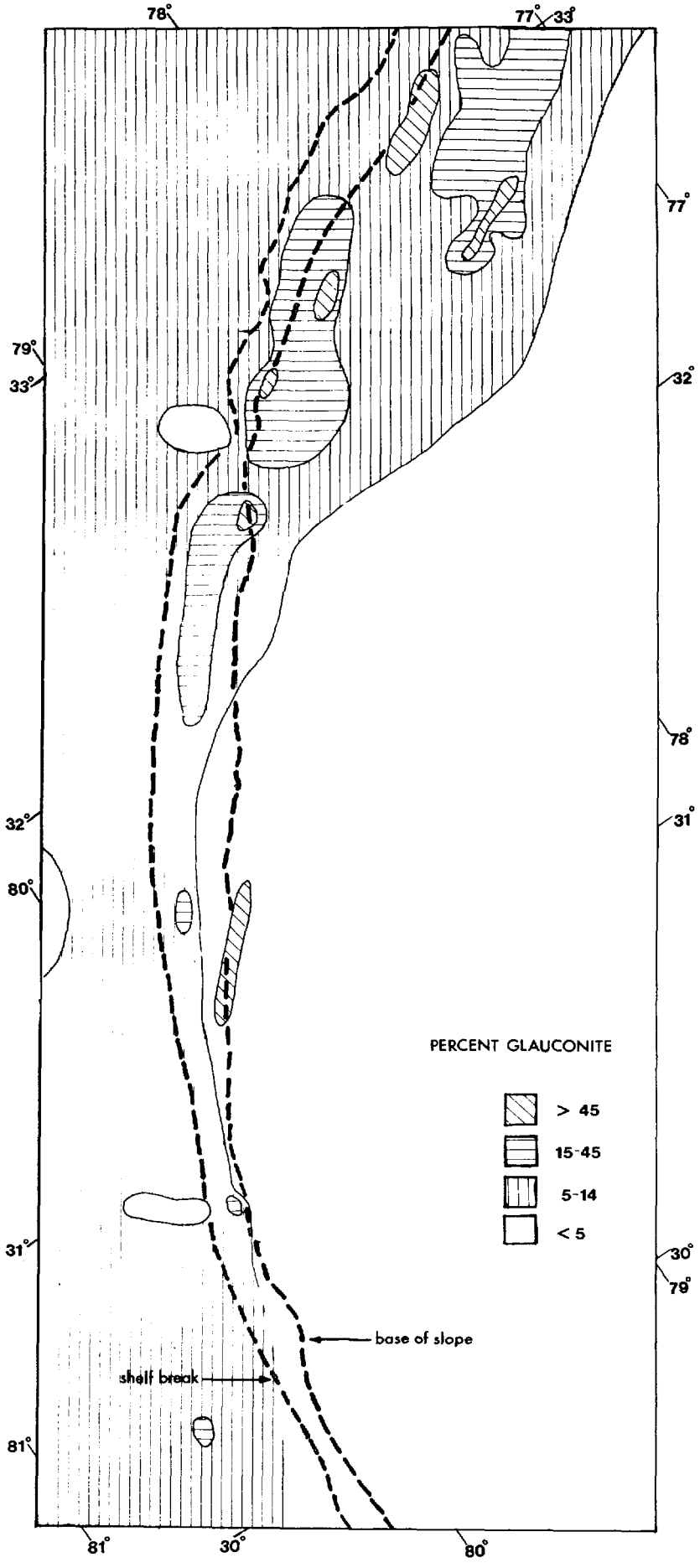
78°
77°
33°
77°
79°
33°
32°
78°
32°
31°
80°
PERCENT GLAUCONITE
> 45
15-45
5-14
< 5
31°
30°
79°
base of slope
shelf break
81°
81°
30°
80°

Figure 5-15. Bottom profiles across coral banks in the southernmost part of the study area.

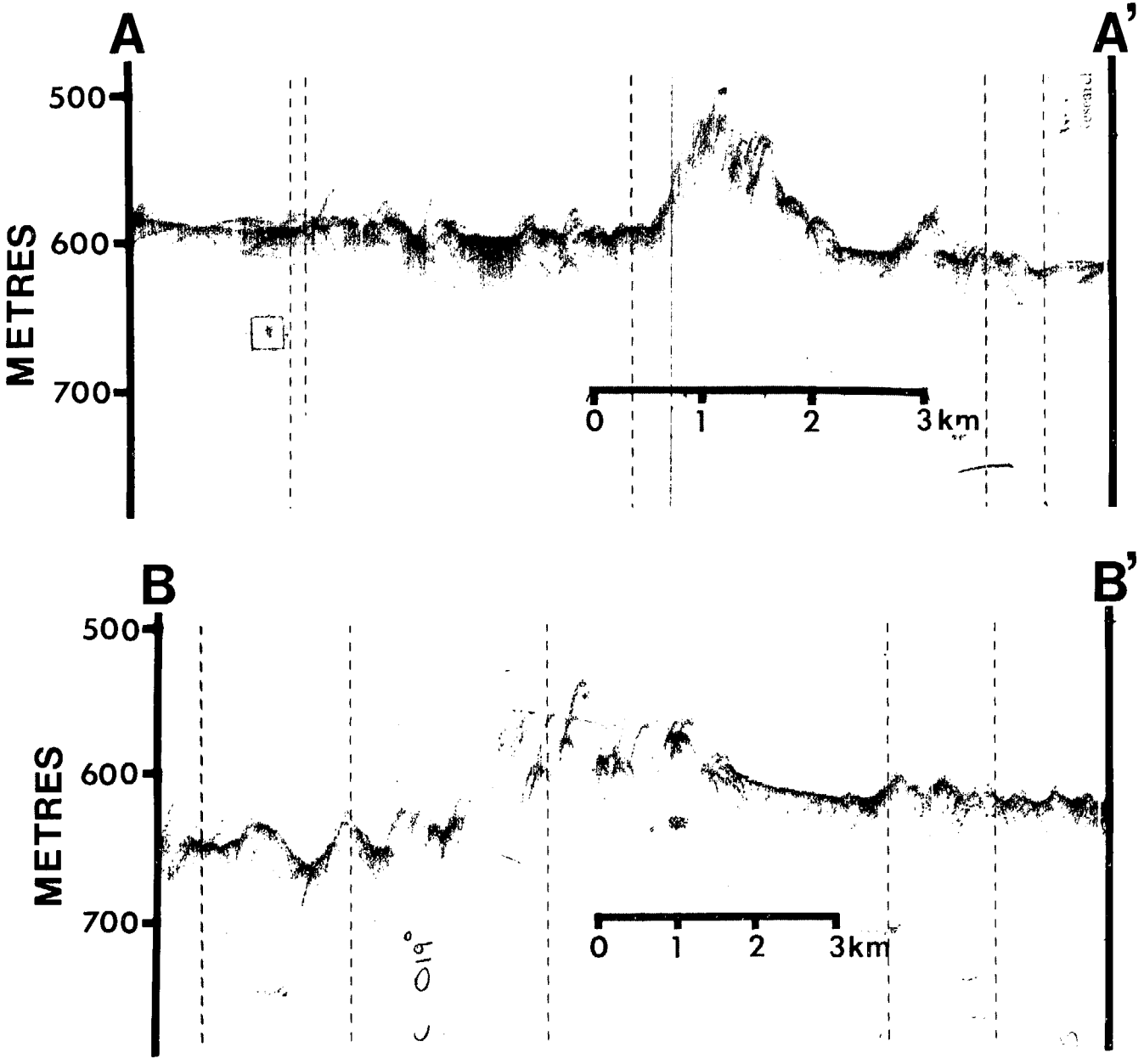

Figure 5-15

Figure 5-16. Ship's track of the R/V EASTWARD within the study area. Groups of coral banks are delineated. Sample locations that are indicated as having come from coral banks (triangles) but that have no station numbers are coral bank samples from the Smithsonian collection.

Figure 5-16

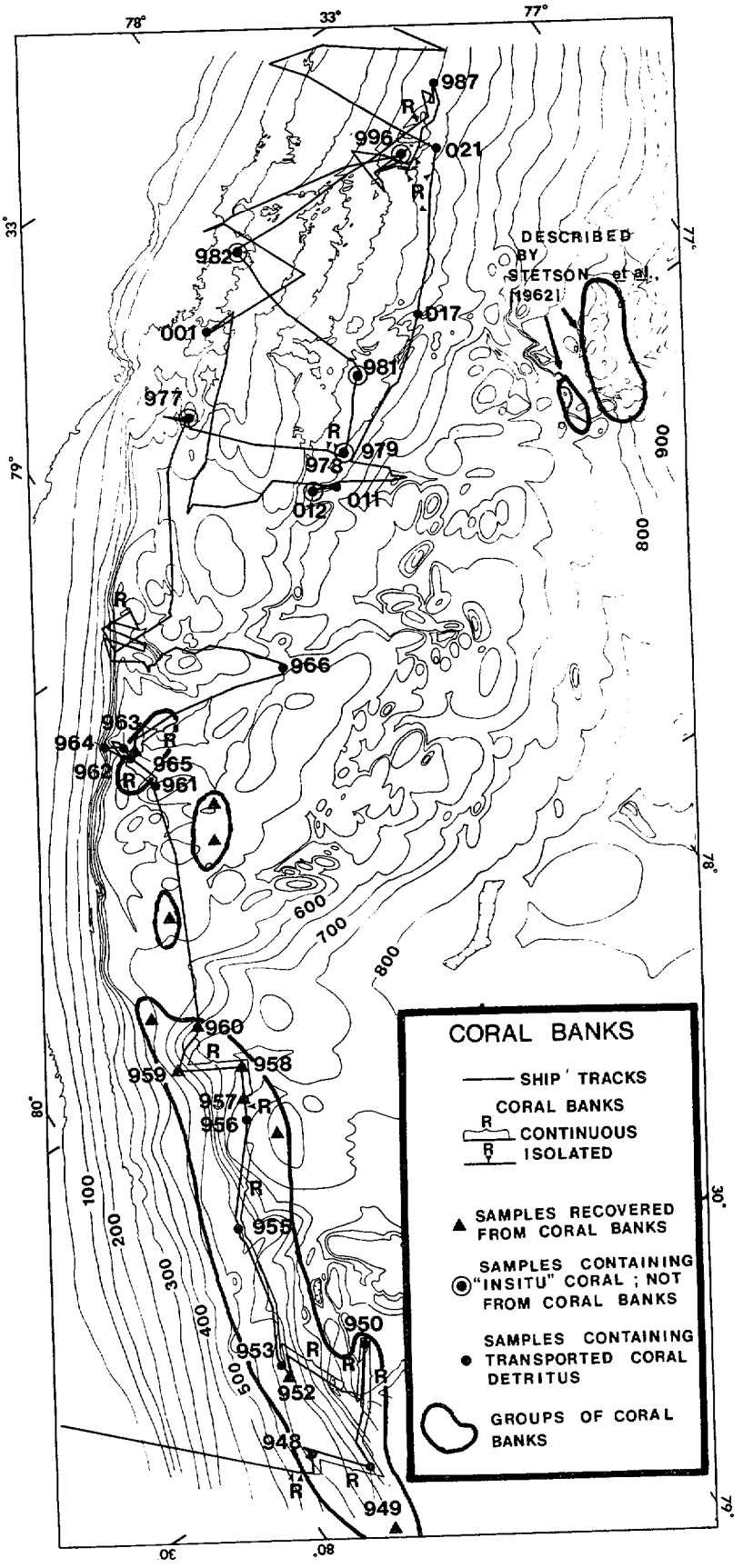
78°
33°
77°
987
996
021
982
001
017
981
977
979
978
012
011
966
963
964
965
962
961
960
959
958
957
956
955
950
953
952
948
949
DESCRIBED BY STETSON et al. (1962)
900
800
600
700
800
100
200
300
400
500
CORAL BANKS
SHIP TRACKS
CORAL BANKS
CONTINUOUS
ISOLATED
SAMPLES RECOVERED FROM CORAL BANKS
SAMPLES CONTAINING "INSITU" CORAL ; NOT FROM CORAL BANKS
SAMPLES CONTAINING TRANSPORTED CORAL DETRITUS
GROUPS OF CORAL BANKS

Table 5-9. Coral assemblages in selected samples from the Florida-Hatteras Slope. Corals identified by Cairns; all specimens were dead when collected unless otherwise specific.

Sample Number	
952	Lophelia prolifera (Pallas) Enallopsammia profunda (Pourtalès) Bathypsammia fallosocialis Squires Thecopsammia socialis Pourtalès Bathypsammia tintinnabulum (Pourtalès)
957	Lophelia prolifera (Pallas) Enallopsammia profunda (Pourtalès)
960, 310-333 cm	Lophelia prolifera (Pallas) Enallopsammia profunda (Pourtalès) Bathypsammia fallosocialis Squires
240-260 cm	Lophelia prolifera (Pallas) Bathypsammia fallosocialis Squires Enallopsammia profunda (Pourtalès)
66- 81 cm	Lophelia prolifera (Pallas) Enallopsammia profunda (Pourtalès)
979	Enallopsammia profunda (Pourtalès)(live) Lophelia prolifera (Pourtalès)(live) Thecopsammia socialis (Pourtalès)(live) Concenthrotheca laevigata (Pourtalès)
994	Bathypsammia tintinnabulum (Pourtalès)
013	Bathypsammia fallosocialis Squires (1 live)
041	Thecopsammia socialis Pourtalès (probably live, poor specimen) Bathypsammia tintinnabulum (Pourtalès)

Piston cores (957, 958, 959, 960, and 962) that were recovered from the coral banks give us some idea of the bank stratigraphy. The coral banks are composed of thick sequences (1-3 metres) of coral gravels floating in a matrix of yellowish and greenish-gray muds and muddy sands. Hydrotroilite was noted in a few of the cores from the banks. Most of the recovered bank sediments were unstructured (fig. 5-17). However, a few current laminations were noted in core 959 (fig. 5-17).

The composition of the coarse fractions in piston cores from the coral banks was essentially the same in every core (table 5-10). Only one core (958) contained any glauconite or quartz. The other cores contained sand fractions composed entirely of foraminifera, siliceous sponge spicules, pteropods, gastropods, and coral debris. Large aggregates of sponge spicules were observed in the cores suggesting that sponges died and were subsequently buried *in situ*.

No living colonial corals were collected from the coral banks during Eastward cruise E-2E-78. Living colonial corals were, however, collected from coral banks in the study area on an Albatross cruise in 1886. Using radiocarbon techniques, these corals dated 680 B.P. Such an old date obtained from a living coral probably reflects the age of the carbon pool in the water above the plateau. No dead radiocarbon dates (>45,000 yrs B.P.) were obtained from any of the coral samples dated in this study (table 5-1).

Slump Mass on the Lower Florida-Hatteras Slope

The areal extent of a slump mass first described by Edsall (1979) was delineated during Eastward cruise E-2E-78. Over 120 kilometres of high-resolution seismic profiles were taken in order to delineate the slump (fig. 5-18). Attempts to core into the main body of the slump failed because of its impenetrable nature which is apparently the result

Figure 5-17. Core X-radiographs of coral bank deposits. Core 959 contained several current laminations (arrows).

Figure 5-17

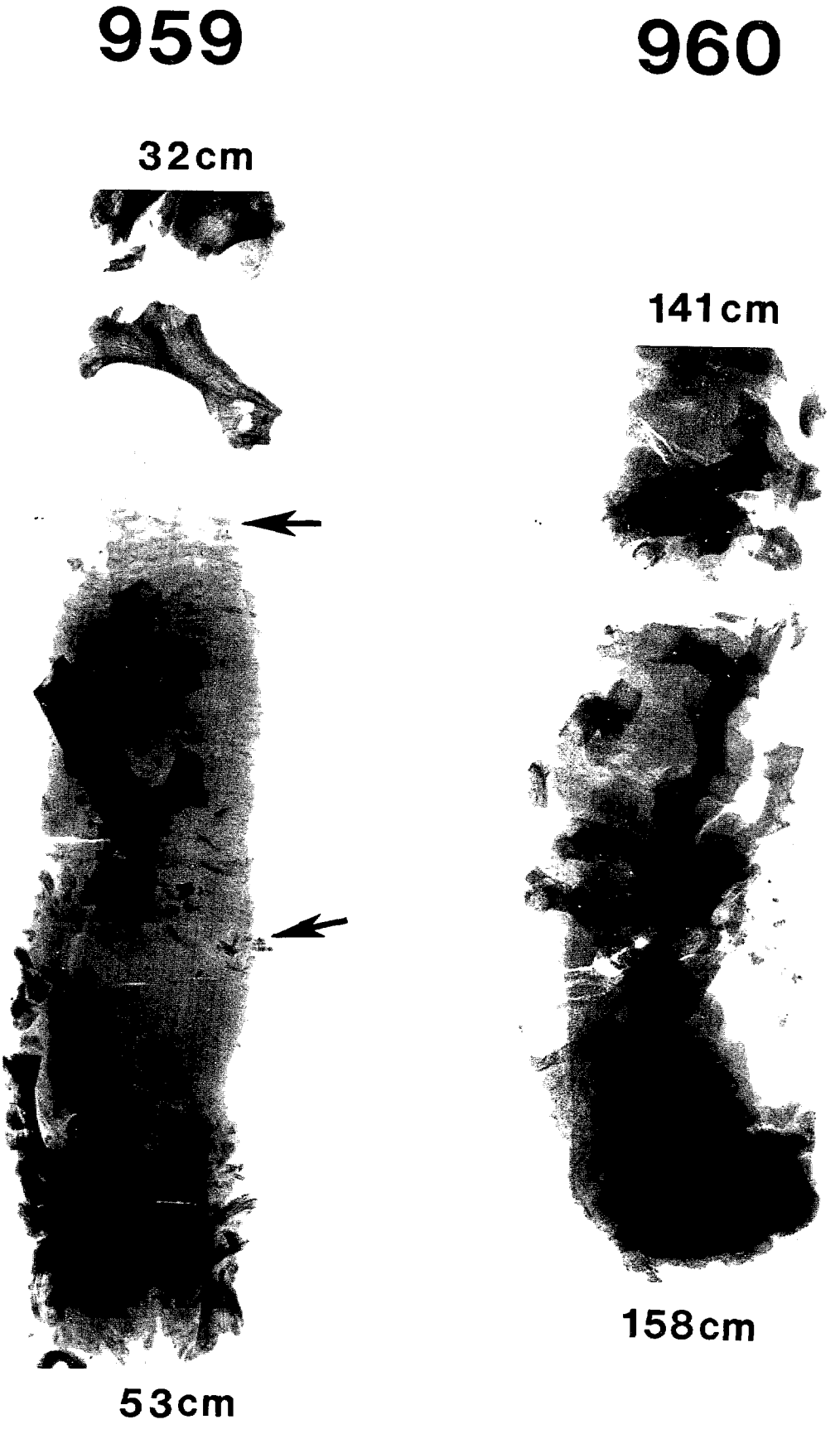

Table 5-10. Average composition and texture in select subsamples of cores recovered from the coral banks.

	Range in Values Hi	→	Lo	$\bar{x}$	sd
Percent Gravel	63	-	0	28	16
Percent Sand	86	-	14	37	20
Percent Mud	72	-	1	36	18
Percent $CaCO_3$	84	-	64	74	6
Mean Grain Size Φ	7.4	-	-0.9	3.2	1.9
Sorting Φ	5.6	-	1.2	4.4	1.3
Constitutents in Sand Fraction					
Quartz	49	-	0	2	9
Spicules	30	-	0	3	6
Phosphorite	--		--	0	0
Forams	86	-	25	54	17
Glauconite	9	-	0	1	2
Pteropods	38	-	0	14	12
Gastropods	32	-	0	11	9
Coral	58	-	0	10	12

Figure 5-18. Location of a slump mass (stippled) on the lower slope-inner plateau. Seismic profile lines (dashed lines) used to delineate the mass are shown. Bathymetry is taken from N.O.S. bathymetric charts (contoured in metres). The outlined area is shown in greater detail in figure 5-19.

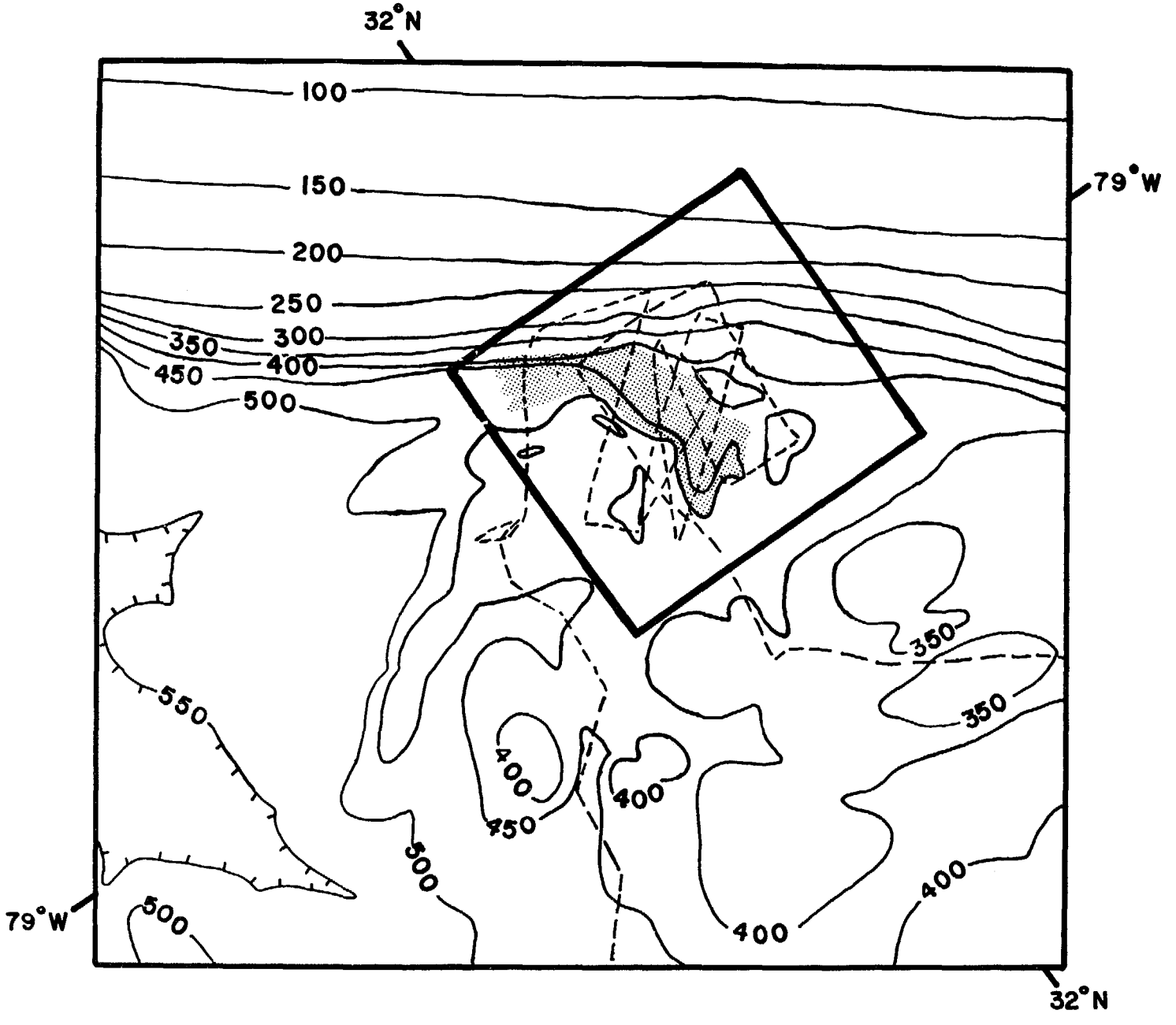
32°N
79°W
100
150
200
250
300
350
400
450
500
550
500
500
450
400
400
400
400
350
350
79°W
32°N

Figure 5-18

of a large phosphorite gravel content.

The slump mass covers 136 km^2. Figure 5-19 shows the distribution and thickness of the mass. The volume of the slump mass is 1.34×10^8 m^3. Assuming the sediment in the slump is the same density of that from the adjacent slope, its total mass would be roughly 2.38×10^8 metric tons. Table 5-11 is a comparison of this slump mass with others described in the literature.

Figure 5-20 is a profile taken across the thickest part of the slump. Evidence from this profile suggests the slump scarp is on the lower slope immediately above the slump mass. The slope of the scarp is approximately 10°.

No cores were recovered from the main body of the slump although cores 969 and 970 were taken near the slump (fig. 5-19). X-radiography of core 970 indicates it penetrated a debris flow. Core 969 was disturbed during extrusion so no attempts were made to X-ray it. However, visually, 969 resembles core 970, indicating it also penetrated the same debris flow. Radiocarbon dates of mud in the debris flow varied from 31,290 to 20,225 yrs B.P. Because of the proximity of cores 969 and 970 to the slump (<0.5 miles) they may have penetrated a debris flow that was associated with the slumping. If this is the case, the slumping must have occurred during the late Quaternary.

The section of the lower Florida-Hatteras Slope near the slump slopes steeply at an angle of 7°. Similar slumps have been triggered by earthquakes along other slopes that have gradients that are similar to those along the section of the Florida-Hatteras Slope near the slump mass (table 5-12). It is tempting to hypothesize that the slump on the Florida-Hatteras Slope was initiated by the Charleston earthquake of 1886. However, we have no evidence at this time that proves or

Figure 5-19. Location of the slump mass and the locations of piston core sites on or near the mass. The lower half of this figure is an isopach of the slump mass (isopached in metres).

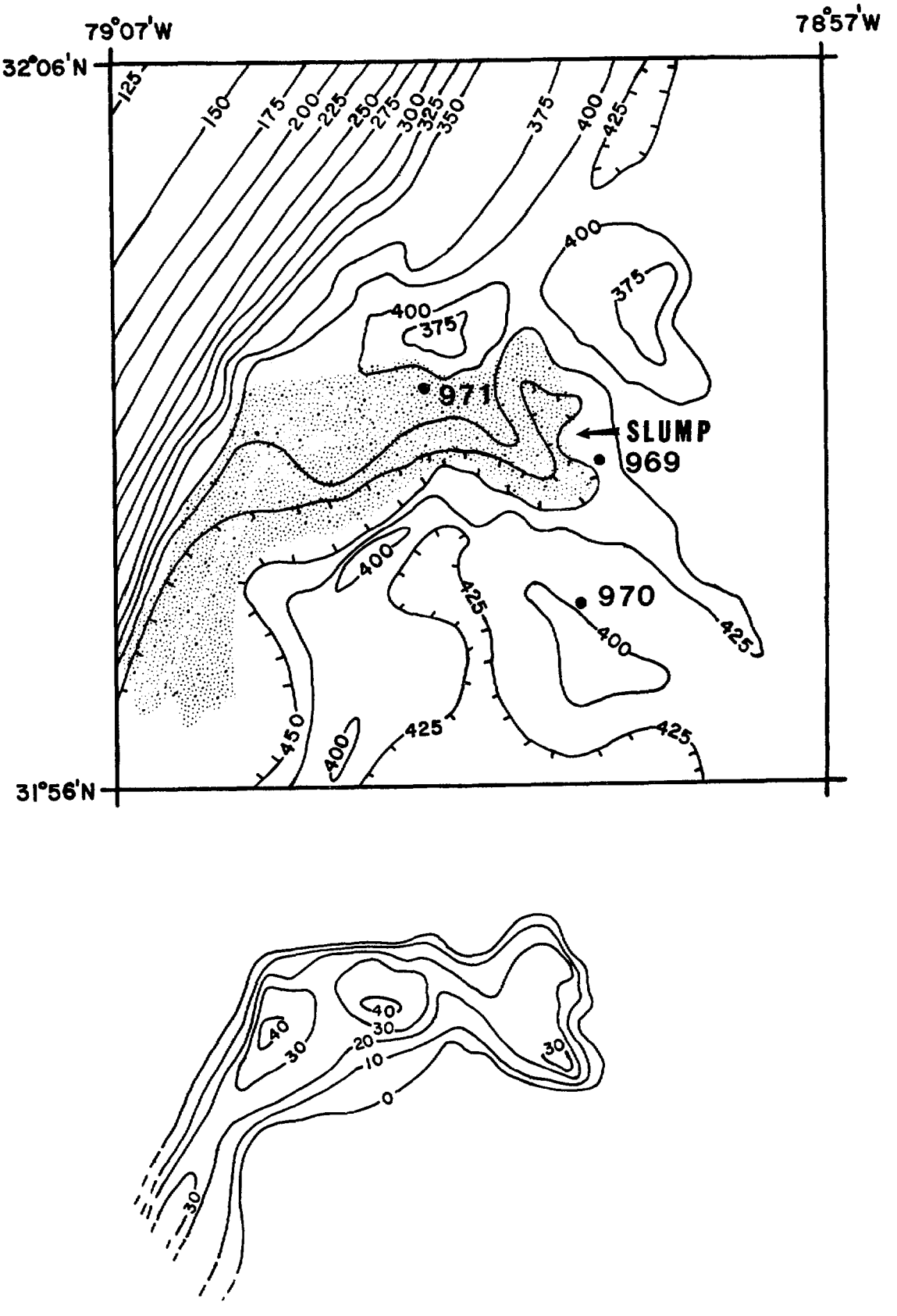
79°07'W
78°57'W
32°06'N
31°56'N
125
150
175
200
225
250
275
300
325
350
375
400
425
450
971
969
970
SLUMP
40
30
20
10
0

Table 5-11. Volumes of submarine slumps (after Scott and Zuckerman, 1970).

Location	Volume m^3
Magdalena River Delta, Colombia	3×10^8
Mississippi River Delta, USA	4×10^7
Suva, Fiji	1.5×10^8
Valdez, Alaska	7.5×10^7
Folla Fjord, Norway	3×10^5
Orkdals Fjord, Norway	10^7
Sagami Wan, Japan	7×10^{10}
Base of the Florida-Hatteras Slope*	1.3×10^8

*This study.

Figure 5-20. A seismic profile across the thickest part of the slump mass showing our interpretations of various features related to the slump.

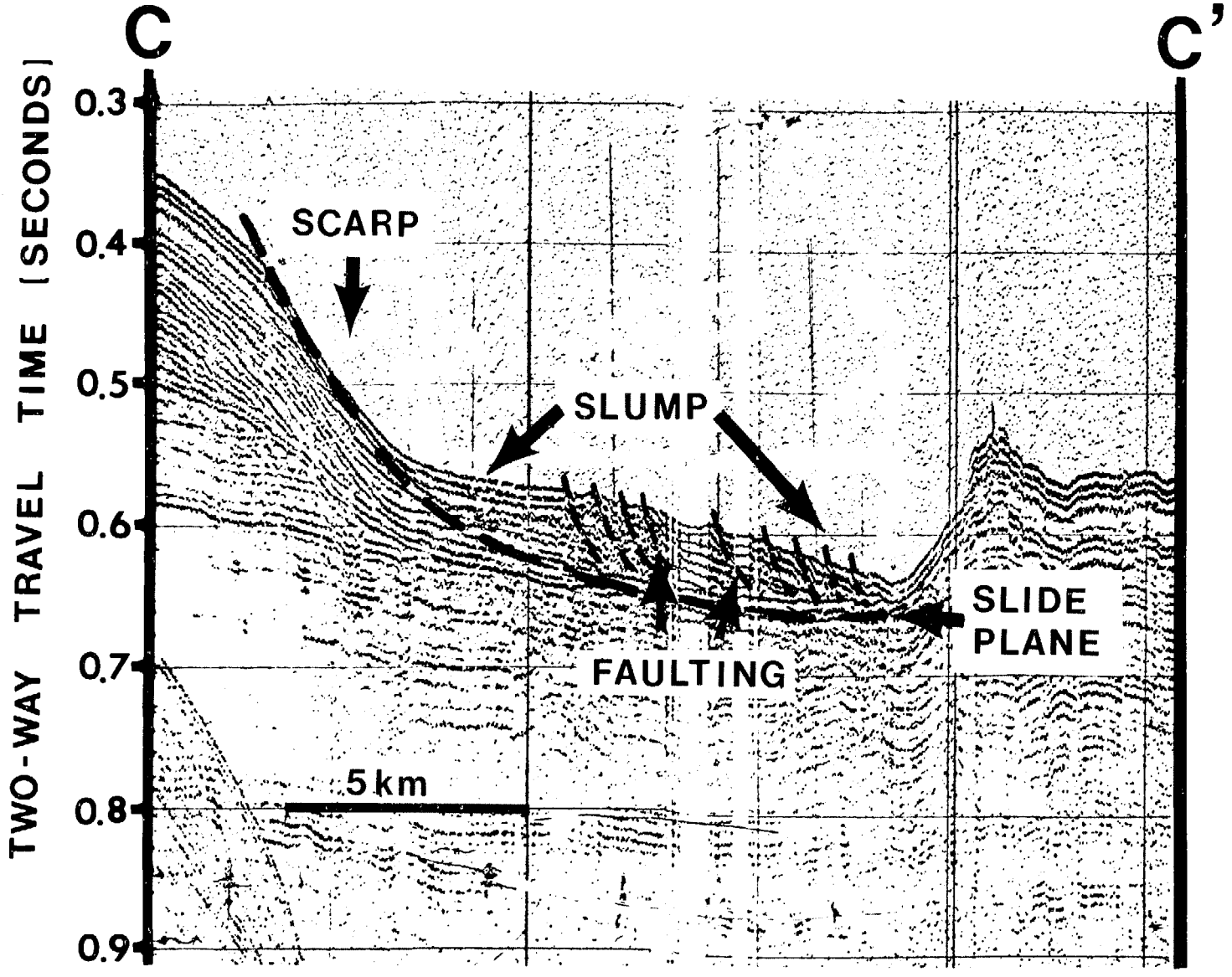
C
C'
TWO-WAY TRAVEL TIME (SECONDS)
0.3
0.4
0.5
0.6
0.7
0.8
0.9
SCARP
SLUMP
FAULTING
SLIDE PLANE
5 km

Figure 5-20

Table 5-12. Some slumps caused by earthquakes (from Scott and Zuckerman, 1970).

Location and Date	Slope Degrees	Magnitude (M)	Focal Depth (km)	Within Epicentral Region	Reference
Grand Banks, 1929	3.5	7.2	Shallow	Yes	Heezen and Ewing (1952)
Orleansville, 1954	4-20	6.7	7	No	Heezen and Ewing (1955)
Strait of Messina, 1908	4	7.5	8	Yes	Ryan and Heezen (1965)
Suva, 1953	3	6.75	60	Yes	Houtz (1962)
Chile, 1922	6	8.3	Shallow	No	Gutenberg (1939)
Valdez, 1964	6	8.5	Shallow	Yes	Coulter and Migliaccio (1966)
Aegean Archipelago, July 9, 1956	10	7.5	15	No	Ambraseys (1960) and Admiralty Chart No. 1866 (1951), Royal Hellenic Navy

disproves this hypothesis.

DISCUSSION

Origin of the Coral Banks on the Blake Plateau

Coral banks on the Blake Plateau have previously been described (Stetson and others, 1962). The framework of the banks are two species of ahermatypic and colonial coral (*Lophelia prolifera* and *Enallopsammia profunda*). Coral banks occur on the plateau primarily in linear groups although isolated banks were also observed (fig. 5-16). In Stetson's study area the individual banks average 0.5 miles in diameter and occur in groups of 200 or more. The largest bank described by Stetson and others (1962) is 480 feet high. Banks on the inner plateau described in this study are of lower relief, the highest being 300 feet. However, the areal extent of the group of banks on the inner plateau is much larger (fig. 5-16).

Factors controlling the distribution of these deepwater corals are not well known. It is likely, however, that at least three factors influence the location of coral banks on the Blake Plateau (Cairns, 1979). The optimum water temperature for deepwater corals varies but is always below the thermocline. Cairns (1979) reports near-bottom water temperatures at sites on the Blake Plateau where living corals were collected range from 6.0-12.0^{o}C. Stetson and others (1962) report bottom water temperatures near the coral banks that range from 7-10°C. Strong bottom currents are also needed to: 1) supply the coral with plankton; 2) keep the polyps clean of fine sediments; 3) help remove metabolic wastes; and 4) help promote the growth and distribution of the coral banks. Finally, there must be a clean hard surface where the coral larvae and living coral branches that are broken off the main

colony can attach and grow. Stetson and others (1962) suggest the attachment surfaces on the Blake Plateau are outcropping lithified carbonate rocks. Evidence here suggests that on the inner plateau the attachment surface is typically the surficial cover of Miocene phosphorite gravels and pavements. Phosphorite gravels and pavements recovered from the plateau often have solitary and colonial corals attached (Appendix 5-2). These gravels and pavements act as "hard grounds" like those found on the shelf, serving as an attachment surface not only for the corals but also for bryozoans, sponges, and worms. Wilson (1979) has found that under certain conditions large pieces of coral detritus that become partially buried in sediment can serve as attachment surfaces.

One of the major questions about these deepwater corals that still remains unanswered concerns the mechanism by which they are broken down. Stetson and others (1962) suggest that boring annelid worms, Ennicia, are capable of breaking down the coral or that fish that swim into the colonial corals seeking shelter might break off coral branches. Wilson (1979) has found evidence that clionid boring sponges attack dead parts of the coral colonies thus weakening branches which eventually break off. More recent work (Perkins, pers. comm., 1979) indicates that deepwater corals are attacked and weakened by a host of additional microboring organisms. During a dive on a deepwater coral bank, Wilson (1979) noted that the relatively weak currents created by the submersible were capable of breaking branches off the *Lophelia prolifera* colonies. If bottom currents are indeed capable of breaking down coral colonies, we would have a mechanism for the distribution of corals that would explain the long linear groups of coral banks such as those observed on the Blake Plateau. With this mechanism living coral

branches are broken off by the current and moved downstream along with coral larvae to a point where they settle on the bottom. Once on the bottom the detached living coral branches can reattach themselves and develop into a branching colony (Wilson, 1979).

A scenario is suggested here that would explain the dramatic difference in the relief of the coral banks on the inner plateau that were described farther seaward by Stetson and others (1962). The banks described by Stetson and others were located beneath a former course of the Gulf Stream (fig. 5-2) while the banks described here lie beneath the present course of the Gulf Stream. The meandering flow of the Gulf Stream periodically crosses the coral banks causing the breakdown of the colonial corals. In this manner the frequency with which the Gulf Stream meanders across the banks controls the height of the banks. The banks studied by Stetson and others (1962) are no longer subjected to the strong Gulf Stream bottom currents and can therefore grow to much greater heights.

Radiocarbon dates of colonial corals (table 5-1) from the plateau indicate the corals have existed on the inner plateau at least since late Pleistocene time. On the basis of seismic data, Edsall (1979) suggests the banks on the inner plateau could not have existed prior to the Quaternary because in seismic profiles the reefs on the inner plateau do not appear to have a substantial base of older reefal material.

It is important that the distinction be made between the coral banks of the Blake Plateau and the lithoherms described by Neumann and others (1975) in the Florida Straits. The two features cannot be differentiated in bottom profiles because they have similar morphologies and produce similar hyperbolic bottom returns. The colonial corals

Lophelia prolifera and *Enallopsammia profunda* grow on both the lithoherms and the coral banks. Because of these similarities the two features could incorrectly be considered synonymous. Lithoherms are mounds of indurated calcareous sands and the corals are only one part of the associated epifaunal assemblage that inhabit the lithoherms. Conversely, colonial corals form the framework for the coral banks which are composed mainly of unconsolidated sediments. Only two possible lithoherms on the plateau were identified during this study. At these two sites rock dredges (996 and 017) recovered large pieces of indurated sandstone with attached coral (Appendix 5-2).

Sedimentation on the Florida-Hatteras Slope and Inner Blake Plateau

The distribution of sediment on the continental shelf, the Florida-Hatteras Slope, and the inner Blake Plateau indicates there are five sources for the sediment that is currently being deposited. Shelf sands cover much of the slope south of 32°N. latitude (fig. 5-21). Normal slope muds like those found on the continental slope north of Cape Hatteras (Doyle and others, 1979) occur only along a narrow band at the base of the slope between 31°30′N. and 32°30′N. Between the shelf sand and the slope muds the slope is covered by a thin zone of transitional sediment. This transitional zone can be subdivided into two parts on the basis of quartz vs. foraminifera content. The transitional zone closest to the shelf sands contains a high percentage of quartz (68%) relative to foraminifera (7%). This is, therfore, considered a shelf dominant transitional sediment. Seaward of this is a zone of transitional sediment that contains a higher relative percentage of foraminifera (29%) and a lower relative percentage of quartz (31%). This zone contains a slope-dominant transitional sediment. On the basis

Figure 5-21. Sources of surficial sediments in the study area.

Figure 5-21

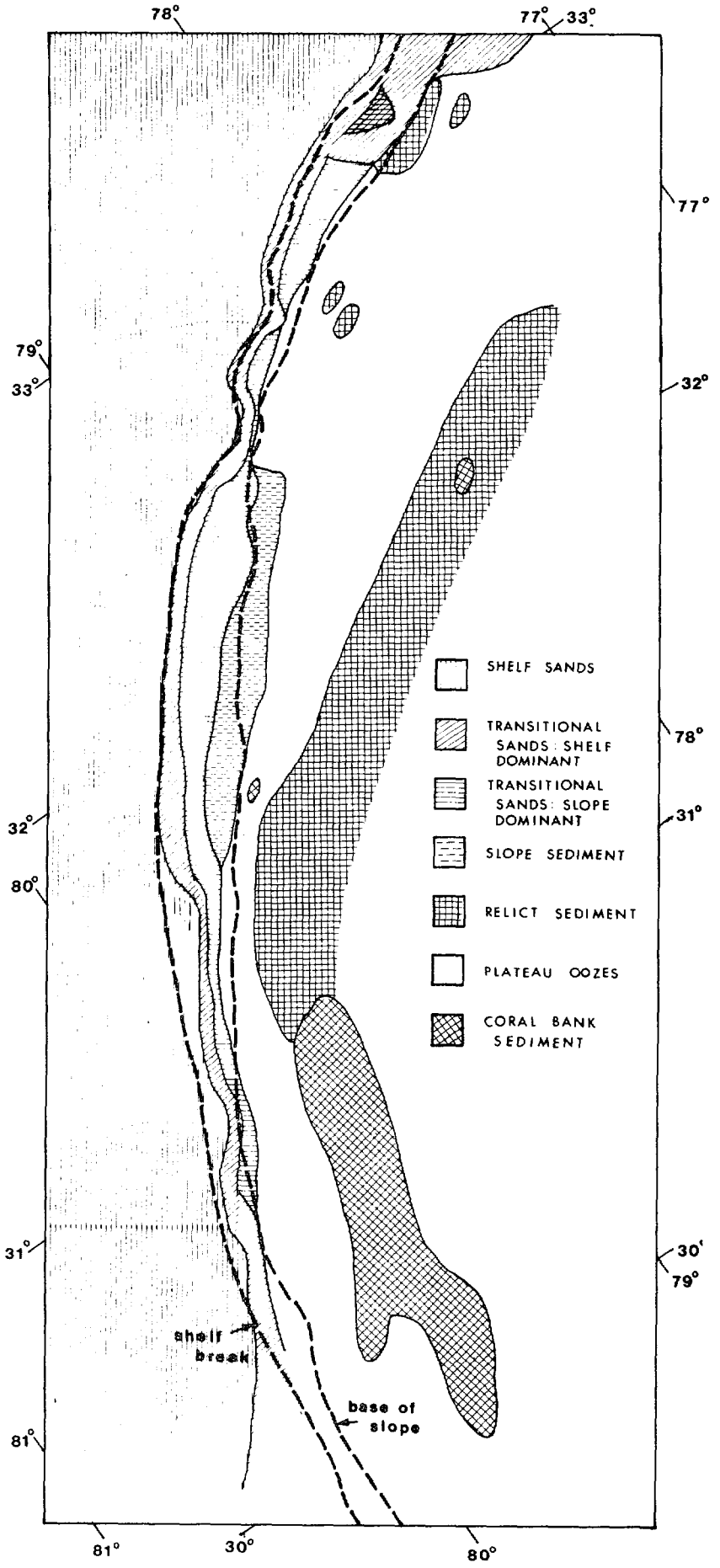
78°
77°
33°
77°
79°
33°
32°
78°
32°
31°
80°
31°
30'
79°
81°
81°
30°
80°
SHELF SANDS
TRANSITIONAL SANDS: SHELF DOMINANT
TRANSITIONAL SANDS: SLOPE DOMINANT
SLOPE SEDIMENT
RELICT SEDIMENT
PLATEAU OOZES
CORAL BANK SEDIMENT
shelf break
base of slope

of these sediment distributions the shelf appears to be an important source of slope sediment.

Doyle and others (1979) have previously suggested that shelf sands are carried over the shelf break and onto the Florida-Hatteras Slope by shelf-edge spillover. Unfortunately, the mechanics of shelf-edge spillover are not well known. It is likely that the spillover results when shelf sands are swept over the shelf break by high wave energy during storms, incursions of the Florida Current (Gulf Stream) onto the shelf, or the Gulf Stream Counter Current. The high energy bottom current regime makes it difficult to explain the deposition of muds on the slope. Doyle (pers. comm., 1979) believes the slope muds are hemipelagic. He suggests they reach the bottom aggregated in fecal pellets. Mud patches on the inner plateau (fig. 5-2) are probably outcropping muddy pre-Holocene sediments.

Most of the Blake Plateau sediments being deposited today contain a residual component. Residual sediments are those sediments reworked from outcropping and subcropping units of the inner plateau. In figure 5-21, only those inner plateau sediments that contain an abundance of nonbiogenic constituents (glauconite, phosphorite, and quartz) are labeled as residual. No attempt was made to evaluate the relative contribution of residual foraminifera to the sediment. Accordingly, sediment labeled as "plateau ooze" in figure 5-21 is not necessarily a first cycle pelagic deposit like that found on the outer plateau (Milliman, 1972). Coral banks are significant sources of coral detritus on most parts of the inner plateau (fig. 5-16). The sediments labeled "coral bank" in figure 5-21 are only those that were actually recovered from the coral banks. These are typically yellowish-gray, muddy, and sometimes sandy coral gravels. Sediments in piston cores

from the inner plateau are residual, relict (from pre-Holocene strata) or first cycle biogenic. The downslope movement of sediment from the shelf or slope does not appear to be an important source of sediment on the inner plateau. No sedimentary structures indicative of turbidites were observed in the cores. There were also no units of quartzose-shelly shelf sands found in the cores.

The most striking feature of the inner plateau cores was the lack of thick current-laid deposits. Sedimentary structures indicative of current deposition such as laminations and cross-beds were observed in the cores (figs. 5-6A through 5-6D). However, these were typically thin units that were separated by zones of highly mottled and unstructured sediment. This intermittent occurrence of current-laid deposits suggests bottom currents on some parts of the plateau are ephemeral short-lived events. Changes in sediment texture throughout the cores (fig. 5-4) also indicate that radical changes in the energy of the prevailing bottom current regime at the point of deposition has occurred throughout time.

Several features of the water circulation above the plateau could explain this apparently temporal nature of the bottom currents. Seasonal meanders of the Gulf Stream have been thoroughly documented (Iselin, 1940). Eddy currents are known to exist along the eastern margin of the Gulf Stream. Warren (1967) observed one of these eddy currents that became detached and flowed away from the Gulf Stream with maximum surface velocities of 200 $cm.s^{-1}$.

Indirect evidence for the velocity of the inner plateau bottom currents is presented here. Phosphorite gravel beds occur in the tops of cores 987 and 989. The phosphorite gravels are known to be Miocene in age (Manheim and others, 1979) and commonly occur as lag deposits on

the plateau. Radiocarbon dates beneath these two gravel beds, however, are late Pleistocene indicating the gravels were deposited since that time. Because of the low regional slope in the area of cores 987 and 989 (fig. 5-1) and because of the sedimentary structures of these two gravel beds (fig. 5-9) it is unlikely they are slump or density current deposits. The most likely explanation is that these are current deposits. Gravels in the beds range from 2 to 25 mm. Assuming the slope of the bottom over which the gravels were transported was negligible, bottom current velocities needed to move these gravels would have been in excess of 80 $cm.s^{-1}$ (Nevin, 1946). It is possible that these gravels were transported during the late Pleistocene when bottom currents were thought to be much stronger (Uchupi, 1967).

CONCLUSIONS: POTENTIAL HAZARDS IMPLIED BY THIS STUDY

There are several phenomena in the study area that may be of interest to individuals concerned with the evaluation of potential hazards on the Florida-Hatteras Slope and inner Blake Plateau. The Gulf Stream may cause problems with its strong bottom currents (at least 40 $cm.s^{-1}$). Temporal variations in the velocities of bottom currents on the Blake Plateau are implied by sedimentary textures and structures. Meandering of the Gulf Stream and also eddy currents that become detached from the main flow are capable of creating short-lived bottom currents on the Blake Plateau. The temporal nature of bottom currents on the Blake Plateau must, therefore, be considered to correctly evaluate potential bottom current related hazards.

Slumping is not an important process on most of the Florida-Hatteras Slope since the regional slope is typically less than 2°. However, on the central portions ($31^{\circ}10'$-$32^{\circ}15'$N.) the

Florida-Hatteras Slope between the 100-500 metre isobaths is often as steep as 7° (fig. 5-18). This is also the area where the slump mass was observed on the inner plateau. Accordingly, slumping must be considered a potential hazard along this part of the slope.

On the inner plateau the deposition of sediments transported by gravity-induced flows is not important. Doyle (pers. comm., 1979) has, however, found turbidites on the Florida-Hatteras Slope. Gravity-induced sediment flows such as turbidity currents are known to result from slope failure triggered by slope disequilibrium or earthquakes. Sediment overbuilding or erosional undercutting can lead to slope disequilibrium that can ultimately result in slope failure. This is the mechanism which is thought to have triggered numerous turbidity currents on the northeastern U. S. continental margin during the Pleistocene (Cleary and others, 1977). During the twentieth century several earthquakes are also known to have caused submarine slumping which in turn triggered turbidity currents.

On the Florida-Hatteras Slope, gravity-induced flows can be triggered by earthquakes. Alternatively, upper slope sediment overbuilding as a result of shelf-edge spillover may lead to slope disequilibrium and failure. The unequal distribution of shelf sediments on certain parts of the Florida-Hatteras Slope indicates the frequency of downslope movement of shelf sediments by gravity-induced flows is variable along the length of the slope. Zones where the gravity-induced flows are more frequent are consequently higher risk sites for drilling structures.

To determine the importance of gravity-induced flows as potential hazards we must know more about the frequency and magnitude of these sediment flows. High-resolution seismic data cannot be used to

determine this information because of the size of the deposits. For example, the turbidite deposited as a result of the Grand Banks earthquake is less than one metre thick. Preliminary work by the authors indicates the Orleansville turbidite is only a few centimeters thick. Yet both of these turbidity currents were strong enough to break submarine telephone cables. A study of piston core stratigraphy is the only way we can properly evaluate the role gravity-induced current deposits play in the formation of the slope. To date we have recovered over 90 piston cores from the Florida-Hattera Slope and inner Blake Plateau. These cores provided an inadequate coverage for defining areas on the slope that are subjected to frequent density flows. However, because the turbidites are found only in cores from the Florida-Hatteras Slope and not in cores from the inner Blake Plateau we can infer that the gravity-induced flows within the study area are probably not as large as the Orleansville or Grand Banks turbidity currents.

REFERENCES CITED

Cairns, S., 1979, personal communications, Smithsonian Institute, Washington, D.C.

Charlot, G., 1965, Rapid detection of Cations and Anions: Chemical Publishing Company, Inc., New York, 106 p.

Charm, W. B., Nesteroff, W. D., and Valdes, S., 1969, Detailed stratigraphic description of the JOIDES cores on the continental margin off Florida: U. S. Geological Survey Professional Paper 581-D, 13 p.

Cleary, W. J., Pilkey, O. H., and Ayers, M. W., 1977, Morphology and sediments of three ocean basin entry points, Hatteras Abyssal Plain: Journal Sed. Petrology, v. 47, p. 1157-1170.

Doyle, L. J., Pilkey, O. H., and Woo, C. C., 1979, Sedimentation on the eastern United States continental slope: in Slope Sedimentation, Soc. Economic Paleontologists and Mineralogists Special Publication No. 27, p. 119-129.

Edsall, D. W., 1979, Southeast Georgia Embayment high resolution seismic reflection survey: U. S. Geological Survey Open-File Report 78-800, 90 p.

Folk, R. L., 1974, Petrology of sedimentary rocks: Austin, Texas, Hemphill Publishing Co., 181 p.

Hawkins, L. K., 1969, Visual observations of manganese deposits on the Blake Plateau: J. Geophy. Res., v. 74, p. 7008-7017.

Heezen, B. C., and Hollister, C. D., 1971, The face of the deep: New York, Oxford Univ. Press, 659 p.

Hollister, G. D., 1973, Atlantic continental shelf and slope of the United States - texture of surface sediments from New Jersey to southern Florida: U. S. Geological Survey Professional Paper 529-M, 23 p.

Hunt, R. E., Swift, D. J. P., and Palmer, H., 1975, Constructional shelf topography - Diamond Shoals, North Carolina: Geol. Soc. Am. Bull., v. 86, p. 143-147.

Iselin, C. O.'D., 1940, Preliminary report on long-period variations in the transport of the Gulf Stream system: papers in Physical Oceanography and Meteorology, v. 8, 40 p.

Krinitzsky, E. L., 1970, Radiography in the earth sciences and soil mechanics: New York, Plenum Press, 163 p.

Manheim, F. T., Pratt, R. M., and McFarlin, P. F., 1979, Composition and origin of phosphorite deposits of the Blake Plateau: in Marine Phosphate, Soc. Econo. Paleontologists and Mineralogists Special

Publication (in press).

Milliman, J. D., 1972, Atlantic continental shelf and slope of the United States - petrology of the sand fraction of sediments, northern New Jersey to southern Florida: U. S. Geological Survey Professional Paper 529-J, 40 p.

Neumann, A. C., Kofoed, J. W., and Keller, G. H., 1977, Lithoherms in the Straits of Florida: Geology v. 5, p. 4-10.

Paull, C. K., and Dillon, W. P., 1979, The subsurface geology of the Florida-Hatteras shelf, slope, and inner Blake Plateau: U. S. Geological Survey Open-File Report 79-448, 93 p.

Poag, C. W., 1978, Stratigraphy of the Atlantic continental shelf and slope of the United States: in Annual Review of Earth and Planetary Sciences, v. 6, p. 251-280.

Pratt, R. M., 1963, Bottom currents on the Blake Plateau: Deep-Sea Research, v. 10, p. 245-249.

Pratt, R. M., 1966, The Gulf Stream as a graded river: Limnology and Oceanography, v. 11, p. 60-67.

Scott, R. F., and Zuckerman, K. A., 1970, Study of slope instability in the ocean floor: California Inst. of Technology Report No. CR-70.007, 61 p.

Stetson, T. R., Squires, D. F., and Pratt, R. M., 1962, Coral banks occurring in deep water on the Blake Plateau: American Museum Novitates, No. 2114, 39 p.

Stetson, T. R., Uchupi, E., and Milliman, J. D., 1969, Surface and subsurface morphology of two small areas of the Blake Plateau: Transactions - Gulf Coast Association of Geological Societies, v. 19, p. 131-142.

Uchupi, E., 1967, The continental margin south of Cape Hatteras, North

Carolina: Shallow structure: Southeastern Geology, v. 8, p. 155-177.

Warren, B. A., 1967, Notes on translatory movement of rings of current with application to Gulf Stream eddies: Deep-Sea Reseach, v. 14, p. 505-524.

Wilson, J B., 1979, "Patch" development of the deep-water coral Lophelia Pertusa on Rockall Bank: Journal Marine Biological Association of the United Kingdom, v. 59, p. 165-177.

CHAPTER 6

OCEAN BOTTOM SURVEY OF THE GEORGIA BIGHT

Vernon J. Henry, Jr.[1], Charles J. McCreery[1], Francis D. Foley[1], and David R. Kendall[1]

[1]Skidaway Institute of Oceanography, University of Georgia, Savannah, Georgia 31406

[2]U.S. Army Corps of Engineers, Savannah, Georgia 31406

CHAPTER 6

Table of Contents

Page

Abstract. 6- 1

Introduction. 6- 2

Bottom features and sediment character. 6- 6

Textural characteristics of the bottom sediments. 6- 6

Bed forms 6-12

Ripples 6-12

Megaripples 6-12

Sand waves. 6-12

Other bottom textures 6-26

Areas of local scour. 6-26

Bioturbation. 6-31

Hard bottoms. 6-31

Low-relief hard bottom. 6-37

Moderate-relief hard bottom 6-37

High-relief hard bottom 6-44

Live bottom 6-44

Reefs and hard bottoms as biologically sensitive features

and geologic hazards. 6-55

Shallow subsurface geology. 6-60

Seismic stratigraphy. 6-60

Upper acoustic reflector. 6-61

Lower acoustic reflector. 6-64

Channeling. 6-64

Deep channels 6-64

Shallow channels. 6-67

Table of Contents

(continued)

Page

Large sedimentary structures. 6-67

Faulting. 6-74

Video (CCTV) interpretation of benthic environments 6-74

Interpretation scheme 6-74

Distribution of benthic environments. 6-79

References cited. 6-83

CHAPTER 6

OCEAN BOTTOM SURVEY OF THE GEORGIA BIGHT

Vernon J. Henry, Jr., Charles J. McCreery, Francis D. Foley,

and David R. Kendall

ABSTRACT

During the period July 1978 through May 1979, four cruises were conducted on the continental shelf of the Georgia Bight by the University of Georgia Marine Geology Program personnel to determine the occurrence and distribution of biologically sensitive areas (reefs/live bottoms) and shallow geological hazards (channels, faults, scour, etc). Instrumentation used consisted of Uniboom[1], 3.5 kHz, side-scan sonar, and towed underwater television.

Surface texture of coarse sediment gave strong returns and finer sediment gave weaker returns on sonograms. In most instances, the former represented outcrops of shallow, acoustically hard reflectors, often supporting reefs, and/or live bottoms, and the latter indicated a thin mobile veneer of finer material associated with the latest rise of sea level.

At least two shallow subsurface reflectors were present that appear to represent separate exposure of the continental shelf during lower sea-level stands. Numerous channels and cut-and-fill structures reflect fluvial process active at such times. The larger channels, up to 40 m in depth, are downcut through the deeper reflector while the smaller channel and cut-and-fill structures are generally established upon the

---

[1]Use of brand names in this report is for descriptive purposes only and does not constitute endorsement by the U.S. Geological Survey.

shallower reflector. A tentative correlation of the shallower reflector with the Pleistocene erosion surface and the deeper with the top of the middle Pliocene is suggested based on their relationship to wedges of large foreset beds and similar stratigraphic features described by other workers for the inner shelf of Georgia and Florida.

The distribution of sessile benthic and pelagic biota appears random but related to the presence of reefs and hard bottoms. Rock dredging and shallow vibracoring is needed to determine the age relationships of the reflector outcrops and live-bottom substrates.

INTRODUCTION

A series of four cruises, designated as GS-1 through GS-4, were conducted on the continental shelf of the Georgia Bight by University of Georgia Marine Geology Program personnel between July 1978 and May 1979. This survey was made to identify types and distribution of hard bottom/live bottom of environmental concern and areas where geological conditions on the ocean bottom and shallow subsurface may present a hazard or constraint to potential hydrocarbon development.

The survey area was limited by the 50-m bathymetric contour to the east; Jacksonville, Florida, to the south; and Beaufort, South Carolina, to the north; totalling approximately 18,150 km^2. Average dip-line spacing is 10 km with strike lines located approximately at the 10 m, 25 m, 40 m, and 45 m bathymetric contours (fig. 6-1). Lease blocks of Sale 43 and Proposed Sale 56 traversed during the cruises are given in table 6-1.

Systems used in the survey were an O.R.E. 3.5-kHz tuned transducer; EG&G model 225 Uniboom transducer; EG&G Mark IB side-scan sonar; and a Jay-Mar Ocean Eye 1000 black and white underwater

Figure 6-1. Location of University of Georgia cruises GS-1 through 4, July 1978 - May 1979.

Figure 6-1

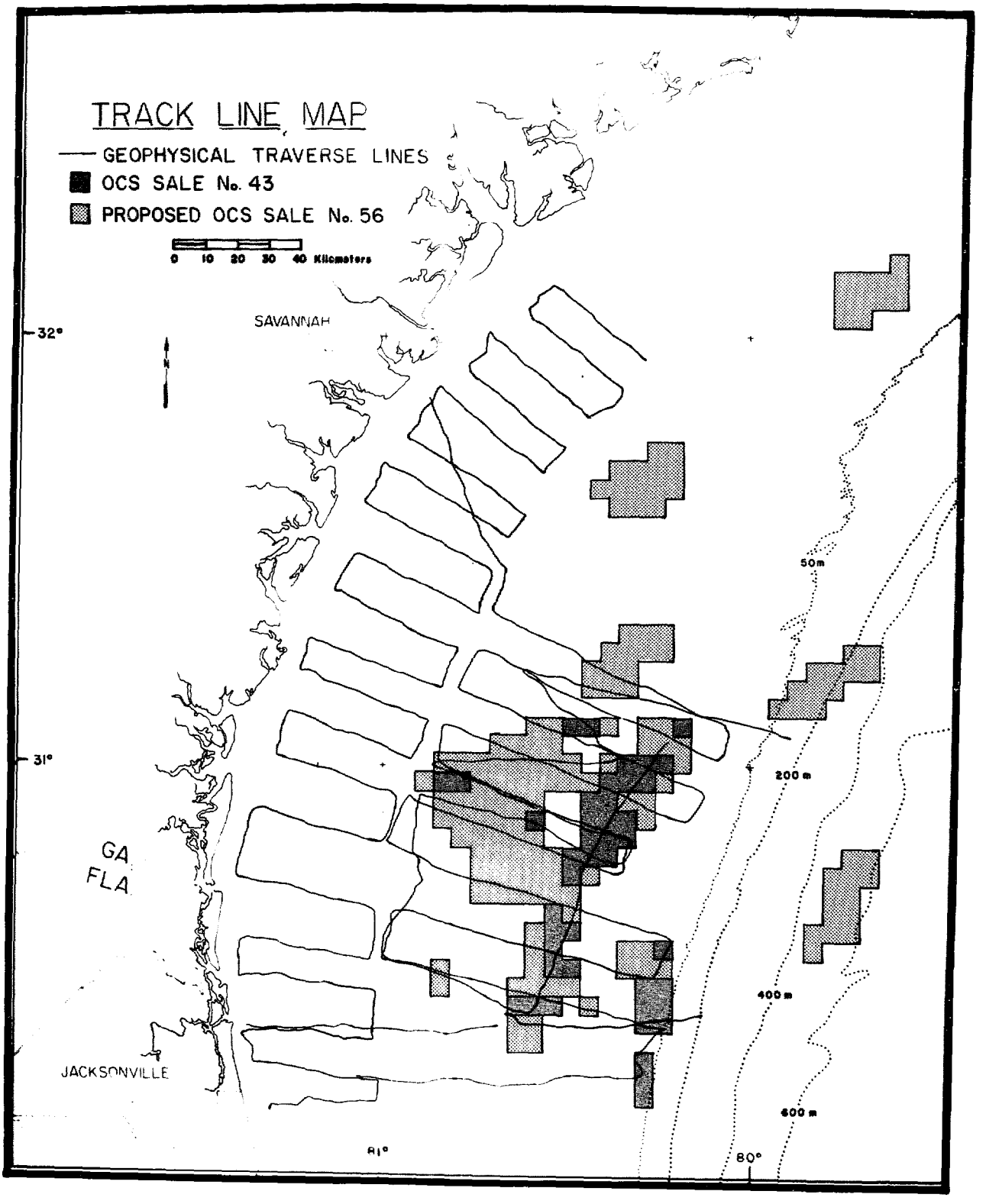
TRACK LINE MAP
GEOPHYSICAL TRAVERSE LINES
OCS SALE No. 43
PROPOSED OCS SALE No. 56
0 10 20 30 40 Kilometers
SAVANNAH
32°
31°
GA
FLA
JACKSONVILLE
81°
80°
50m
200 m
400 m
600 m

Table 6-1. Lease Blocks Traversed

OCS Sale No. 43

Brunswick Quadrangle (NH 17-2)	Jacksonville Quadrangle (NH 17-5)	
912	34	210
913	35	252
918	36	384
1003	78	427
1004	118	433
1005	121	471
	122	557
	123	558
	165	564
	167	565
	208	608
	209	609
		696

OCS Proposed Sale No. 56

Brunswick Quadrangle (NH 17-2)	Jacksonville Quadrangle (NH-17-5)		
781	24	114	340
782	27	115	382
783	28	116	426
825	29	117	465
826	33	161	475
827	69	162	476
910	70	247	513
911	71	248	514
916	72	249	515
917	73	253	561
961	74	294	601
962	79	295	602
	80	296	

television, mounted on a tow sled so as not to compromise traverse speed. Position was verified at 15-min intervals by a Northstar 6000 Loran-C receiver.

The following line kilometres of continuous data were collected:

3.5-kHz tuned transducer	2,163 km
Uniboom	2,228 km
Side-scan sonar	2,255 km
Underwater-towed television	550 km

An in-house designed prototype acoustic sediment probe was tested during the survey. The Uniboom system and a production version of the probe will be used on future surveys in conjunction with a micro-processor-controlled frequency spectrum analyzer to determine sediment textural characteristics.

BOTTOM FEATURES AND SEDIMENT CHARACTER

Side-scan sonar is the primary tool in determining conditions on the bottom, whether it be mobile, inactive, scour dominated, or hard bottom capable of supporting abundant benthic populations. With the exception of hard bottoms which are treated separately, these bottom conditions, some of which pose engineering constraints, are plotted on the "Texture/Bed Forms" Map Series A (plate in pocket in back cover).

Textural Characteristics of the Bottom Sediments

Bed forms and textural patterns were mapped based upon interpretation of side-scan sonar and 3.5-kHz data. Textural changes were plotted as plan-view contacts. Based on these plots, texture between contacts may be interpolated to be gradational or continuous, as indicated.

Subbottom profiles and sonograms indicate that the bottom is

largely covered by a relatively thin veneer of sand. The decreased thickness of the sand veneer on the outer part of the shelf is probably due both to scour during storm events as well as the increased distance from any modern coastal sediment source. Up to 90% of the inner shelf and as much as 50% of the outer shelf is overlain by this veneer. Thickness of the deposit ranges from 0 to 3 m or more, as indicated by 3.5-kHz records.

Sediments underlying the surficial sand appear to be more indurated or of a slightly coarser grain size or higher shell content, yielding a stronger return on sonograms when outcropping. Apparently this sediment is unconsolidated in the upper portion as it will support the formation of small-scale bed forms. For this reason, areas showing strong returns do not alone imply scour zones. This evaluation can be made in conjunction with "Hard bottom/Live bottom" Map Series B (plate in pocket in back cover) showing areas where the strong subsurface reflector, described below, outcrops. The actual petrology of the sand veneer as well as the strong reflector layer is still largely unknown due to the lack of ground-truth samples.

Records indicate that sediment types, including that of the sand veneer tend to migrate as units or patches. Plan-view contacts of sediment of different grain size may be found to be sharp or gradational probably dependent on water depth, current activity, and bed-form morphology. Changes in sediment texture, not necessarily related to bed forms, occur on the shelf as a result of scour into differing strata such as channel fills, accumulation of coarse sediment in troughs and depressions (fig. 6-2), and terminations of overlying veneers of sediment (fig. 6-3).

Figure 6-2. Strong return on sonogram (lower record) produced by coarse sediment in topographic trough. Note presence of shallow strong reflector on 3.5 kHz profile. (Line 1_4 @ 1300 hours.)

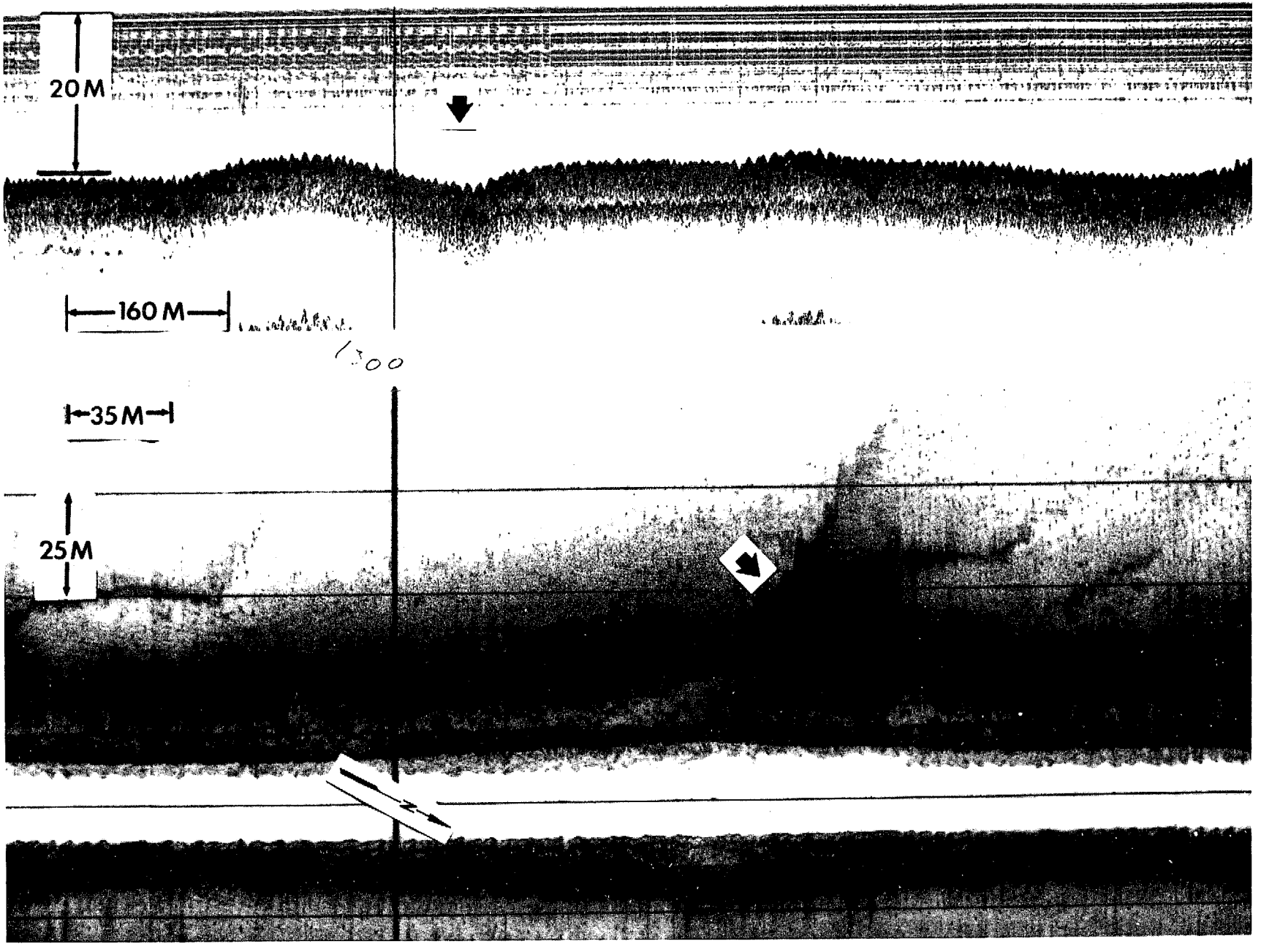

Figure 6-2

Figure 6-3. Sharp contact of sand veneer (light return) and underlying sediments (strong return). Note "bump" on 3.5-kHz profile representing contact. North is to the right (line 36_4 at 2034 hours).

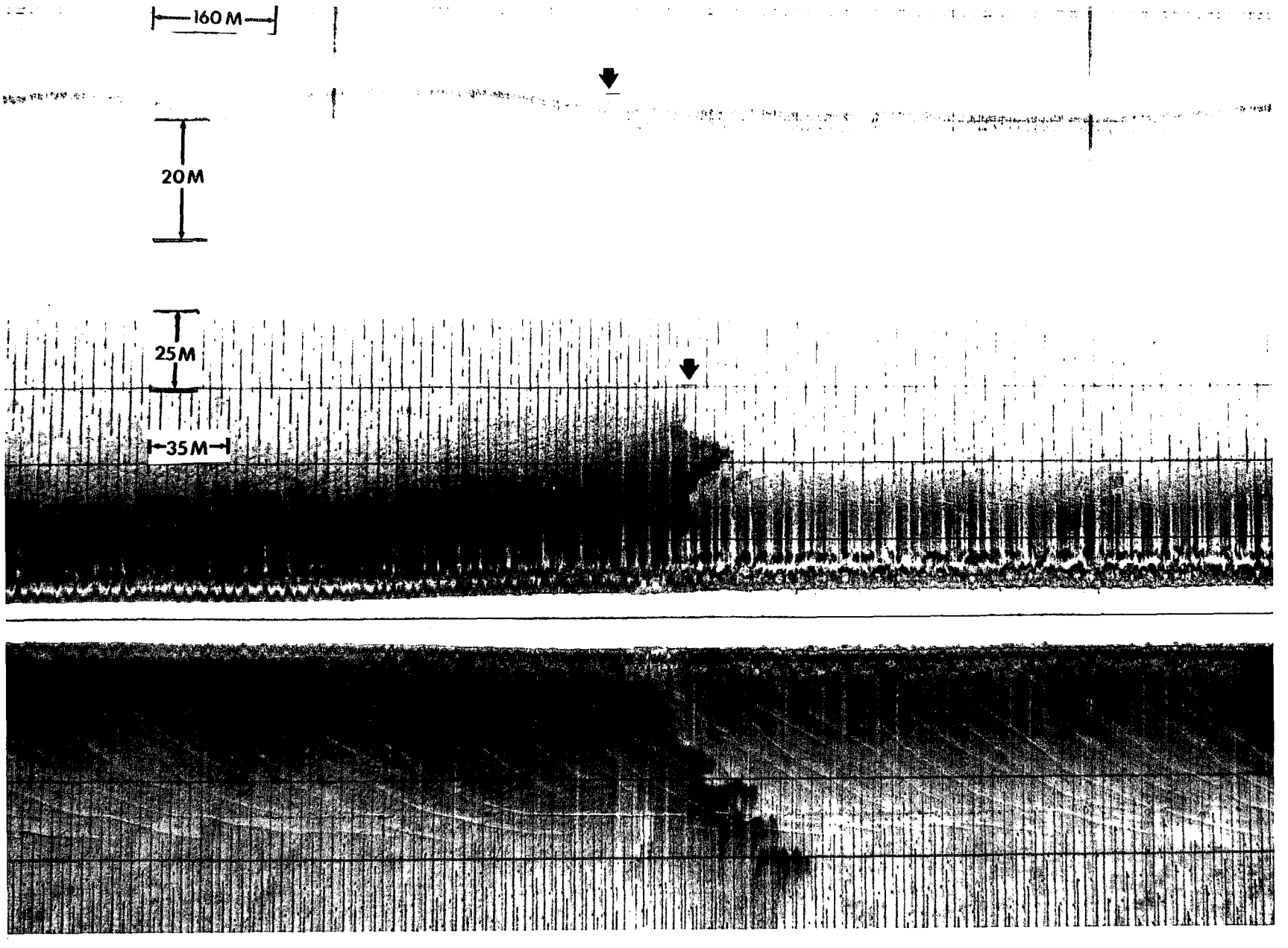

Figure 6-3

Bed Forms

Ripples

Mobile bed forms, occurring in varying types and sizes, are very common on the Georgia shelf. Closed-circuit underwater-towed television shows that small ripples (wave length <0.5 m) are common across the shelf independent of water depth (fig. 6-4). Ripple crests are commonly oriented north-south.

Sharp boundaries of grain size are shown by underwater-towed television and at times display different ripple morphology across these boundaries - finer grained sediments forming longer wave length and highly asymmetric ripples while coarser-appearing sediments support shorter wave length ripples that are slightly asymmetric.

The presence of algal growth along the crests of many of the ripples infers inactivity, indicating that shear stress on bottom sediments sufficient for bed-form migration is probably present only during storm events.

Megaripples

Megaripples of 0.5 to 1 m wave length are also common on the shelf (fig. 6-5). These bed forms are on the lower limit of resolution for the side-scan sonar system at the 200 m range and often are not observed if the crest orientation is perpendicular to the traverse direction. For this reason, many of the megaripple fields mapped were located on the midshelf strike lines, showing northerly orientation of the crest.

Sand Waves

Large-scale sand waves of up to 100 m wave length are common especially in the nearshore, where wave action has greater impact. Three different morphologies of large-scale sand waves have been recognized in this size category: linear parallel sand waves with

Figure 6-4. Underwater-towed television image of ripples. Wave length is approximately 30 cm. Camera is looking seaward (line 13_3 at 0931 hours).

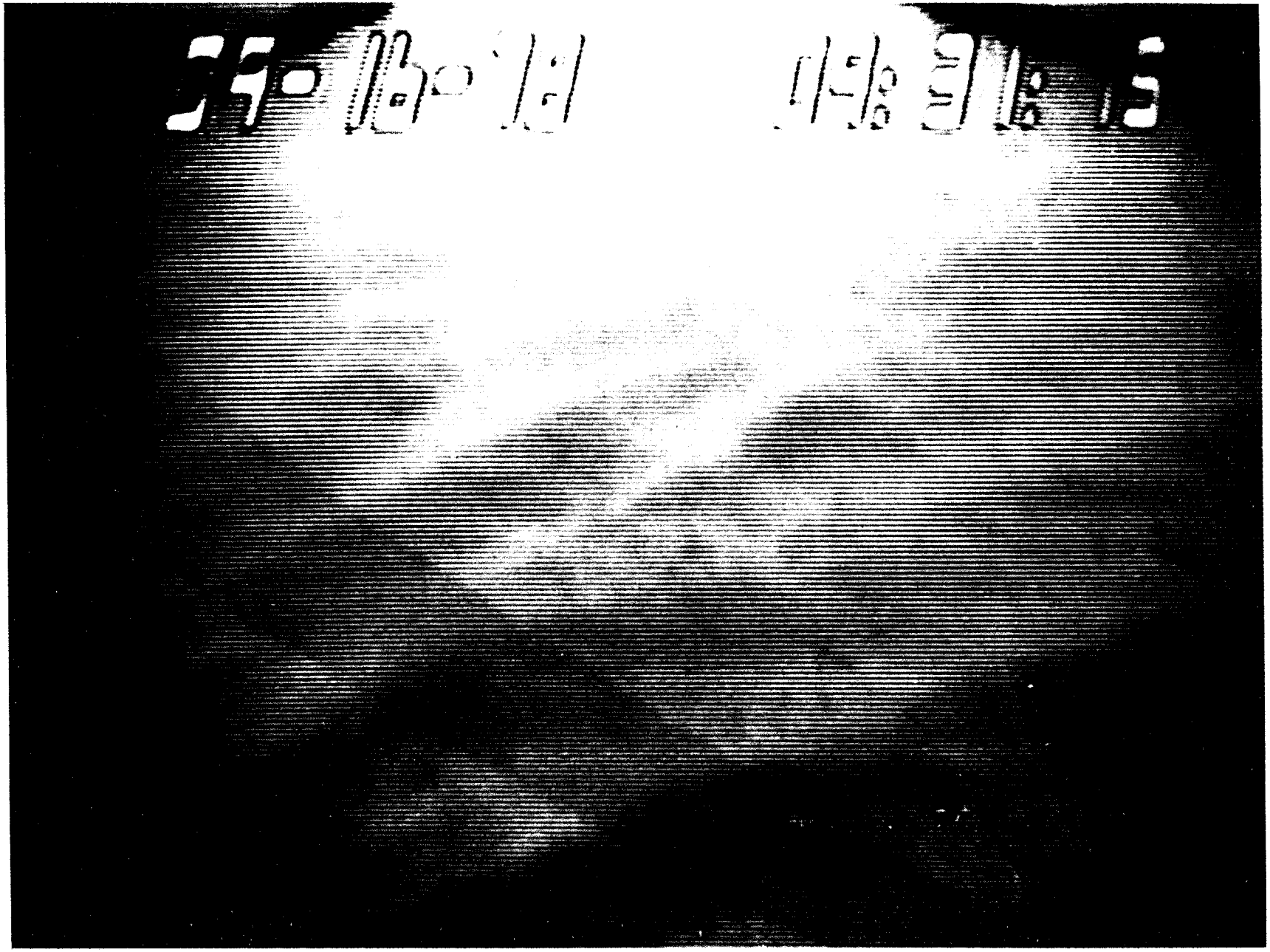

Figure 6-4

Figure 6-5. Sonogram of a well developed megaripple field located near the shelf edge. Wave length is approximately .5 m. Note topographic expression at arrow indicating migration offshore (line 15_3 at 1417 hours).

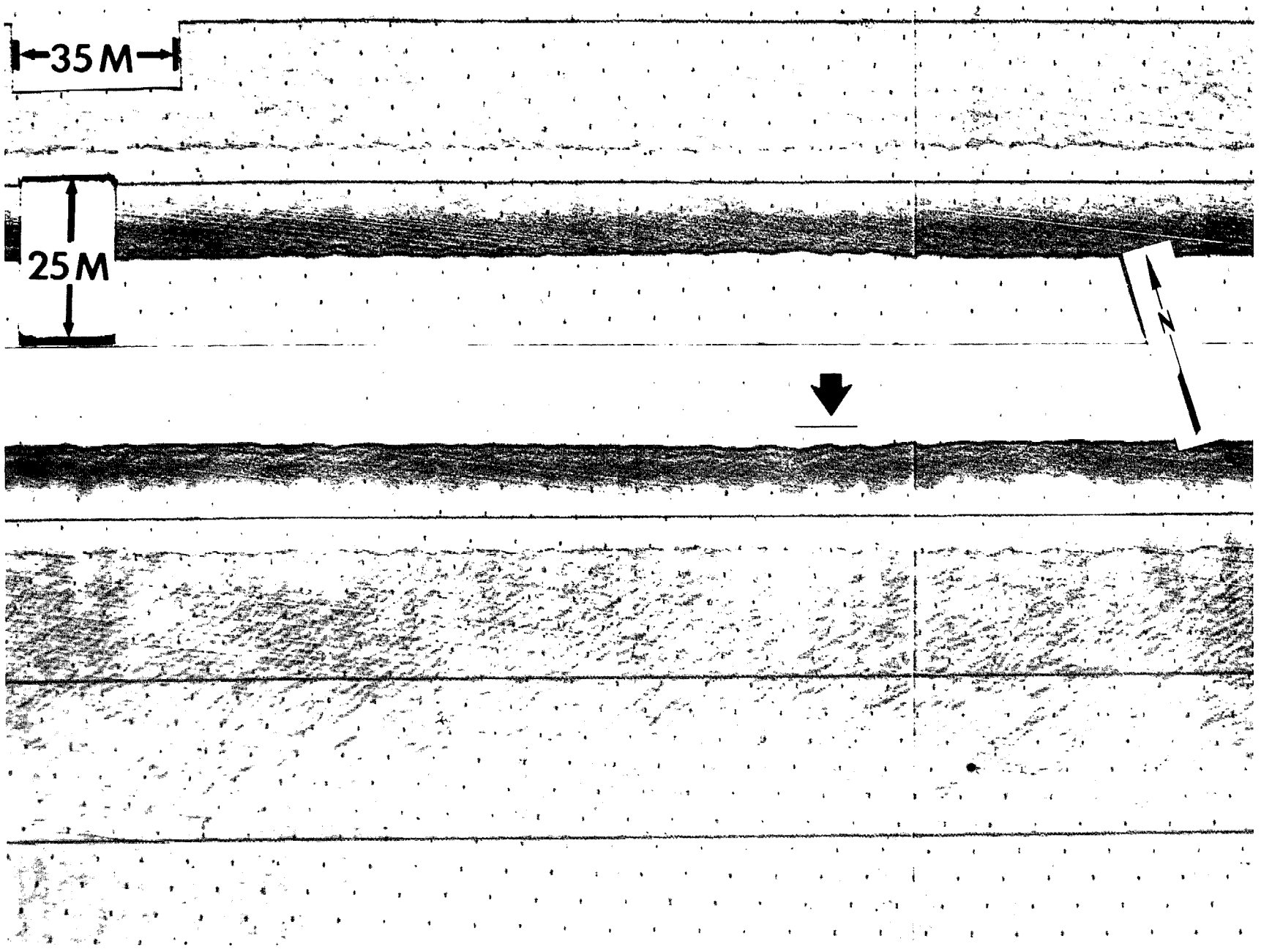

Figure 6-5

generally straight, continuous crests with little bifurcation (fig. 6-6), rhomboid sand waves with straight crests that intersect to form a diamond-shaped pattern (fig. 6-7), and irregular sand waves with sinuous, irregular crests that bifurcate in an unpredictable manner (fig. 6-8).

These different morphologies probably result from varying current regime and combinations of sand-wave types from different storm directions. Rhomboid sand waves may be a combination of linear parallel sand waves produced by two major storm directions. Irregular sand-wave morphology may be produced by multiple events. Orientation is difficult to determine for many of these sand waves and must be deduced by the plan-view shape of the bed form.

Of all the major sand-wave fields mapped, over 90% fell within the 25-m bathymetric contour. These fields are mostly linear in form, oriented north-south, with local relief of up to 3 m and are often evenly spaced and bounded by a sharp seaward and gradational landward contact suggesting migration of discrete sand-wave fields. Average width of these sand-wave fields is 3 km or more.

In the offshore area, sand waves are less frequent but, nevertheless, prominent (fig. 6-9). They may be relict features of the last major storm or perhaps even stranded by a rising sea level and modified by present-day current and wave activity.

With regard to the hazards aspect of sand waves to pipeline placement or shallow burial, the risks appear greater inside the 25-m isobath where, apparently, storms of even moderate intensity cause bedload transport. Seaward of this depth only the higher energy, but less frequent, disturbances initiate sand-wave development. If pipeline routes must traverse sand-wave fields, it would seem that burial to a

Figure 6-6. 3.5 kHz profile (upper record) and sonogram (lower record) showing linear parallel sand waves, crests oriented east-west, intersected by possible larger scale bed form feature. Arrows are time equivalent. (line 2_4 @ 1545 hours.)

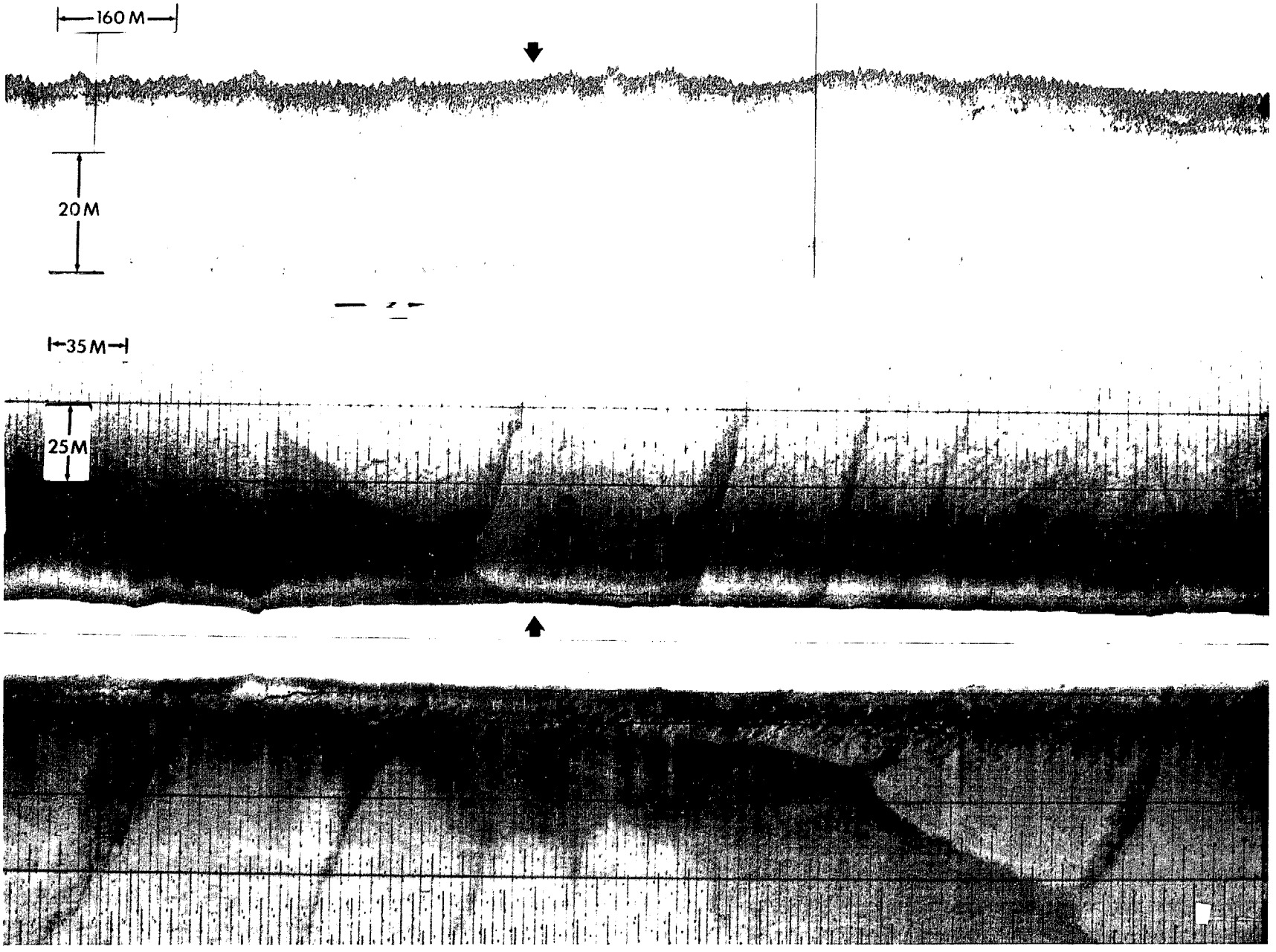

Figure 6-6

Figure 6-7. 3.5 kHz profile (upper record) and sonogram (lower record) showing rhomboid sand waves with straight crests that intersect to form a diamond-shaped pattern. Arrows are time equivalent. (Line 9_4 @ 0605 hours.)

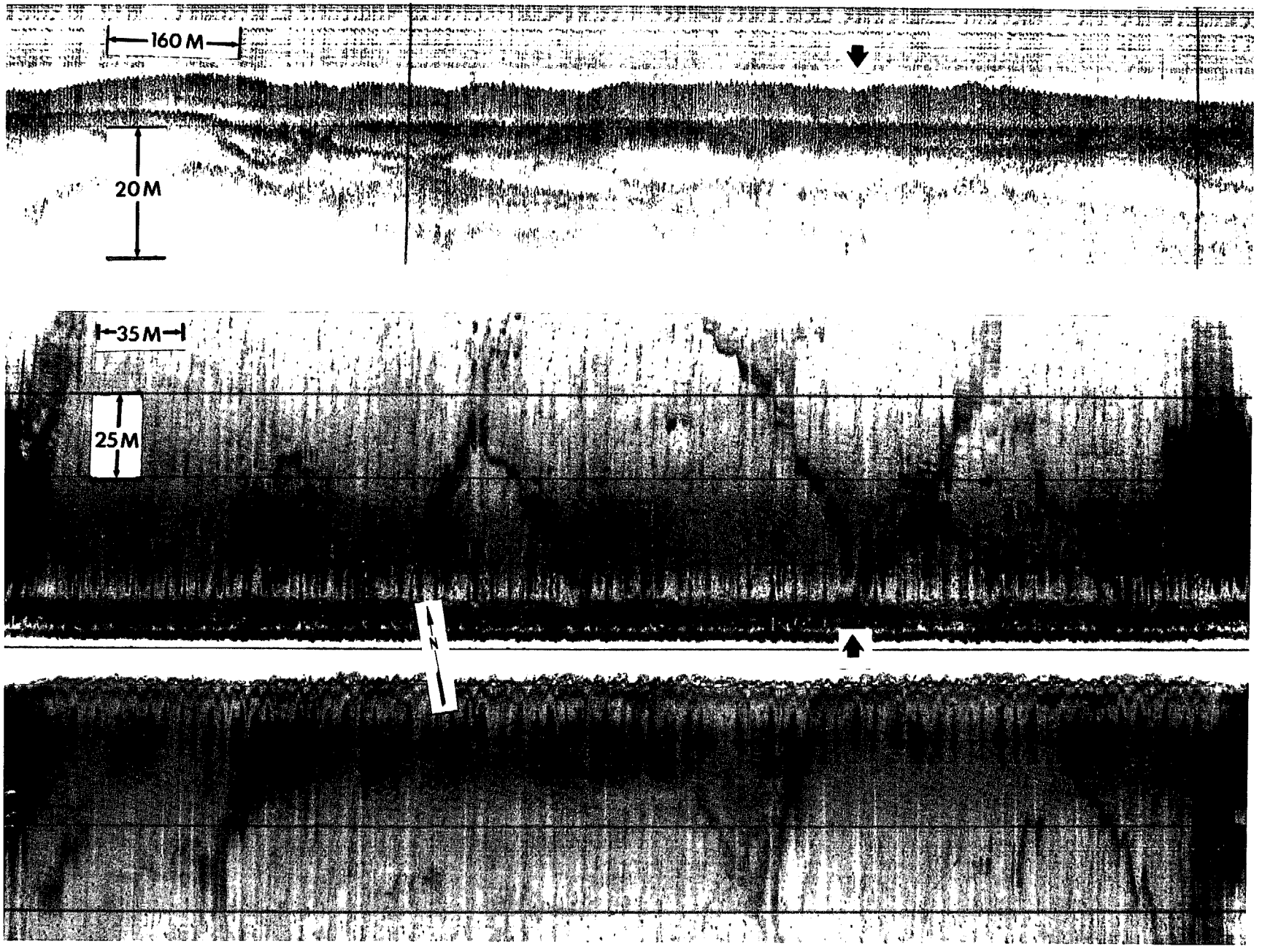

Figure 6-7

Figure 6-8. 3.5 kHz profile (upper record) and sonogram (lower record) showing sand waves with irregular morphology. Note north-south orientation of sand wave field. Bed-form shape suggests migration to the south. (Line 7_4 @ 0200 hours.)

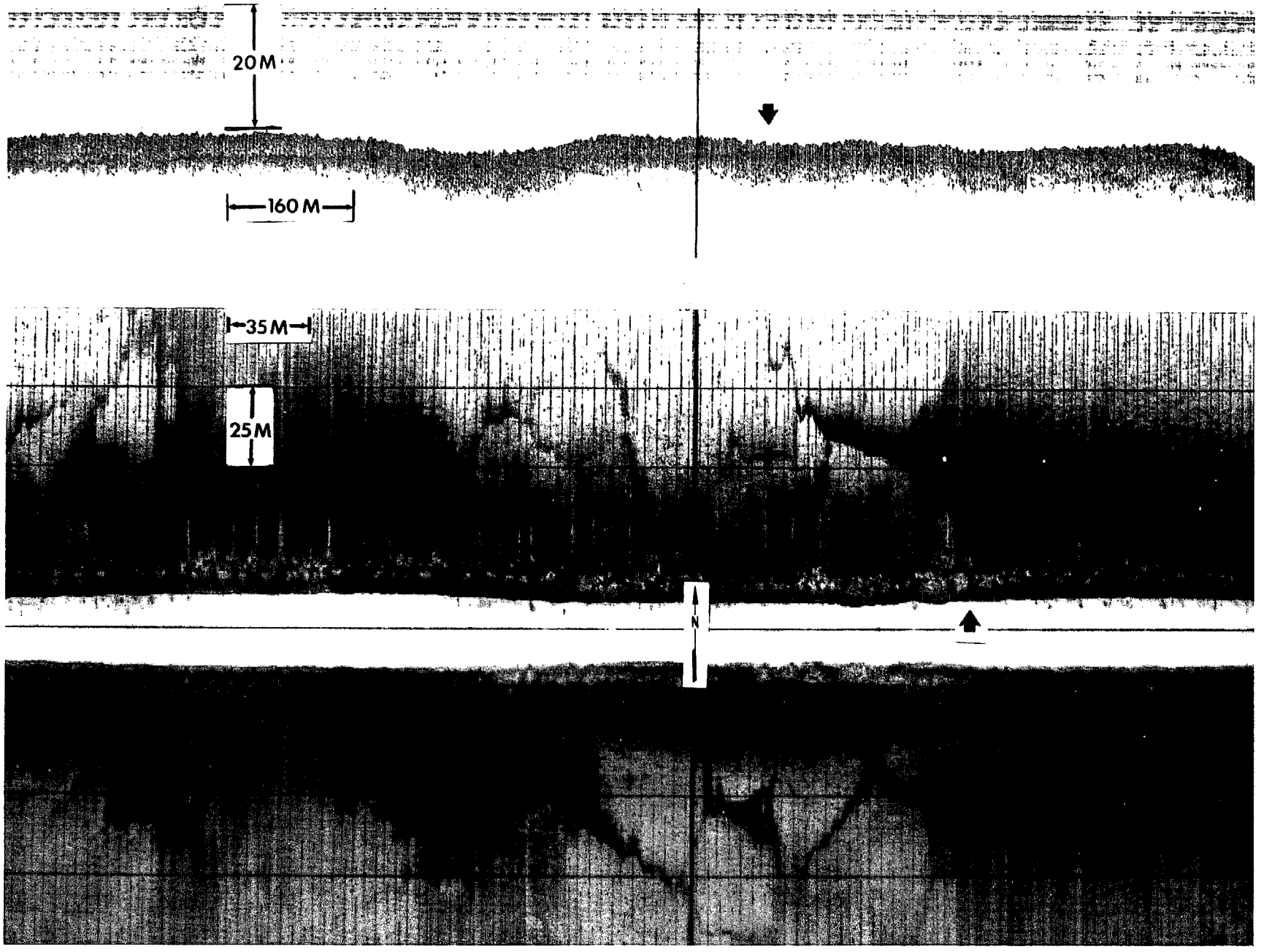

Figure 6-8

Figure 6-9. 3.5 kHz profile (upper record) and sonogram (lower record) showing offshore "relict" sand fields with sharp seaward and gradational landward contact. Sand waves are notably rare on the outer shelf although this textural pattern is common. (Line 8_2 @ 0600 hours.)

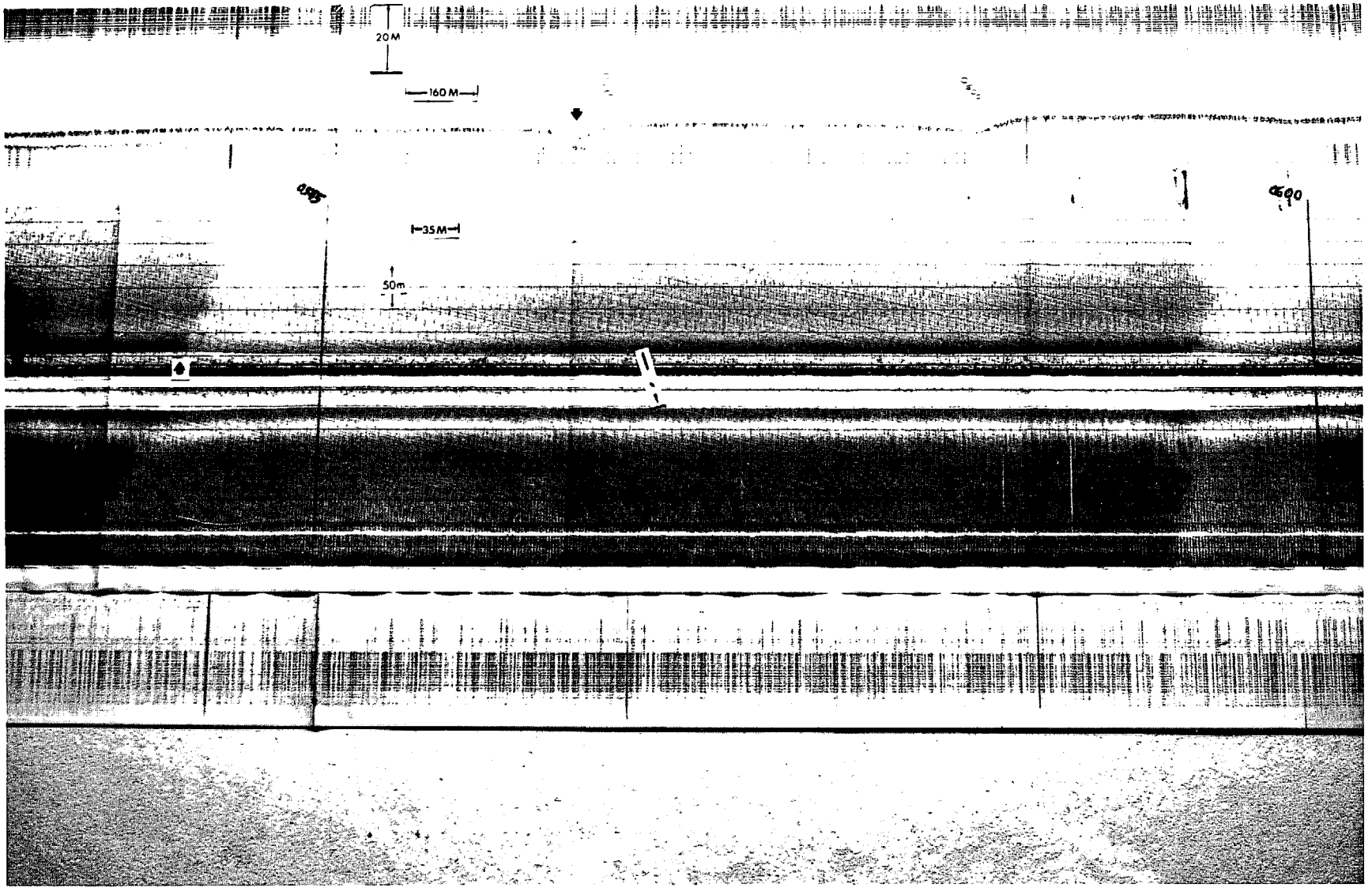

Figure 6-9

depth of at least one-third the sand-wave height in the offshore areas and one-half the sand wave height in the inshore areas would be prudent as pipeline spanning would be less likely to occur given the length/height ratios in these areas.

Other Bottom Textures

A pattern noted as significantly recurrent on the sonogram is best described as reticulated or weblike (fig. 6-10). Reticulation rings are oval in shape, the long axis length ranging from 5 to 30 m. Different examples of reticulated bottom vary in return strength as well as web size. The origin of this "texture" is not fully understood; however, it has been noted that reticulation is found only on the outer shelf, especially in areas of scour where it is sometimes gradational into areas of strong return. Although proximal track lines suggest reticulation as true bottom, towed underwater television and minisub observations failed to reveal such features. These patterns may result from water-column density anomalies related to temperature/salinity structure.

Areas of Local Scour

Areas of local scour, inferred by mobile bed-form fields and/or outcrop of the shallow reflector, are present across the shelf. Apparent scour most commonly occurs on the outer shelf (see Map Series A and B), especially in the southern portion of the study area where the surficial sand veneer is notably absent and the shallow reflector is truncated and discontinuous in outcrop. In this area, scour may be caused by periodic incursions of Gulf Stream meanders.

Tidal-dominated scour was noted in the area of Tybee Trough, an arcuate asymmetric depression located 45 km east of Savannah, Georgia (fig. 6-11). This feature is believed to be a partially filled meander

Figure 6-10. Sonogram of reticulated texture of unknown origin showing variation in web size. This texture may be due to bottom conditions or water mass properties. 3.5 kHz profile shown in upper portion of figure. (Line 3_3 @ 0030 hours.)

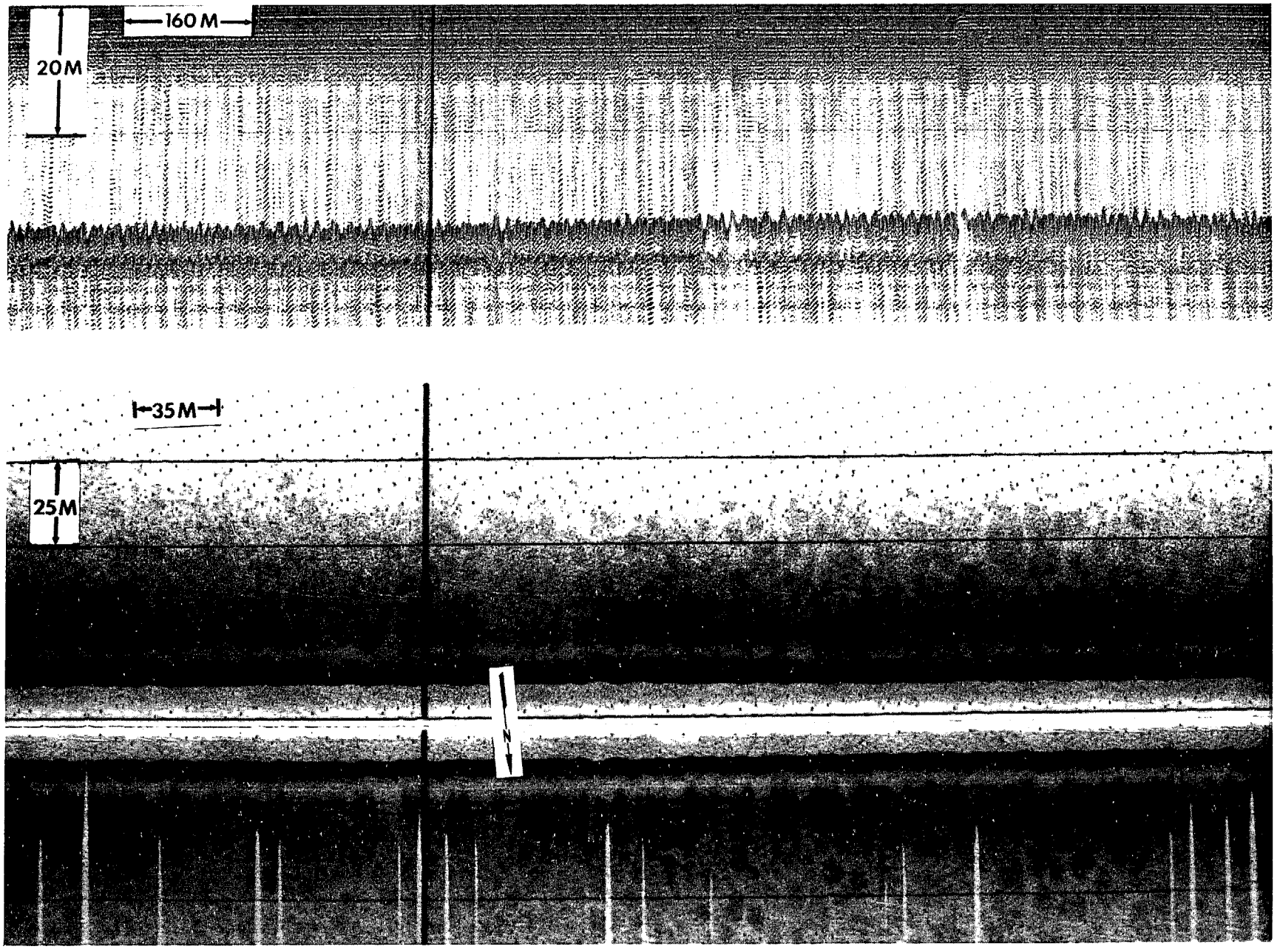

Figure 6-10

Figure 6-11. Map showing bathymetry and location of Tybee Trough, 45 km east of Savannah, Georgia.

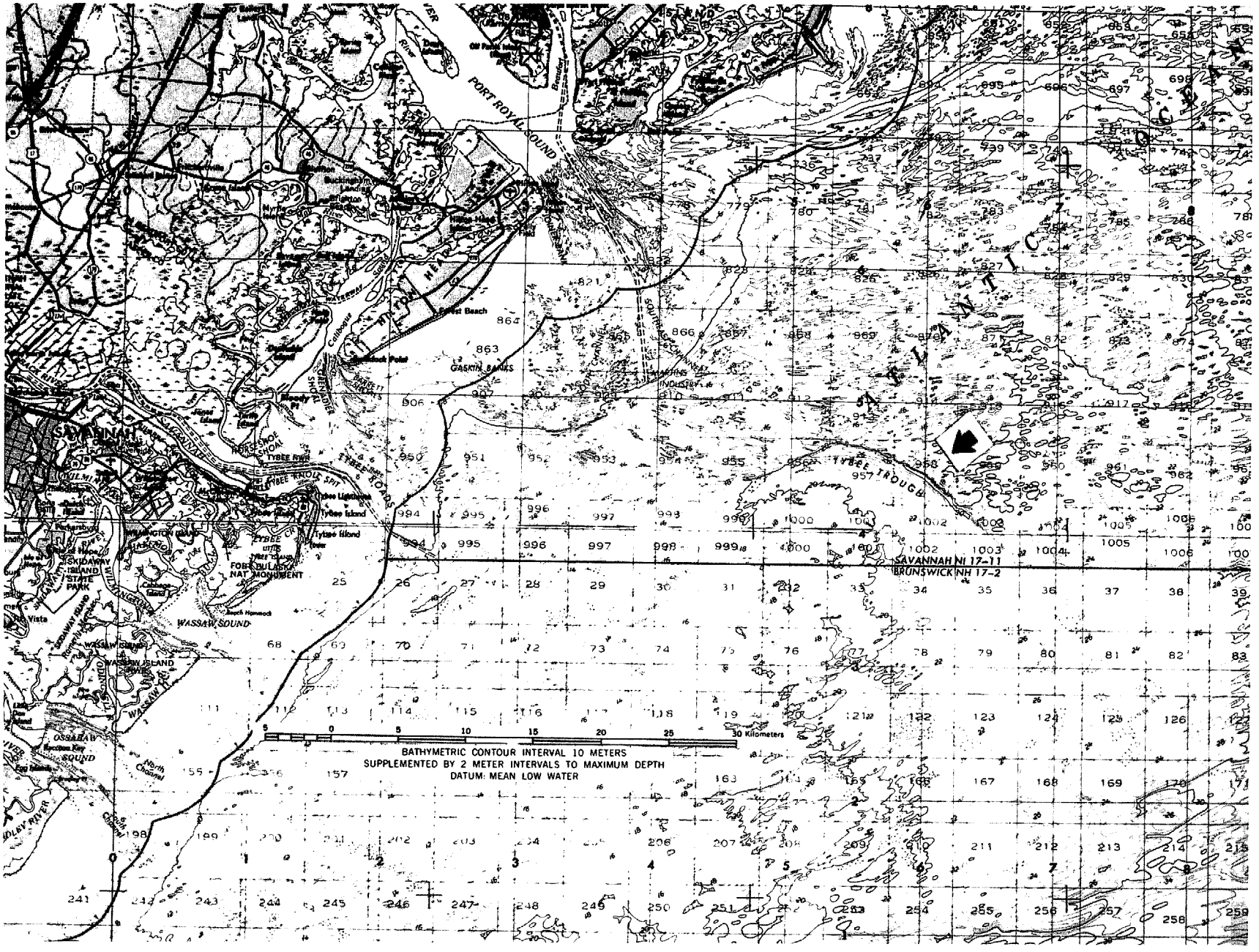
PORT ROYAL SOUND
SAVANNAH
GASKIN BANKS
TYBEE ROADS
TYBEE TROUGH
FORT PULASKI NAT MONUMENT
WASSAW SOUND
OSSABAW SOUND
SAVANNAH NI 17-11
BRUNSWICK NH 17-2
30 Kilometers
BATHYMETRIC CONTOUR INTERVAL 10 METERS
SUPPLEMENTED BY 2 METER INTERVALS TO MAXIMUM DEPTH
DATUM: MEAN LOW WATER

Figure 6-11

of the ancestral Savannah River channel. At the time of traverse, the trough was under ebb tidal influence and contained a suspended sediment load of sufficient density to mask the channel bank morphology on seismic records (fig. 6-12).

Bioturbation

Relative degrees of bioturbation were noted and mapped in the interpretation of underwater-towed television videotapes as discussed in a later section. Degree of bioturbation indicates how attractive a particular bottom is to benthos and how recently the bottom has been active or mobile. Mapped degrees of bioturbation in most cases transcended textural boundaries, probably due to the quiescent period previous to the survey cruises, which were conducted during the late spring and summer months. A slightly higher density of bioturbation was noted in the coarser, less mobile sediments (fig. 6-13) and in the hard-bottom/live-bottom areas.

Hard Bottoms

Another constraint to hydrocarbon development operations is the presence of hard bottoms and reefs and the environmentally sensitive benthic communities that they support.

Henry and Giles (1979) classified Georgia Bight reefs and hard bottoms into three general morphotypes based on relief as detected by side-scan sonar, 3.5 kHz, Uniboom, and underwater-towed television system (see table 6-2). Classification boundaries were chosen according to grouping of natural occurrence. Although an outcrop of the shallow subsurface reflectors often produces a strong return on the sonogram, such signatures do not always indicate a live bottom or even a hard bottom. Nevertheless, even in the absence of ground truth and fish signatures, such outcrops may be considered as possible or potential

Figure 6-12. Sonogram (above) and 3.5 kHz profile (below) of Tybee Trough. Located 45 km east of Savannah, Georgia. Local scour is indicated by containment of suspended sediment (indicated by arrow) of sufficient density to mask channel morphology on seismic records. (Line 41_4 @ 0630 hours.)

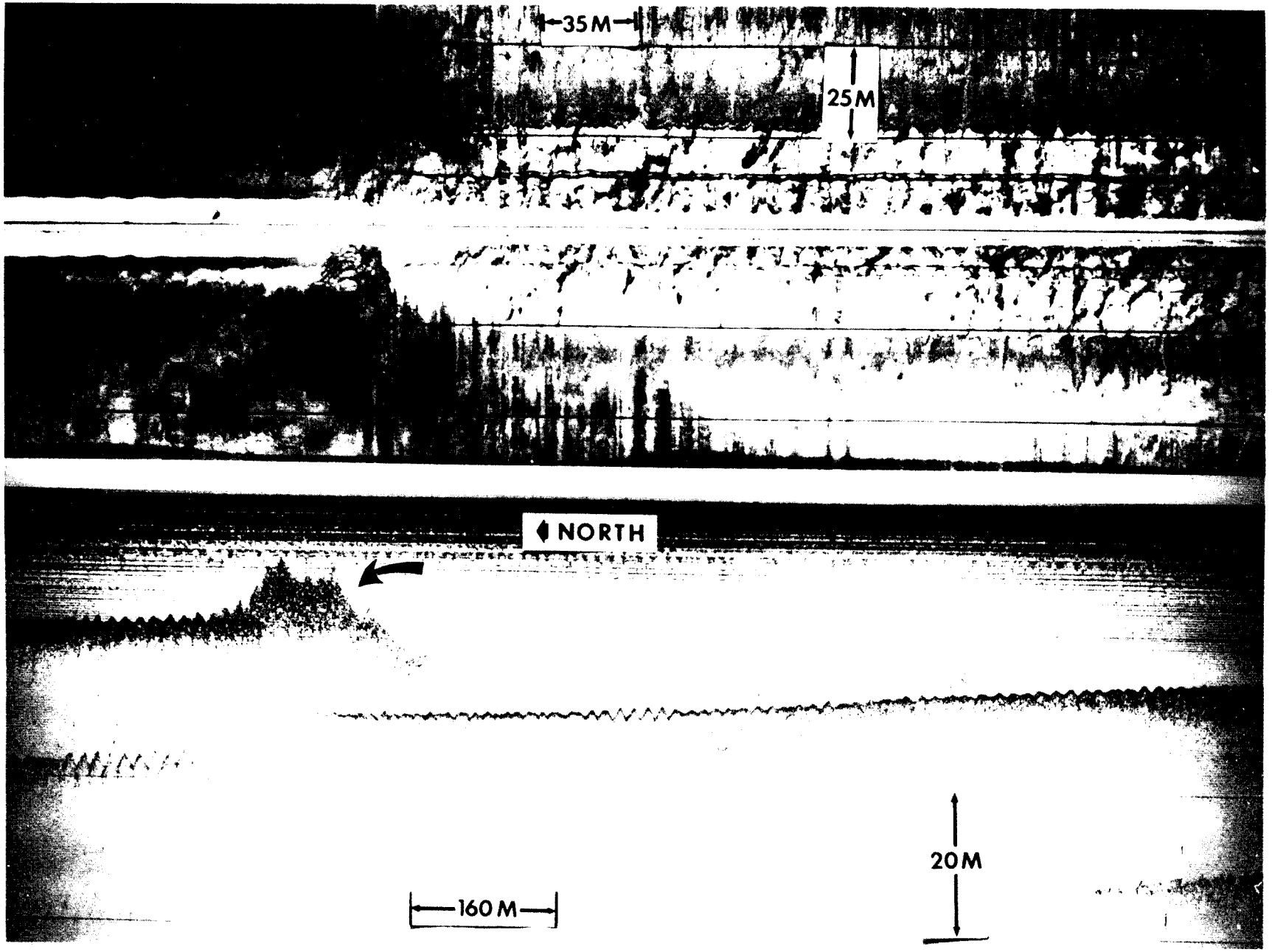

Figure 6-12

Figure 6-13. Underwater-towed television image of extensively bioturbated bottom sediments (line 13_3 at 1048 hours).

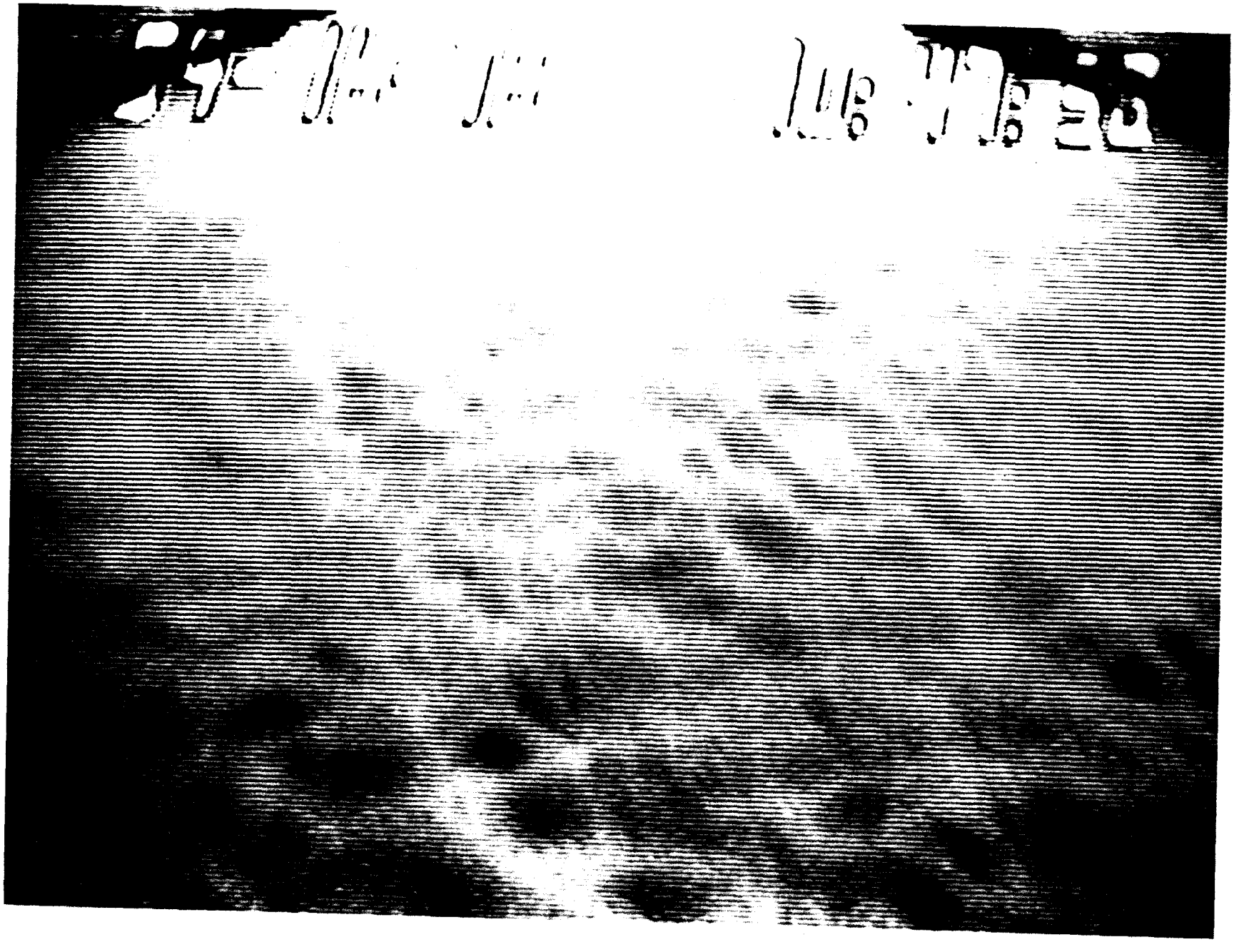

Figure 6-13

Table 6-2. Morphological classification of reefs and hard grounds in the Georgia Bight

Type I - Low-Relief Hard Grounds

<0.5 m relief

Substrate commonly covered by thin veneer of sand

Sparse to moderate occurrence of sessile epibenthos, principally sponges and octocorals

Widely distributed across the shelf

Generally difficult to detect by sonar technique

Type II - Moderate-relief reefs

Up to 2 m relief

Moderate to abundant occurrence of epibenthos, principally sponges, octocorals, and algae

Generally restricted occurrence but most commonly found off north Florida and the Carolinas in inner and middle shelf depths

Moderate to abundant reef fish community

Generally easy to detect using side-scan and fish-finding sonar

Type III - Shelf-edge reef

Up to 15 m relief

Moderate to abundant occurrence of epibenthos, principally sponges, octocorals, and algae

Occur as discontinuous ridge or ridges at or near the initial break in slope - 30 to 100 m water depth

Abundant reef fish community

Easily detected by sonar technique

hard-bottom loci. Hard bottoms and shallow reflector outcrops are plotted on Map Series B. The geological nature of the shallow reflectors and most reef substrates is still to be determined.

Low-Relief Hard Bottom

Low-relief hard bottoms occur as relatively smooth, flat-lying substrates of less than 0.5 m relief. Due to their low relief, this type of hard bottom is subject to periodic covering by the surficial sand veneer and as a result does not support abundant benthic populations.

Side-scan sonar without benefit of other systems is often of little assistance in locating low-relief hard bottoms due to a lack of shadowing, low population density, and the presence of the sand veneer (fig. 6-14). Underwater-towed television offers the best detection method for this type of hard bottom (fig. 6-15).

Although the regional distribution of this hard-bottom type is not known due to limited underwater-towed television coverage, low-relief hard bottoms were noted on all areas of the shelf.

Moderate-Relief Hard Bottom

Moderate-relief hard bottoms occur as irregular, discontinuous, rocky outcrops displaying relief of 0.5 to 2 m. These hard bottoms may be considered to be true reefs supporting abundant benthic and pelagic communities.

This type of hard bottom/reef is easily detected by side-scan sonar, displaying irregular topography with a high percentage of acoustic shadowing (fig. 6-16). Moderate-relief hard bottoms occur in highest frequency between the 15 and 30 m isobaths and in most cases are related to outcrop of a strong subsurface reflector.

A typical example of a moderate-relief hard bottom is Grays Reef,

Figure 6-14. 3.5 kHz (above) and sidescan sonar (below) records of low-relief hard bottom, located to right (east) of arrows as confirmed with towed underwater television shown in figure 15. Arrows are time equivalent indicating contact of sand veneer with hard bottom. (Line 41_4 @ 0900 hours.)

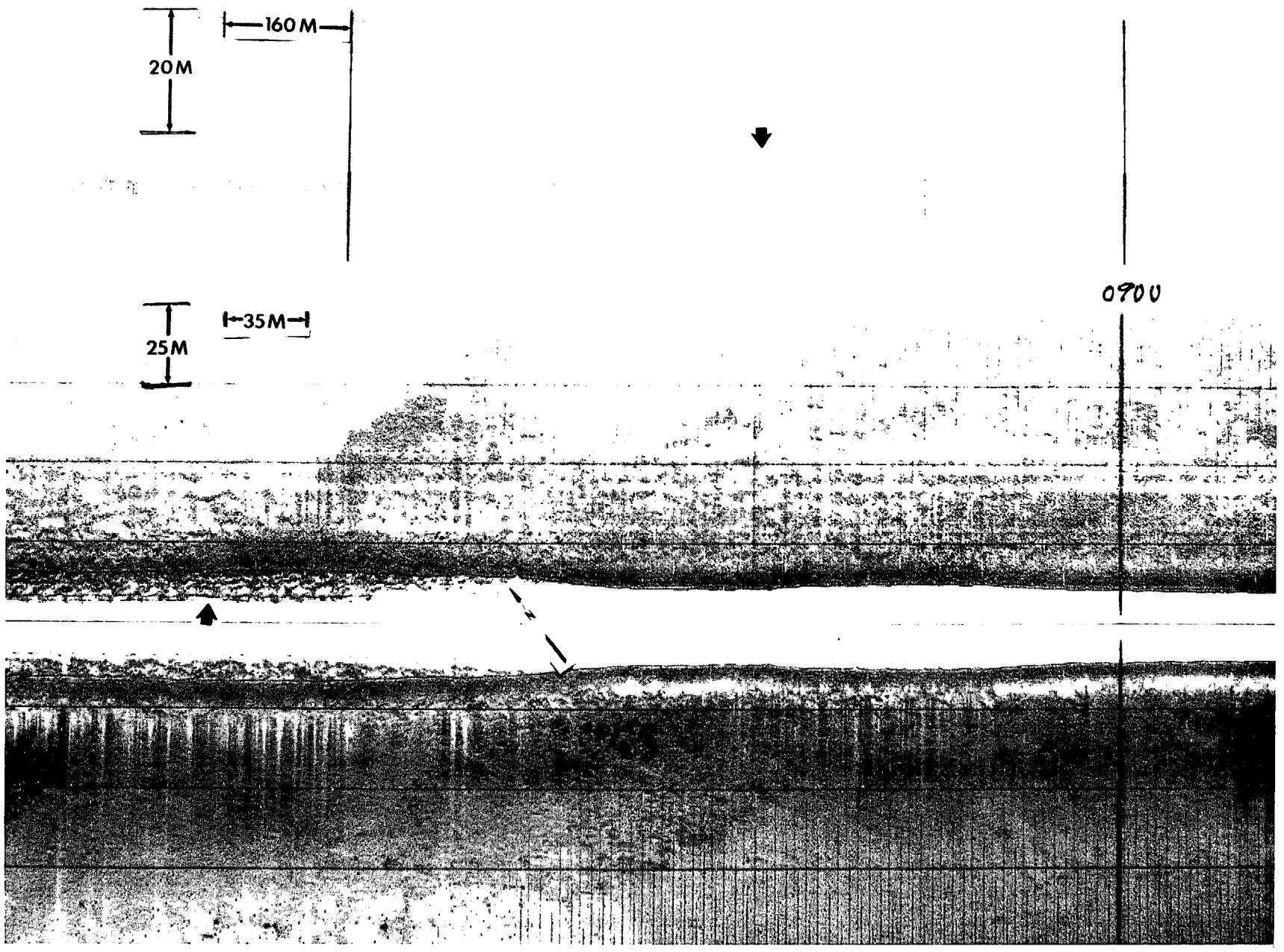

Figure 6-14

Figure 6-15. Underwater-towed television image of low-relief hard bottom shown in figure 6-14. Note basket sponge in right foreground and water turbidity as limiting factor in the use of television as a ground-truth method (line 41_4 at 0901 hours).

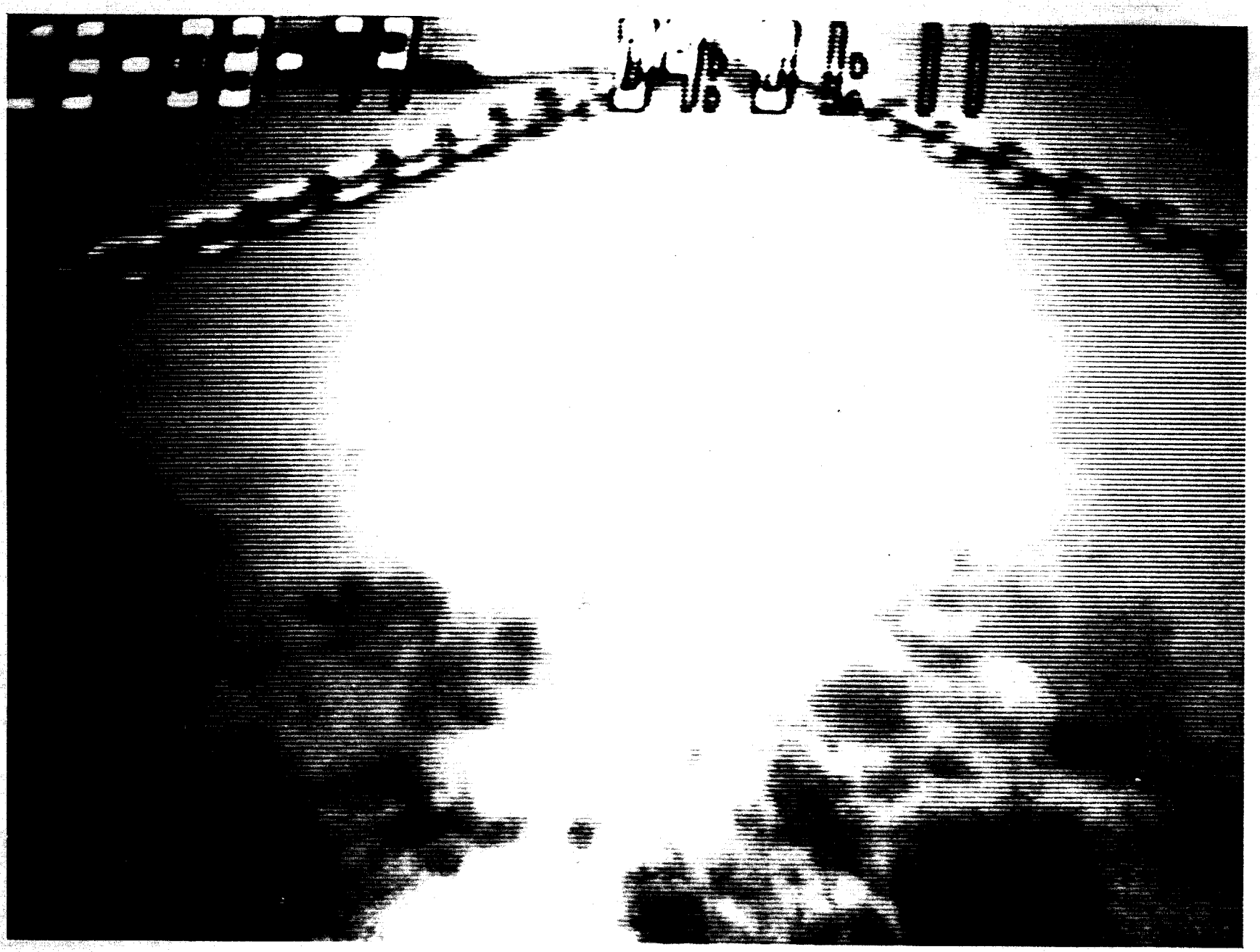

Figure 6-15

Figure 6-16. 3.5 kHz (above) and sidescan sonar (below) records of moderate-relief hard bottom indicated by arrows. Note shadowing on sonogram and parabolic fish signatures on profile. (Line 11_4 @ 1220 hours.)

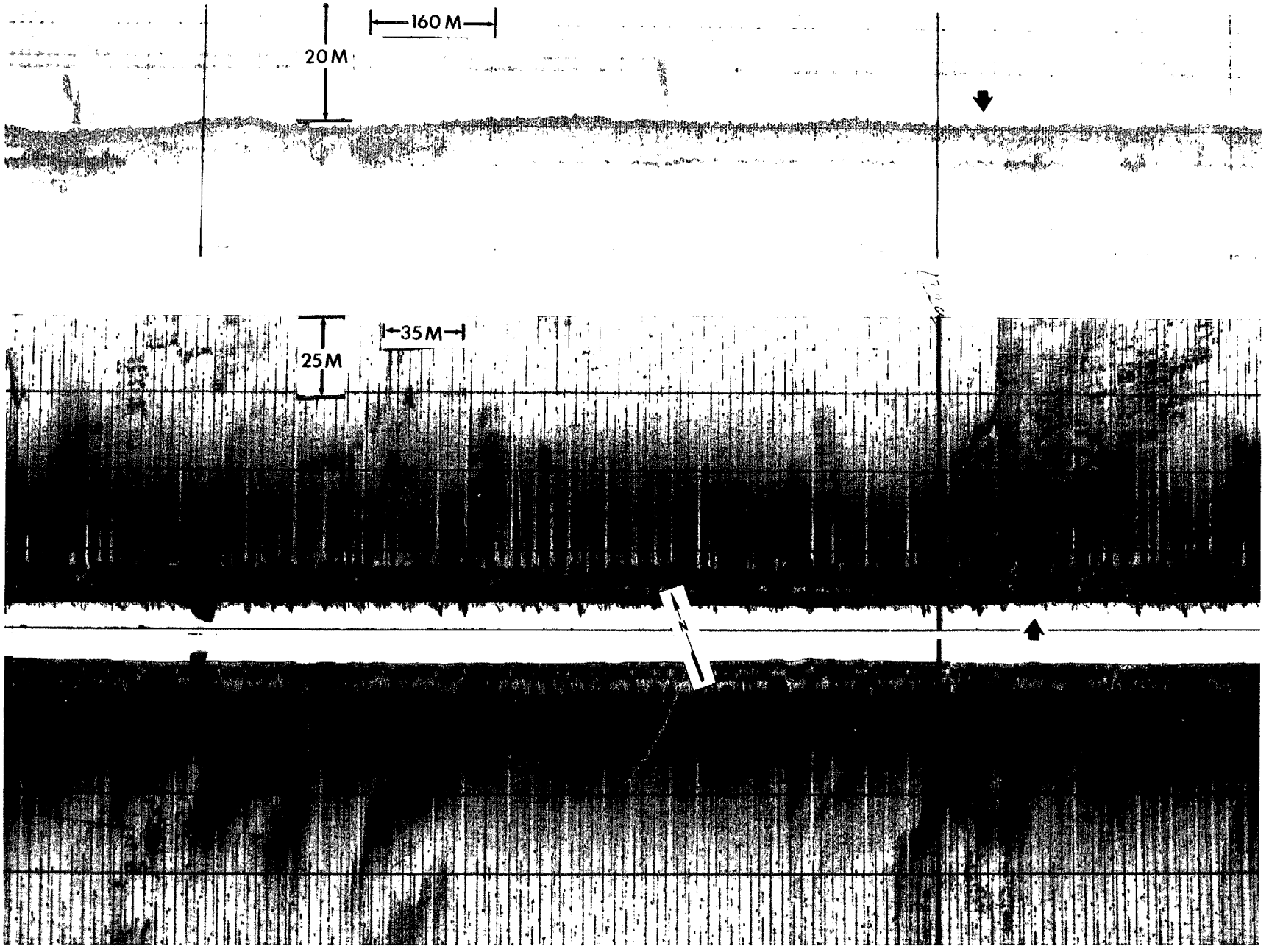

Figure 6-16

located 33 km due east of Sapelo Island, Georgia (fig. 6-17). According to Hunt (1974), the Grays Reef substrate is Pliocene in age.

High-Relief Hard Bottom

High-relief hard bottoms, displaying relief of 2 m or more, comprise the third classification of hard bottoms. Most hard bottoms of this type are located in the vicinity of the shelf break, between the 30 and 100-m isobath and are termed shelf-edge reefs. Figure 6-18 indicates the location of fathometer profiles across the shelf break made by the South Carolina Wildlife and Marine Resources Department, Charleston, South Carolina. These data are being examined to determine the occurrence, morphology, and trend of the shelf-edge reefs and associated features.

Reef morphology ranges from rounded, gentle gradient outcrops of relatively low relief, to steep scarps (fig. 6-19) or a series of stepped scarps. Scoured depressions often occur at the base of scarped shelf-edge reefs while a ridge may form at the top (fig. 6-20). Maximum local relief noted in shelf-edge reef is 15 m.

Both moderate and high-relief hard bottoms are typified by blocky, irregular rock outcrops with sand filling cracks and joints. In some cases, scarped shelf-edge strata may be traced landward and seaward under surficial sediments to become a shallow, strong subsurface reflector. Seismic profiles from a location 110 km due east of Jacksonville, Florida, show what is apparently a buried shelf-edge reef 2 km landward of the present-day shelf edge suggesting an earlier shelf-edge position (fig. 6-21).

Live Bottom

Plots of fish signatures of both side-scan sonar and 3.5-kHz records indicate that target schools are highly mobile. Although

Figure 6-17. Diver-held television image of Grays Reef, typical of moderate-relief hard bottom in the Georgia Bight. Location is shown on Map Series B.

Figure 6-17

Figure 6-18. Map of fathometer data presently available to University of Georgia Marine Geology Program by the South Carolina Wildlife and Marine Resources Development for purposes of mapping continuity of the shelf-edge reef complex.

LEGEND

A. Distinct scarp, well defined.

B. Scarp rounds slightly and divides. The feature pinches out north and south.

C. Pronounced scarp continues.

D. Transitional zone. No scarp present.

E. Scarp appears again, although well rounded.

F. Intermittent occurrence of low-relief scarp.

G. Distinct scarp present.

H. Very low-relief scarp, nearly undiscernable.

I. Scarp not present.

J. Two scarps present, very distinct and prominent.

K. Low relief scarp landward of edge; two apparent outcrops occur downslope.

L. Where present, scarp is low relief and located landward from usual shelf-edge position.

M. Scarp not present or poorly defined.

N. Well defined scarp.

Figure 6-18

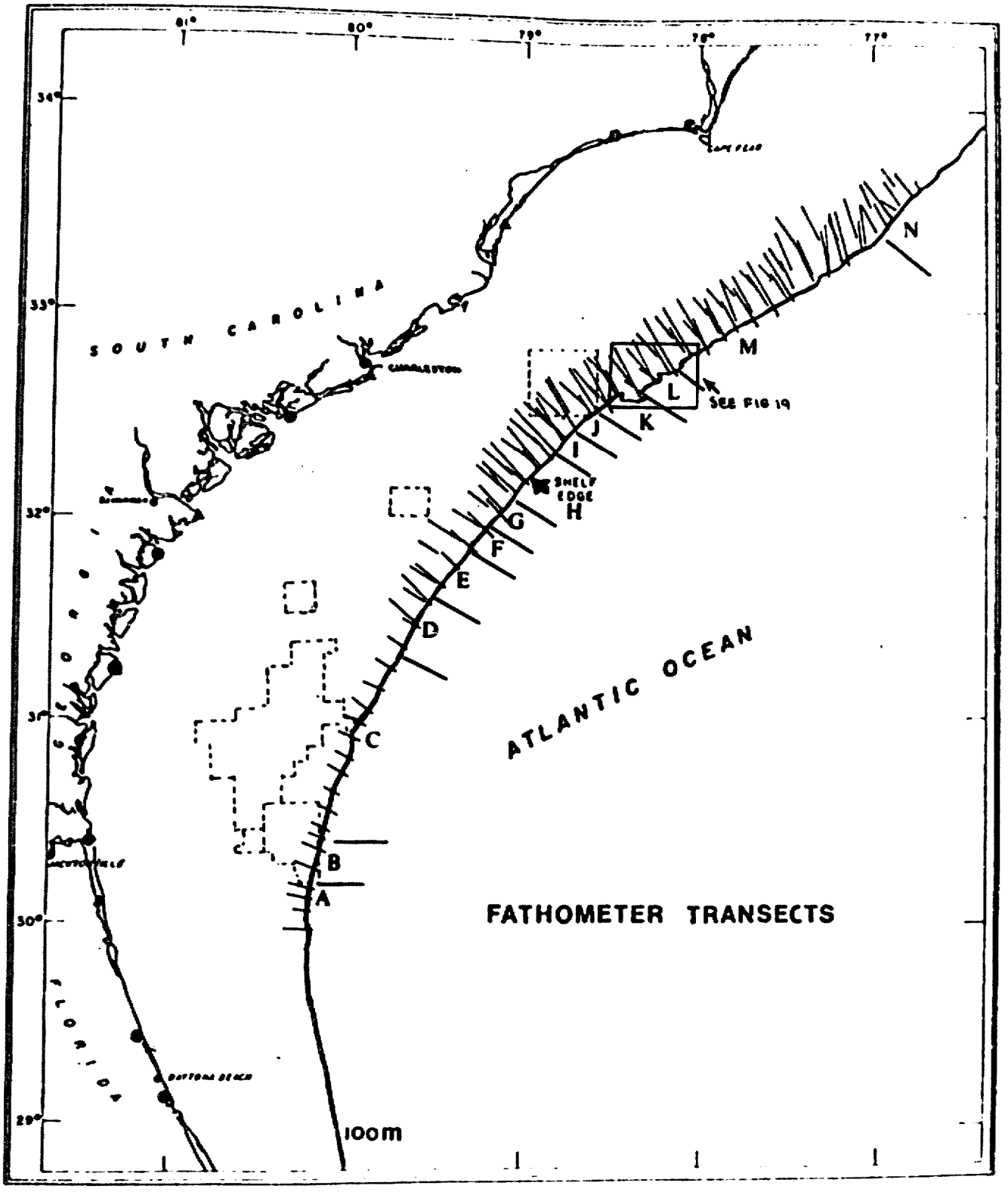
81°
80°
79°
78°
77°
34°
33°
32°
31°
30°
29°
SOUTH CAROLINA
CHARLESTON
CAPE FEAR
SEE FIG 19
SHELF EDGE
ATLANTIC OCEAN
FATHOMETER TRANSECTS
100m
A
B
C
D
E
F
G
H
I
J
K
L
M
N

Figure 6-19. 3.5 kHz (above) and sidescan sonar (below) records of high-relief hard bottom/shelf-edge reef with 9 m local relief. Note shallow subsurface reflector in vicinity of shelf-edge reef. Arrows are time equivalent. (Line 1_1 @ 0607 hours.)

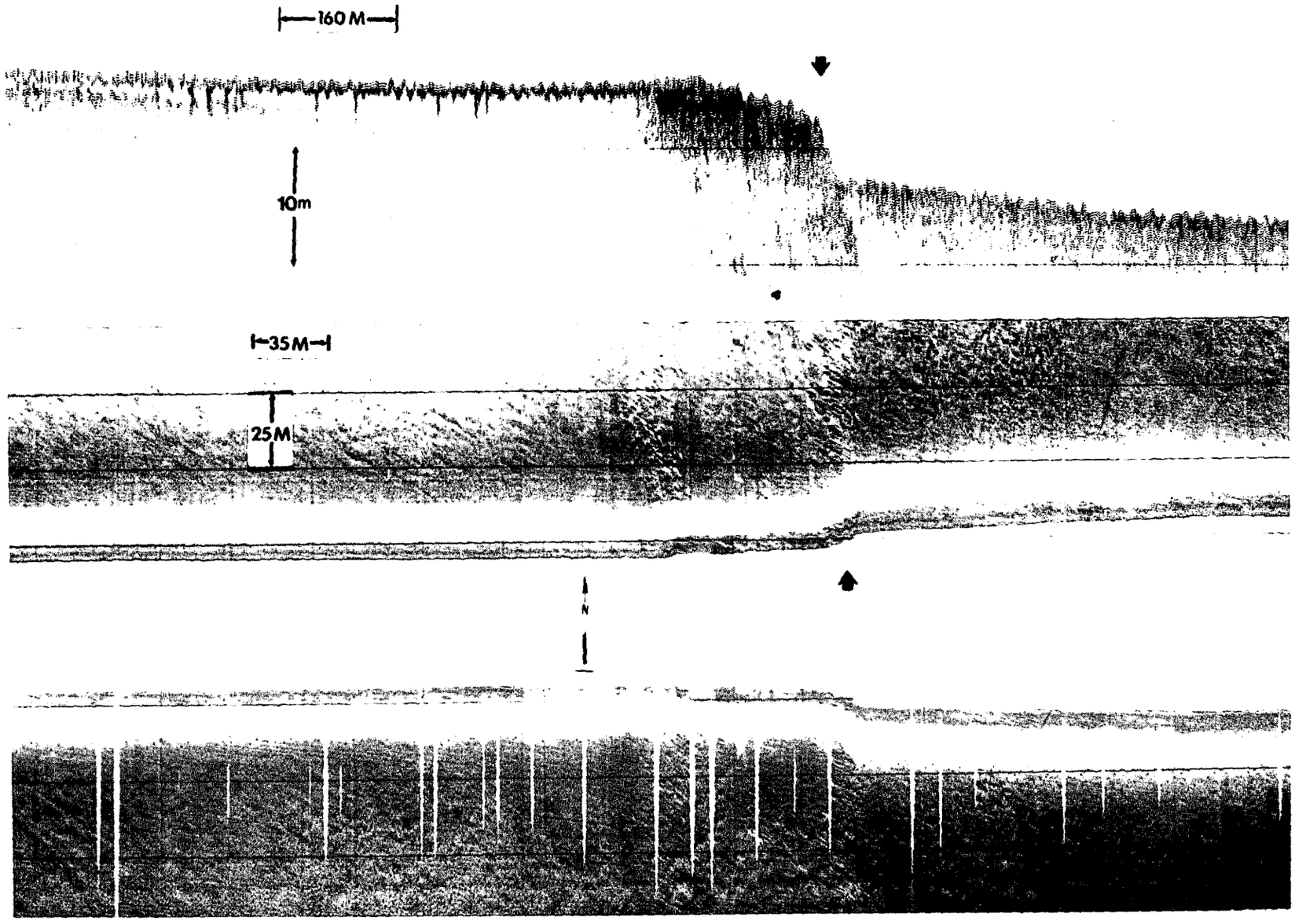

Figure 6-19

Figure 6-20. Fathometer record showing shelf-edge escarpment. Note ridge at top and scoured (?) depression at base of the scarp.

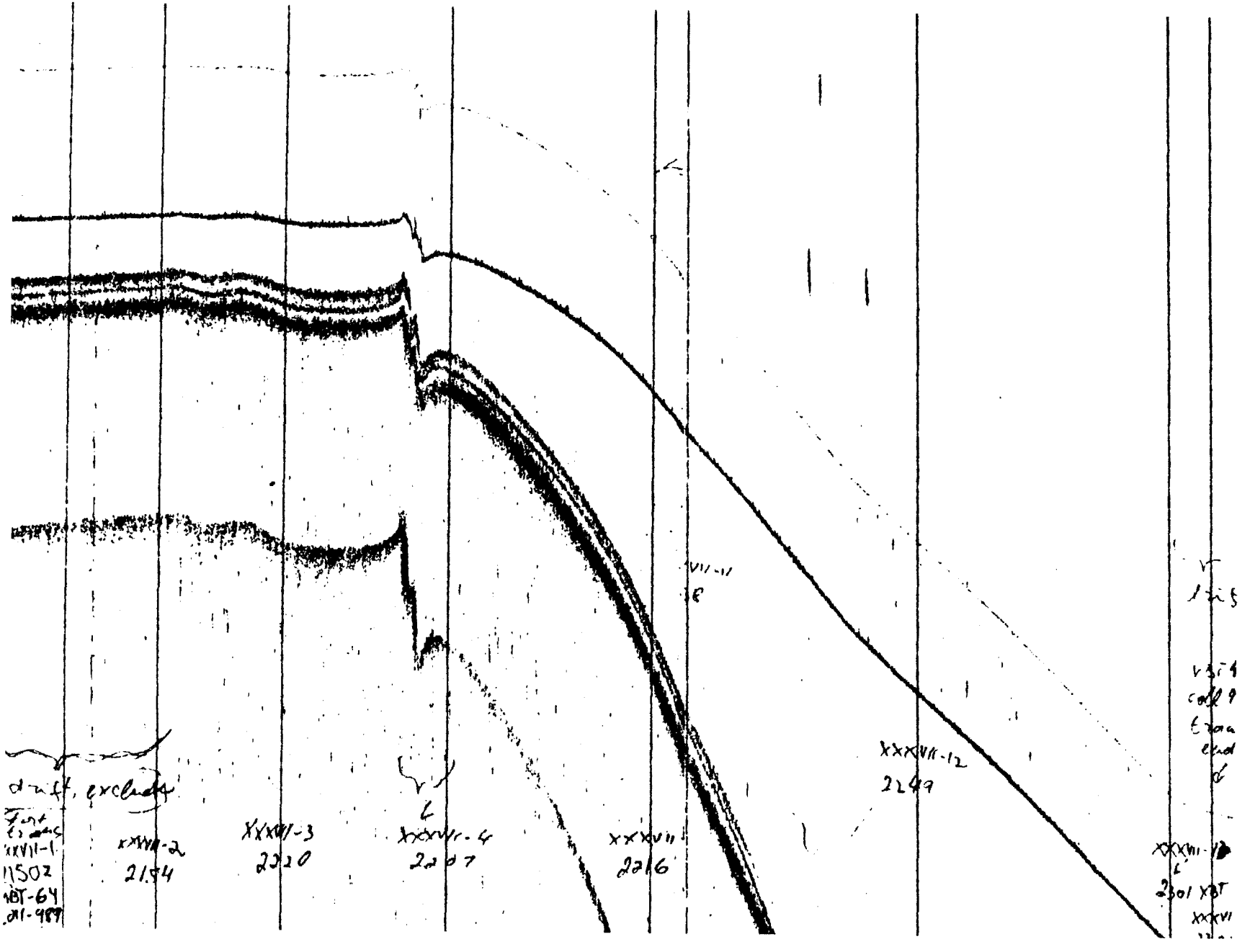

Figure 6-20

Figure 6-21. 3.5-kHz profile showing buried reefs developed on sections of previously exposed shallow subsurface reflector. Inset shows scarp of reef located 2,000 m landward of the present shelf-edge reef (line 1_1 at 0553 hours).

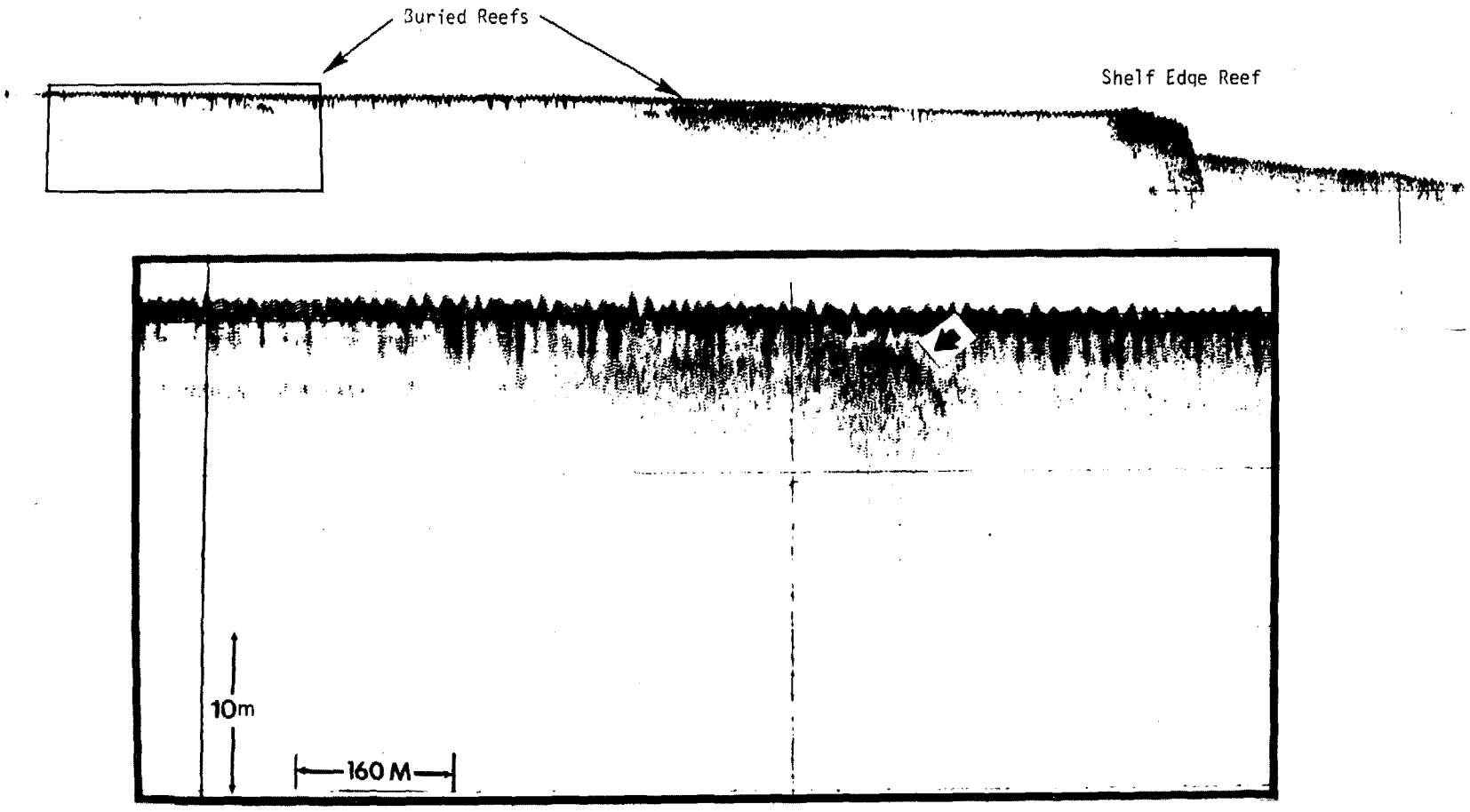

Figure 6-21

concentrations of fish were often found irregularly distributed across the shelf with only slight preference of hard bottom and outcrop areas over featureless, sandy bottom, it is highly possible that hard bottoms were present nearby but out of detection range. In any case, the distribution of fish may also be controlled by water mass conditions as indicated by high concentrations in Tybee Trough (fig. 6-22).

Fish signature distribution is shown on Map Series B. Hard-bottom areas ground-truthed by underwater-towed television generally display large and diverse populations of sessile benthic and pelagic organisms. Areas of reflector outcrop where hard bottom has not been indicated often reveal no more to towed television than a slight change in sediment texture, thus explaining strong returns on the sonogram.

A preliminary estimate of the relative occurrence of low-relief hard bottom (LRHB), moderate-relief reef (MRR), shelf-edge reef (SER) and outcrop of the shallow acoustic reflector (SAR) along track lines of cruises GS1-4 is given in table 6-3. Vagaries in this presentation are that track lines often did not always extend to the shelf edge and closed-circuit television ground truth was sparse to lacking in the inshore areas. Therefore, while the estimated percentage of occurrence of moderate-relief reef is probably good, the figures for low-relief hard bottom and shelf-edge reef are minimal. Also, a significant percentage of the outcrop areas of the shallow acoustic reflector probably support low-relief hard bottom.

Reefs and Hard Bottoms as Biologically Sensitive Features and Geological Hazards

From the standpoint of environmental impact on live bottoms resulting from the effects of oil and gas production, it would seem

Figure 6-22. Tybee Trough profile showing cut-and-fill structure of the probable ancestral Savannah River channel. Note high density of parabolic fish signatures possibly in response to nutrient-rich water contained in the trough (line 41_4 at 0630 hours). See figure 6-11 for location of Tybee Trough.

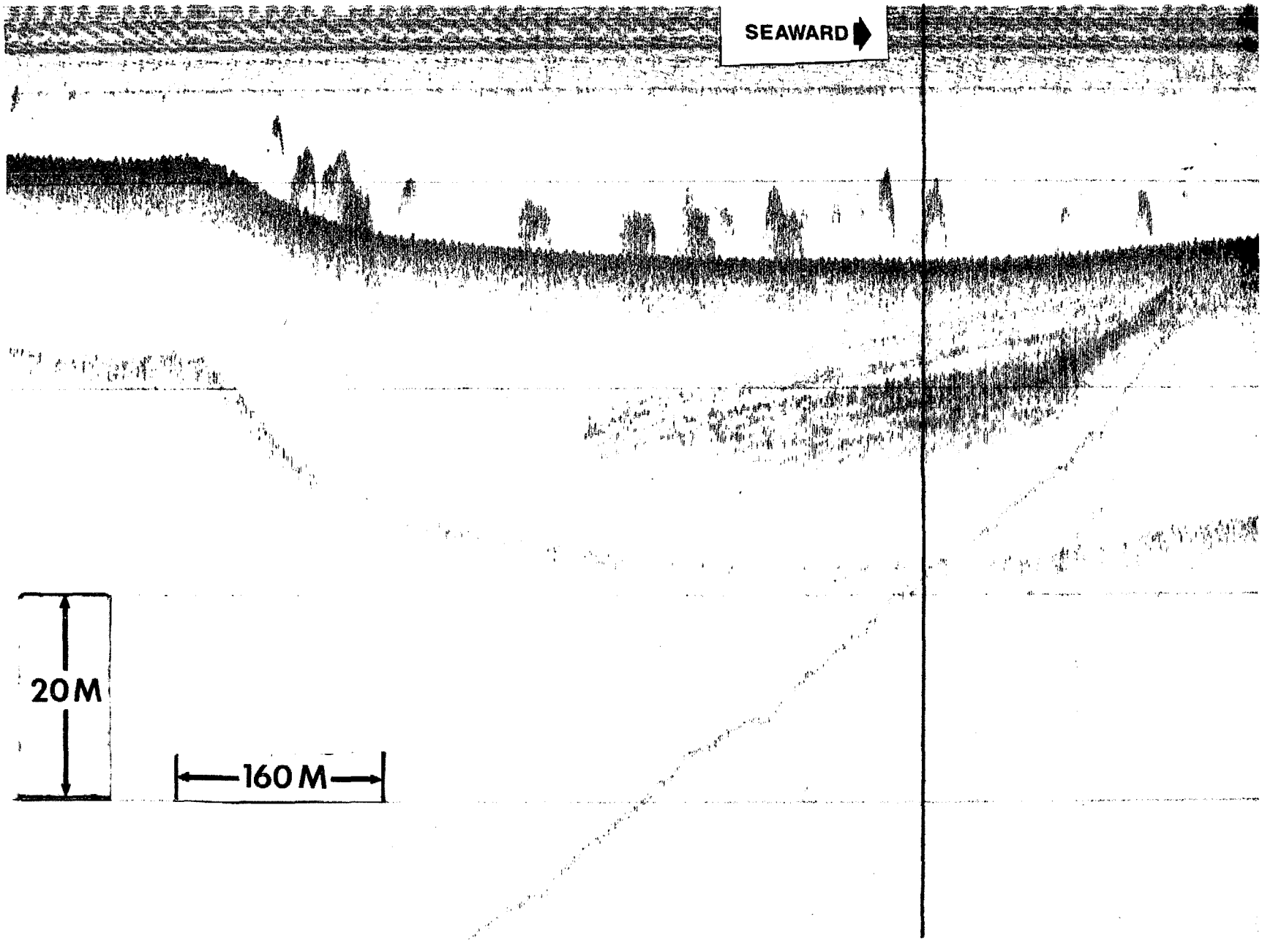

Figure 6-22

Table 6-3. ESTIMATED HARDBOTTOM OCCURRENCE ALONG GS1-4 TRACK LINES

CRUISE	QUADRANGLE	TOTAL TRACK (km)	OUTCROP OF SHALLOW ACOUSTIC REFLECTOR	LRHB	MRR	SER
GS-1	Jacksonville	125 km	3 km 2.4%	5.5. km 4.4%	6.0 km 4.8%	3 km 2.4%
GS-2	Brunswick	327 km	56 km 17.1%	0 km 0%	4.5 km 1.4%	0 km 0%
	Jacksonville	640 km	90 km 14.1%	0 km 0%	7.5 km 1.2%	4 km .6%
	Combined	967 km	146 km 15.1%	0 km 0%	12 km 1.2%	4 km .4%
GS-3	Brunswick	161 km	70 km 43.5%	1 km .6%	0 km 0%	2 km 1.2%
	Jacksonville	279 km	26 km 9.3%	0 km 0%	0 km 0%	0 km 0%
	Combined	440 km	96 km 21.8%	1 km .2%	0 km 0%	2 km .5%
GS-4	Brunswick	600 km	94 km 15.7%	12 km 2.0%	44 km 7.3%	0 km 0%
	Jacksonville	352 km	64 km 18.2%	5 km 1.4%	9 km 2.6%	0 km 0%
	Combined	952 km	158 km 16.6%	17 km 1.8%	53 km 5.6%	0 km 0%
TOTAL INSHORE LINES (Cruise GS-4)		952 km	158 km 16.6%	17 km 1.8%	53 km 5.6%	0 km 0%
TOTAL OFFSHORE LINES (Cruises GS-1 thru 3)		1532 km	245 km 16.0%	6.5 km .4%	18 km 1.2%	9 km .6%
TOTAL TRACK LINES		2484	403 km 16.2%	23.5 km 1.0%	71 km 2.9%	9 km .4%

obvious that impact would increase relative to the productivity of the biotope. Consequently, moderate-to-high-relief reefs would be more sensitive to pipeline emplacement, rig siting, and drilling activities than low-relief hard bottoms. Such conclusions are yet to be established, however, and the possibility exists that because of their innate productivity and topographic expression, the impact gradient may be more narrow and the impact area more confined in moderate and high-relief reefs than would be the case in low-relief, less productive live bottoms. Widespread burial of low-relief hard grounds by drilling mud and other drill-hole effluvia is a possible case in point. Also, a pile-supported or submersible platform would cause more immediate impact than a drill ship or semisubmersible platform.

On the other hand, reefs and hard bottoms may present significant geological and/or economic hazards to pipelines and drilling operations. Because little knowledge exists on the lithology, thickness, and geotechnical properties of the reef substrates, it is difficult to assess the feasibility of laying pipelines and spudding-in in such areas. In the latter case, Hathaway and others (1976) described the necessity of moving the drill site of hole 6003 because the presence of a rock outcrop caused severe mooring difficulties and made drilling impossible.

It is likely, therefore, that pipeline routes through, and the use of certain types of drilling platforms on, reefs and hard grounds should be avoided from both a geological hazards and environmental standpoint. In any case, a great deal more information is needed concerning the effects of natural processes and man's activities on these features that can only be learned by *in situ* time-lapse photography and shallow drilling into the substrate. In several areas, for example,

high-resolution seismic profiles show what appears to be a moderate-relief reef buried by a sand wave (see fig. 6-21). Drilling (vibracore) into such a feature would provide valuable information on the biologic nature of the reef, the lithology of the substrate, the time of burial, and, possibly, the rate of movement of the sand wave.

Small samples of reef substrate that have been collected from several localities in the Georgia Bight by dredging and SCUBA indicate that the shallow acoustic reflector may, in fact, be strata of more than one geologic age and lithology. Understanding the stratigrahpic and structural relationship by more extensive dredging and by drilling in selected areas would provide the basis for predicting and understanding the occurrence of reefs and live bottoms. Process analysis and stratigraphic studies are strongly recommended.

SHALLOW SUBSURFACE GEOLOGY

Seismic Stratigraphy

Eustatic sea-level fluctuations in response to global climactic changes have resulted in periods of partial to complete subaerial exposure of the shelf (Blackwelder and others, 1979). Regression of the shoreline across the shelf with lowering of sea level would expose the shelf surface to processes operating on the coastal plain today. Fluvial processes would cause incisement of this surface with possible delta formation at the mouths of major rivers. Given enough time, weathering processes would develop soil horizons. Subsequent transgression of the sea would tend to destroy some or all of these features by landward erosion of the shoreface leaving distinctive shoreline features and an erosional surface cut by channels. The resulting horizon(s) is the reflector(s) observed on the seismic

records.

Two, perhaps more, shallow reflectors seem to be fairly continuous over the survey area. However, even though the distribution of the acoustic horizons is nearly ubiquitous, the relationship of these reflectors is complex.

The two prominent reflectors occur at depths from approximately 7-10 m to where they outcrop and are rarely separated vertically by more than 5 m. Generally, they form a relatively low-relief, flat-lying surface. Outcrops appear to be controlled by changes in bathymetry or slight changes in attitude which bring them to the surface. Numerous channels of differing size and morphology often cut through the reflectors. Also, cut-and-fill structures are seen within larger channels and indicate at least two phases of fluvial activity.

An attempt has been made to map these horizons as separate and distinct. However, regional correlation is difficult because the reflectors are hummocky or erosional in appearance and locally discontinuous. The occurrence of the channels and cut-and-fill structures is shown in Map Series C (plate in pocket in back cover).

Upper Acoustic Reflector

The shallower of the two principal acoustic reflectors seems to be less continuous and is seen most commonly in the inner to midshelf. In some areas, this horizon is seen only as the bottoms of truncated channels (fig. 6-23). The smaller areal extent is possibly due to erosional processes active on the shelf today or in the past, from subaerial erosion during lower stands of the sea and/or restricted depositional environment. Also, this horizon is generally absent on the outer shelf possibly due to the scouring effects of the Gulf Stream or shoreface erosion at a lower sea level.

Figure 6-23. 3.5-kHz record showing shallow reflector (indicated by arrow) seen as the bottoms of truncated channels (line 29_4 at 0550 hours).

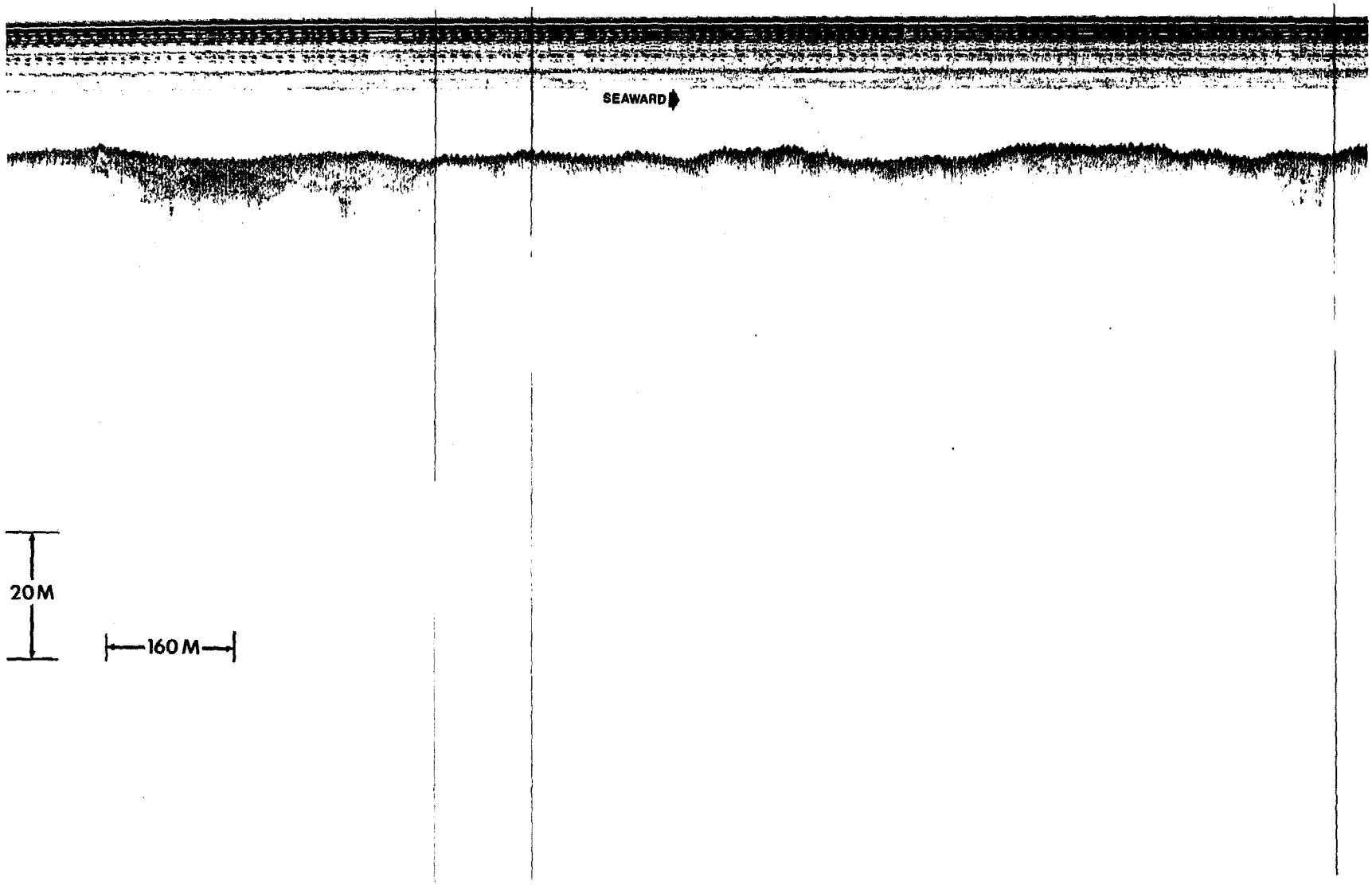

Figure 6-23

Lower Acoustic Reflector

The deeper of the shallow reflectors is more extensive in occurrence and shows a hummocky erosional surface (fig. 6-24). This horizon can be seen to be developed between unconformable units and is incised by channels probably of fluvial origin. Work done by Woolsey (1977) on the inner shelf shows a horizon which is at about the same depth and characteristically channeled. This unconformity apparently separates the underlying Pliocene to Miocene age beds from the overlying Pleistocene to Holocene material.

Channeling

Channels of various sizes and morphologies are seen cutting into the shelf sediments. These features are important for the reconstruction of paleodrainage patterns because they are often the only preserved structures related to subaerial exposure on the shelf which record former lowstands of the sea. Being sheltered by their own incisement, the channels have not been planed off by the subsequent transgression or incorporated into the surficial sand sheet by present-day processes.

Deep Channels

Shallow seismic records show the presence of channels which are conspicuous due to their great depth and which have large apparent width due to lateral migration or the angle at which the seismic line cuts the features. Some channels are up to 40 m in depth and many are in excess of 20 m. When comparing these channels to present fluvial systems, depths of the order of 20-40 m are formed only in major rivers or at intersections of larger tidal channels and inlet throats of estuaries.

The time necessary for development of a tidally scoured channel would require a lengthy period of sea-level stability, thus indicating a

Figure 6-24. 3.5-kHz record showing deeper reflector (indicated by arrow) overlain by shallower reflector (line 18_4 at 0530 hours).

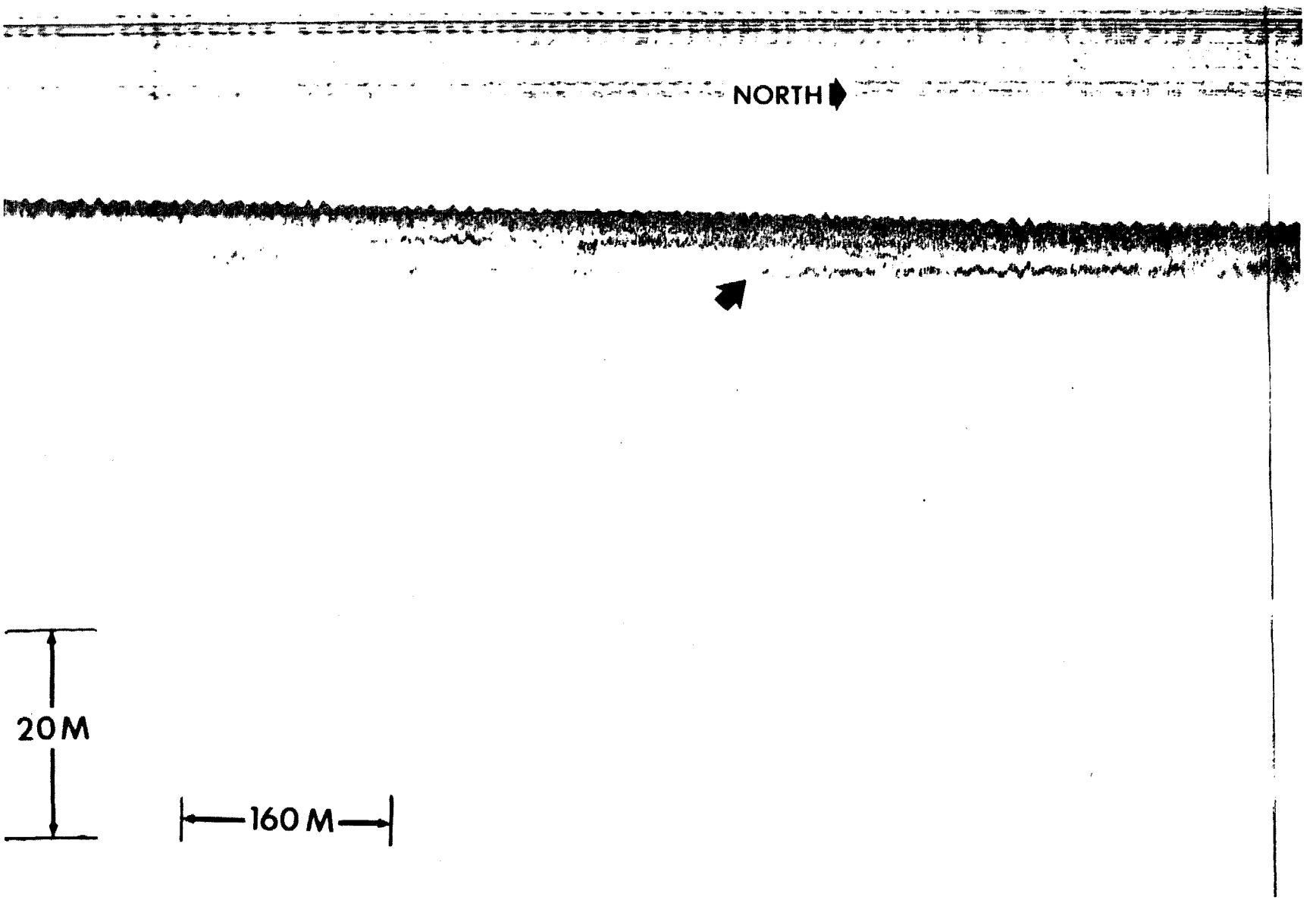

Figure 6-24

stillstand or at least a slowing rate of sea-level change, either transgression or regression. The isolated occurrence of deep channels suggests a localized feature rather than a continuous incised channel extending across the shelf resulting from a single, prolonged episode of falling sea level.

Where these channels are not truncated by erosion they seem to be established on the deeper reflector and are subsequently infilled and overlain by the shallower reflector where present. The deeper channels also show smaller channels within the infilling sediment, indicating a change in the base level from transgression of the sea (fig. 6-25).

Shallow Channels

Channels whose depths are <15 m are by far the most common and show a great diversity in morphology, ranging from cut-and-fill structures to channellike depressions devoid of internal structures (fig. 6-26). The smaller channels can be seen in both the shallow or deeper reflector, but in general the shallow reflector seems to show only the small channels, rarely exceeding 5 m depth.

The nearshore profiles from Tybee Island to St. Catherines Island show a high density of channeling. This may be the offshore expression of the ancestral Savannah and/or Ogeechee Rivers.

Offshore of St. Catherines Sound on GS-4 lines 26 and 27 is a buried erosional surface with approximately 10 m relief (fig. 6-27). It is possible that this is a channel surveyed at an acute angle, but the lack of structures such as cut and fill or superimposed channeling leaves interpretation open to conjecture.

Large Sedimentary Structures

An extensive wedge of large foreset beds previously described by Woolsey (1977) and Henry and others, (1978) occurs on the nearshore

Figure 6-25. Uniboom profile showing deep channel (approximately 40 m) established upon and cutting into deeper reflector. Note smaller channel superimposed indicating a change of base level during transgression. Smaller channel is established upon the shallower reflector (line 12_3 at 0615 hours).

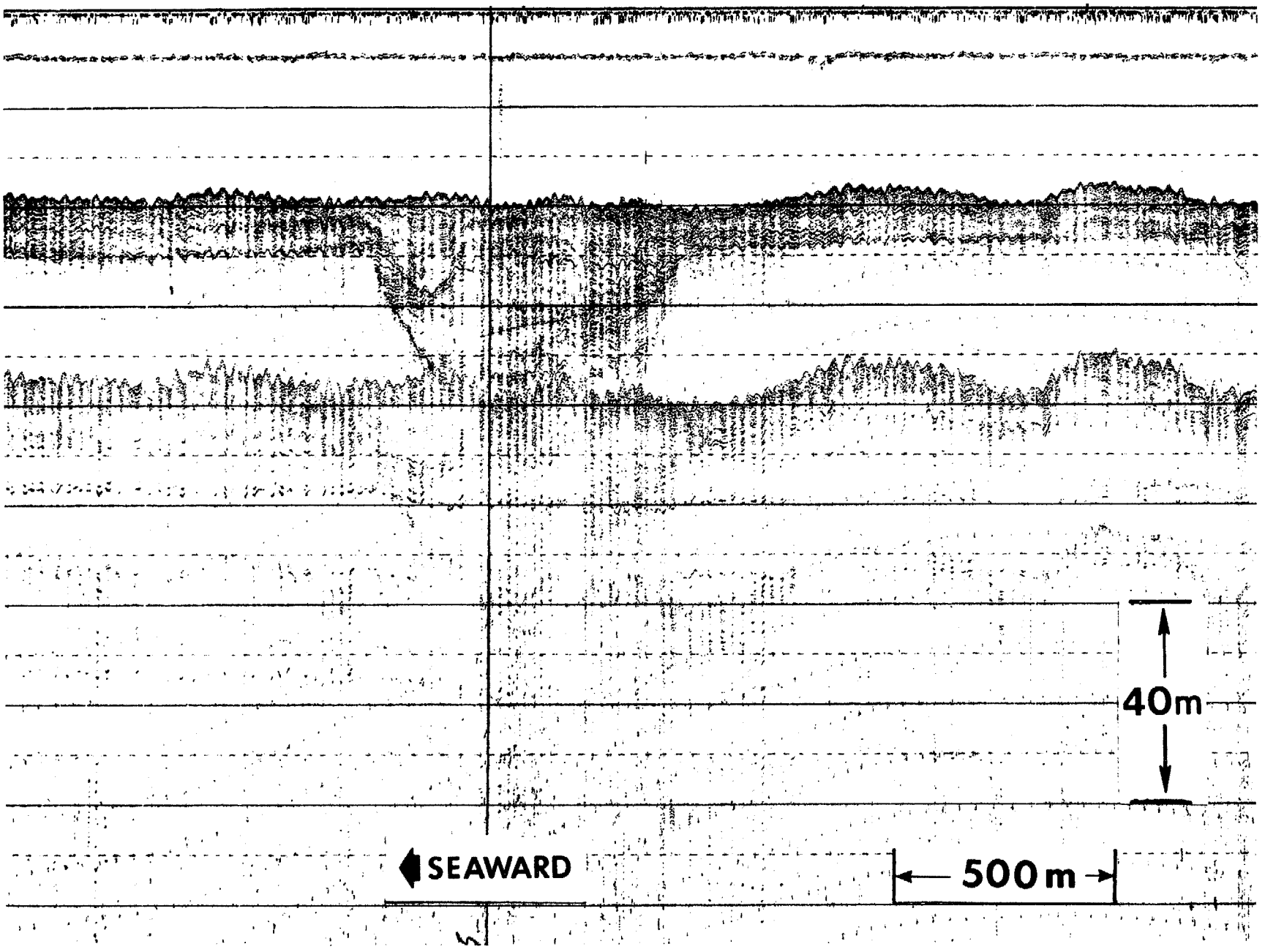

Figure 6-25

Figure 6-26. 3.5-kHz records showing channeling with internal structure (top) and without (bottom) (top-line 21_4 at 1345 hours; bottom-line 8_2 at 0700 hours).

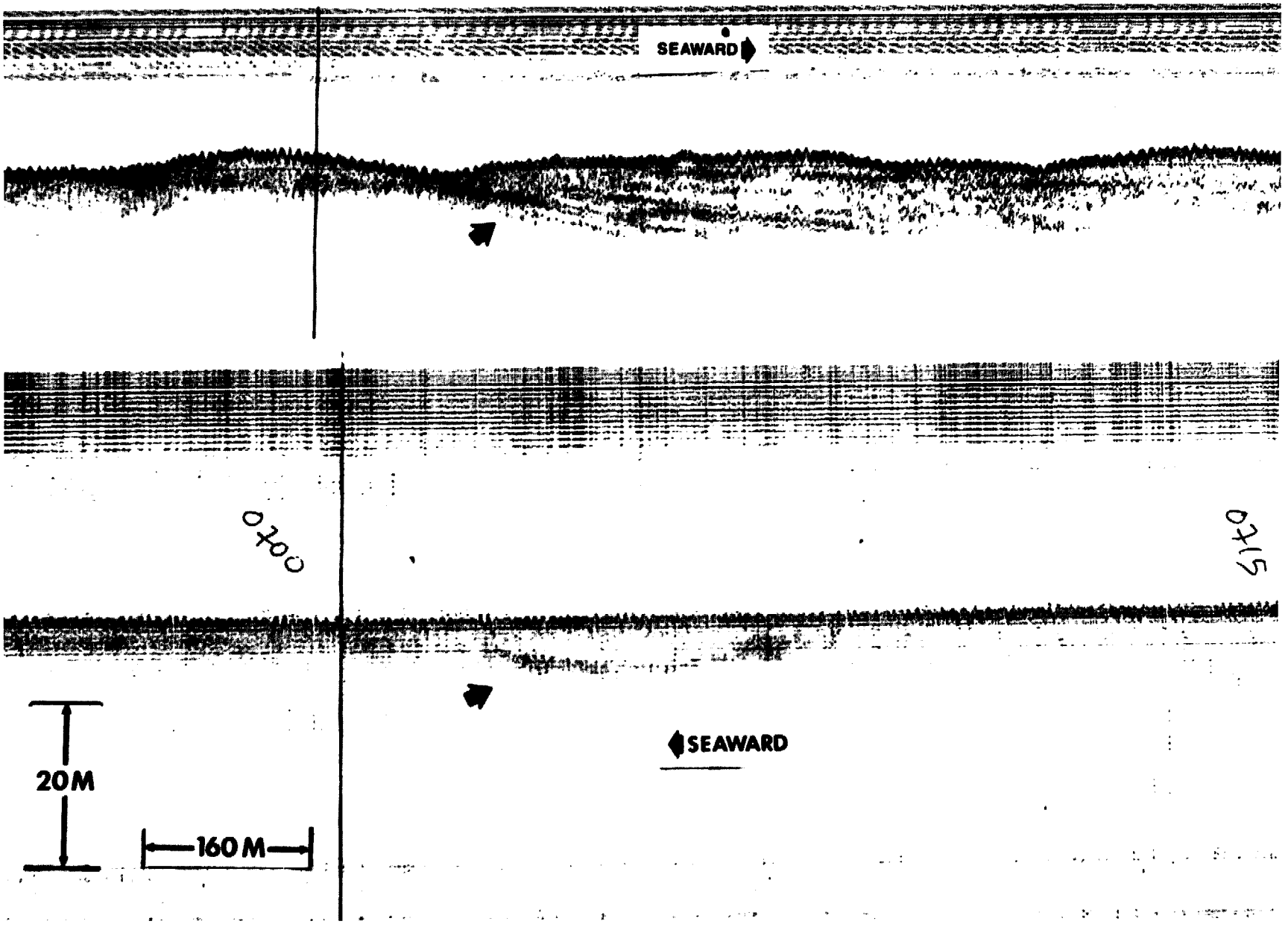

Figure 6-26

Figure 6-27. Uniboom profile showing erosional surface and unconformable relationship between units above and below the deeper reflector (line 26_4 at 2240 hours).

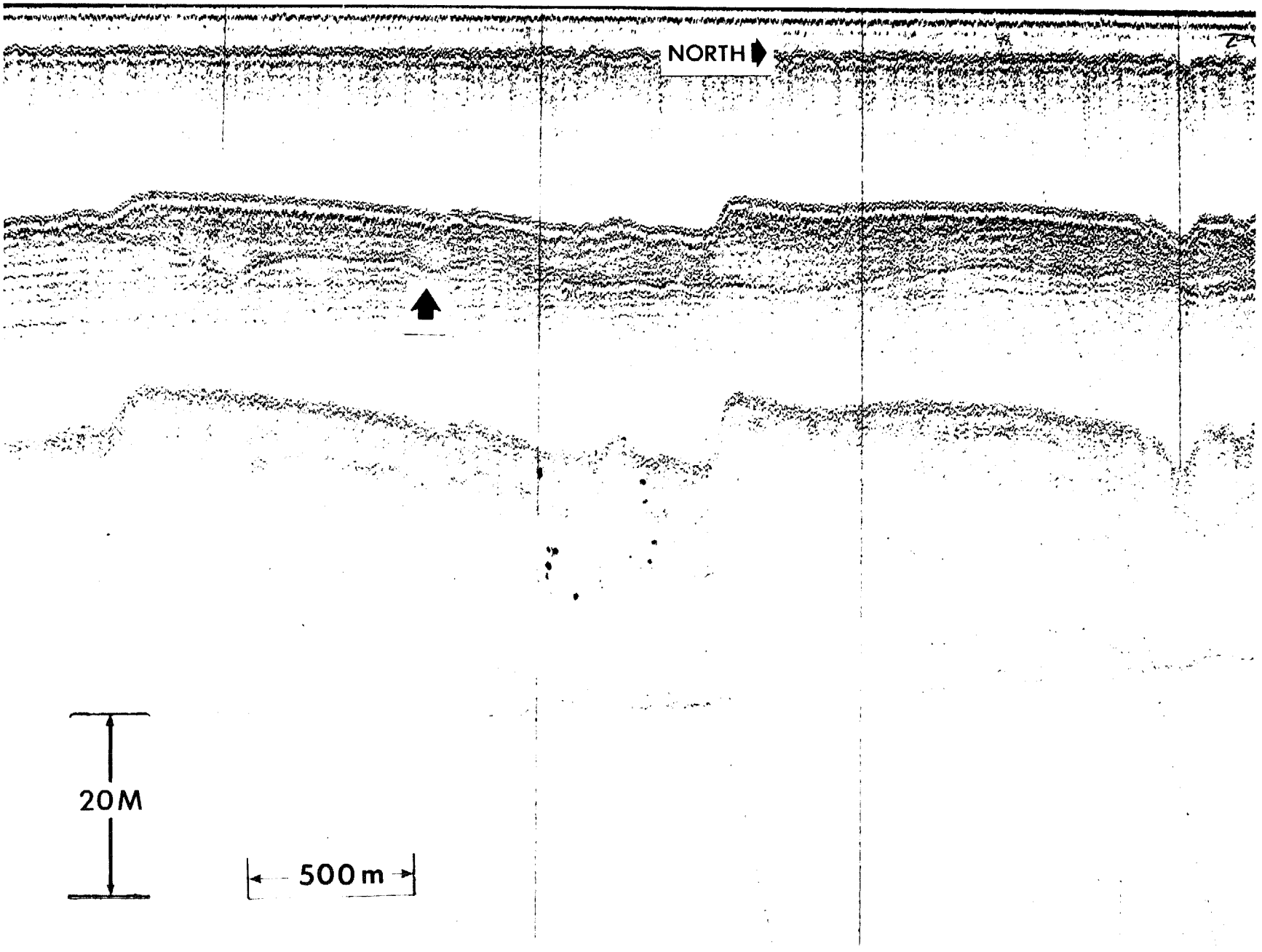

Figure 6-27

transects from Jacksonville to Jekyll Island in sediments of Pliocene age (fig. 6-28). These features follow a northerly trend at an angle to the coast and have been documented on the inner shelf of Florida between Jacksonville and Cape Canaveral by Field and Duane (1974). The offshore margins of these structures are irregular, extending farther seaward off modern rivers. This relationship together with their bedding character suggests that they are coalescing fan deltas deposited during a period of increased coastal sedimentation.

Lines 8_2, 10_2, 11_2, 12_2, 10_3, 11_3, and 12_3 show such large-scale foresets prograding seaward over a buried erosional scarp of approximately 8-10 m relief. A filled channel of approximately 2 km apparent width and 20 m depth is located just landward of this sequence suggesting a distributary channel/deltaic sequence.

Faulting

Based on examination of the seismic records, the tectonic activity associated with the southeast Georgia Embayment has not been expressed in this area in the form of shallow faulting.

VIDEO (CCTV) INTERPRETATION OF BENTHIC ENVIRONMENTS

Interpretation Scheme

The following discussion is based on the biological geological interpretation of sixty-two one-hour closed-circuit television tapes from cruises GS-1 through 4 (fig. 6-21) and 22 submersible dives in R/S DIAPHUS in August 1978 (fig. 6-29). The 550 km of video coverage obtained during these surveys was correlated with side-scan sonar, 3.5 kHz, and Uniboom seismic records to delineate the occurrence, distribution, gross species composition, and community structure. Results are summarized in Map Series D (plate in pocket in back cover).

Figure 6-28. Uniboom record showing foreset bedding of probable deltaic origin (line 9_4 at 0600 hours).

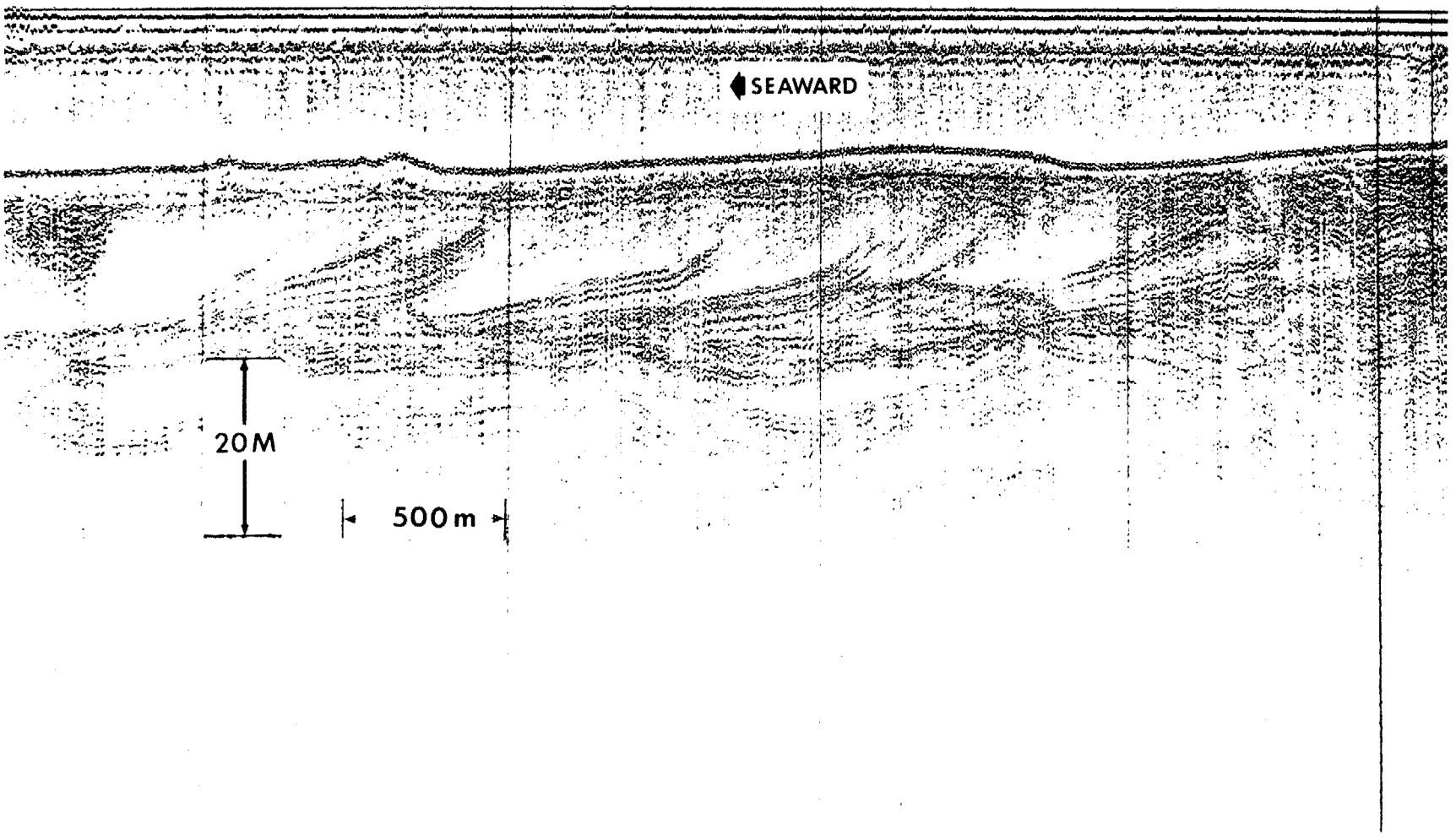

Figure 6-28

Figure 6-29. Dive sites, submersible DIAPHUS, STATE ARROW leg 3, August 1978.

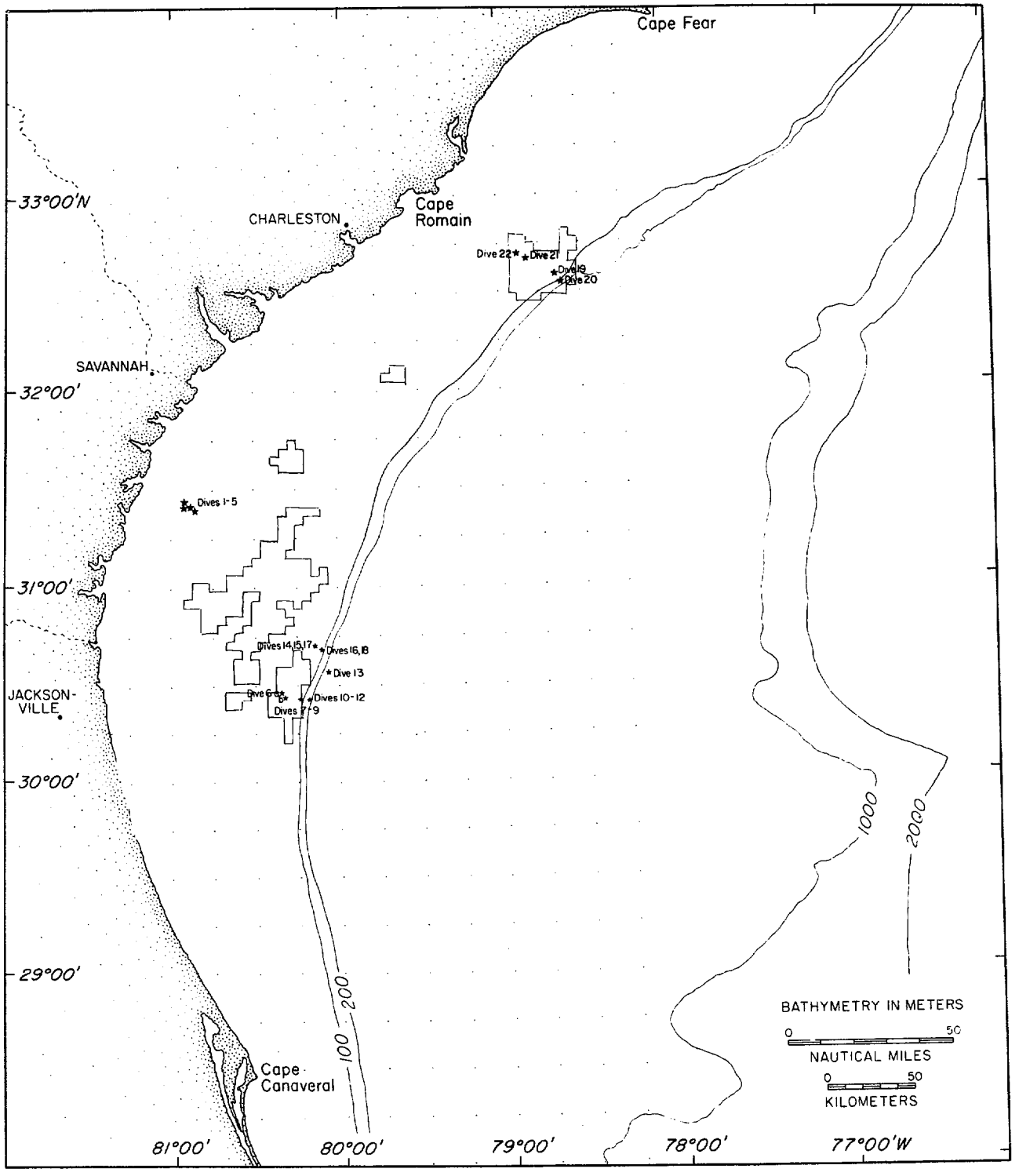
Cape Fear
33°00'N
CHARLESTON
Cape
Romain
Dive 22
Dive 21
Dive 19
Dive 20
SAVANNAH
32°00'
Dives 1-5
31°00'
Dives 14,15,17
Dives 16,18
Dive 13
Dive 6
Dives 10-12
Dives 7-9
JACKSON-
VILLE
30°00'
1000
2000
29°00'
200
100
Cape
Canaveral
BATHYMETRY IN METERS
0
50
NAUTICAL MILES
0
50
KILOMETERS
81°00'
80°00'
79°00'
78°00'
77°00'W

In most cases, precise species identification of benthic organisms observed was not possible due to the absence of samples for laboratory verification, however, an attempt was made to at least broadly classify benthic organisms observed on the videotapes. In addition, tentative interpretations of sediment texture and bottom features associated with the live bottoms were made.

Map symbols were chosen that closely resembled the organism or geological feature in question, so as to minimize the confusion in data interpretation as presented on the maps. The relative abundance of each organism depicted is indicated by the frequency of that symbol along each video track line and is highly subjective. Live-bottom habitats were so structurally diverse that faunal symbols were necessarily limited to major epifaunal taxa for the most part (i.e., soft corals, sponges, macroalgae, and fish) due to space limitations.

The relative degree of bioturbation was subjectively determined along each towed underwater television track line reflecting both infaunal and epifaunal action on surficial sediments. Small-scale bed forms were noted on the maps but not differentiated as to size or morphology.

Distribution of Benthic Environments

Coarse sand/shell bottom was characterized by low to high concentrations of shell hash, primarily bivalve shell halves heavily encrusted with algae. Also observed on this type of bottom were varying amounts of "rocklike" debris, which appear to be a conglomerate of shell, algae (*Lithothamnion* balls), and other material, perhaps bryozoa. Outcropping rocks associated with moderate and high-relief reef types were observed on the videotapes in the inshore areas at Grays Reef (Hunt, 1974) and at shelf-edge localities off Jacksonville, Brunswick,

and Charleston. More abundant were low-relief live bottoms characterized by the occurrence, on an otherwise flat, sandy bottom, of a structurally diverse attached sessile community (i.e., soft coral, sponges, etc.) signifying an underlying hard layer.

The living fauna observed on videotapes was highly diversified but generally restricted to epibenthic species and demersal fish, although some pelagic species also were noted. The resolution of the TV camera varied from poor to excellent depending on the water.

An analysis of videotapes suggests in general a nonrandom distribution of epibenthos and spatial heterogeneity in the surficial sedimentary environment over the Georgia shelf. The biological interpretation of videotapes focused primarily on epibenthic faunas and demersal and pelagic fish within visual range of the TV camera. Infaunas were rarely observed due to their cryptic nature and habitat preferences. Densities of infaunal burrows were noted whenever possible and are generally reflected in the degree of bioturbation noted from the tapes. Individual species were identified to the lowest possible taxa within the limitations of the TV resolution capabilities. Taxa of major importance were generally widely distributed over the study area. Echinoderms were the single most common taxa of fauna observed over the Georgia shelf, especially in the soft bottom areas. Of these, starfish (Asteroidea), sea urchins (Echinoidea), and sea cucumbers (Holothuroidea) were most commonly observed. As depicted in Map Series D, large aggregates of sea urchins and sea cucumbers were observed along a number of midshelf and shelf-edge locations, especially due east of Brunswick. These deposit-feeding organisms are capable of completely reworking the soft surficial sediments, and video observations gave ample evidence of this from their numerous trails. Another biogenic

structure of some significance in the soft bottom areas was the abundance of shallow depressions. These shallow depressions varied in diameter from less than 0.5 m to almost 1 m. The smaller depressions were probably fish nesting or resting sites, while the larger depressions were most likely generated by stingrays (David Miller, personal communication). These depressions were most commonly located in medium-fine to medium sand in the midshelf region. Stanley and Fenner (1973) have observed fish "nesting sites" concentrated in fine-grain sediment below the shelf break off North Carolina. Also, commonly associated with or near these depressions were large numbers of burrowing wrasses. These fish were quite numerous and widely distributed primarily within the midshelf region. Crustaceans were quite ubiquitous over the entire CCTV study area but were generally too small to be clearly resolved for specific identification. Portunid crabs, however, were readily identifiable and were widely distributed over the entire study area. Microflora, such as diatoms, thickly covered surficial sediments on the shelf except in areas where there was heavy sediment biogenesis due to grazing by epifaunas and infaunal burrowers or bed forms indicating active or recent sediment movement from tide or storm action. Macroalgae/bryzoa were nonrandomly distributed over the entire study area primarily in areas of consolidated sediments devoid of bed forms.

Sessile epifaunas associated with live bottoms were typically composed of species of sponges (Porifera), soft corals (Octocorals), bryozoans, and macroalgae, all of which require the presence of a hard substrate for attachment. Demersal and pelagic fish were very numerous over reef areas because of the spatial heterogeneity of the reef habitat, which provides both food and refuge for many invertebrate and

vertebrate species. Many of the fish observed on the CCTV tapes in the reef habitats were tropical species, such as groupers, snappers, angelfish, butterfly fish, and damselfish. Struhsaker (1969) noted the distribution and composition of demersal fish on the continental shelf between North Carolina and north Florida. He found the fish in live-bottom reef habitats were typically tropical species. Tropical invertebrates, such as the Florida spiny lobster were observed frequently on the shelf-edge reefs and have been observed on inshore reefs infrequently, such as Grays Reef. In general, most inshore and midshelf reefs observed on CCTV were of the low-relief form, although relatively extensive moderate-relief areas were also observed on videotapes at Grays Reef and at another inshore reef located 37 km due east of St. Catherines Island. The inshore reefs, although patchy and discontinuous, are quite extensively distributed along the 20-25 m isobath, extending through the survey area from Jacksonville, Florida, to Savannah, Georgia. High-relief hard-bottom areas were restricted to the shelf edge 30-100 m isobath, exhibiting extensive rock outcrops and topographic relief. These areas, as well as the low to moderate-relief hard-bottom reefs, exhibited a highly diverse flora and fauna compared with soft bottom areas, where epifaunal diversity was markedly low for the most part. Schooling fish (Clupidae, etc.) were frequently observed over both soft and hard-bottom areas, exhibiting no discernible habitat preferences.

Studies of the benthic community distribution, composition, and structure over the continental shelf extending from the Carolinas to north Florida have confirmed the existence of a highly diverse benthic fauna in both soft and hard-bottom areas (Pearse and Williams, 1951; Cereme-Vivas and Gray, 1966; Menzies and others, 1966; Day and Field,

1971; Avent and others, 1977). Benthic faunas observed belong primarily to two biogeographical provinces. Those benthic organisms distributed within the inner shelf soft bottom areas lie principally within the Carolinian Province, while those found in the reef habitats and outer continental shelf belong principally to the Tropical Province.

REFERENCES CITED

Avent, R.M., King, M.E., and Gore, R.H., 1977, Topographic and faunal studies of shelf-edge prominences off the Central Eastern Florida coast: Int. Revue gesamten Hydrobiol., v. 62, no. 1, p. 185-208.

Blackwelder, B.W., Pilkey, O.H., and Howard, J.D., 1979, Late Wisconsinan sea levels on the Southeast U.S. Atlantic Shelf based on in-place shoreline indicator: Science, v. 204, p. 618-620.

Cereme-Vivas, M.J., and Gray, I.E., 1966, The distributional pattern of benthic invertebrates of the continental shelf off North Carolina: Ecology, v. 47, no. 2, p. 260-270.

Day, J.H., and Field, J.G., 1971, The use of numerical methods to determine the distribution of the benthic fauna across the continental shelf of North Carolina: J. Animal Ecology, v. 40 p. 93-125.

Field, M.E., and Duane, D.B., 1974, Geomorphology and sediments of the inner continental shelf, Cape Canaveral, Florida: Technical Memorandum no. 41, March 1974, U.S. Army, Corps of Engineers, Coastal Engineering Research Center, Ft. Belvoir, VA.

Hathaway, J.C., Schlee, J.S., Poag, C.W., Valentine, P.C., Weed, E.G.A., Bothner, M.H., Kohout, F.A., Manheim, F.T., Schoen, R., Miller, R.E., and Schultz, D.M., 1976, Preliminary Summary of the 1976 Atlantic Margin Coring Project of the U.S. Geological Survey: U.S.

Geolgical Survey Open-File Report 76-844.

Henry, V.J., and Giles, R.T., 1979, Distribution and occurrence of reefs and hard grounds in the Georgia Bight:, Chapter 8, Environmental Geologic Studies Southeastern United States Atlantic Outer Continental Shelf, U.S. Geological Survey Office of Marine Geology, Woods Hole, MA, Draft Final Report to the Bureau of Land Management.

Henry, V.J., Giles, R.T., and Harding, J.L., 1978, Geological evaluation of potential pipeline corridor sites along the Georgia Coast: Final Report to the Georgia Office of Planning and Budget, Atlanta, Georgia, 36 p.

Hunt, J.L., 1974, The geology and origin of Grays Reef, Georgia Continental Shelf: MS. Master's Thesis, University of Georgia, Athens, Georgia.

Menzies, R.J., Pilkey, O.H., Blackwelder, B.W., Dexter, D., Huling, P., and McCloskey, L., 1966, A submerged reef off North Carolina: Int. Revue gesamten Hydrobiol, v. 51, no. 3, p. 393-431.

Miller, D., 1979, Personal communication, Georgia Marine Extension Center, Savannah, Georgia.

Pearse, A.S., and Williams, L.G., 1951, The biota of the reefs off the Carolinas: J. Elisha Mitchell Scientific Society, v. 67, p. 133-161.

Stanley, D.J., and Fenner, P., 1973, Underwater television survey of the Atlantic outer continental margin near Wilmington Canyon: Smithsonian Contrib. Earth Sciences, no. 11, p. 1-54.

Struhsaker, P., 1969, Demersal fish resources: composition, distribution, and commercial potential of the continental shelf stocks of the southeastern United States: Fish. Ind. Res. v. 4,

no. 4, p. 261-300.

Woolsey, J.R., 1977, Neogene Stratigraphy of the Georgia Coast and Inner Continental Shelf: unpublished Ph.D. dissertation, University of Georgia, Athens, Georgia.

CHAPTER 7

SEISMIC STRATIGRAPHY OF THE NORTHERN AND CENTRAL BLAKE PLATEAU

Paul R. Pinet[1], Peter Popenoe[2], Susan M. McCarthy[2], and Marshall L. Otter[2]

[1]U.S. Geological Survey and Colgate University, Department of Geology, Hamilton, New York 13346

[2]U.S. Geological Survey, Woods Hole, Massachusetts 02543

CHAPTER 7

Table of Contents

Page

Abstract. 7- 1

Introduction. 7- 2

Purpose 7- 2

Physiography. 7- 3

Previous work 7- 3

Methods and materials 7- 7

Results and Discussion. 7-10

Upper Cretaceous unit 7-10

Albian sequence 7-10

Coniacian-Turonian sequence 7-24

Santonian sequence. 7-36

Campanian-Maestrichtian sequence. 7-42

Summary of Late Cretaceous environments 7-49

Cenozoic section. 7-54

Paleocene sequence. 7-54

Eocene-Oligocene sequence 7-64

Post-Oligocene sequence 7-77

Structural and stratigraphic development of the northern

Blake Plateau 7-83

Summary 7-85

References cited. 7-88

CHAPTER 7

SEISMIC STRATIGRAPHY OF THE NORTHERN AND CENTRAL BLAKE PLATEAU

Paul R. Pinet, Peter Popenoe, Susan M. McCarthy, and Marshall L. Otter

ABSTRACT

The stratigraphic framework of the northern half of the Blake Plateau was interpreted from over 4,700 km of single-channel, air gun and sparker, seismic-reflection profiles. Age control for the seismic stratigraphy is based on drill data from three well sites on the plateau and on correlations to seismic sequences beneath the Florida-Hatteras Continental Shelf and Slope.

The Blake Plateau represents the frontal edge of a thick continental margin sedimentary prism. The shallow stratigraphy of the plateau consists of a thick Upper Cretaceous sequence that is capped by thin and discontinuous Cenozoic deposits.

Upper Cretaceous strata are divided into four major units that are most distinguishable beneath the northernmost part of the plateau. Here, a basal Albian sequence is overlain by three progradational wedges (a Coniacian-Turonian sequence, a Santonian sequence, and a Campanian-Maestrichtian sequence) that are composed of sediments deposited in continental shelf and slope environments. Depocenters shifted markedly throughout the Late Cretaceous, probably in response to variations in sediment input and to fluctuations of sea level. South of 31°N., Upper Cretaceous sediments accumulated seaward of the shelf break in a slowly subsiding basin that was flanked on the east by a topographically prominent, but dead Albian reef complex. Environmental conditions in the basin likely were uniform, as inferred from the acoustically transparent character of the deposits.

Three thin, but mappable, units whose ages are inferred to be Paleocene, Eocene-Oligocene, and post-Oligocene comprise the Cenozoic section. Well data from three well sites indicate that foraminiferal ooze, limestone, and calcarenitic sand are the dominant lithologies comprising the Cenozoic sequence. The major geologic agent at this time was the Gulf Stream; it appeared over the plateau during the early Tertiary and profoundly affected sedimentation patterns, controlling the location of the shelf edge and scouring the plateau's surface. Continued slow crustal subsidence in conjunction with low rates of sedimentation throughout the Cenozoic transformed the Blake Plateau into a deepwater environment where thin carbonate oozes accumulated.

INTRODUCTION

Purpose

Previous work has delineated the broad structural, stratigraphic, and sedimentological framework of the Blake Plateau. However, because of a recent resurgence of interest in evaluating the petroleum prospects and environmental hazards to exploration of the region, refinements in our understanding of the area's geology are required. In this context, our intent is 1) to define the seismic stratigraphy of the plateau, noting in particular regional variations in acoustical appearance, thickness, and overall geometry of each seismic unit; 2) to ascertain the probable age of each stratigraphic sequence, utilizing well data at three drill sites and previously interpreted seismic lines; and 3) to determine environments of deposition for the Blake Plateau during the Late Cretaceous and Cenozoic. A discussion of environmental hazards to petroleum exploration and development of the northern Blake Plateau from the examination of seismic profiles is presented in chapter 8 of this volume.

Physiography

The morphology of the continental margin that adjoins the Carolinas, Georgia, and Florida is atypical, because of the presence of the Blake Plateau (fig. 7-1). The western edge of the plateau abuts the toe of the Florida-Hatteras Continental Slope at water depths ranging between 300 and 600 m. The declivity of the plateau surface is slight, but is inclined to the east, the bottom gradients being somewhat steeper at its northern limit than its southern end (Pratt and Heezen, 1964). The broad plateau occupies an area of about 128,000 km^2 (fig. 7-1). The steep Blake Escarpment forms the seaward edge of the plateau at a water depth of about 1,000 m. To the south, the escarpment is separated from the Florida-Hatteras Slope by over 250 km, but to the north, these two entities merge into one physiographic unit off Cape Lookout, North Carolina.

Previous Work

Numerous bathymetric, sedimentological, and geophysical surveys of the Blake Plateau and environs have been completed during the past two decades. Initial summaries of the physiography (Heezen and others, 1959) and of the structure of the northern part of the plateau (Hersey and others, 1959) provided the broad framework for planning subsequent studies. Pratt and Heezen (1964) not only incorporated many new sounding lines into an updated version of the plateau's topography, but also emphasized the role played by the Gulf Stream in shaping its surface and in determining the distribution and texture of its sediment (Pratt, 1966).

By the mid-1960's, the systematic geophysical surveys provided invaluable data related to the structural development of the Florida-Hatteras Shelf and Slope, Blake Plateau, and Blake Escarpment.

Figure 7-1. Physiography and bathymetry of the continental margin of the southeastern United States. Isobaths are in metres.

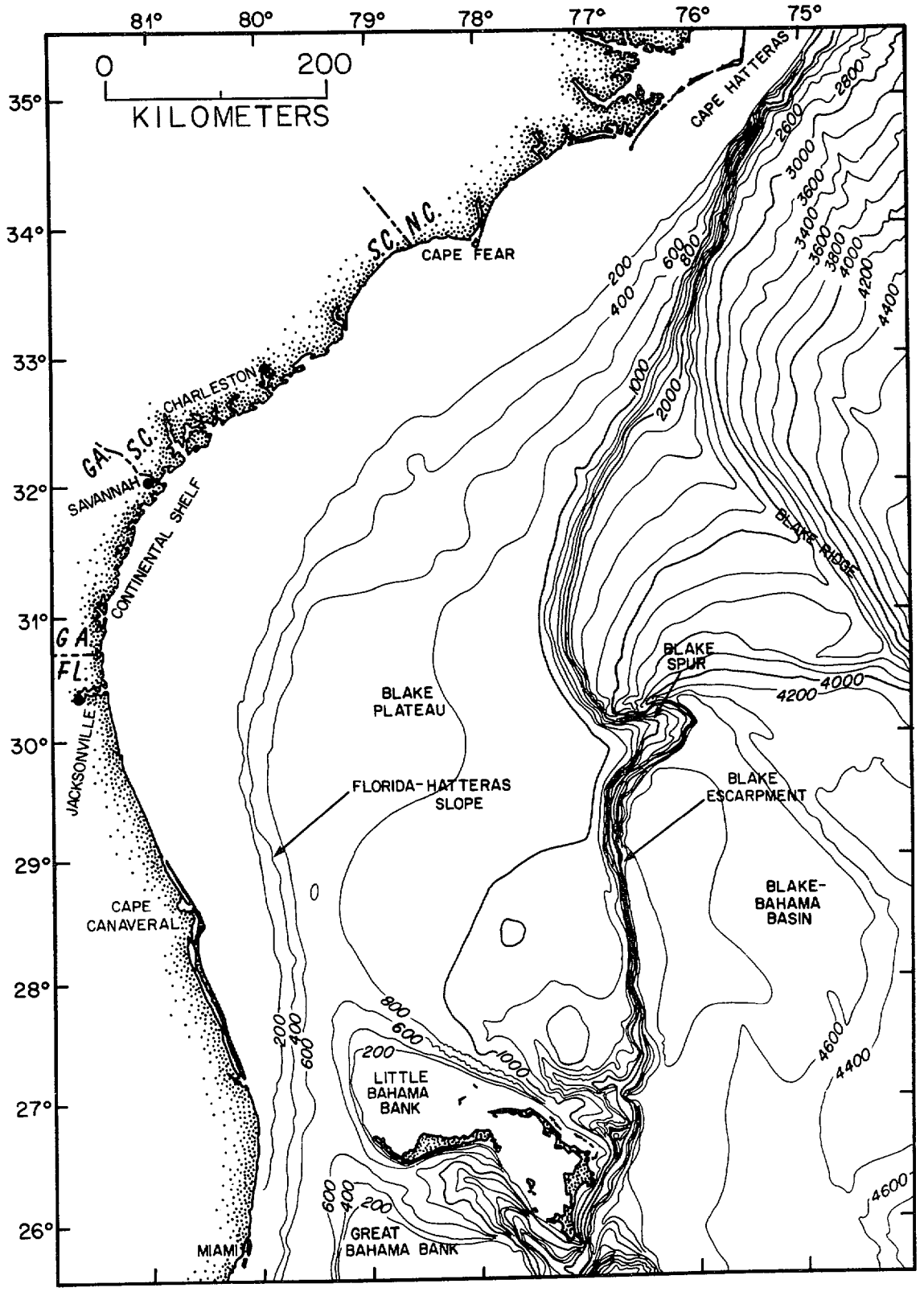
81°
80°
79°
78°
77°
76°
75°
35°
34°
33°
32°
31°
30°
29°
28°
27°
26°
0
200
KILOMETERS
CAPE HATTERAS
CAPE FEAR
S.C.
N.C.
CHARLESTON
GA.
S.C.
SAVANNAH
CONTINENTAL SHELF
GA
FL.
JACKSONVILLE
CAPE CANAVERAL
MIAMI
BLAKE PLATEAU
FLORIDA-HATTERAS SLOPE
BLAKE SPUR
BLAKE RIDGE
BLAKE ESCARPMENT
BLAKE-BAHAMA BASIN
LITTLE BAHAMA BANK
GREAT BAHAMA BANK
200
400
600
800
1000
2000
2600
2800
3000
3400
3600
3800
4000
4200
4400
4600

Ewing and others (1966) established that prominent seismic reflectors beneath the plateau to a depth of 1 km are continuous and dip to the west towards the continental shelf; refraction velocity data (Antoine and Henry, 1965; Sheridan and others, 1965) enabled them to correlate stratigraphic units beneath the shelf with those beneath the plateau.

Subsequent drilling on the plateau under the auspices of the JOIDES program yielded lithological, thickness, fossil, and age data that provided a firmer footing for geophysical interpretations. For example, Emery and Zarudski (1977) integrated JOIDES drill data and seismic units, concluding that the Cenozoic section beneath the plateau is abbreviated and that deeper reflecting horizons are Cretaceous or older in age. Ewing and others (1966) synthesized available refraction and reflection data, well logs, and core samples into an evolutionary model for the late Mesozoic-Cenozoic development of the Blake Plateau and Blake Escarpment. They proposed that the plateau had been the site of shallow-water carbonate deposition behind a massive coral-reef barrier that grew just landward of the Blake Escarpment during much of the Cretaceous. Death of the reef mass and crustal subsidence and Gulf Stream erosion throughout the Cenozoic produced the deep submerged plateau.

High-resolution, shallow-penetration seismic reflection of the continental margin of the southeastern United States (Uchupi, 1967; Uchupi and Emery, 1967; Uchupi, 1970) indicated that the prism of sediment comprising the shelf and slope had prograded across the inner Blake Plateau during the Cenozic, the seaward growth being controlled largely by the Gulf Stream. Drilling of three additional JOIDES holes on the Blake Plateau confirmed the broad outlines of the plateau's development as a deepwater basin that underwent scouring by vigorous

bottom currents throughout most of the Tertiary (Schlee, 1977). Recently, common-depth-point (CDP) multichannel seismic data indicated that the Blake Plateau is a sediment depocenter containing over 10 km of largely Mesozoic fill that accumulated in a progressively widening Atlantic Ocean (Dillon and others, 1979a; Klitgord and Behrendt, 1979).

METHODS AND MATERIALS

During ISELIN cruise 78-3, about 4,700 km of single-channel, continuous seismic-reflection profiles were obtained in the area of the Blake Plateau bounded by the 28°N. and 32°N. lines of parallel (fig. 7-2). The grid pattern consists of 14 east-west trending dip lines spaced about 30 km apart and two north-south trending tie lines that converge towards the north. Tracklines connect the three drill sites located in the southern half of the study area, permitting age and lithological data to be tied into the seismic stratigraphy.

Three acoustical energy sources were utilized simultaneously throughout the survey, a Bolt[1] pneumatic acoustic repeater, a Teledyne sparker unit, and a 3.5-kHz tuned transducer. The sparker had a power of 600 joules and was activated at a repetition rate of 1.5 s. Two air guns with a chamber capacity of 40 in^3 each were fired simultaneously at 10 s intervals at a pressure of 2,000 psi. Returning signals were gathered by a 300 m-long hydrophone array, consisting of 200 elements. A shorter 20-element array received the sparker signal. Towing speeds were maintained at between 5 and 6 knots whenever possible, and the hydrophone was streamed at a depth of about 4 to 5 m. Analog signals

---

[1]Use of brand names in this report is for descriptive purposes only and does not constitute endorsement by the U.S. Geological Survey.

Figure 7-2. Tracklines along which both air-gun and sparker seismic profiles were obtained. The thick segments of the lines are portions of profiles that are reproduced in this report. J4, J6, and ASP 3 are drill sites that provided lithological and age data used in interpreting the seismic stratigraphy.

Figure 7-2

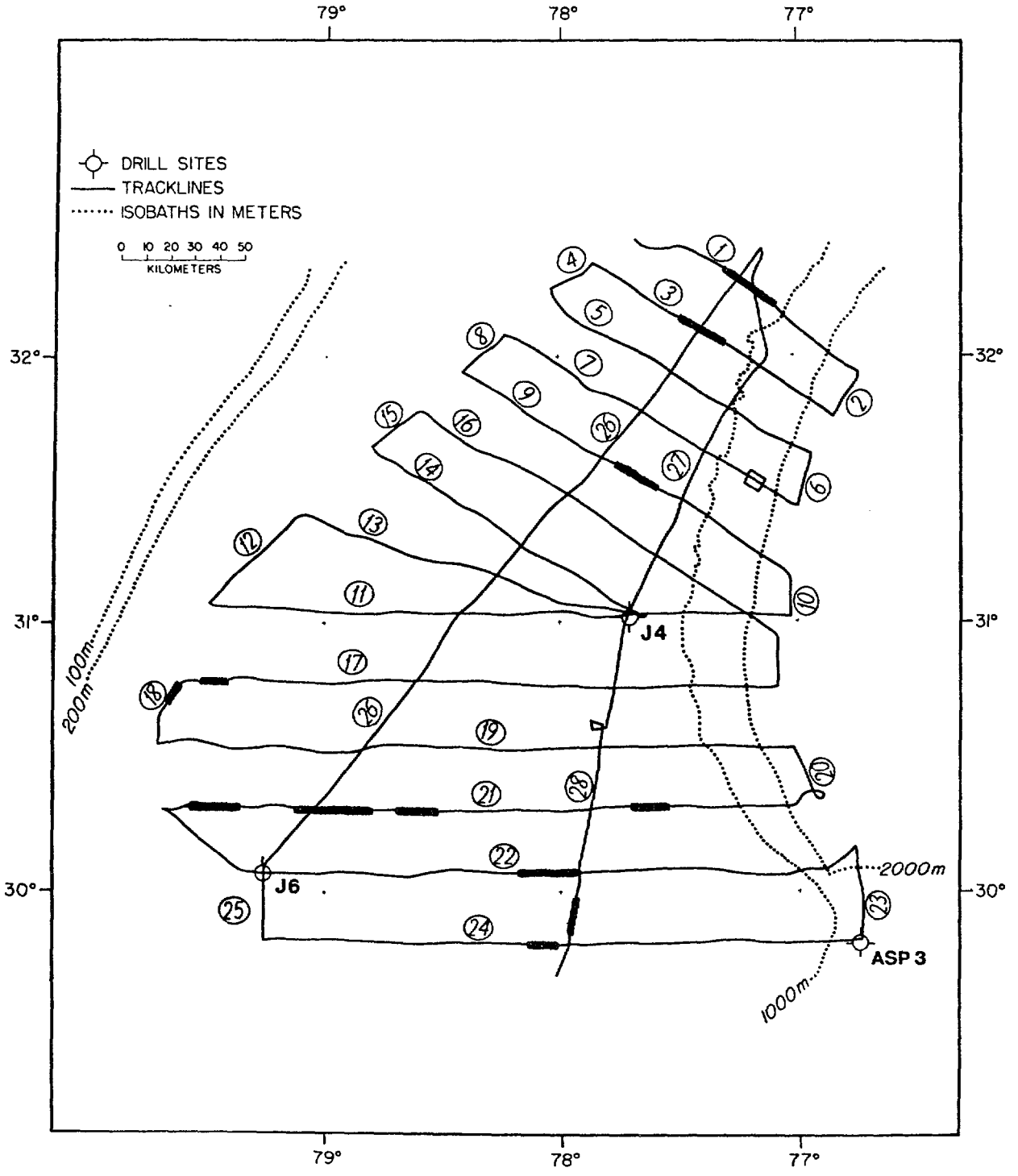
79°
78°
77°
32°
31°
30°
DRILL SITES
TRACKLINES
ISOBATHS IN METERS
0 10 20 30 40 50
KILOMETERS
J4
J6
ASP 3
100m
200m
1000m
2000m

were recorded on magnetic tape, after passing through band pass filters set at 150/300 Hz for the sparker system and 65/150 Hz for the air-gun unit. Signals also were displayed graphically on separate recorders with a 0.5/s sweep for the sparker and a 2.0/s sweep for the air gun.

RESULTS AND DISCUSSION

Analysis of stratigraphy from seismic data is a three-step process: definition of seismic sequences based on acoustical character, determination of the probable age of each unit relying on drill data, and facies interpretation utilizing the geometry, and internal reflector configuration of each sequence. Boundaries between most seismic sequences in the study represent stratigraphic discontinuities, below which reflectors are truncated by erosion or over which reflectors onlap or downlap older beds. In broadest outline, the stratigraphy as defined by this seismic survey, consists of thick Upper Cretaceous units that are overlain by thin Cenozoic deposits (fig. 7-3). The character and deposition of each unit are described below.

Upper Cretaceous Units

Albian Sequence

Two prominent reflectors, Al_a and Al_b, are associated with Albian sediments. The former defines the top of the Albian sequence, the latter a possible unconformity within the sequence (fig. 7-3). Age control is good and relies on a depth comparison of both reflectors to the stratigraphic interpretation of deep-penetration seismic line TD-5 that passes through the COST GE-1 well on the Florida-Hatteras Shelf and the ASP 3 well near the Blake Escarpment (Dillon and others, 1979b). Depth agreement between our survey lines and profile TD-5 is within 0.04 s of two-way travel time for both reflectors. Reflector Al_a also

Figure 7-3. Line drawings of air-gun seismic profiles that reveal the Upper Cretaceous stratigraphy of the Blake Plateau. Figures 7-3a, 3b, and 3c show dip lines; 3c also shows tie lines. Trackline locations are depicted in figure 7-2.

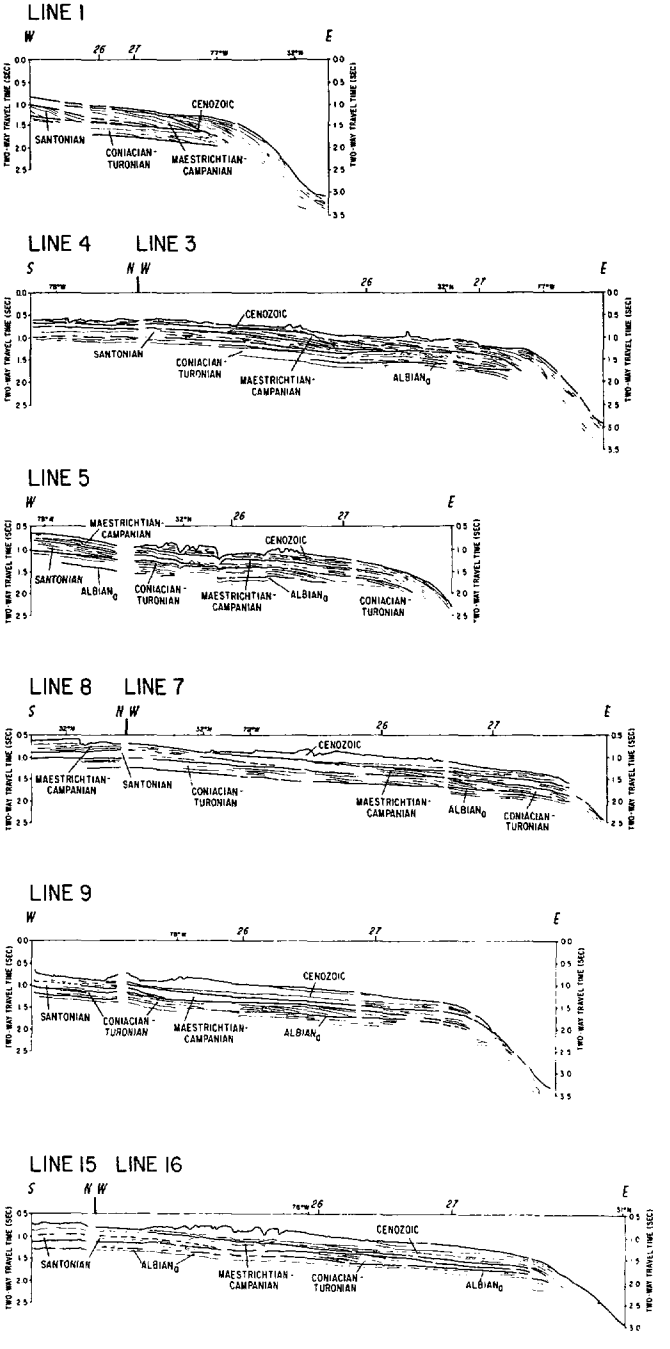
LINE 1
W
E
26
27
CENOZOIC
SANTONIAN
CONIACIAN-TURONIAN
MAESTRICHTIAN-CAMPANIAN
LINE 4
LINE 3
S
N W
E
26
27
CENOZOIC
SANTONIAN
CONIACIAN-TURONIAN
MAESTRICHTIAN-CAMPANIAN
ALBIAN
LINE 5
W
E
26
27
MAESTRICHTIAN-CAMPANIAN
CENOZOIC
SANTONIAN
ALBIAN
CONIACIAN-TURONIAN
MAESTRICHTIAN-CAMPANIAN
ALBIAN
CONIACIAN-TURONIAN
LINE 8
LINE 7
S
N W
E
26
27
CENOZOIC
MAESTRICHTIAN-CAMPANIAN
SANTONIAN
CONIACIAN-TURONIAN
MAESTRICHTIAN-CAMPANIAN
ALBIAN
CONIACIAN-TURONIAN
LINE 9
W
E
26
27
CENOZOIC
SANTONIAN
CONIACIAN-TURONIAN
MAESTRICHTIAN-CAMPANIAN
ALBIAN
LINE 15
LINE 16
S
N W
E
26
27
CENOZOIC
SANTONIAN
ALBIAN
MAESTRICHTIAN-CAMPANIAN
CONIACIAN-TURONIAN
ALBIAN
TWO-WAY TRAVEL TIME (SEC)

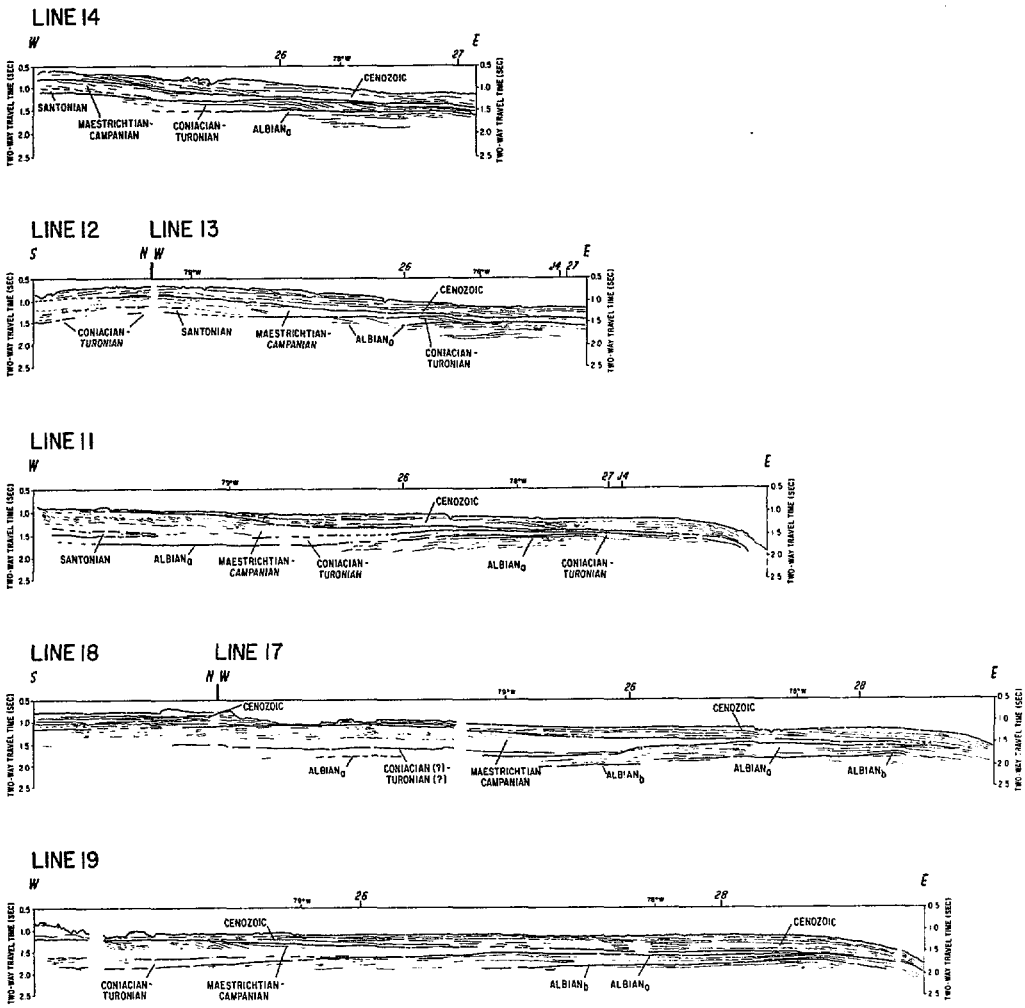
LINE 14
W
E
26
27
CENOZOIC
SANTONIAN
MAESTRICHTIAN-CAMPANIAN
CONIACIAN-TURONIAN
ALBIAN$_a$
TWO-WAY TRAVEL TIME (SEC)
LINE 12
LINE 13
S
N W
E
26
J4 27
CENOZOIC
CONIACIAN-TURONIAN
SANTONIAN
MAESTRICHTIAN-CAMPANIAN
ALBIAN$_b$
CONIACIAN-TURONIAN
LINE 11
W
E
26
27 J4
CENOZOIC
SANTONIAN
ALBIAN$_a$
MAESTRICHTIAN-CAMPANIAN
CONIACIAN-TURONIAN
ALBIAN$_a$
CONIACIAN-TURONIAN
LINE 18
LINE 17
S
N W
E
26
28
CENOZOIC
CENOZOIC
ALBIAN$_a$
CONIACIAN (?)-TURONIAN (?)
MAESTRICHTIAN CAMPANIAN
ALBIAN$_b$
ALBIAN$_a$
ALBIAN$_b$
LINE 19
W
E
26
28
CENOZOIC
CENOZOIC
CONIACIAN-TURONIAN
MAESTRICHTIAN-CAMPANIAN
ALBIAN$_b$
ALBIAN$_a$

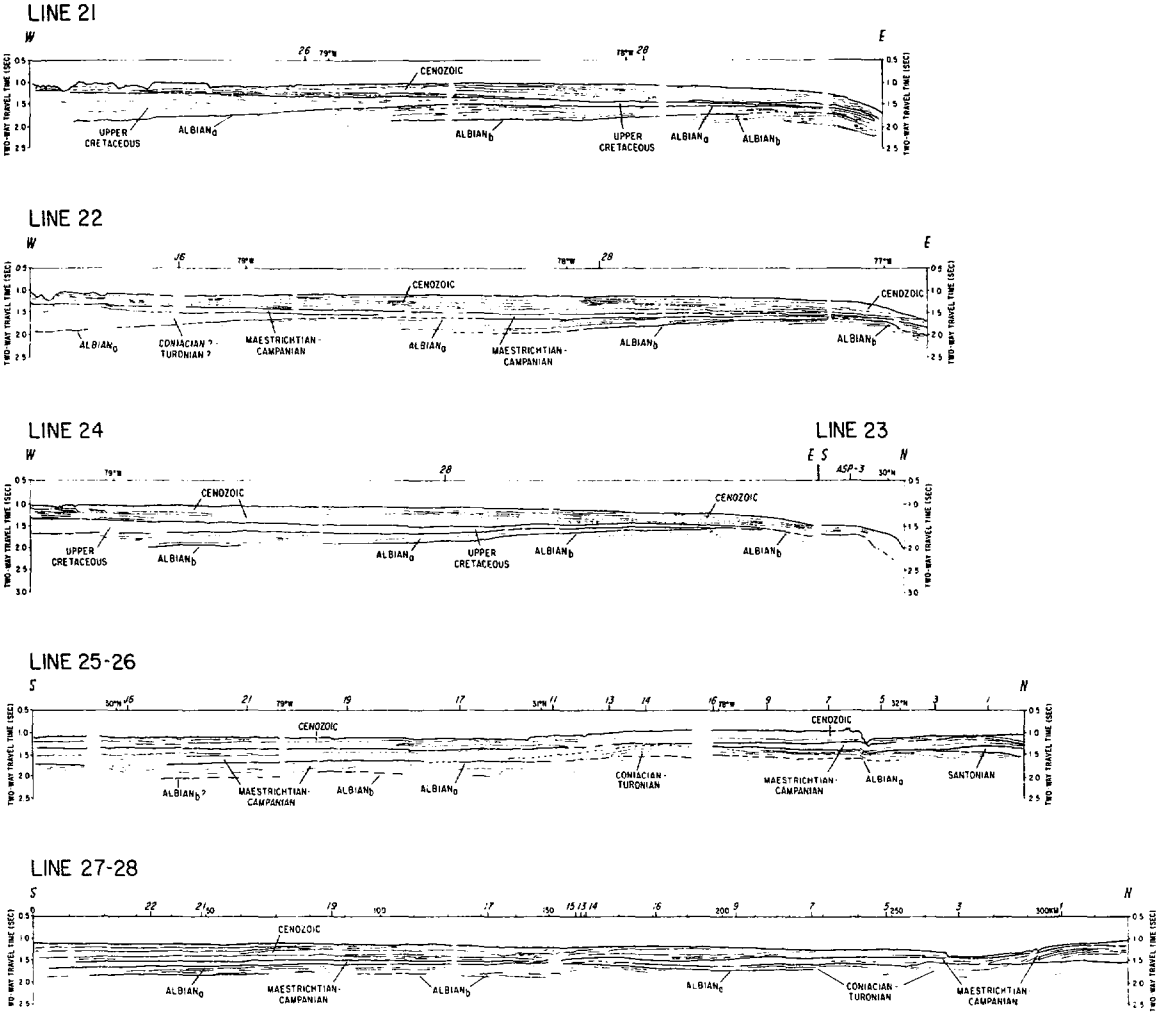
LINE 21
W
E
CENOZOIC
UPPER CRETACEOUS
ALBIAN$_a$
ALBIAN$_b$
UPPER CRETACEOUS
ALBIAN$_a$
ALBIAN$_b$
TWO-WAY TRAVEL TIME (SEC)
LINE 22
W
E
CENOZOIC
CENOZOIC
ALBIAN$_a$
CONIACIAN ? - TURONIAN ?
MAESTRICHTIAN - CAMPANIAN
ALBIAN$_a$
MAESTRICHTIAN - CAMPANIAN
ALBIAN$_b$
ALBIAN$_b$
TWO-WAY TRAVEL TIME (SEC)
LINE 24
LINE 23
W
E S
N
ASP-3
CENOZOIC
CENOZOIC
UPPER CRETACEOUS
ALBIAN$_b$
ALBIAN$_a$
UPPER CRETACEOUS
ALBIAN$_b$
ALBIAN$_b$
TWO-WAY TRAVEL TIME (SEC)
LINE 25-26
S
N
CENOZOIC
CENOZOIC
ALBIAN$_b$?
MAESTRICHTIAN - CAMPANIAN
ALBIAN$_b$
ALBIAN$_a$
CONIACIAN - TURONIAN
MAESTRICHTIAN - CAMPANIAN
ALBIAN$_a$
SANTONIAN
TWO-WAY TRAVEL TIME (SEC)
LINE 27-28
S
N
CENOZOIC
ALBIAN$_a$
MAESTRICHTIAN - CAMPANIAN
ALBIAN$_b$
ALBIAN$_c$
CONIACIAN - TURONIAN
MAESTRICHTIAN - CAMPANIAN
TWO-WAY TRAVEL TIME (SEC)

has been correlated with a distinct erosion surface apparent on seismic lines collected during FAY 017 and 018 cruises across the Florida-Hatteras Slope and inner Blake Plateau (Paull and Dillon, 1979).

The deeper reflector Al_b is traceable only in the southern part of the study area. Although few reflectors are apparent beneath the Al_b horizon, they are parallel to one another when present on the records (fig. 7-4). The Al_b reflector is deepest along the inner Blake Plateau and rises to the east, culminating in a broad NNW.-SSE.-trending ridge near the Blake Escarpment (fig. 7-5). The ridge which is crossed by lines 21 (fig. 7-6), 22, and 24 likely is the surface expression of an Albian reef bank identified by Dillon and others (1979b) on seismic line TD-5. However, because of the limited number of line crossings and difficulties in distinguishing the Al_b reflector in many profiles, the ridge is not delineated well nor is its reef composition confirmed. Hence, the ridge tentatively is interpreted as an Albian reef mass whose upward growth formed the eastern margin of a subsiding basin that was coincident with the Blake Plateau.

Reflector Al_a defines the top of the Albian sequence. Unlike Al_b, this surface can be mapped throughout the survey area. A major difference from north to south is apparent in the configuration of the Al_a reflector (fig. 7-7). North of 31°N., the top of the Albian series slopes seaward, the surface displaying a few irregularities east of tie line 26. Although acoustical penetration of the Al_a unconformity was poor along the western ends of the northern tracklines, the Albian sequence crossed by the eastern line segments (fig. 7-3) consists of a series of parallel reflectors (lines 7, 9, and 16), or of a combination of parallel and chaotic reflectors (lines 13 and 14). South of 31°N., in contrast to the north, the stratigraphic interval bounded by Al_a and

Figure 7-4. Photograph of portion of original air-gun profile. Coordinates for middle of this line segment are 30°05'N.,77°58'W. Location is shown on figure 7-2 as a thickened trackline segment. Note that Cretaceous reflectors all rise to the east, particularly Al_a and Al_b, two reflectors within the Albian sequence.

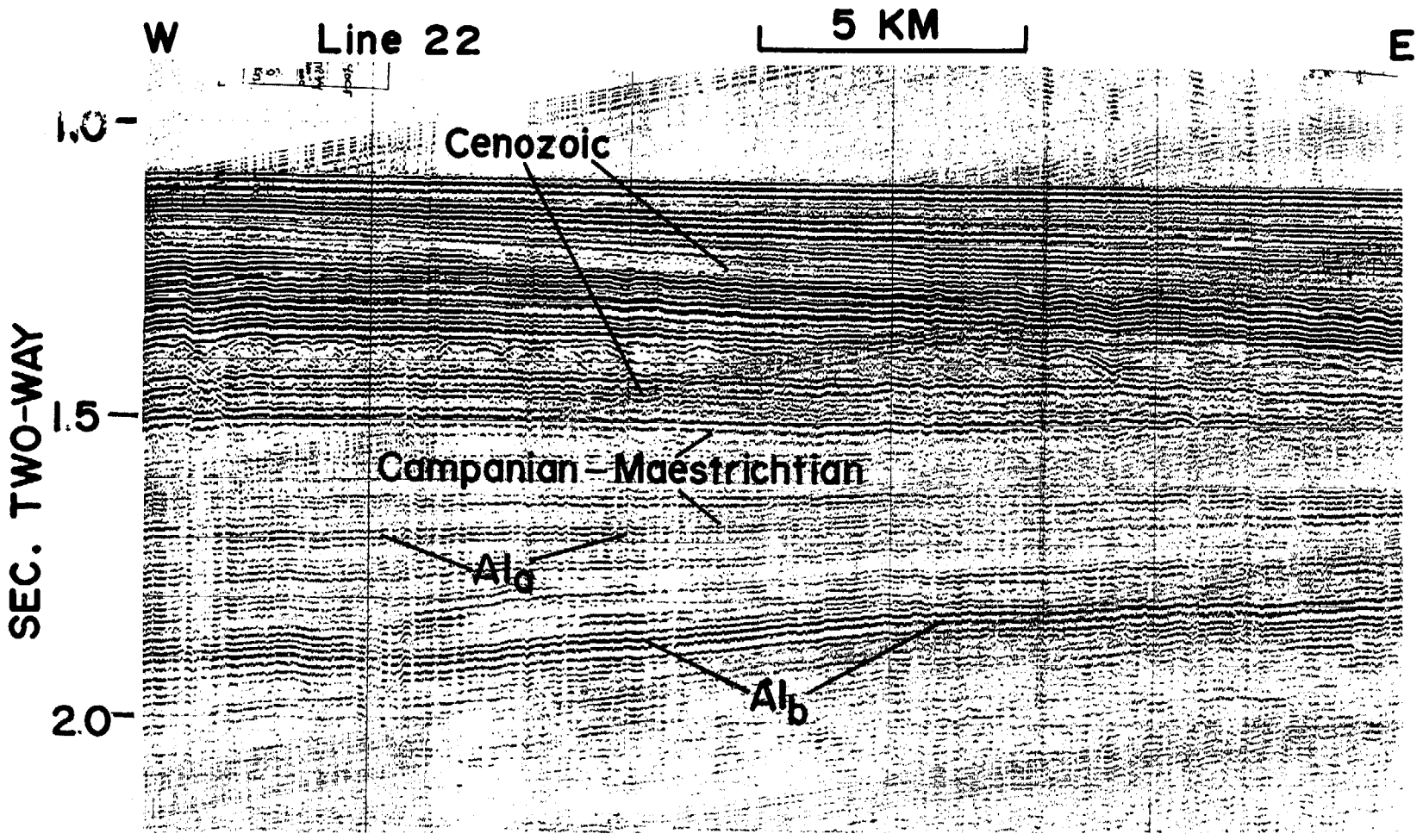
W
Line 22
5 KM
E
1.0
1.5
2.0
SEC. TWO-WAY
Cenozoic
Campanian - Maestrichtian
Al$_a$
Al$_b$

Figure 7-4

Figure 7-5. Structure contours on reflector Al_b, the oldest mappable reflector on the seismic records. Data are absent for the northern plateau, because of the difficulty of distinguishing the Al_b horizon. Note prominent ridge west of well ASP 3, believed to be the expression of a buried reef mass.

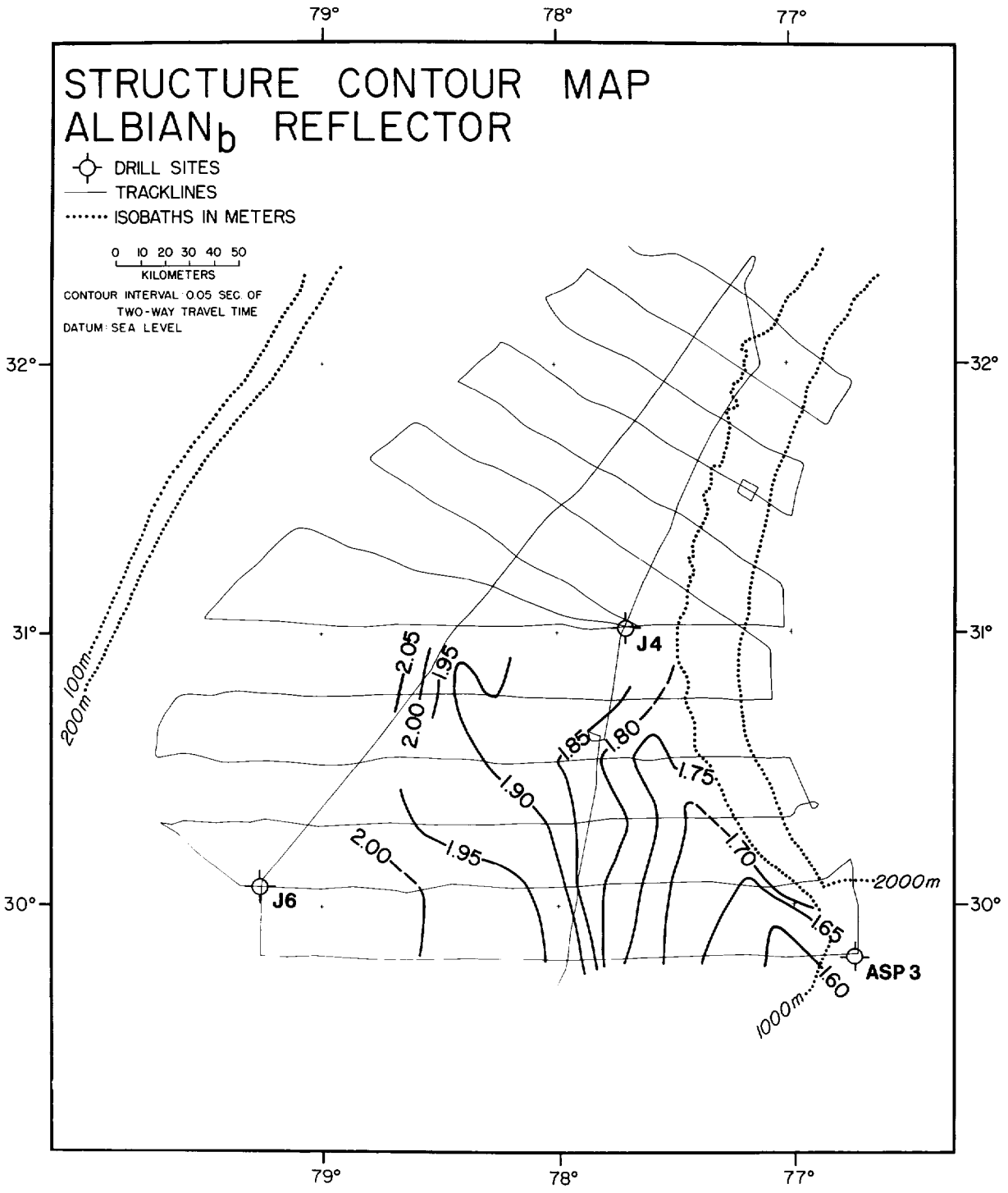
STRUCTURE CONTOUR MAP
ALBIAN$_b$ REFLECTOR
DRILL SITES
TRACKLINES
ISOBATHS IN METERS
0 10 20 30 40 50
KILOMETERS
CONTOUR INTERVAL 0.05 SEC. OF TWO-WAY TRAVEL TIME
DATUM: SEA LEVEL
79°
78°
77°
32°
31°
30°
J4
J6
ASP 3
2.05
2.00
1.95
1.90
1.85
1.80
1.75
1.70
1.65
1.60
100m
200m
1000m
2000m

Figure 7-6. Photograph of portion of original air-gun profile. Coordinates for middle of this line segment are 30°19'N.,78°51'W. Location is shown on figure 7-2 as a thickened trackline segment. Note gradual rise of reflector $A1_a$ to the east and absence of mappable units in the Upper Cretaceous interval. Cenozoic section shows excellent reflector definition and continuity, as well as a prominent unconformity.

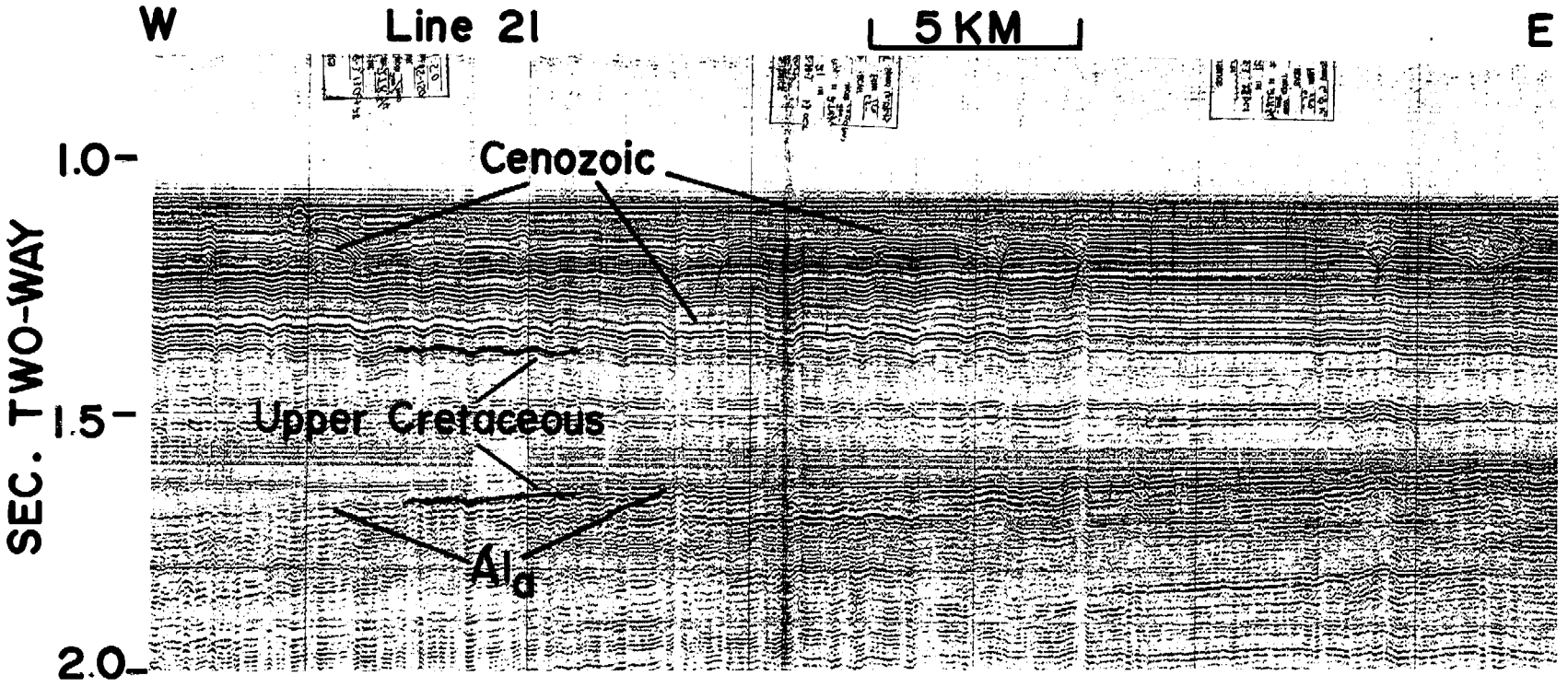
W
Line 21
5 KM
E
1.0
1.5
2.0
SEC. TWO-WAY
Cenozoic
Upper Cretaceous
Al_a

Figure 7-6

Figure 7-7. Structure contours for the top of the Albian sequence (reflector Al_a). Note complex configuration of the Al_a surface in the northern part of the study area in contrast to its simpler character to the south.

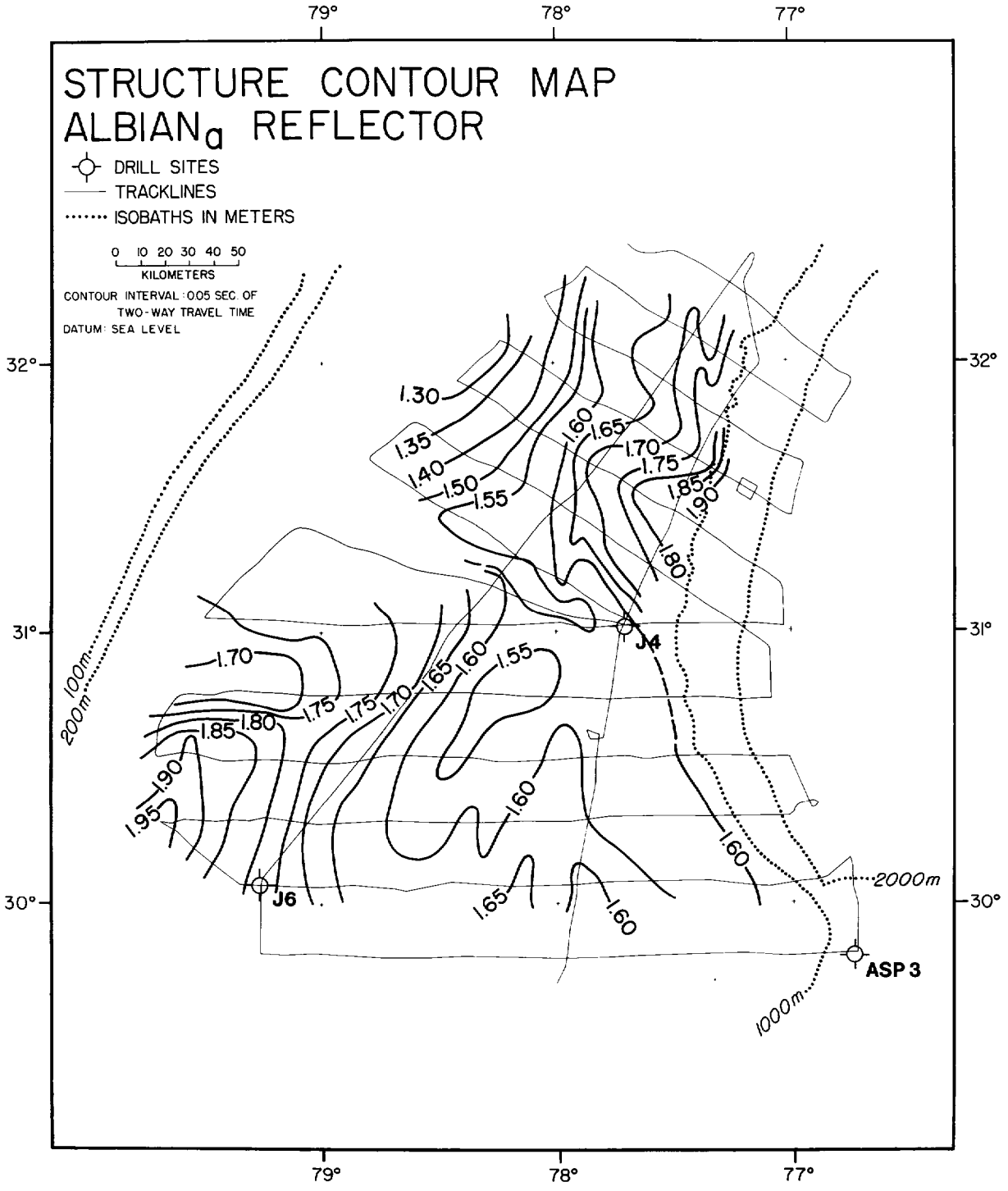
STRUCTURE CONTOUR MAP
ALBIAN$_a$ REFLECTOR
DRILL SITES
TRACKLINES
ISOBATHS IN METERS
0 10 20 30 40 50
KILOMETERS
CONTOUR INTERVAL: 0.05 SEC. OF TWO-WAY TRAVEL TIME
DATUM: SEA LEVEL
79°
78°
77°
32°
31°
30°
1.30
1.35
1.40
1.50
1.55
1.60
1.65
1.70
1.75
1.80
1.85
1.90
1.95
J4
J6
ASP 3
100m
200m
1000m
2000m

Al_b is poorly reflective and rises rather than dips to the east (fig. 7-8), onlapping the presumed Al_b reef bank near the Blake Escarpment. A few reflectors are evident along the seaward portions of the southern lines, and consist largely of weak discontinuous, parallel reflectors.

Isopach data (fig. 7-9) are available only for the southern region where both the Al_a and Al_b reflectors can be identified with confidence. The thickest part of the unit occurs as a broad bank (0.35/s thick) that trends north-south across the middle third of each line. The unit becomes thinner to the east where it onlaps the Al_b reefal mass. The isopach contours adjacent but landward of the Blake Escarpment (fig. 7-9) closely parallel the structure contours of the Al_b surface (fig. 7-5), suggesting that sediment deposition during Albian time was controlled by the topographically high reef structure. Dillon and others (1979b) concluded that carbonate buildup probably had ceased along the outer reef bank sometime during the Albian, the death of the reef being attributed to a major transgression during this time interval (Poag and Hall, 1979).

Coniacian-Turonian Sequence

The stratigraphic unit above reflector Al_a comprises the oldest of three progradational wedges of the Late Cretaceous (fig. 7-3). It is assigned tentatively to the Coniacian-Turonian based on a correlative unit beneath the Florida-Hatteras Slope and inner Blake Plateau identified on seismic lines from an earlier survey (Paull and Dillon, 1979). Additionally, the top of the sequence extends to COST GE-1 well where it appears to coincide with a stratigraphic break between Coniacian and Santonian sediments (Poag and Hall, 1979; Valentine, 1979).

Figure 7-8. Photograph of portion of original air-gun profile. Coordinates for the middle of this line segment are 30°20'N.,79°32'W. Location is shown on figure 7-2 as a thickened trackline segment. Note the irregular nature of reflector Al_a as well as its shoaling attitude to the east. South of 31°N. it is not possible to divide the Upper Cretaceous into discrete units, because of the poorly reflective nature of this interval. The Cenozoic sequence shows numerous excellent reflectors. Gulf Stream scouring has excavated the erosional topography evident at the surface.

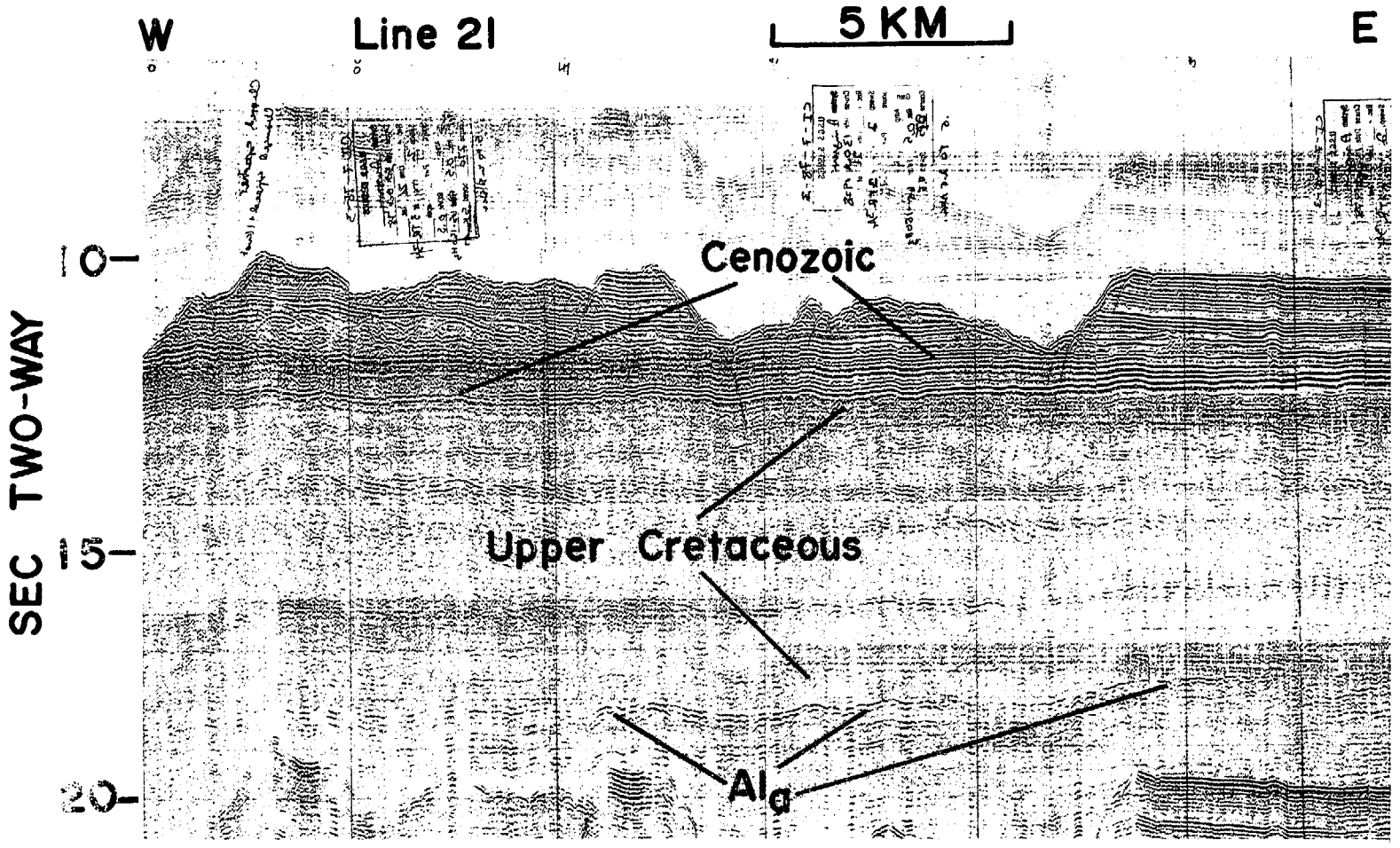
W
Line 21
5 KM
E
SEC TWO-WAY
1.0
1.5
2.0
Cenozoic
Upper Cretaceous
Alg

Figure 7-8

Figure 7-9. Thickness variations for the stratigraphic interval bounded by the Al_a and Al_b reflectors. Note the sparse sediment cover northwest of ASP 3 that overlies a prominent, but buried Albian reef mass.

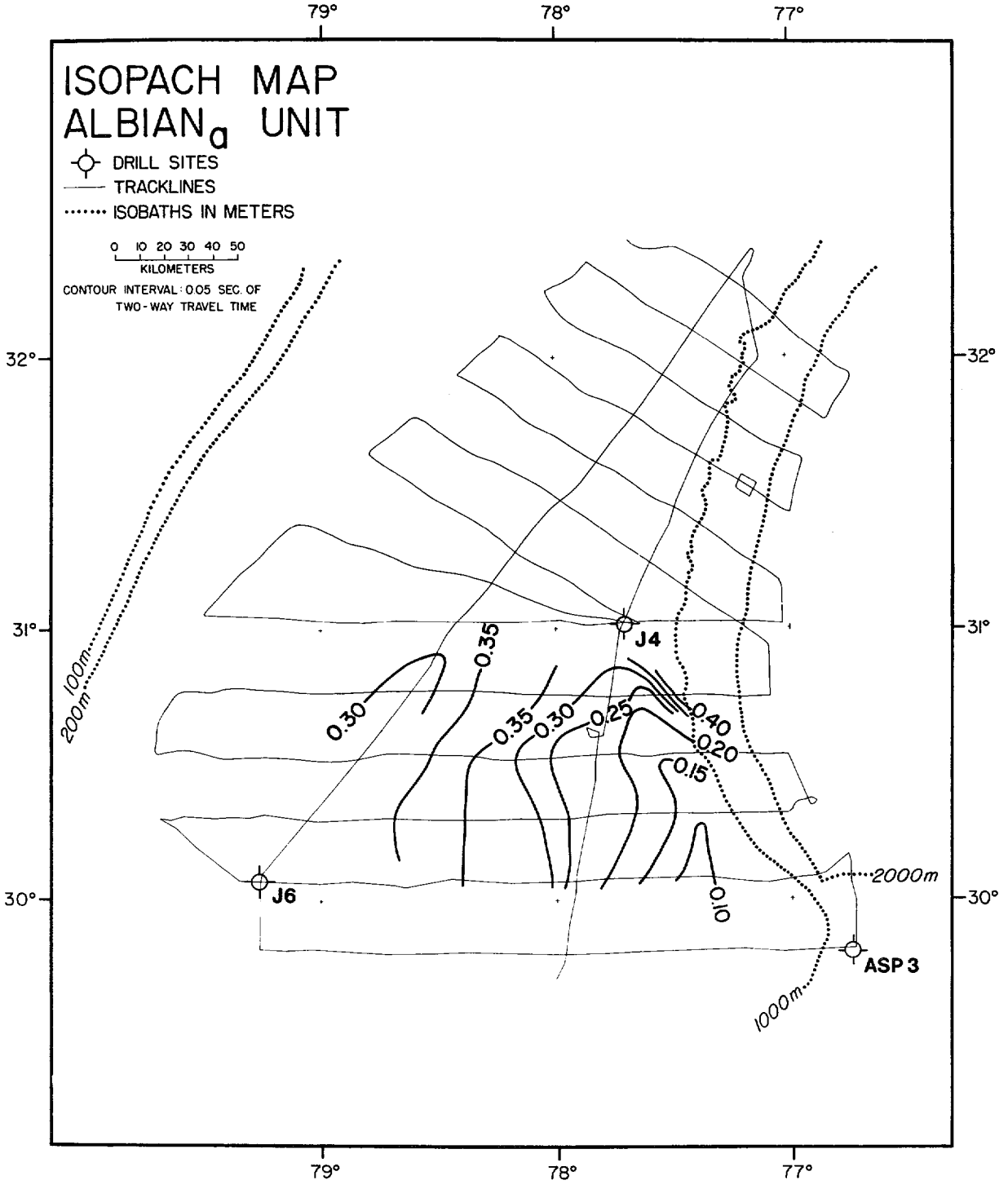
ISOPACH MAP
ALBIAN$_a$ UNIT
DRILL SITES
TRACKLINES
ISOBATHS IN METERS
0 10 20 30 40 50
KILOMETERS
CONTOUR INTERVAL: 0.05 SEC. OF TWO-WAY TRAVEL TIME
79°
78°
77°
32°
31°
30°
J4
J6
ASP 3
0.30
0.35
0.35
0.30
0.25
0.40
0.20
0.15
0.10
100m
200m
1000m
2000m

Along the northern dip lines, the Coniacian-Turonian sequence is distinguishable readily from the underlying Albian unit by a series of parallel to slightly divergent reflectors that grade eastward into a sigmoidal or an oblique progradational wedge (figs. 7-3 and 7-10). The dip of the prograded reflectors increases from north to south. The seaward terminus of the progradational facies is delimited on the isopach map (fig. 7-11) by the 0.10/s contour line. Reflectors at the base of the wedge undergo thinning to the east and downlap the older Albian unconformity. These characteristics indicate a shelf-break and prograded-slope facies that was outbuilding during Coniacian-Turonian times. The edge of this ancient continental margin had a markedly different orientation than the present-day Florida-Hatteras Slope, as indicated by the strike of the structure contours near line 9 which changes from a northeast-trend in the north to an east-trend in the south (fig. 7-12). Paull and Dillon (1979) show a similar pattern for the top of the Coniacian sediments that underlie the inner Blake Plateau.

Coniacian-Turonian strata beneath the central Blake Plateau have a different seismic appearance than their correlatives to the north (fig. 7-3). South of 31°N., the unit is ill defined (fig. 7-8) and when distinguishable essentially is reflection-free. Although data are limited, the unit along southern dip lines appears to onlap and pinch out to the east against the Albian reef mass (fig. 7-3) which persisted as a topographic high during this time interval.

The reflection character, thickness variations, structural attitude, and seismic facies of the Coniacian-Turonian unit to the north indicate that it represents a shelf edge and slope that was prograding across the Blake Plateau. The copious supply of sediment likely was

Figure 7-10. Photograph of portion of original air-gun profile. Coordinates for middle of this line are 32°17'N.,77°11'W. Location is shown on figure 7-2 as a thickened trackline segment. Portions of three Cretaceous progradational wedges are apparent. Note that the Santonian sequence, the middle progradational wedge, pinches out just to the right of the center of the photograph. The Cenozoic cover here is quite thin.

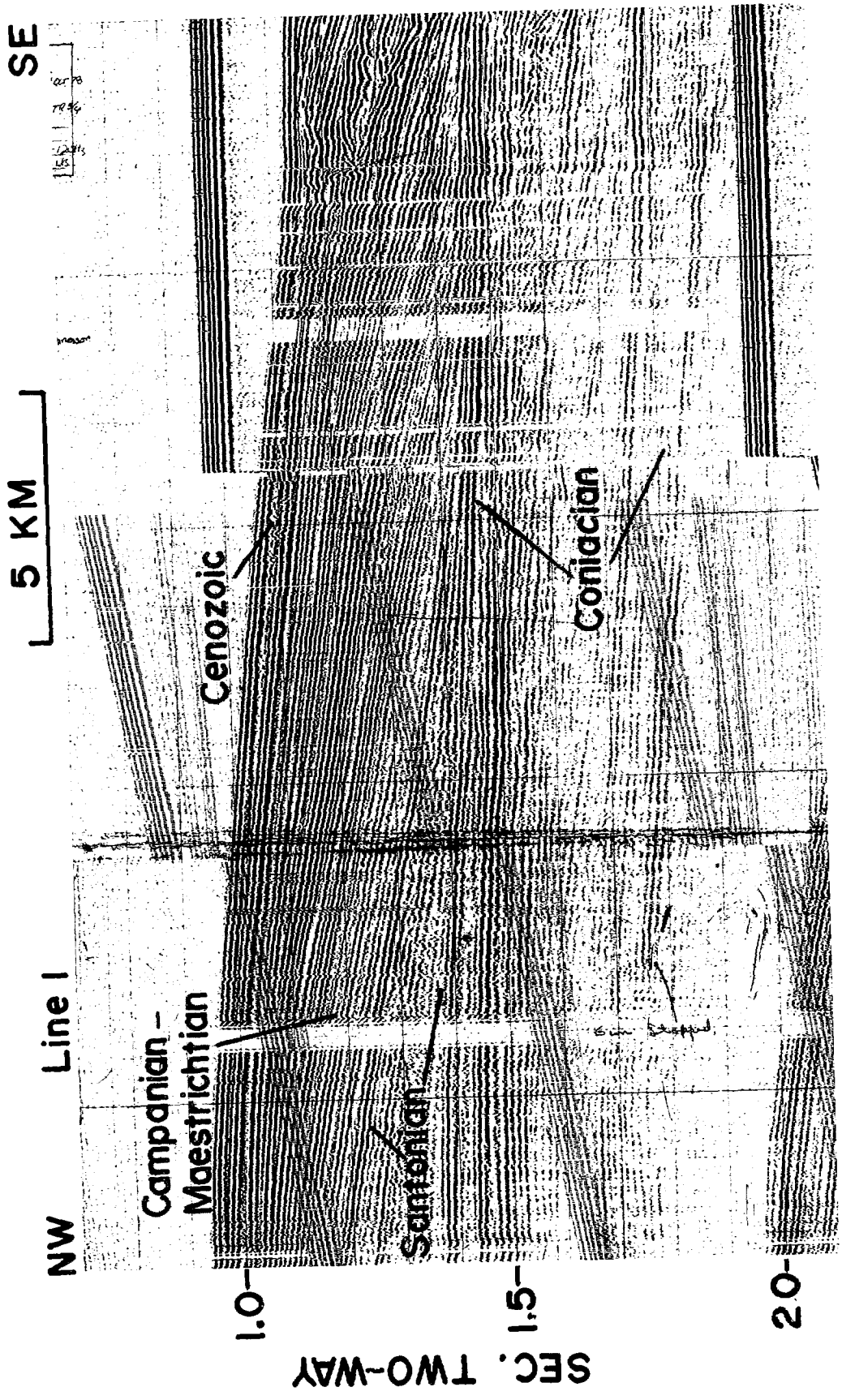
NW
SE
Line I
5 KM
Campanian - Maestrichtian
Santonian
Cenozoic
Coniacian
1.0
1.5
2.0
SEC. TWO-WAY

Figure 7-11. Thickness data for Coniacian strata. The seaward terminus of the progradational wedge is broadly lobate in plan view and is delimited by the 0.10/s contour line.

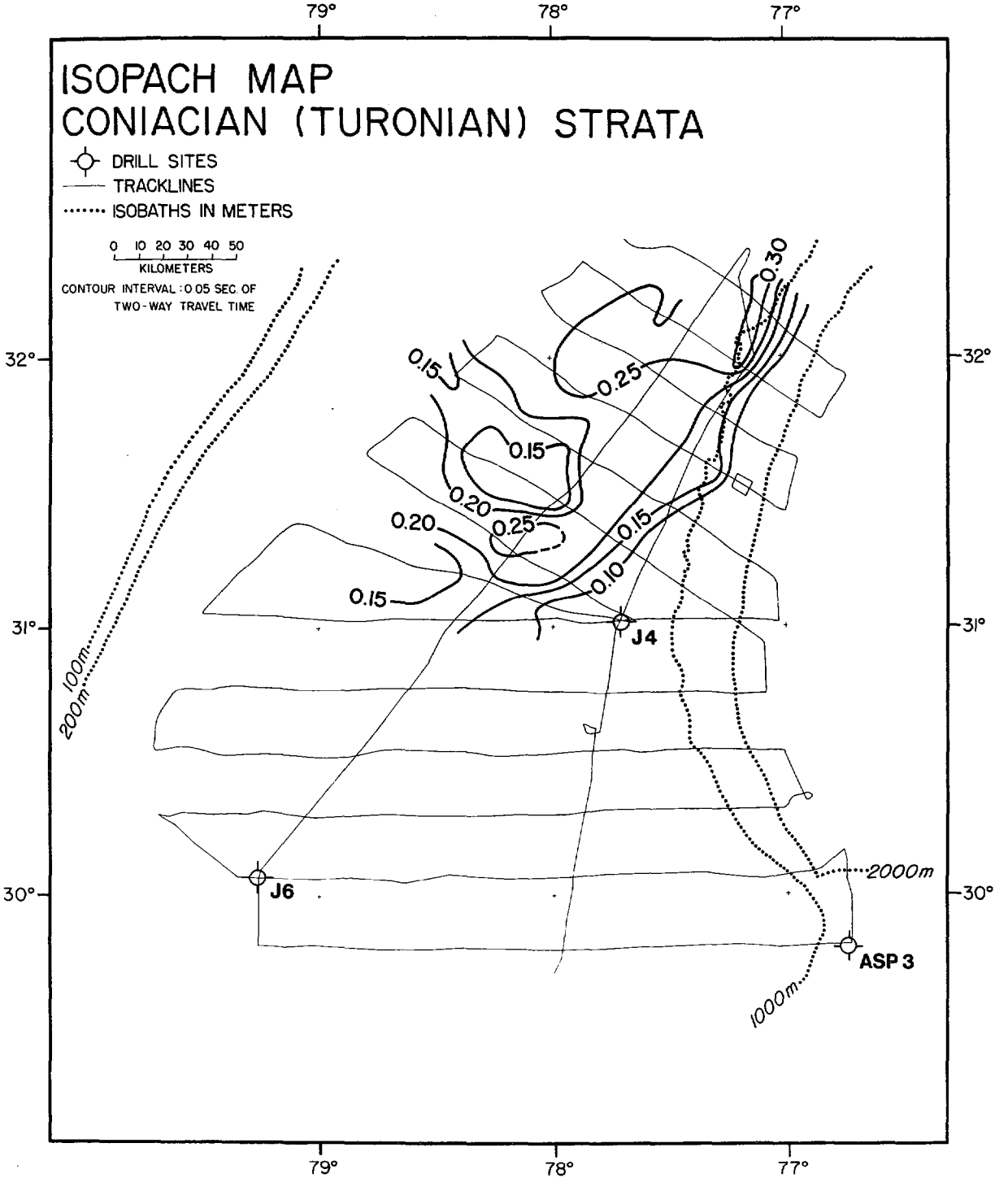
ISOPACH MAP
CONIACIAN (TURONIAN) STRATA
DRILL SITES
TRACKLINES
ISOBATHS IN METERS
0 10 20 30 40 50
KILOMETERS
CONTOUR INTERVAL : 0.05 SEC. OF TWO-WAY TRAVEL TIME
79°
78°
77°
32°
31°
30°
0.30
0.25
0.15
0.20
0.10
J4
J6
ASP 3
100m
200m
1000m
2000m

Figure 7-12. Structure contours on the top of the Coniacian unit, showing its relatively simple attitude of sloping gently to the east. Note change in strike of contour lines to the west of well J4.

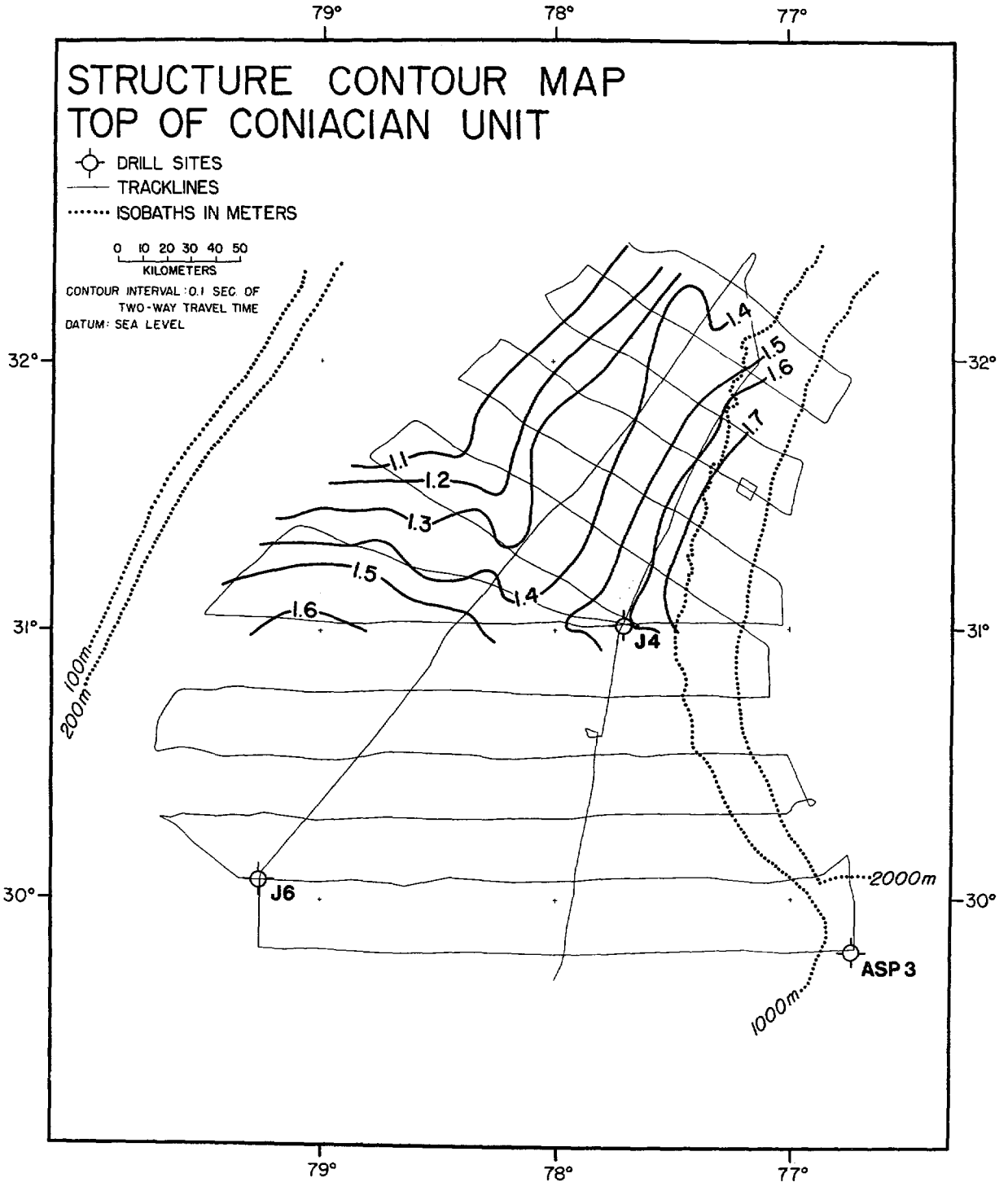
STRUCTURE CONTOUR MAP
TOP OF CONIACIAN UNIT
DRILL SITES
TRACKLINES
ISOBATHS IN METERS
0 10 20 30 40 50
KILOMETERS
CONTOUR INTERVAL: 0.1 SEC OF TWO-WAY TRAVEL TIME
DATUM: SEA LEVEL
79°
78°
77°
32°
31°
30°
1.1
1.2
1.3
1.4
1.5
1.6
1.7
J4
J6
ASP 3
100m
200m
1000m
2000m

being derived from a source area located to the northwest of the margin wedge, as inferred from the broadly lobate form of the deposit. An ample sediment influx to the outer perimeter of the prograding margin also is supported by the fact that the Coniacian-Turonian sediments smooth out all the large irregularities found on the top of the underlying Al_a unconformity.

Seaward of the margin deposits, the Blake Plateau consisted of a slowly subsiding basin during Coniacian-Turonian time that was bounded on the east by an ancient reef complex whose crest remained topographically higher than the adjoining basin floor. Sediment bypassing of the shelf edge and biogenic production injected sediment into the basin that accumulated slowly under relatively uniform depositional conditions as inferred from the largely transparent character of the basin facies. Infilling basin sediments onlapped the Albian reef mass at the Blake Escarpment.

Santonian Sequence

A prominent stratigraphic sequence that overlies Coniacian-Turonian strata on the inner Blake Plateau comprises a second progradational series (fig. 7-3). First noted by Paull and Dillon (1979), this interval is regarded as Santonian in age based largely on core-hole data from the Florida Shelf. Overlapping grid lines clearly establish equivalency between this seismic unit on ISELIN 78-3 lines and those on FAY 017 and 018 lines (Paull and Dillon, 1979).

The unit, consisting largely of a series of oblique progradational reflectors, undergoes considerable thinning to the east (figs. 7-10 and 7-13), not unlike the underlying Coniacian-Turonian facies. The top of the unit slopes eastward in the northern part of the survey area, the seaward margin of the progradational wedge striking N.-S. (fig. 7-14).

Figure 7-13. Thickness data for Santonian strata that represent a progradational shelf-slope facies. Unit thins abruptly to the east.

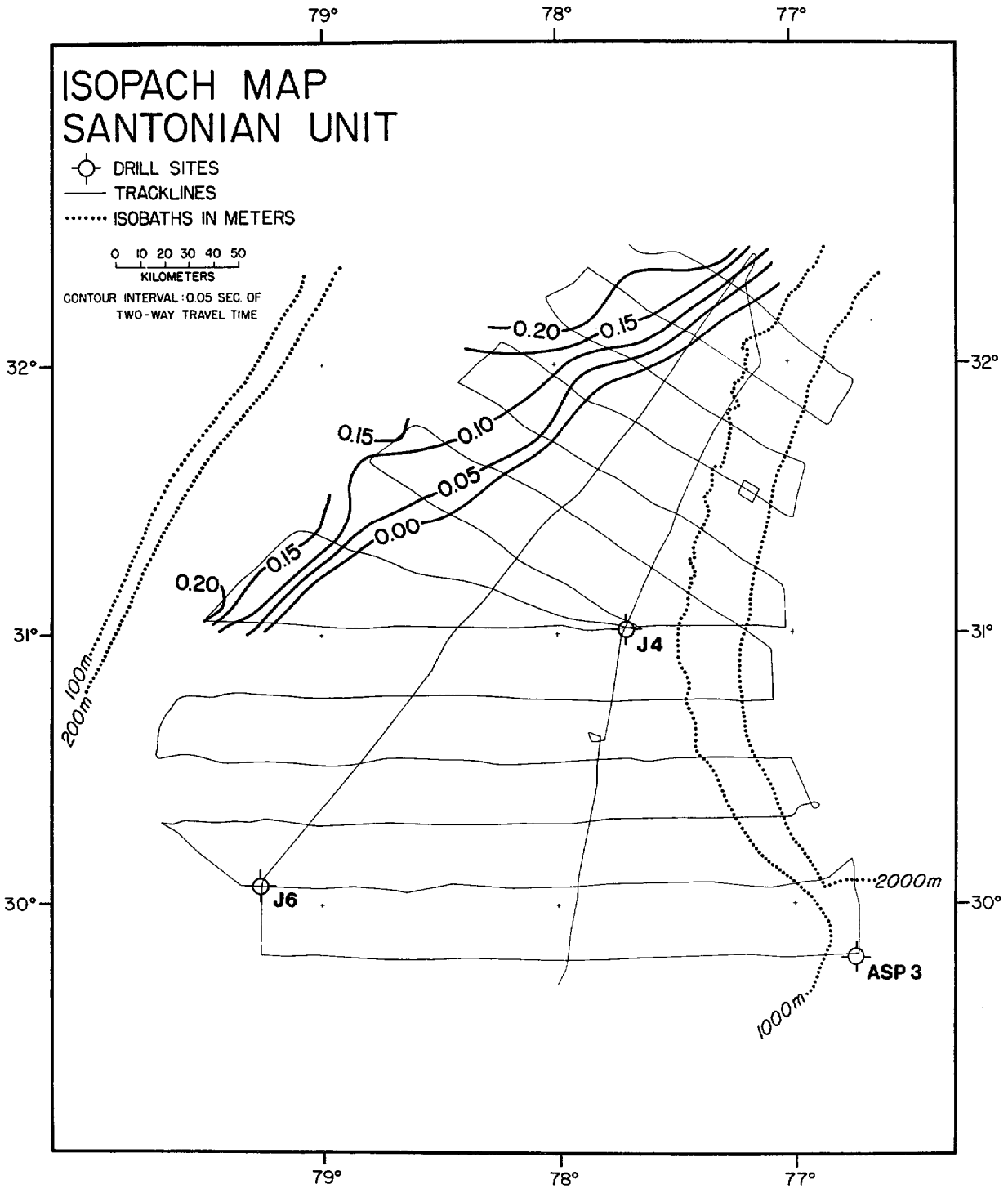
ISOPACH MAP
SANTONIAN UNIT
DRILL SITES
TRACKLINES
ISOBATHS IN METERS
0 10 20 30 40 50
KILOMETERS
CONTOUR INTERVAL: 0.05 SEC. OF TWO-WAY TRAVEL TIME
79°
78°
77°
32°
31°
30°
0.20
0.15
0.10
0.05
0.00
J4
J6
ASP 3
100m
200m
1000m
2000m

Figure 7-14. Structure contours on top of Santonian unit showing relatively simple configuration of gradual deepening to the east.

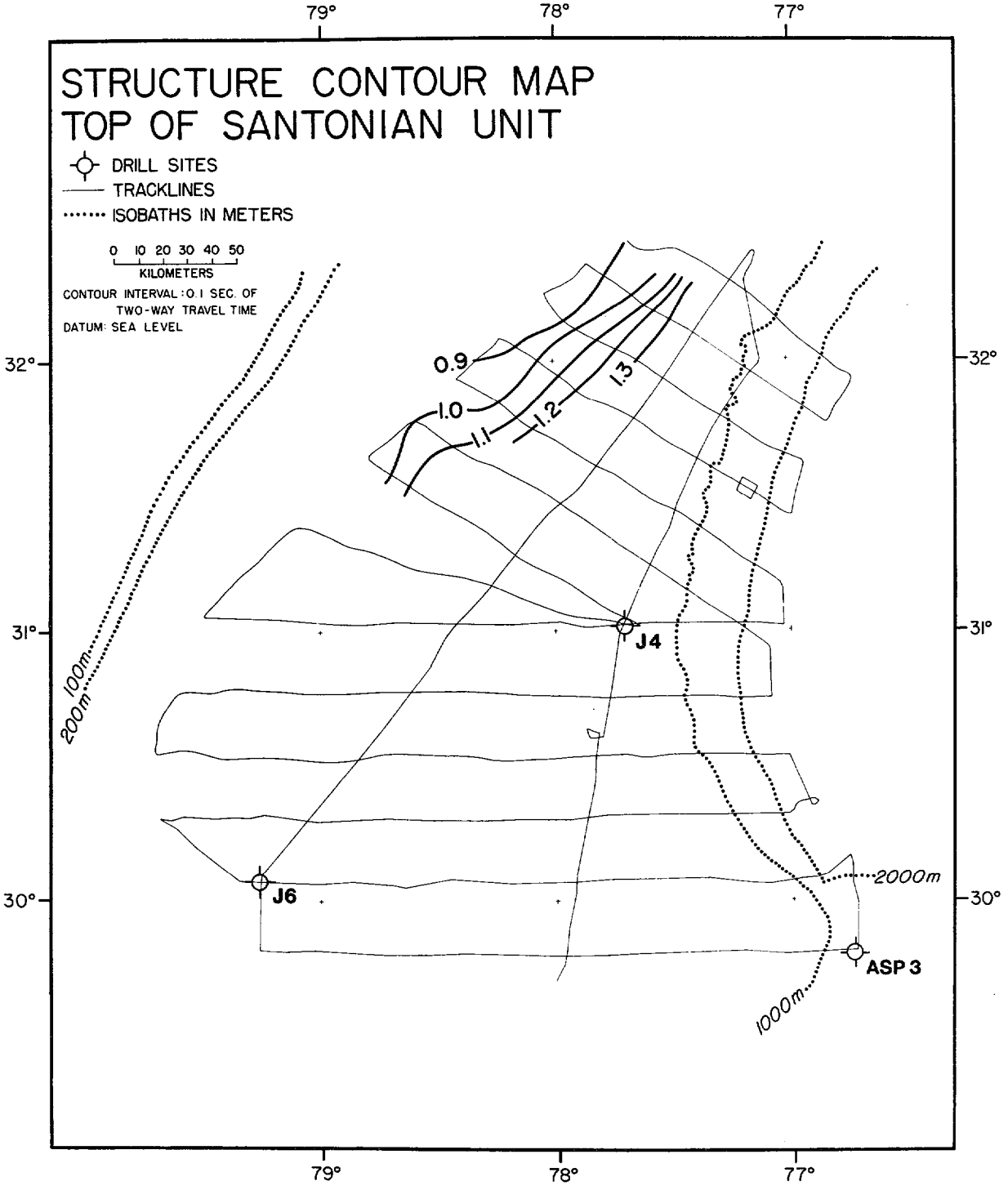
STRUCTURE CONTOUR MAP
TOP OF SANTONIAN UNIT
DRILL SITES
TRACKLINES
ISOBATHS IN METERS
0 10 20 30 40 50
KILOMETERS
CONTOUR INTERVAL: 0.1 SEC. OF TWO-WAY TRAVEL TIME
DATUM: SEA LEVEL
79°
78°
77°
32°
31°
30°
0.9
1.0
1.1
1.2
1.3
J4
J6
ASP 3
100m
200m
1000m
2000m

At 31°N., the structure contours assume an E.-W. trend and extend beneath the Florida-Hatteras Shelf and Slope (Paull and Dillon, 1979), paralleling the structure contours of the underlying Coniacian-Turonian wedge.

South of 31°N., reflectors equivalent to the Santonian unit to the north are not apparent on the seismic lines, because the Upper Cretaceous stratigraphic interval essentially is acoustically transparent in this region (fig. 7-8). Undoubtedly, sediments of Santonian age are present and probably pinch out against the Albian reef mass that lies adjacent to the Blake Escarpment.

Available geophysical information indicates that the sedimentological system during the Santonian was similar to the older Coniacian-Turonian system. Sediment was derived from a source area located apparently to the northwest and was dispersed seaward along a brcad progradational lobe, resulting in outbuilding of the shelf edge and slope. Sediment that bypassed the shelf-slope environments presumably settled to the bottom of a slowly subsiding deepwater basin. Sediment buildup on the basin floor likely continued to cover and onlap the western shoulder of the massive Albian reef complex.

Particularly noteworthy is the fact that the Santonian shelf edge was positioned about 50 km to the west (landward) of the older Coniacian-Turonian shelf edge. This pronounced shift or relocation of depositional environments may reflect a major transgression of sea level that affected the area during the Santonian. For example, Poag and Hall (1979), based on a detailed examination of foraminiferal assemblages from the COST GE-1 well on the Florida Shelf, interpreted a marked change from middle-shelf to outer-shelf water depths during the Santonian.

Campanian-Maestrichtian Sequence

The youngest Cretaceous sediments beneath the Blake Plateau are considered to be Campanian-Maestrichtian in age (fig. 7-3). Beds at the top of the sequence show erosional truncation that defines a regional unconformity traceable throughout the survey area. This erosional surface clearly matches a Maestrichtian unconformity mapped beneath the Florida-Hatteras Shelf and Slope (Paull and Dillon, 1979) whose age, based on well data, is well established.

The Campanian-Maestrichtian unit represents the youngest progradational facies of the Cretaceous. The acoustical characteristics of the unit are well displayed along dip lines 1 (fig. 7-10) and 3 (fig. 7-15) where it consists of divergent seaward-dipping reflectors that are eroded deeply and covered by chaotic Tertiary infill along the eastern end of both lines. Equivalent reflectors along the inner portions of dip lines 5 and 7 (fig. 7-3a) likewise are inclined seaward, but become more concordant with the lower and upper boundaries of the sequence to the east. Farther southward beyond seismic line 13, the Campanian-Maestrichtian unit becomes acoustically transparent or exhibits discontinuous, parallel reflectors that have been segmented by numerous small faults (fig. 7-16).

The unconformity that defines the top of the Campanian-Maestrichtian strata slopes uniformly eastward along the full extent of the northernmost seismic lines (fig. 7-17). However, south of 31°N., the erosion surface dips seaward along the inner Blake Plateau, but flattens out and reverses its slope as it rises towards the Albian reef structure at the Blake Escarpment. Thickness data could only be assembled for the northern sector of the survey area, because of the difficulty of distinguishing confidently the various Upper Cretaceous

Figure 7-15. Photograph of portion of original air-gun profile. Coordinates for middle of this line are 32°09'N.,77°20'W. Location is shown on figure 7-2 as a thickened trackline segment. The Santonian and Campanian-Maestrichtian progradational wedges display reflectors that dip and thin to the east. Upper surface of Campanian-Maestrichtian unit is a distinct regional disconformity.

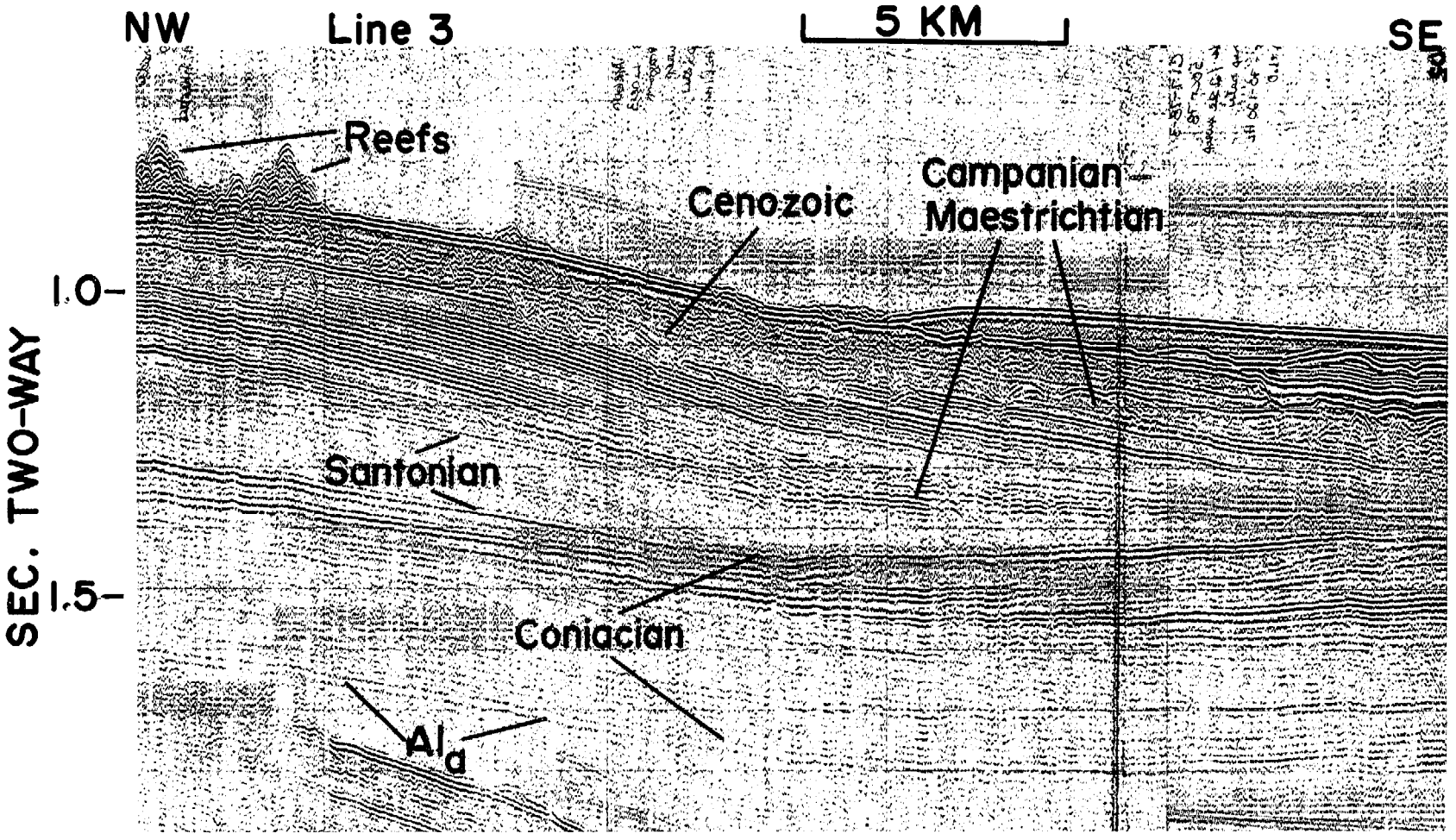
NW
Line 3
5 KM
SE
Reefs
Cenozoic
Campanian-
Maestrichtian
1.0
SEC. TWO-WAY
1.5
Santonian
Coniacian
Al$_d$

Figure 7-15

Figure 7-16. Photograph of portion of original sparker profile. Coordinates for middle of this line segment are 30°47'N.,79°26'W. Location is shown on figure 7-2 as a thickened trackline segment. Note how the Upper Cretaceous contact with the Paleocene is sharply delineated on the seismic record. Also evident are numerous small faults that are confined to the Cretaceous sequence.

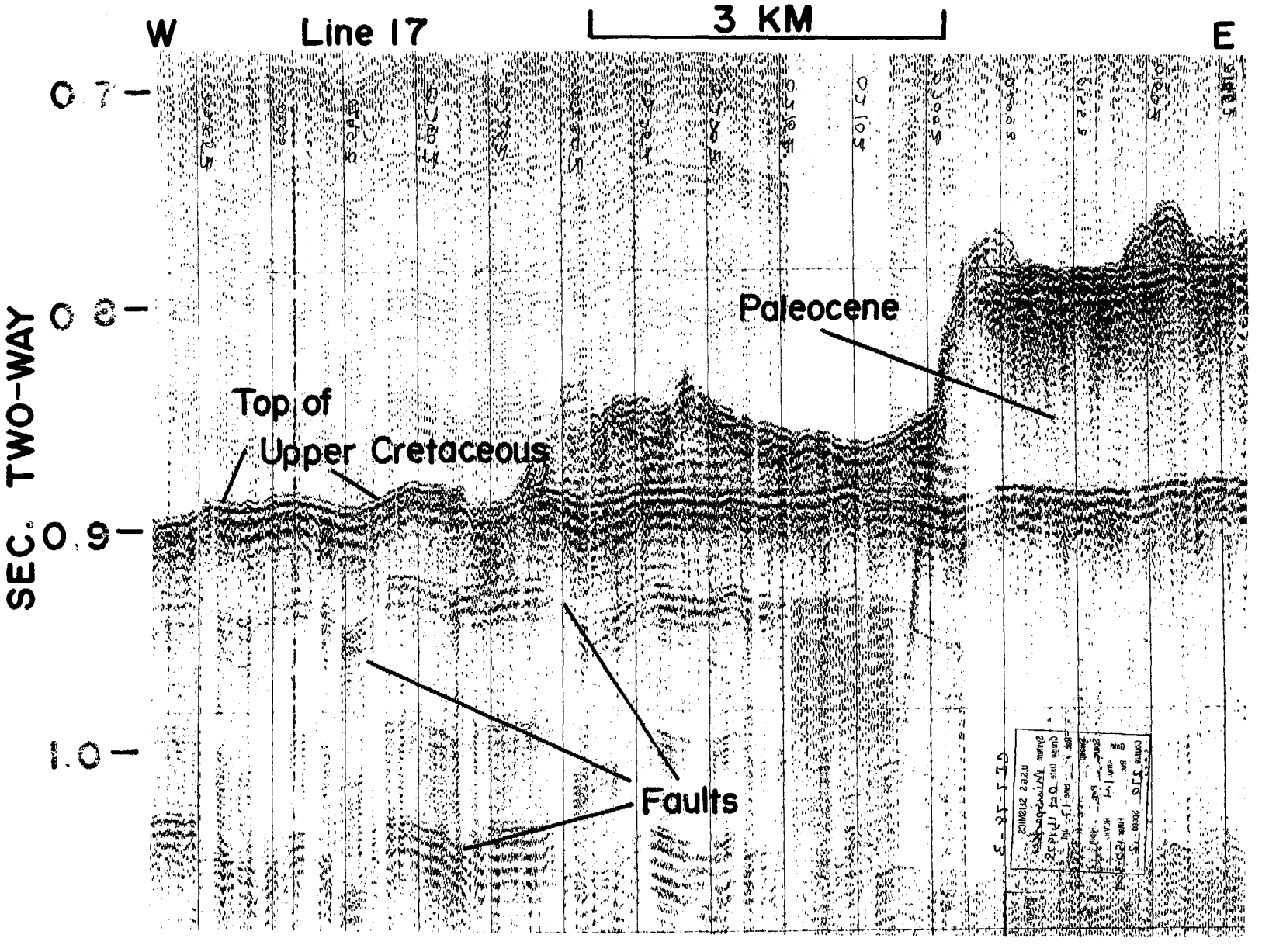
W
Line 17
3 KM
E
SEC. TWO-WAY
0.7
0.8
0.9
1.0
Paleocene
Top of
Upper Cretaceous
Faults

Figure 7-16

Figure 7-17. Structure contours on top of Campanian-Maestrichtian strata. Note regional eastward dip of this surface; expression of an Albian reef mass still evident to the west of drill site ASP 3.

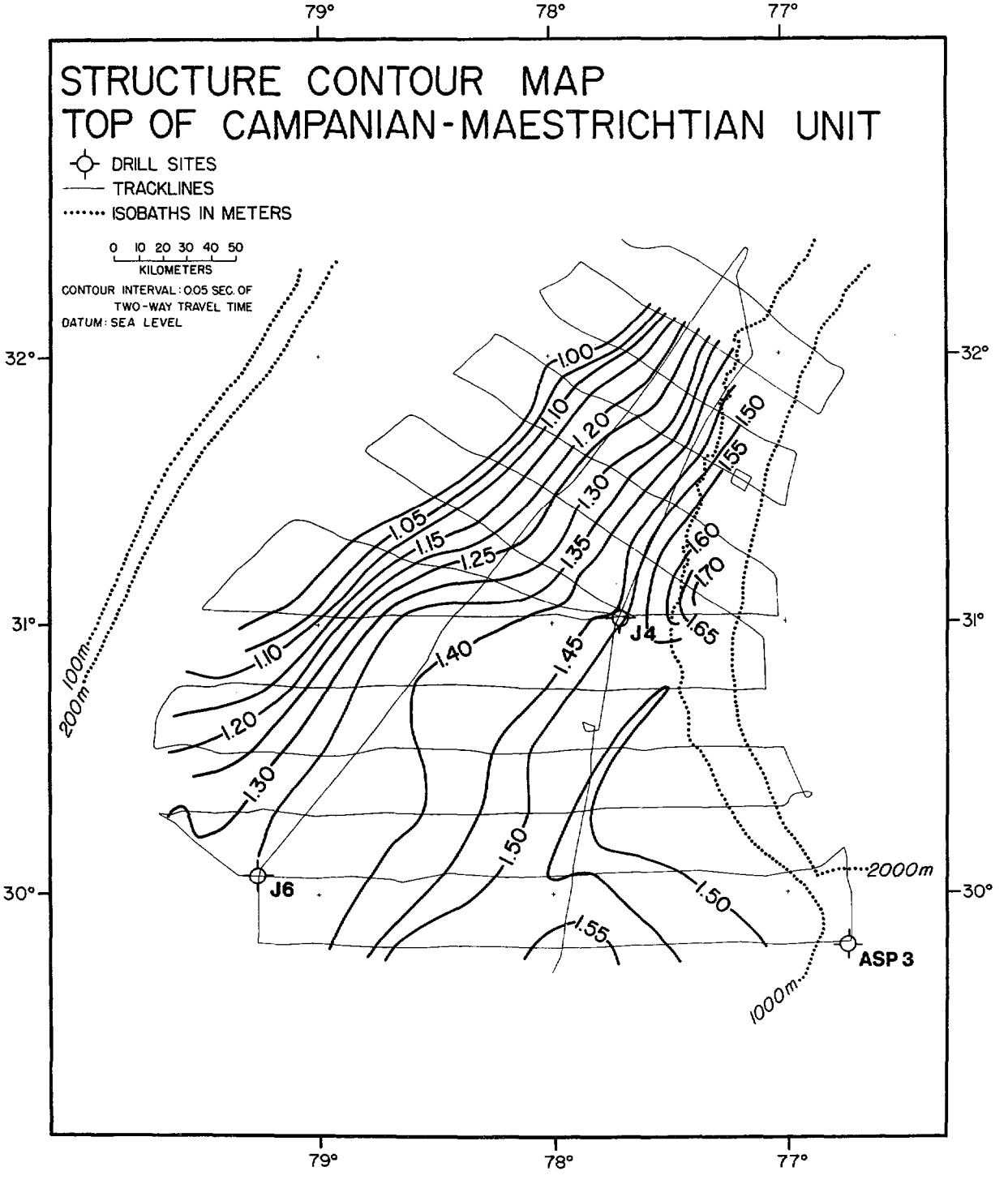
STRUCTURE CONTOUR MAP
TOP OF CAMPANIAN-MAESTRICHTIAN UNIT
DRILL SITES
TRACKLINES
ISOBATHS IN METERS
0 10 20 30 40 50
KILOMETERS
CONTOUR INTERVAL: 0.05 SEC. OF TWO-WAY TRAVEL TIME
DATUM: SEA LEVEL
79°
78°
77°
32°
31°
30°
1.00
1.05
1.10
1.15
1.20
1.25
1.30
1.35
1.40
1.45
1.50
1.55
1.60
1.65
1.70
J4
J6
ASP 3
100m
200m
1000m
2000m

units south of 31°N. The limited isopach data (fig. 7-18) reveal two depositional loci; one appears as a local accumulation in the northwest corner of the study area, the other forms a NE.-trending deposit that runs along the central inner Blake Plateau. The unit undergoes marked thinning along the distal end of each northern line.

The depositional environment of the inner Blake Plateau during Campanian-Maestrichtian time is reconstructed as an outbuilding shelf and slope complex, with characteristics that are similar to the depositional model that was applied to the two older Cretaceous progradational sequences. Apparently, the sediment supply was abundant, as the base of the continental slope during Campanian-Maestrichtian time was extended eastward to a greater extent than during Santonian time. Also, the seaward shift of the continental-margin edge occurred during the latest Cretaceous in spite of an apparent rise of sea level (Poag and Hall, 1979).

In the southern part of the survey area, Campanian-Maestrichtian sediments accumulated in a subsiding basin that was bounded to the north by the accreting shelf and slope deposits described above and to the east by a dead Albian reef system. Basin sediments onlapped the reef mass and eventually spilled over the crest of the Albian reef tract, although the reef remained a topographically positive feature on the Maestrichtian seafloor. Structure-contour data (Paull and Dillon, 1979) indicate that the deepest part of the basin extended from 31°N. to beyond 29.5°N. parallel to the western edge of the inner Blake Plateau.

Summary of Late Cretaceous Environments

Isopach data for the entire Upper Cretaceous (fig. 7-19) effectively summarize general depositional patterns for this time period. Thick Upper Cretaceous deposits that underlie the inner Blake

Figure 7-18. Thickness data for the Campanian-Maestrichtian interval. Two depocenters are evident, one a local accumulation in the northwest corner of the map, the other, a northeast-trending deposit that runs along the central inner Blake Plateau.

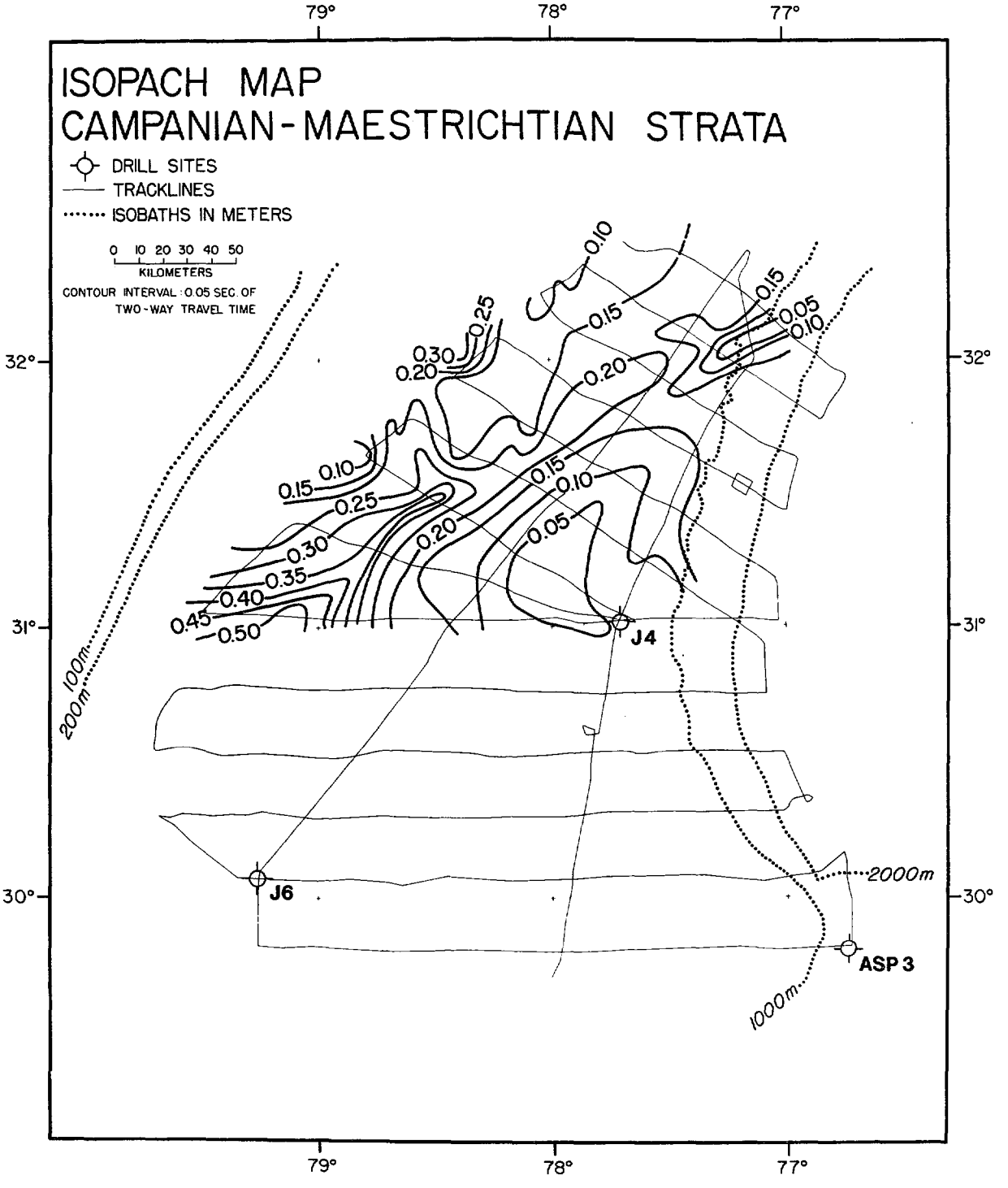
ISOPACH MAP
CAMPANIAN-MAESTRICHTIAN STRATA
DRILL SITES
TRACKLINES
ISOBATHS IN METERS
0 10 20 30 40 50
KILOMETERS
CONTOUR INTERVAL: 0.05 SEC. OF TWO-WAY TRAVEL TIME
79°
78°
77°
32°
31°
30°
0.10
0.15
0.05
0.10
0.25
0.30
0.20
0.20
0.15
0.10
0.25
0.30
0.35
0.40
0.45
0.50
0.15
0.10
0.20
0.05
J4
J6
ASP 3
100m
200m
1000m
2000m

Figure 7-19. Thickness data for the combined Upper Cretaceous units. Map shows how bulk of sediment accumulated over the inner Blake Plateau.

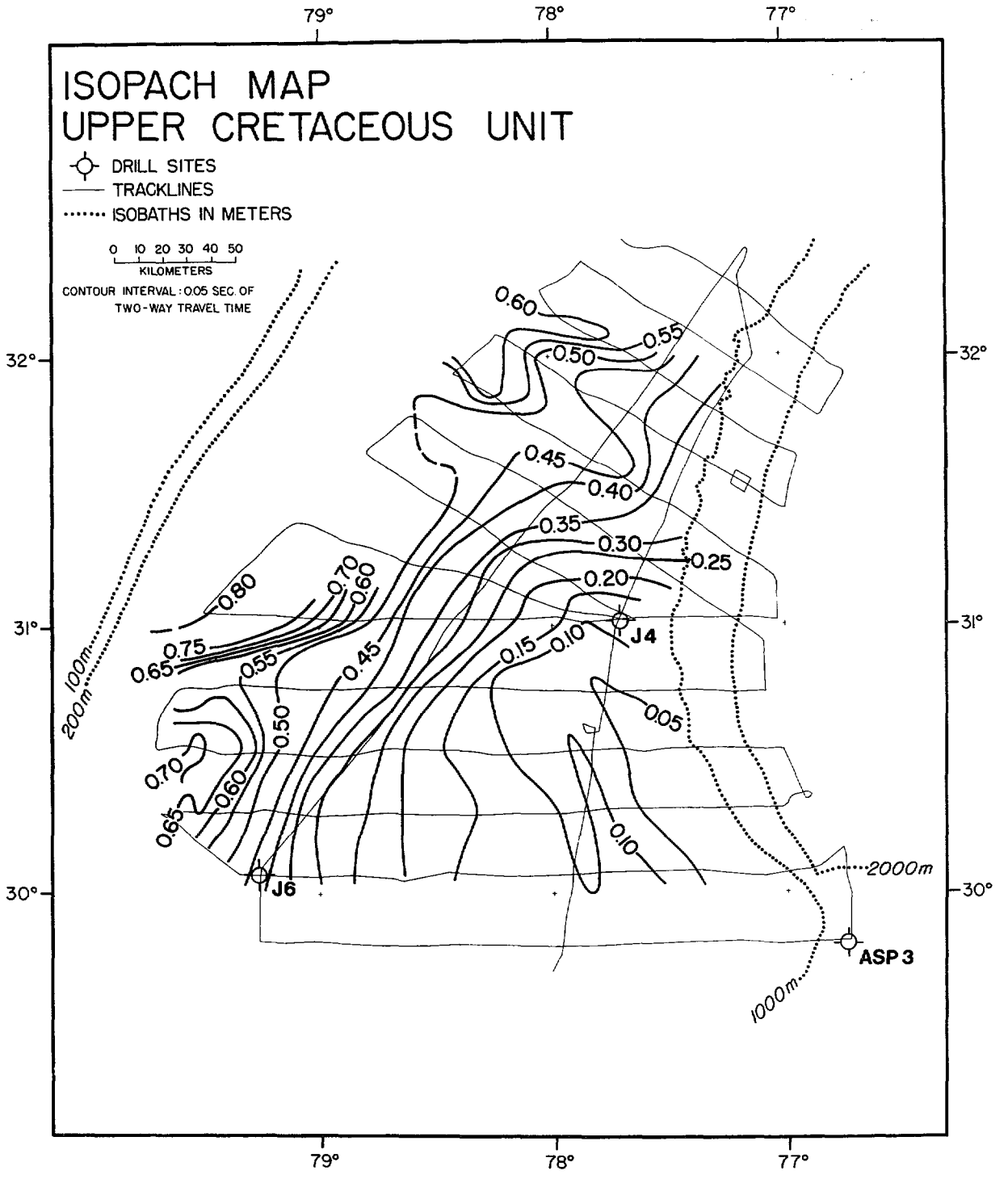
ISOPACH MAP
UPPER CRETACEOUS UNIT
DRILL SITES
TRACKLINES
ISOBATHS IN METERS
0 10 20 30 40 50
KILOMETERS
CONTOUR INTERVAL: 0.05 SEC. OF TWO-WAY TRAVEL TIME
79°
78°
77°
32°
31°
30°
0.60
0.55
0.50
0.45
0.40
0.35
0.30
0.25
0.20
0.15
0.10
0.05
0.80
0.75
0.70
0.65
0.60
0.55
0.50
0.45
0.70
0.65
0.60
0.10
J4
J6
ASP 3
100m
200m
1000m
2000m

Plateau are the product of the influx of abundant detritus to an ancient continental shelf and slope environment; three distinct progradational cycles are evident. The shelf break trended NE.-SW. at the north end of the plateau, and E.-W. near 31°N., so that the shape of the Late Cretaceous continental margin along the southeast United States was markedly different than at present. A broad basin located seaward (south and east) of the shelf edge presumably received an input of biogenic and fine clastic material. Deposition in the basin was slow. A discontinuous Albian reef or carbonate bank defined the eastern lip of the subsiding basin. Slow filling of the basin caused sediment to onlap gradually the submarine ridge, blanketing the dead reef mass by Maestrichtian time. The ridge, however, was not engulfed totally, for it maintained its topographic expression throughout the Late Cretaceous.

CENOZOIC SECTION

Age assignments to Cenozoic seismic units are reliable south of 31°N., but are tenuous at best across the northern half of the survey area for two principal reasons. First, no well data are available north of drill site J4. Second, unconformities that define the seismic sequences in the Cenozoic section are very irregular, and in some localities merge, making it on occasion very difficult to trace reflectors northward with confidence. Hence, definition of seismic sequences and ages for units north of J4 should be regarded as interpretive in nature, requiring corroboration by drilling.

Paleocene Sequence

The Upper Cretaceous erosion surface is covered by a widespread basal Tertiary unit whose upper surface is a well defined, strong reflector that represents a major regional unconformity of the Cenozoic

(fig. 7-20). Extrapolation of this stratigraphic unit to FAY 017 and 018 seismic profiles (Paull and Dillon, 1979) indicates that the unit is Paleocene in age. Confirmation of this age assignment is provided by well data on the Blake Plateau (fig. 7-2) at drill sites J4, J6, and ASP 3 (Charm and others, 1969; Schlee, 1977). Although the unit consists mainly of Paleocene sediments, it is possible that thin lower Eocene sediments are present at its top.

Internal reflectors of the Paleocene interval are arranged in distinct parallel configurations with either a regular or wavy pattern. The unit tends to be less reflective near its base than within its upper half (fig. 7-21), although this relation is reversed occasionally. On a few lines, strong, coherent sets of wavy reflectors divide the unit into two parts, as exemplified along the western half of dip line 13. Over most of the Blake Plateau, Paleocene strata are near horizontal, but pass laterally into eastward (seaward) dipping sequences adjacent to the Blake Escarpment (figs. 7-20, 7-21).

The three-dimensional configuration of the Paleocene unconformity is defined in figure 7-22. In the northern region, the erosion surface generally deepens eastward. Its attitude in the southern region, however, is more complex with a steeper seaward gradient over the central part of the inner Blake Plateau and a gentler seaward gradient along the outer plateau. Quite noteworthy is the fact that the Albian reef mass is not apparent on the structure contour map of the top of the Paleocene. This indicates that sediment burial during the early Tertiary completely obliterated this Upper Cretaceous feature so that it no longer exerted an influence on the seaward dispersal of sediment across the plateau.

Sediment thicknesses for the Paleocene are quite variable

Figure 7-20. Line drawings of sparker profiles that reveal the shallow stratigraphy of the Blake Plateau. Figures 7-20a, 20b, and 20C show dip lines; 20c also shows tie lines. Trackline locations are depicted in figure 7-2.

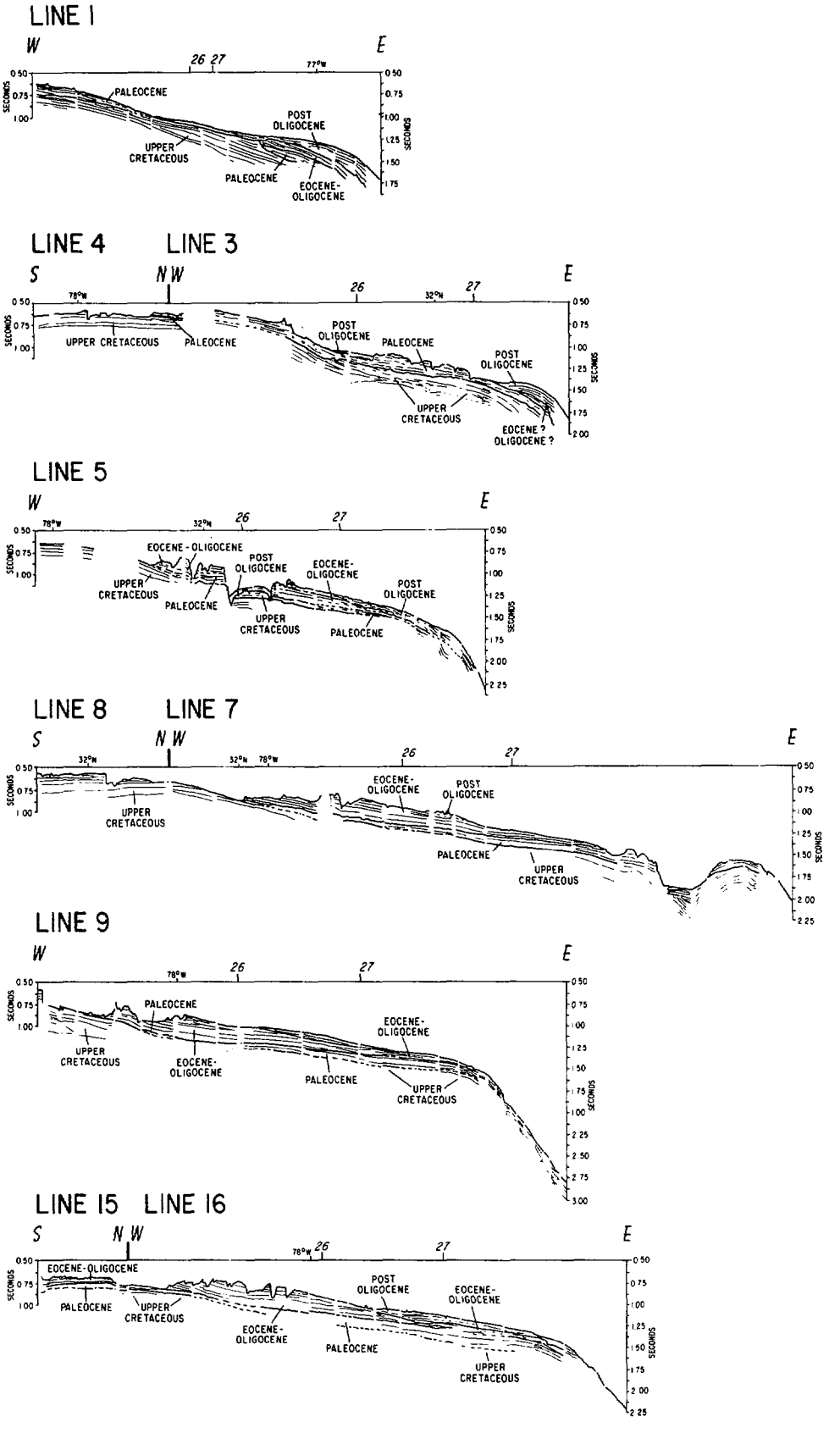
LINE 1
W
E
26 27
77°W
PALEOCENE
POST OLIGOCENE
UPPER CRETACEOUS
PALEOCENE
EOCENE-OLIGOCENE
SECONDS
LINE 4
LINE 3
S
NW
E
26
27
78°W
32°N
UPPER CRETACEOUS
PALEOCENE
POST OLIGOCENE
PALEOCENE
POST OLIGOCENE
UPPER CRETACEOUS
EOCENE ? OLIGOCENE ?
LINE 5
W
E
78°W
32°N
26
27
EOCENE-OLIGOCENE
POST OLIGOCENE
EOCENE-OLIGOCENE
UPPER CRETACEOUS
PALEOCENE
POST OLIGOCENE
UPPER CRETACEOUS
PALEOCENE
LINE 8
LINE 7
S
NW
E
32°N
32°N 78°W
26
27
EOCENE-OLIGOCENE
POST OLIGOCENE
UPPER CRETACEOUS
PALEOCENE
UPPER CRETACEOUS
LINE 9
W
E
78°W
26
27
PALEOCENE
EOCENE-OLIGOCENE
UPPER CRETACEOUS
EOCENE-OLIGOCENE
PALEOCENE
UPPER CRETACEOUS
LINE 15
LINE 16
S
NW
E
78°W
26
27
EOCENE-OLIGOCENE
POST OLIGOCENE
EOCENE-OLIGOCENE
PALEOCENE
UPPER CRETACEOUS
EOCENE-OLIGOCENE
PALEOCENE
UPPER CRETACEOUS

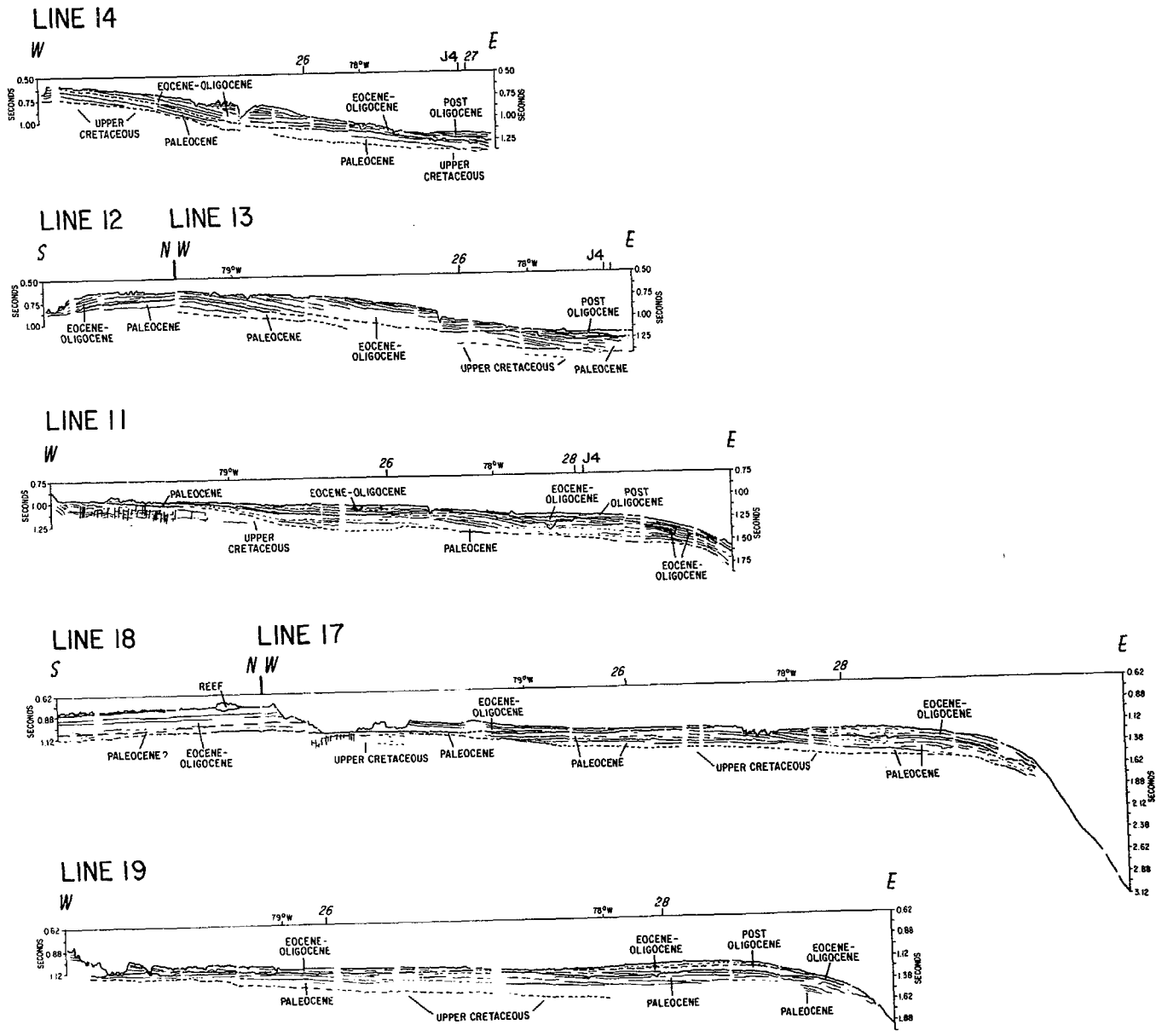
LINE 14
W
E
26
78°W
J4
27
SECONDS
EOCENE-OLIGOCENE
EOCENE-OLIGOCENE
POST OLIGOCENE
UPPER CRETACEOUS
PALEOCENE
PALEOCENE
UPPER CRETACEOUS
LINE 12
LINE 13
S
N W
E
79°W
26
78°W
J4
EOCENE-OLIGOCENE
PALEOCENE
PALEOCENE
EOCENE-OLIGOCENE
POST OLIGOCENE
UPPER CRETACEOUS
PALEOCENE
LINE 11
W
E
79°W
26
78°W
28 J4
PALEOCENE
EOCENE-OLIGOCENE
EOCENE-OLIGOCENE
POST OLIGOCENE
UPPER CRETACEOUS
PALEOCENE
EOCENE-OLIGOCENE
LINE 18
LINE 17
S
N W
E
REEF
79°W
26
78°W
28
EOCENE-OLIGOCENE
EOCENE-OLIGOCENE
PALEOCENE ?
EOCENE-OLIGOCENE
UPPER CRETACEOUS
PALEOCENE
PALEOCENE
UPPER CRETACEOUS
PALEOCENE
LINE 19
W
E
79°W
26
78°W
28
EOCENE-OLIGOCENE
EOCENE-OLIGOCENE
POST OLIGOCENE
EOCENE-OLIGOCENE
PALEOCENE
UPPER CRETACEOUS
PALEOCENE
PALEOCENE

Figure 7-20B

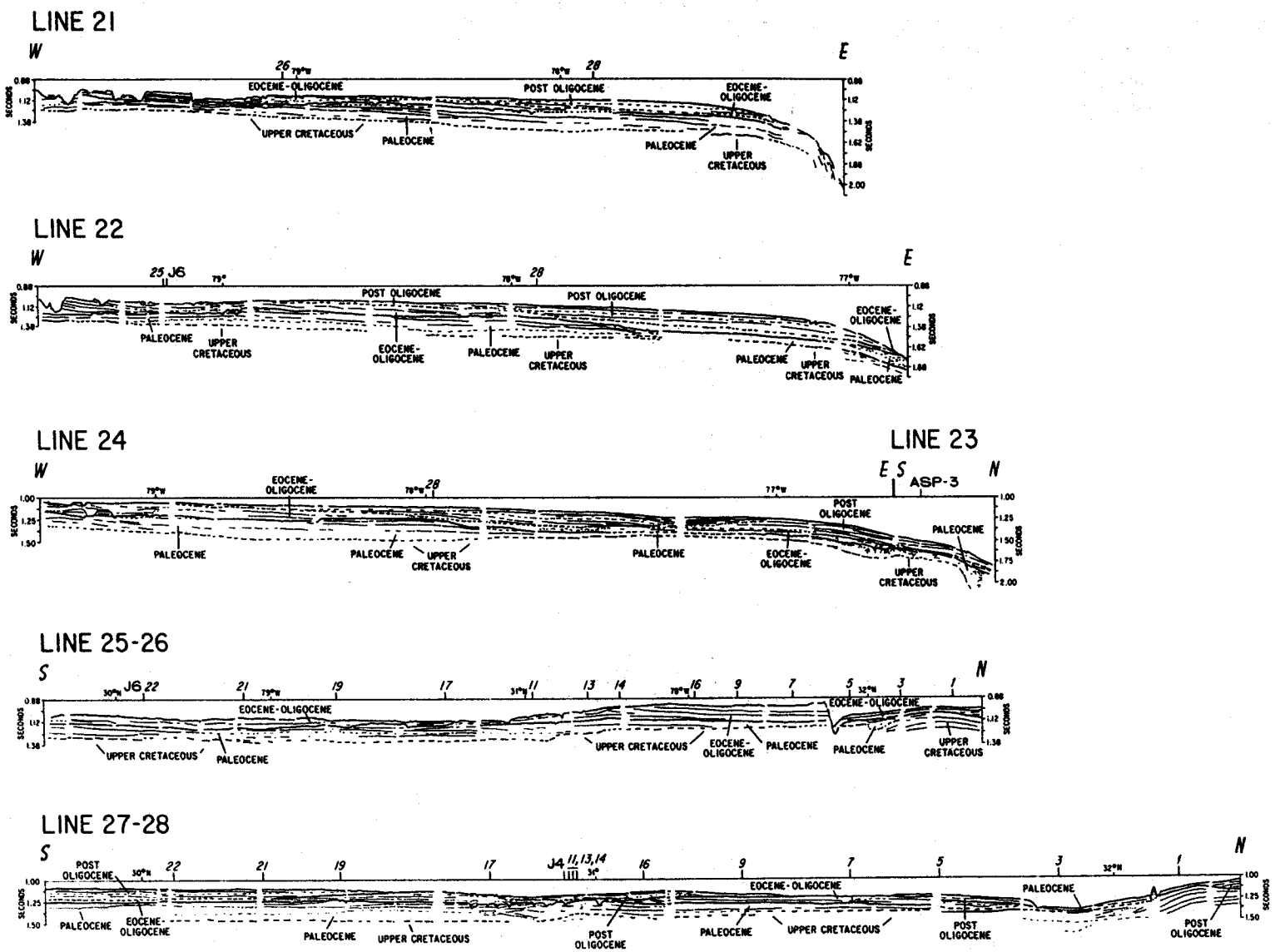
LINE 21
W
E
26
28
EOCENE-OLIGOCENE
POST OLIGOCENE
EOCENE-OLIGOCENE
UPPER CRETACEOUS
PALEOCENE
PALEOCENE
UPPER CRETACEOUS
SECONDS
LINE 22
W
E
25 J6
28
POST OLIGOCENE
POST OLIGOCENE
EOCENE-OLIGOCENE
PALEOCENE
UPPER CRETACEOUS
EOCENE-OLIGOCENE
PALEOCENE
UPPER CRETACEOUS
PALEOCENE
UPPER CRETACEOUS
PALEOCENE
SECONDS
LINE 24
LINE 23
W
E S
ASP-3
N
EOCENE-OLIGOCENE
28
POST OLIGOCENE
PALEOCENE
PALEOCENE
PALEOCENE
UPPER CRETACEOUS
PALEOCENE
EOCENE-OLIGOCENE
UPPER CRETACEOUS
SECONDS
LINE 25-26
S
N
J6 22
21
19
17
11
13
14
16
9
7
5
3
1
EOCENE-OLIGOCENE
EOCENE-OLIGOCENE
UPPER CRETACEOUS
PALEOCENE
UPPER CRETACEOUS
EOCENE-OLIGOCENE
PALEOCENE
PALEOCENE
UPPER CRETACEOUS
SECONDS
LINE 27-28
S
N
POST OLIGOCENE
22
21
19
17
J4 11,13,14
16
9
7
5
3
1
EOCENE-OLIGOCENE
PALEOCENE
PALEOCENE
EOCENE-OLIGOCENE
PALEOCENE
UPPER CRETACEOUS
POST OLIGOCENE
PALEOCENE
UPPER CRETACEOUS
POST OLIGOCENE
POST OLIGOCENE
SECONDS

Figure 7-20C

Figure 7-21. Photograph of portion of original sparker profile. Coordinates for middle of this line segment are 31°35'N.,77°41'W. Location is shown on figure 7-2 as a thickened trackline segment. Note how upper part of Paleocene sequence tends to be more reflective than lower part.

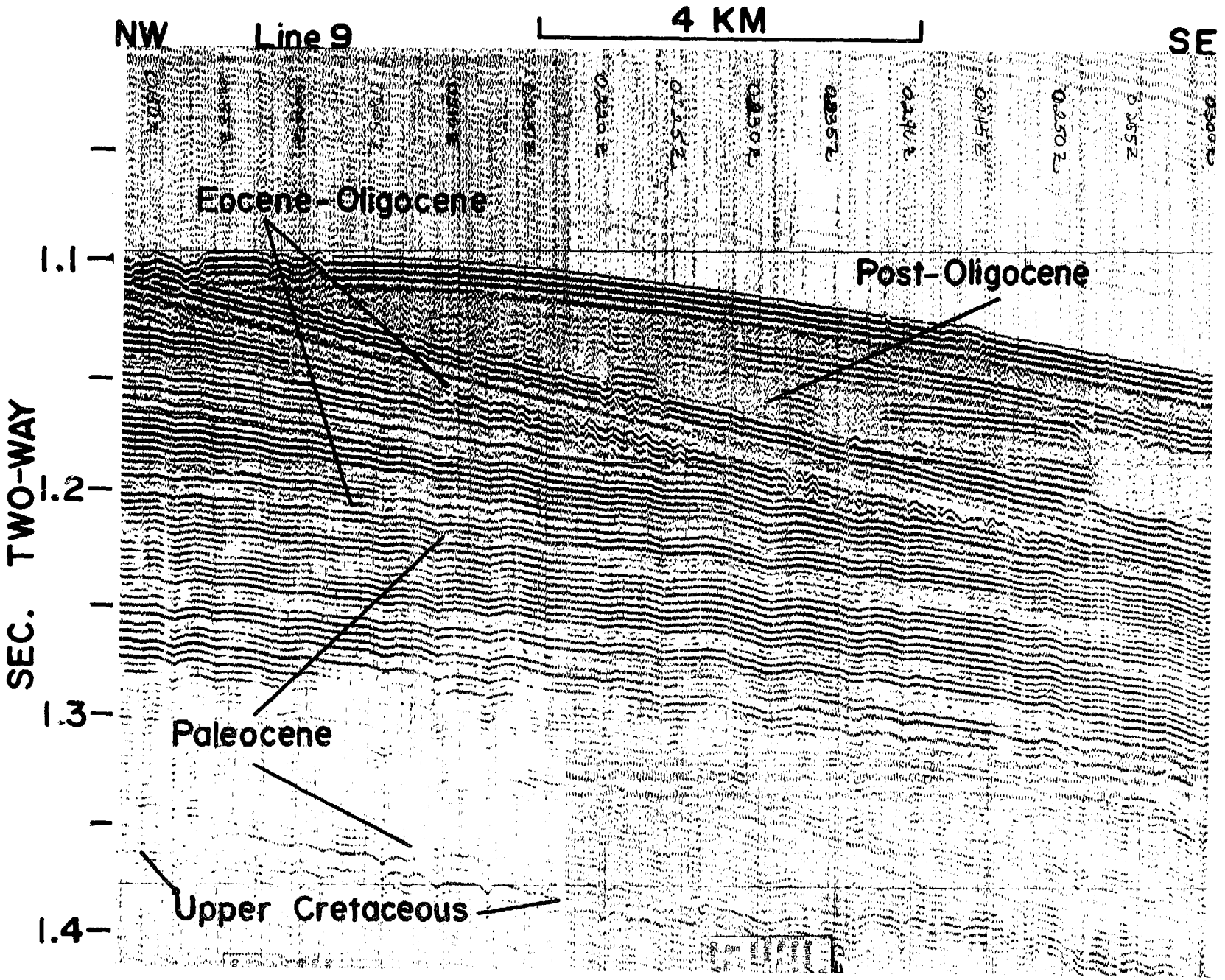
NW
Line 9
4 KM
SE
SEC. TWO-WAY
1.1
1.2
1.3
1.4
Eocene-Oligocene
Post-Oligocene
Paleocene
Upper Cretaceous

Figure 7-21

Figure 7-22. Structure contours on top of Paleocene unit. Surface displays regional dip to the east with only localized deviations from this trend. Note that Albian reef mass located to west of drill site ASP 3 has no expression, indicating that it has been engulfed by sediment.

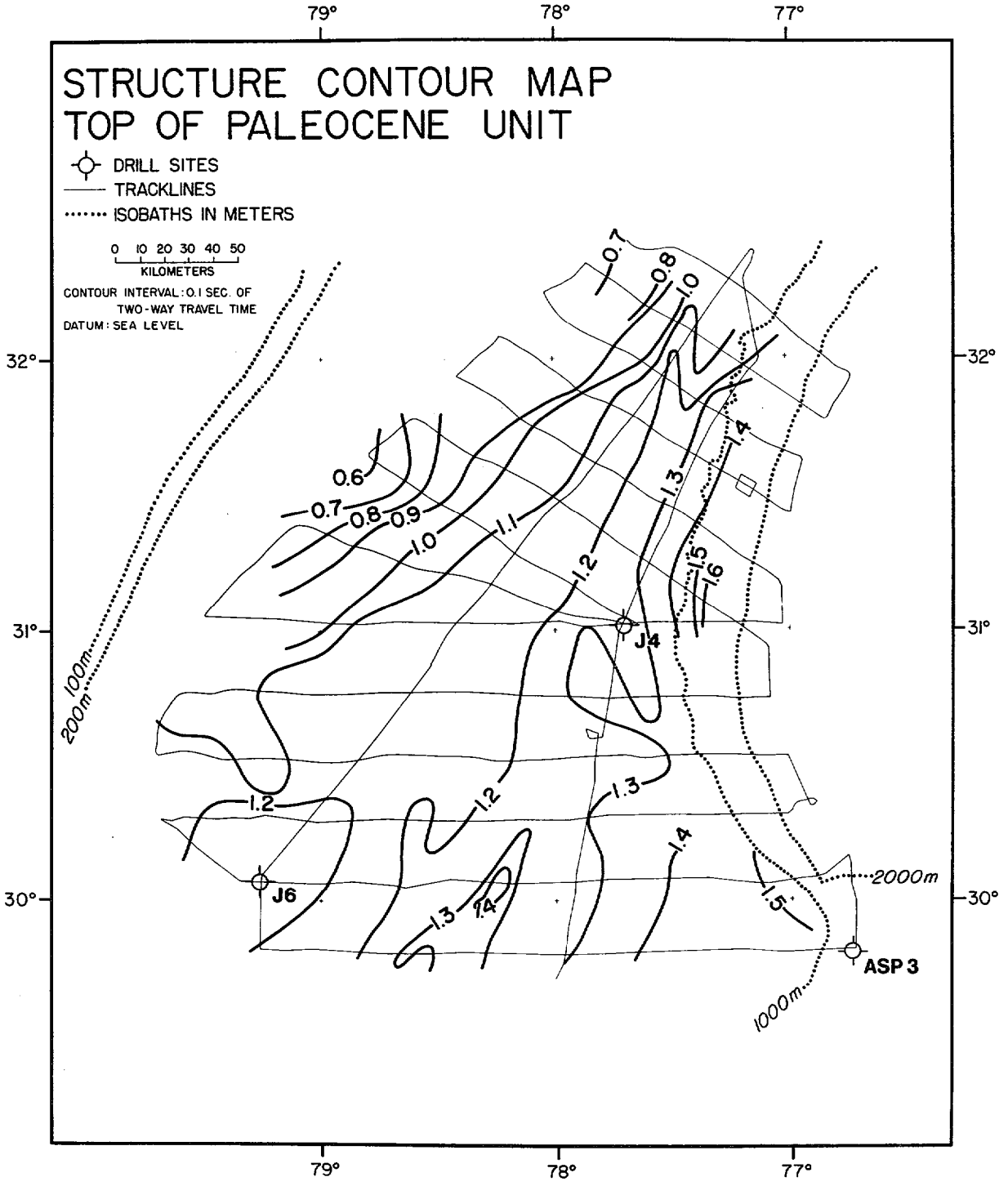
STRUCTURE CONTOUR MAP
TOP OF PALEOCENE UNIT
DRILL SITES
TRACKLINES
ISOBATHS IN METERS
0 10 20 30 40 50
KILOMETERS
CONTOUR INTERVAL: 0.1 SEC. OF TWO-WAY TRAVEL TIME
DATUM: SEA LEVEL
79°
78°
77°
32°
31°
30°
0.6
0.7
0.8
0.9
1.0
1.1
1.2
1.3
1.4
1.5
1.6
J4
J6
ASP 3
100m
200m
1000m
2000m

throughout the survey area (fig. 7-23). Typically, sediment is thin (less than 0.1 s) along the inner Blake Plateau. South of 31°N., this sparse sediment cover grades seaward into a broad band of thicker sediment (greater than 0.25 s). The upper bounding surface of this thick zone displays unusually rugged relief because of the presence of numerous erosional channels cut into the Paleocene deposits (fig. 7-24). Paleocene strata are truncated against the channel walls. Inspection of the seismic profiles reveals that deep channels in the Paleocene unconformity are confined to a broad swath south of 31°N. that runs across the Blake Plateau beginning near well J6 and extending ENE. to the Blake Escarpment. The general morphology of these channels resembles to a remarkable degree the channeled topography that runs across the present-day surface of the inner Blake Plateau. The latter is the product of prolonged scouring activity associated with the main axis of the Gulf Stream (Uchupi and Emery, 1967). This implies that the jagged relief of the Paleocene erosion surface was similarly constructed, and suggests that the Gulf Stream influenced depositional-erosional processes on the Blake Plateau as early as late Paleocene-early Eocene. If this interpretation is correct, the Gulf Stream flowed E.-W. during the early Tertiary in contrast to its modern counterpart which runs N.-S. parallel to the toe of the Florida-Hatteras Continental Slope.

Eocene-Oligocene Sequence

Paleocene sediments are succeeded by a stratigraphic interval whose upper bounding surface is unconformable in character (fig. 7-20). In the northern part of the survey area, this unit is thick and readily delimited, assuming that age inferences are correct. Here, intersection of ISELIN 78-3 lines with FAY 017 and 018 lines (Paull and Dillon, 1979)

Figure 7-23. Thickness data for Paleocene strata. The unit is particularly thin along the inner Blake Plateau, because of the erosional activity of the Gulf Stream.

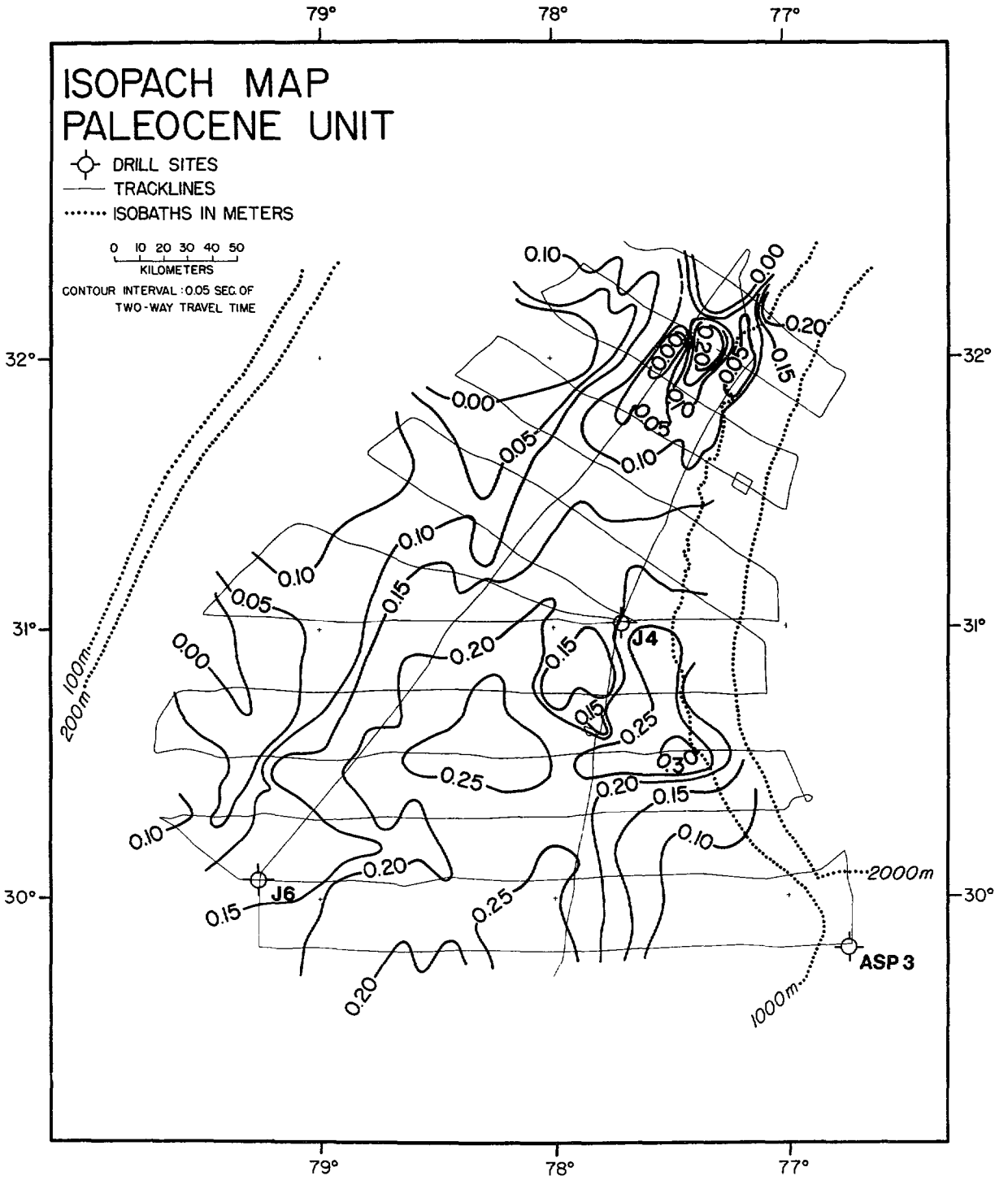
ISOPACH MAP
PALEOCENE UNIT
DRILL SITES
TRACKLINES
ISOBATHS IN METERS
0 10 20 30 40 50
KILOMETERS
CONTOUR INTERVAL : 0.05 SEC. OF TWO-WAY TRAVEL TIME
79°
78°
77°
32°
31°
30°
J4
J6
ASP 3
100m
200m
1000m
2000m

Figure 7-24. Photograph of portion of original sparker profile. Coordinates for middle of this line segment are 30°19'N.,78°45'W. Location is shown on figure 7-2 as a thickened trackline segment. Note the rugged relief evident along the unconformity at the top of the Paleocene unit. Eocene-Oligocene deposits have completely obliterated the irregular topography of the unconformity.

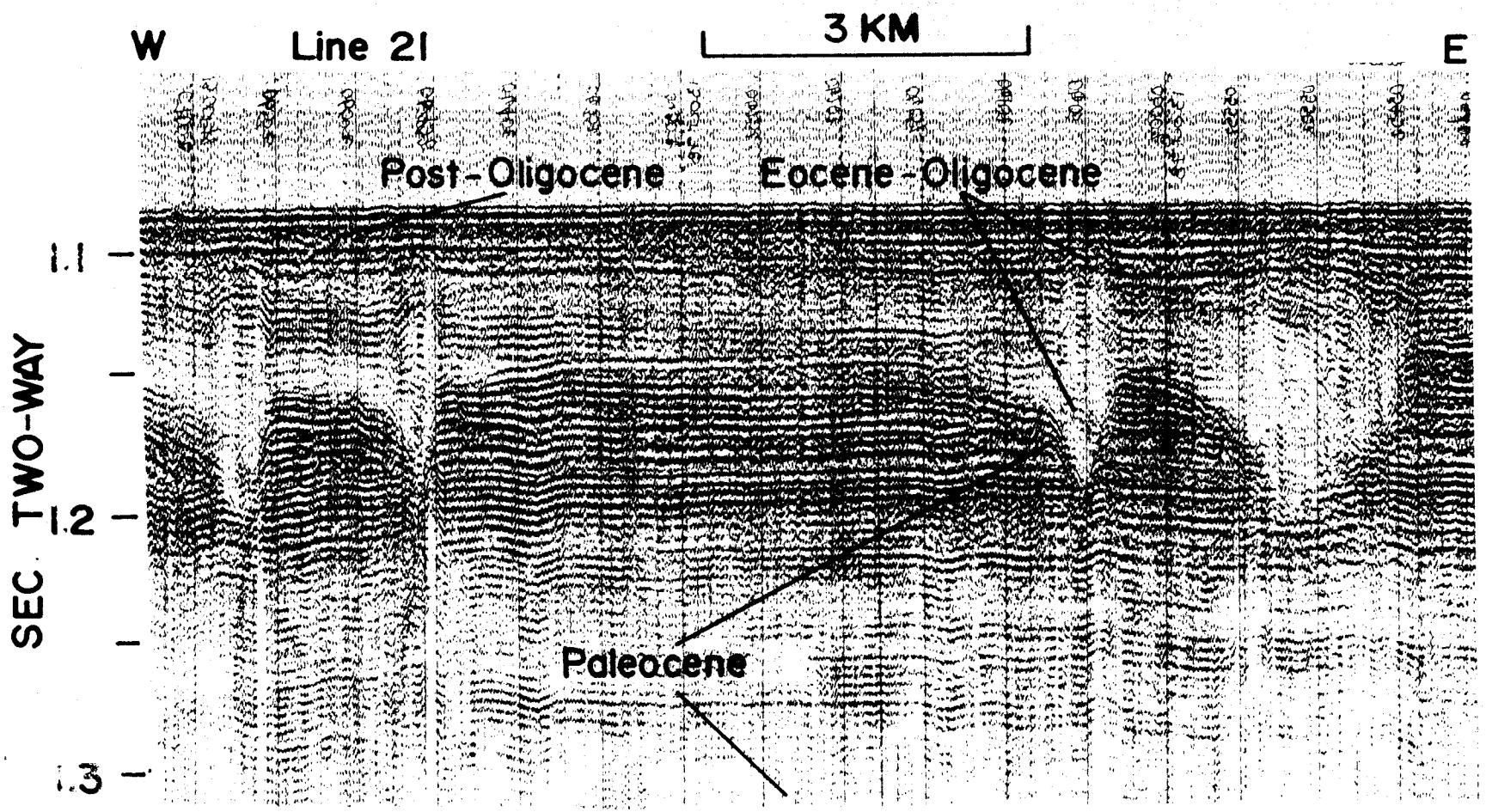
W
Line 21
3 KM
E
Post-Oligocene
Eocene-Oligocene
Paleocene
SEC. TWO-WAY
1.1
1.2
1.3

Figure 7-24

indicates that the unit is equivalent to Eocene-Oligocene strata beneath the Florida-Hatteras Continental Slope. Drill-hole data support this age inference. Assuming a seismic velocity of 2 $km \cdot s^{-1}$ the sequence consists of 113 m of Eocene and Oligocene calcilutite and calcarenite at core hole J6 and of 73 m of lower Eocene and Oligocene calcilutite at core hole J4 (Charm and others, 1969; Schlee, 1977).

Bedding in the Eocene-Oligocene sequence is characterized by even to wavy, parallel reflectors (fig. 7-24), the topmost beds showing weak erosional truncation against overlying units (fig. 7-25). The Eocene-Oligocene sediments smooth out and obliterate the jagged topography of the underlying Paleocene unconformity (fig. 7-24). A distinctive seismic facies is associated with the Eocene-Oligocene sediments that infill the channels and valleys of the Paleocene erosion surface (fig. 7-24). This facies consists of a series of discontinuous, irregular to chaotic reflectors that typically are arranged in a moundlike form. Their appearance on seismic profiles is somewhat similar to those obtained from regions where carbonate buildup has occurred (Bubb and Hatlelid, 1977). As such, the moundlike facies of the Eocene-Oligocene sequence is interpreted as representing localized zones of carbonate buildup along and within erosional channels. It is noteworthy that deepwater coral mounds presently thrive along the floor and edges of channels incised into the present-day surface of the inner Blake Plateau by the Gulf Stream (Uchupi, 1967).

Thicknesses of Eocene-Oligocene sediments (fig. 7-26) are quite variable. North of 31°N., the Blake Plateau is covered by a relatively thick pile of Eocene-Oligocene sediment that undergoes thinning both shoreward and seaward of the main deposit. The sequence is thin or absent farther southward (figs. 7-21 and 7-27). At well J4, this

Figure 7-25. Photograph of portion of original sparker profile. Coordinates for middle of this line segment are 30°45'N.,79°38'W. Location is shown on figure 7-2 as a thickened trackline segment. The Eocene-Oligocene sequence is unusually thick in this area and disconformably overlies a Paleocene unit.

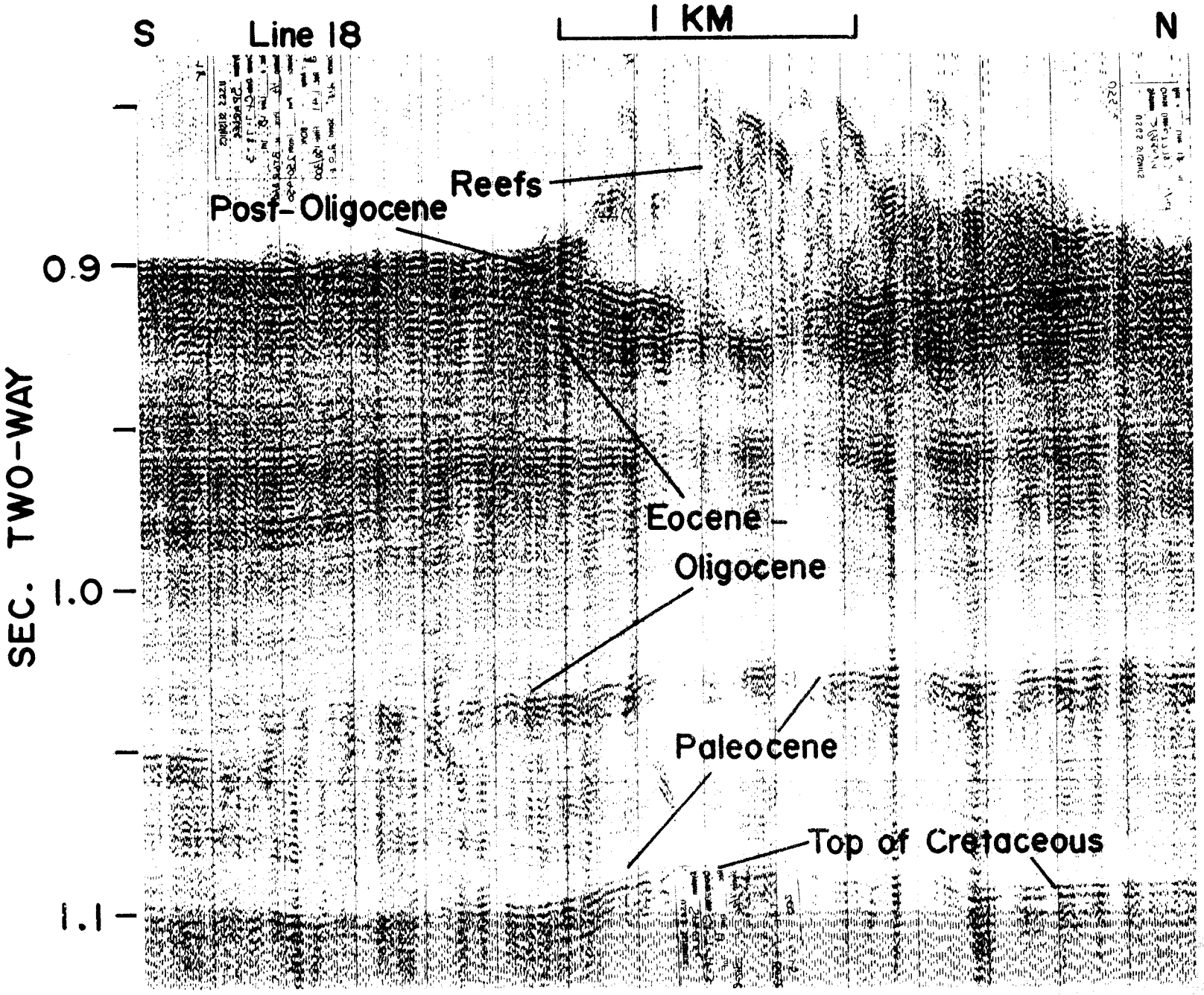
S
Line 18
1 KM
N
SEC. TWO-WAY
0.9
1.0
1.1
Reefs
Post-Oligocene
Eocene-
Oligocene
Paleocene
Top of Cretaceous

Figure 7-25

Figure 7-26. Thickness data for Eocene-Oligocene strata. Note how bulk of material of this age has accumulated north of well J4. This presumably reflects the fact that the prototype Gulf Stream was confined to the plateau south of 31°N. during most of Paleogene time.

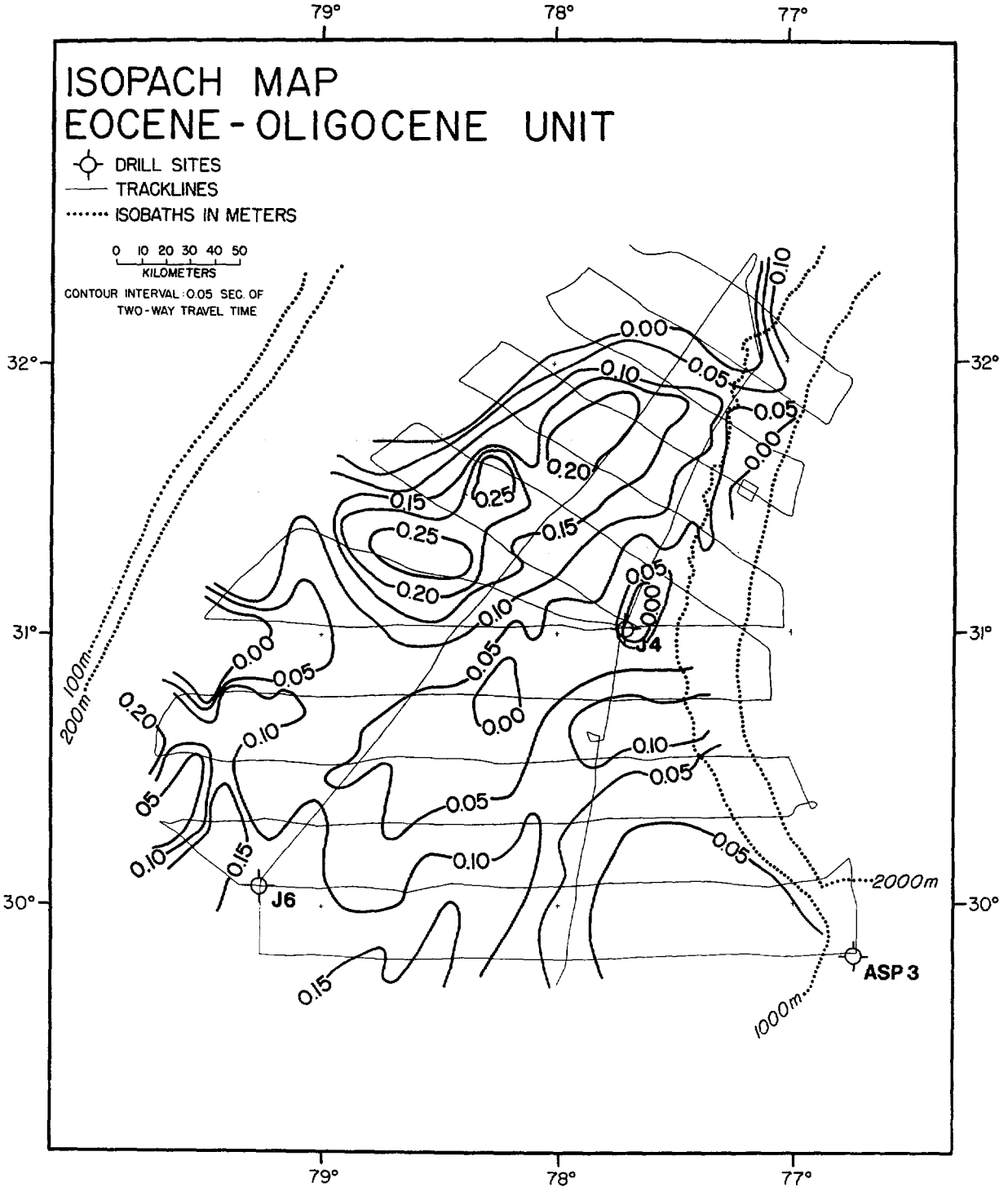
ISOPACH MAP
EOCENE - OLIGOCENE UNIT
DRILL SITES
TRACKLINES
ISOBATHS IN METERS
0 10 20 30 40 50
KILOMETERS
CONTOUR INTERVAL: 0.05 SEC. OF TWO-WAY TRAVEL TIME
79°
78°
77°
32°
31°
30°
J4
J6
ASP 3
100m
200m
1000m
2000m

Figure 7-27. Photograph of portion of original sparker profile. Coordinates for middle of this line segment are 30°20'N.,77°32'W. Location is shown on figure 7-2 as a thickened trackline segment. Note the smoothness of the top of the Paleocene surface along this portion of line 21, as well as the thin character of the Eocene-Oligocene unit.

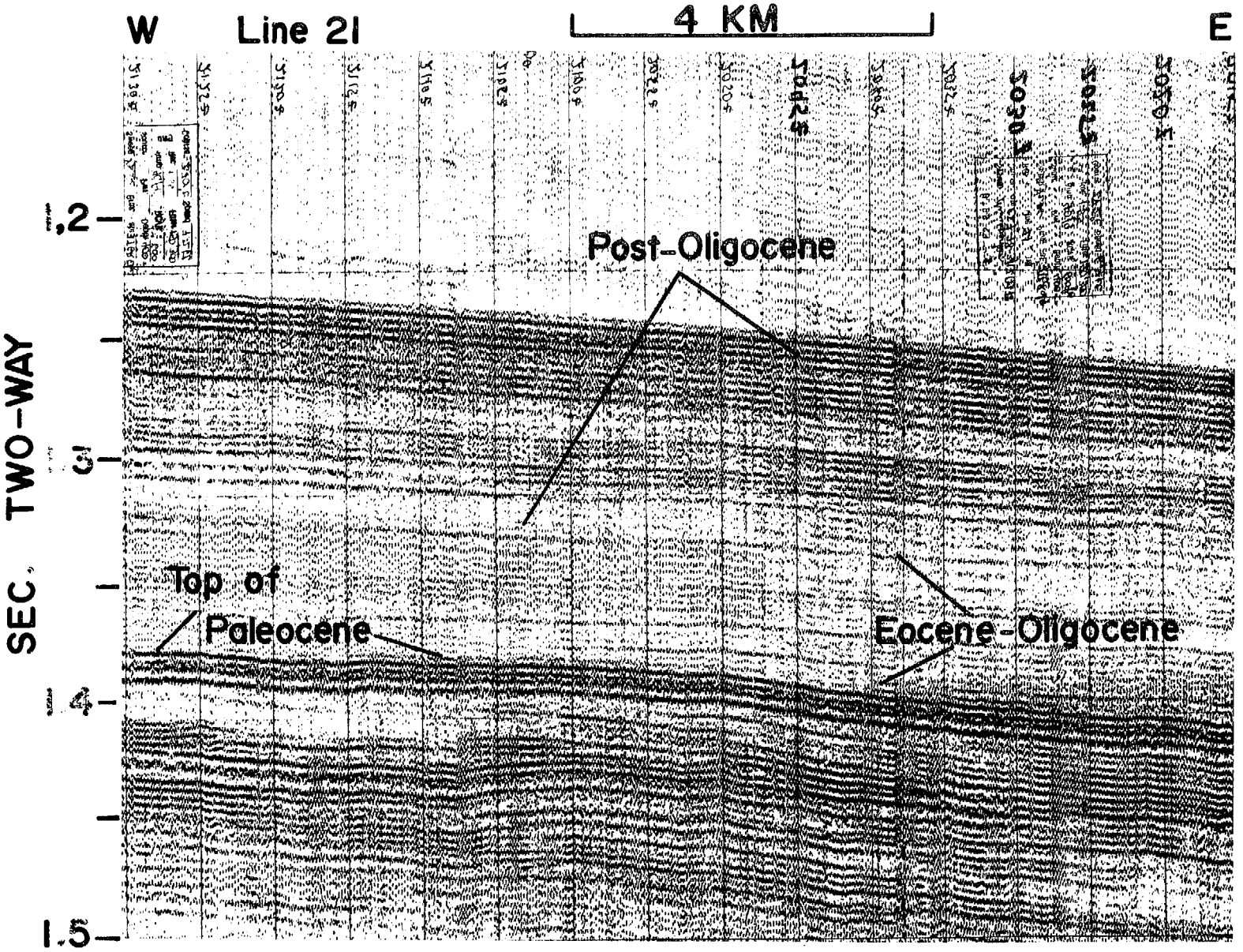
W
Line 21
4 KM
E
SEC. TWO-WAY
.2
.3
.4
1.5
Post-Oligocene
Top of
Paleocene
Eocene-Oligocene

Figure 7-27

stratigraphic interval is composed of about 10 m of lower Eocene ooze and silt and 25 m of Oligocene carbonate sand (Schlee, 1977). The inner plateau at drill site J6 is underlain by about 120 m of ooze equally divided between the Eocene and Oligocene, and an admixture of chert in the lower part of the section (Schlee, 1977). Farther offshore at well ASP 3, the Eocene-Oligocene sequence is thin and poorly sampled. Inshore equivalents beneath the Florida-Hatteras Continental Shelf thicken to as much as 700 m and consist dominantly of Eocene strata, Oligocene sediment being thin or absent in most places (Paull and Dillon, 1979). Also, lithologies are quite variable here and include calcareous silty clays, carbonate sands, and fine-grained limestones, all of which accumulated on a shallow carbonate shelf (Hathaway and others, 1979; Poag and Hall, 1979; Valentine, 1979).

As noted above, the Eocene-Oligocene sequence is thin or absent in the southern part of the survey area, presumably due to the presence at that time of a current sufficiently powerful to not only inhibit deposition, but also erode preexisting materials. Moreover, this region of the plateau is underlain by the rugged erosional surface (fig. 7-24) that defines the top of the Paleocene sequence, which further strengthens the case for strong bottom-current activity. Hence, the abbreviated Eocene-Oligocene section that overlies a deeply incised Paleocene unconformity offers compelling evidence for the appearance of the Gulf Stream system over the Blake Plateau sometime during the early Tertiary (late Paleocene-early Eocene). However, the seismic data indicate that the axis of the prototype Gulf Stream evidently was positioned farther south and was oriented more NE.-SW. than its modern counterpart.

Structure-contour and isopach data indicate that the basic

framework and shape of the present continental margin off the southeastern United States had been established by the Eocene and Oligocene. This contention is supported by the fact that the steepest dip of the top of the Paleogene coincides with the position of the modern continental slope. Also, Paleogene sediments are significantly thicker beneath the Florida-Hatteras Shelf than beneath the Blake Plateau (Paull and Dillon, 1979), a pattern that likewise typifies younger strata of the region. Microfossils collected from Eocene-Oligocene carbonate sands, marls, and limestones beneath the shelf indicate shallow-water carbonate deposition (Poag, 1978). Near the shelf edge, the unit grades into calcilutites and silty clays (Poag, 1978) and thickens considerably to as much as 700 m within a well defined depocenter positioned between 30° and 31°N. latitude (Paull and Dillon, 1979). The latter deposit indicates a high rate of sediment input to the outer shelf. However, despite the voluminous sediment influx, the unit thins abruptly beneath the slope and is exceedingly thin or absent beneath the Blake Plateau. Clearly, these thickness variations reflect the influence of vigorous bottom currents that inhibited the seaward extension of the Eocene-Oligocene depocenter as well as prevented the accumulation of sediment on the Blake Plateau proper. Hence, the stratigraphic record of the region apparently documents the presence of the Gulf Stream as far back as the early Tertiary; this current has controlled directly the development of the Florida Outer Shelf and Slope and the Blake Plateau since that time.

Post-Oligocene Sequence

Volumetrically, post-Oligocene deposits are the least important units of the study area. Significant accumulations of these sediments are confined to the eastern third of the Blake Plateau (figs. 7-28 and

Figure 7-28. Thickness data of Post-Oligocene deposits. Note that they are confined to the eastern third of the Blake Plateau, where the Gulf Stream exerts less of a direct influence on the bottom.

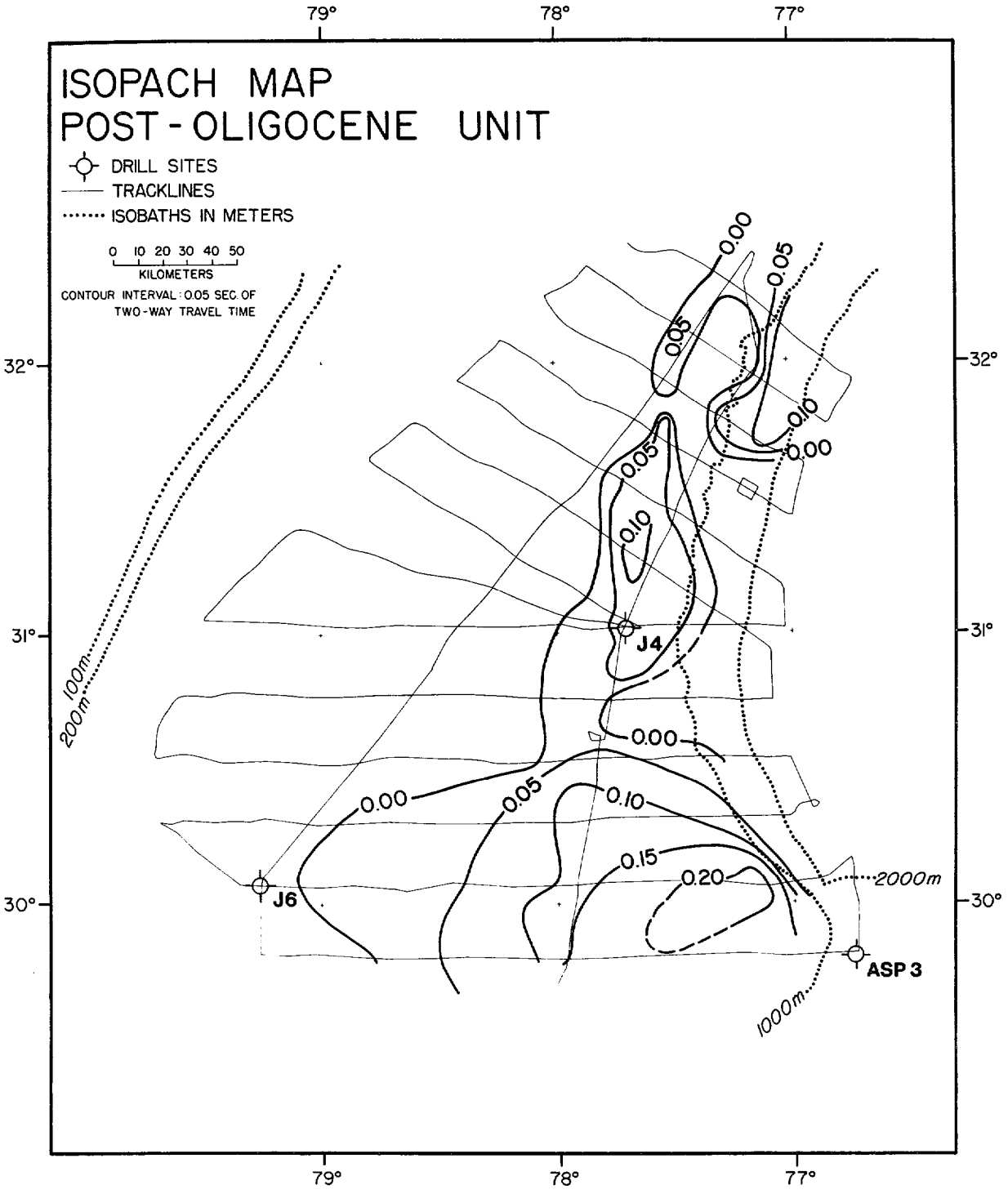
ISOPACH MAP
POST-OLIGOCENE UNIT
DRILL SITES
TRACKLINES
ISOBATHS IN METERS
0 10 20 30 40 50
KILOMETERS
CONTOUR INTERVAL: 0.05 SEC. OF TWO-WAY TRAVEL TIME
79°
78°
77°
32°
31°
30°
0.00
0.05
0.10
0.15
0.20
J4
J6
ASP 3
100m
200m
1000m
2000m

7-29), where they unconformably overlie older units. Elsewhere, they are either absent altogether or too thin to be within the resolution capability of the seismic-profiler system.

Generally, post-Oligocene sedimentary sequences display strong, well defined, even reflectors whose continuity is excellent (fig. 7-20). This type of reflector configuration is exemplified by dip lines 21, 22, and 24 (fig. 7-20C) where post-Oligocene deposits thicken eastward to as much as 200 m as they onlap and downlap an inclined Eocene-Oligocene erosional surface. At the western end of seismic line 22 at drill site J6, sediments of this age essentially are absent, consisting of no more than 6 m of post-Miocene calcilutite. To the northeast at drill site J4, the unit is somewhat thicker, consisting of 35 m of lower Miocene calcilutite that is overlain by 18 m of post-Miocene calcarenite.

A close inspection of internal reflector patterns within the post-Oligocene interval reveals intricate, but localized, cut-and-fill structures. Deposition and erosional processes were undoubtedly complex as indicated by these reflector patterns. Also, unconformities within the sequence are common. For example, the post-Oligocene unit along dip line 24 is composed of two distinct depositional intervals. Reflectors within the basal sequence are prominent and regular, and display erosional truncation. The younger interval consists of an onlapping fill, characterized by a uniform array of even, parallel reflectors. Tracing the unit seaward to drill hole ASP 3 indicates that the post-Oligocene sediments are composed mainly of Miocene calcilutites and calcarenites and minor Pliocene and Pleistocene calcilutite.

The dominant factor in the post-Oligocene development of the Blake Plateau was and continues to be the erosive force of the Gulf Stream, as

Figure 7-29. Photograph of portion of original sparker profile. Coordinates for middle of this line segment are 29°09'N.,77°57'W. Location is shown on figure 7-2 as a thickened trackline segment. Note the great thickness of post-Oligocene deposits that unconformably overlie a thin Eocene-Oligocene unit.

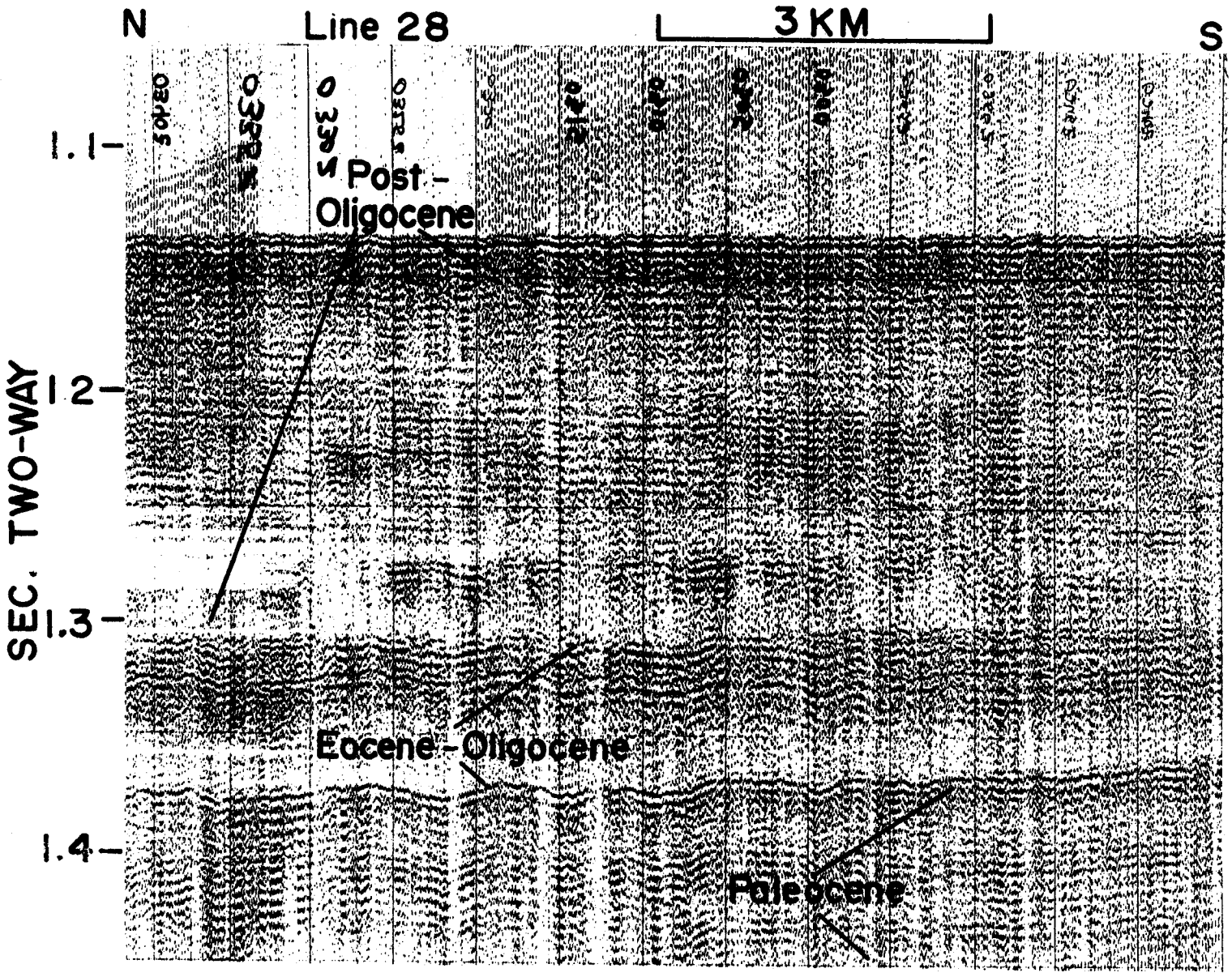
N
Line 28
3 KM
S
SEC. TWO-WAY
1.1
1.2
1.3
1.4
Post-Oligocene
Eocene-Oligocene
Paleocene

Figure 7-29

indicated by the barrenness of the plateau's surface as well as numerous stratigraphic discontinuities within Miocene and younger deposits. Fluctuations in both velocity and volume transport of the Gulf Stream throughout the late Cenozoic are suggested by a biostratigraphic analysis of a suite of piston cores from the southeastern Blake Plateau (Kaneps, 1979). Apparently, deposition of calcareous ooze occurred during low-velocity phases of the current, and erosion of sediment during high-velocity phases (Kaneps, 1979).

Structural and Stratigraphic Development of the Northern Blake Plateau

High-resolution, shallow-penetrating seismic-reflection profiles acquired during ISELIN cruise 78-3 reveal the stratigraphic character of the Blake Plateau extending back in time to the Albian. Earlier development of the plateau and adjoining Florida-Hatteras Continental Shelf and Slope has been reconstructed by others, using deep-penetration, multichannel CDP seismic records, magnetic anomaly patterns of the crust, and deep-sea drill-core data.

Inception of the present-day continental margin of southeastern North America began with thinning and rifting of the continental crust possibly sometime during the Triassic (Dillon and others, 1979a; 1979b), unquestionably by the Jurassic (Klitgord and Behrendt, 1979). This tectonic phase marked the opening of the Atlantic Ocean. Subsequently, ocean spreading at the Mid-Atlantic Ridge translated the margin of eastern North America away from the ridge as production of basaltic crust ensued (Pitman and Talwani, 1972; Vogt, 1973). Concurrently, the continental edge of North America subsided markedly, because of thermal cooling of basement rocks (Folger and others, 1980).

Crustal structure beneath the Blake Plateau is complex and apparently reflects variations in composition as well as segmentation of

the crust by several fracture zones. For example, magnetic-anomaly characteristics of the basement beneath the northern Blake Plateau suggest that it is composed of sialic rock north of 31°N., but of transitional (i.e., nonsialic) rock south of 31°N. (Klitgord and Behrendt, 1979). The two types of basement may be juxtaposed along a fracture zone, because a projection of the Blake Spur Fracture Zone passes beneath the Blake Plateau at about 31°N. (Emery and Uchupi, 1972; Klitgord and Behrendt, 1979). Support for a quasi-independent development of the basement in this area of the plateau is provided by calculations of depth-to-magnetic source that indicate a significantly deeper basement and, thus, greater total subsidence for the crust south of 31°N. than north of this line of parallel (Klitgord and Behrendt, 1979). Furthermore, the southern part of the Blake Plateau overlaps Africa in most predrift reconstructions, suggesting that the crust in this region is not sialic in composition, but was generated by spreading activity at the Mid-Atlantic Ridge (Vogt, 1973). This fundamental difference in crustal composition influenced to a degree the subsequent evolution of the continental margin as indicated by a variety of geophysical data (Dillon and others, 1979a).

During much of the Jurassic and Cretaceous, sedimentation along the northern Blake Plateau was controlled largely by erosional-depositional processes that resulted in upward growth and seaward extension of a thick wedge of sediment on a subsiding basement (Emery and Uchupi, 1972; Sheridan, 1974; Dillon and others; 1979a). A massive reef complex apparently thrived along the southern Blake Plateau, whose prolonged vertical development produced the precipitous Blake Escarpment (Sheridan, 1974; Dillon and others, 1979b). Limited data suggest that this massive offshore reef bank died near the end of Aptian and a

subsequent reef of Albian age developed landward of it. This reef also died at the close of the Albian although it remained a prominent bathymetric high (Dillon and others, 1979a) that influenced the seaward dispersal of sediment particularly in the area south of 31°N. Here, Upper Cretaceous reflectors dip seaward along the inner Blake Plateau, but flatten out further offshore, eventually reversing their dip as post-Albian units onlap the reef structure near the Blake Escarpment. Complete burial of the reef mass was not accomplished until the early Tertiary. The northern extremity of the Blake Plateau apparently was not flanked by massive reefs (Dillon and others, 1979a) and a series of three Upper Cretaceous progradational wedges formed, whose seaward termini shifted position as a function of variations in sediment influx and subsidence rates as well as fluctuations in sea level.

By the early Tertiary, Gulf Stream circulation was established over the Blake Plateau. The erosive force of high-intensity bottom currents produced an abbreviated Tertiary section containing numerous stratigraphic discontinuities. Also significant progradation of the Florida-Hatteras Continental Slope across the Blake Plateau essentially ceased during the Cenozoic, because of the scouring activity of this powerful bottom current (Uchupi, 1967; 1970). Hence, crustal subsidence in conjunction with active transport and erosion by the Gulf Stream throughout the Cenozoic lowered the plateau's surface to its present depth (Ewing and others, 1966).

SUMMARY

The development of the northern Blake Plateau and the contiguous Florida-Hatteras Continental Shelf and Slope since the Late Cretaceous resulted in the accumulation of a thick sedimentary prism. The

stratigraphy of this sediment pile basically consists of thick Upper Cretaceous deposits that are overlain by thin Cenozoic units. The depositional history of the northern Blake Plateau from the Late Cretaceous to the present reflects the interaction of the following processes and events:

i) subsidence of an Albian shallow-water carbonate shelf bank and the accumulation of Upper Cretaceous and Cenozoic deepwater sediments upon it;

ii) formation of a series of progradational shelf and slope facies whose depocenters shift in response to variations in both sediment influx and sea-level fluctuations;

iii) initiation of Gulf Stream current flow perhaps as early as Late Paleocene, followed by a long history of bottom scouring of the Blake Plateau's surface by the current producing an abbreviated Tertiary-Quaternary section with many stratigraphic gaps.

The Upper Cretaceous section beneath the northern Blake Plateau was subdivided into four major seismic sequences, whose ages were inferred by comparing their depths of burial to those of units encountered on a deep-penetration seismic line, TD-5, that crosses the COST GE-1 well site on the inner Blake Plateau and the ASP 3 drill site near the Blake Escarpment (Dillon and others, 1979b). Additionally, our seismic units were correlated to those defined beneath Florida-Hatteras Shelf-Slope and the inner Blake Plateau (Paull and Dillon, 1979).

Albian deposits which comprise the oldest unit apparent on our seismic records generally dip seaward in the northern part of the Blake Plateau, but farther southward near the Blake Escarpment are draped over a massive carbonate reef bank that apparently had died sometime during

the early Albian (Dillon and others, 1979a; 1979b). This basal unit is overlain by three progradational wedges, a Coniacian-Turonian sequence, a Santonian sequence, and a Campanian-Maestrichtian sequence, that grade eastward and southward over the northern Blake Plateau into thin deeper-water deposits that onlap and pinch out against the Albian reef mass. The internal reflector configurations of the three wedges suggest that they represent prograded shelf-slope facies that underwent pronounced shifts in position possibly in response to fluctuations in sediment input and in sea level. Available stratigraphic information indicates that sediment introduced to this ancient continental margin was dispersed seaward along the leading edge of broad progradational wedges. Sediment that bypassed the shelf break accumulated on the floor of a slowly subsiding deepwater basin and blanketed the western shoulder of the massive, but dead, Albian reef complex.

Three distinct seismic units are recognized in the Cenozoic section of the northern Blake Plateau, whose ages are inferred to be Paleocene, Eocene-Oligocene, and post-Oligocene, based on correlations to drill-site data and to seismic sequences beneath the Florida-Hatteras Continental Shelf. The seismic stratigraphy indicates quite clearly that deposition on the Blake Plateau was spasmodic throughout much of the Tertiary and Quaternary. The basal Paleocene unit shows the least variation in thickness and obscures the topographic expression of the underlying Albian reef complex near the Blake Escarpment. The top of the Paleocene unit is a regional unconformity, typified by irregular and, locally, deeply eroded topography that likely was produced by strong bottom currents associated with Gulf Stream activity. This erosional surface suggests that Gulf Stream flow was initiated at least as early as late Paleocene-early Eocene. Since its inception, the Gulf

Stream has dominated sedimentation patterns on the Blake Plateau by inhibiting deposition and eroding preexisting sediment. As a result of current scouring, the Eocene-Oligocene and post-Oligocene units are thin and discontinuous and characterized by complex seismic facies and numerous stratigraphic hiatuses.

REFERENCES CITED

Antoine, J.W., and Henry, V.J., 1965, Seismic refraction study of shallow part of continental shelf off Georgia coast: American Association of Petroleum Geologists Bulletin 49, p. 601-609.

Bubb, J.N., and Hatlelid, W.G., 1977, Seismic recognition of carbonate buildup, in Payton, C.E., ed., Seismic Stratigraphy-Applications to Hydrocarbon Exploration: American Association of Petroleum Geologists Memoir 26, p. 185-204.

Charm, W.B., Nesteroff, W.D., and Valdes, S., 1969, Detailed stratigraphic description of the JOIDES cores on the continental margin off Florida: U.S. Geological Survey Professional Paper 581-D, p. D1-D13.

Dillon, W.P., Paull, C.K., Buffler, R.T., and Fail, J.-P., 1979a, Structure and development of the Southeast Georgia Embayment and northern Blake Plateau: preliminary analysis, in Watkins, J.S. and others, eds., Geological and Geophysical Investigations of Continental Margins: American Association of Petroleum Geologists Memoir 26, p. 27-41.

Dillon, W.P., Paull, C.K., Dahl, A.G., and Patterson, W., 1979b, Structure of the continental margin near the COST GE-1 drillsite from a common depth point seismic reflection profile, in Scholle, P.A., ed., Geological Studies on the COST GE-1 well, U.S. South

Atlantic Outer Continental Shelf Area: U.S. Geological Survey Circular 800, p. 97-114.

Emery, K.O., and Uchupi, E., 1972, Western North Atlantic Ocean: topography, rocks, structure, water, life, and sediments: American Association of Petroleum Geologists Memoir 17, 532 p.

Emery, K.O., and Zarudski, E.R.K., 1967, Seismic reflection profiles along the drill holes on the continental margin off Florida: U.S. Geological Survey Professional Paper 581-A, p. A1-A8.

Ewing, J., Ewing, M., and Leyden, R., 1966, Seismic-profiler survey of Blake Plateau: American Association of Petroleum Geologists Bulletin 50, p. 1948-1971.

Folger, D.W., Dillon, W.P., Grow, J.A., Klitgord, K.D., and Schlee, J.S., 1980, Evolution of the Atlantic Continental Margin of the United States, in Talwani, M., Hay, W., and Ryan, W.B.F., eds., Deep Drilling Results in the Atlantic Ocean: Continental margins and paleoenvironments: American Geophysical Union Maurice Ewing Series 3, p. 87-108.

Hathaway, J.C., and others, 1979, U.S. Geological Survey core drilling on the Atlantic shelf: Science 206, p. 515-527.

Heezen, B.C., Tharp, M., and Ewing, M., 1959, The floors of the oceans, the North Atlantic: Geological Society of America Special Paper 65, 122 p.

Hersey, J.B., Bunce, E.T., Wyrick, R.F., and Dietz, F.T., 1959, Geophysical investigation of the continental margin between Cape Henry, Virginia and Jacksonville, Florida: Geological Society of America Bulletin 70, p. 437-466.

Kaneps, A.G., 1979, Gulf Stream: velocity fluctuations during the late Cenozoic: Science 204, p. 297-301.

Klitgord, K.D., and Behrendt, J.C., 1979, Basin structure of the U.S. Atlantic margin, in Watkins, J.S., and others, eds., Geological and Geophysical Investigations of Continental Margins: American Association of Petroleum Geologists Memoir 29, p. 85-112.

Paull, C.K., and Dillon, W.P., 1979, The subsurface geology of the Florida-Hatteras shelf, slope, and inner Blake Plateau: U.S. Geological Survey Open-File Report 79-448, 94 p.

Pitman, W.C., III, and Talwani, M., 1972, Sea-floor spreading in the North Atlantic: Geological Society of America Bulletin 83, p. 619-649.

Poag, C.W., 1978, Stratigraphy of the Atlantic continental shelf and slope of the United States: Annual Review, Earth and Planetary Sciences 6, p. 251-280.

Poag, C.W., and Hall, R.E., 1979, Foraminiferal biostratigraphy, paleoecology, and sediment accumulation rates, in Scholle, P.A., ed., Geological Studies on the COST GE-1 well, U.S. South Atlantic Outer Continental Shelf Area: U.S. Geological Survey Circular 800, p. 49-63.

Pratt, R.M., 1966, The Gulf Stream as a graded river: Limnology and Oceanography 11, p. 60-67.

Pratt, R.M. and Heezen, B.C., 1964, Topography of the Blake Plateau: Deep-Sea Research 11, p. 721-728.

Schlee, J.S., 1977, Stratigraphy and Tertiary development of the continental margin east of Florida: U.S. Geological Survey Professional Paper 581-F, p. F1-F25.

Sheridan, R.E., 1974, Atlantic continental margin of North America, in Burk, C.A., and Drake, C.L., eds., Geology of Continental Margins: New York, Springer-Verlag, p. 391-407.

Sheridan, R.E., Drake, C.L., Nafe, J.E., and Hennion, J., 1965, Seismic refraction study of the continental margin east of Florida: American Association of Petroleum Geologists Bulletin 50, p. 1972-1991.

Uchupi, E., 1967, The continental margin south of Cape Hatteras, N.C.: shallow structure: Southeastern Geology 8, p. 155-177.

Uchupi, E., 1970, Atlantic continental shelf and slope of U.S.-shallow structure: U.S. Geological Survey Professional Paper 529-I, p. I1-I44.

Uchupi, E., and Emery, K.O., 1967, Structure of continental margins off Atlantic coast of U.S.: American Association of Petroleum Geologists Bulletin 51, p. 223-234.

Valentine, P.C., 1979, Calcareous nannofossil biostratigraphy and paleoenvironmental interpretation, in Scholle, P.A., ed., Geological Studies in the COST GE-1 well, U.S. South Atlantic Outer Continental Shelf Area: U.S. Geological Survey Circular 800, p. 64-70.

Vogt, P.R., 1973, Early events in the opening of the North Atlantic, in Tarling, D.H., and Runcorn, S.K., eds., Implications of Continental Drift to the Earth Sciences: London, Academic Press, p. 693-712.

CHAPTER 8

AN ASSESSMENT OF POTENTIAL GEOLOGIC HAZARDS OF THE NORTHERN AND CENTRAL BLAKE PLATEAU

Paul R. Pinet[1], Peter Popenoe[2], Marshall L. Otter[2], Susan M. McCarthy[2]

[1]U.S. Geological Survey and Colgate University, Department of Geology, Hamilton, New York 13346

[2]U.S. Geological Survey, Woods Hole, Massachusetts 02543

CHAPTER 8

Table of Contents

	Page
Abstract	8- 1
Introduction	8- 2
Potential geologic hazards of the Blake Plateau	8- 2
Structural features	8- 2
Faults	8- 2
Clathrates and accompanying trapped gas	8-10
Diapirs	8-16
Slump masses	8-16
Stratigraphic features	8-26
Cut-and-fill structures	8-26
Cavernous limestone	8-26
Gulf Stream-generated features	8-34
Surface scour	8-34
Channeling	8-37
Biogenic features	8-37
Conclusions	8-40
References cited	8-45

CHAPTER 8

AN ASSESSMENT OF POTENTIAL GEOLOGIC HAZARDS OF THE NORTHERN AND CENTRAL BLAKE PLATEAU

Paul R. Pinet, Peter Popenoe, Marshall L. Otter,

and Susan M. McCarthy

ABSTRACT

A geologic hazards map of the Blake Plateau between 30° and 32°N. latitude was constucted from about 4,700 km of high-resolution seismic-reflection profiles. Although slump masses are prevalent at the precipitous Blake Escarpment, none were detected on the plateau surface proper. Faults are not common in the area, and those that were noted were either small or showed little evidence of recent activity. Cut-and-fill structures and deepwater reef banks are ubiquitous, but pose no insurmountable problems to drilling operations.

Three features are of considerable consequence for successful drilling of the plateau's surface. First, problematical reflector configurations typify Paleocene limestones and some Eocene-Oligocene carbonates in the southeastern portion of the study area that tentatively are interpreted as arising from massive solution features. Second, Gulf Stream-flow consists of not only powerful surface currents but also strong bottom currents that presently scour the plateau's surface and that have a documented erosional history extending back to the early Tertiary. Third, a frozen gas hydrate layer which may trap shallow gas has been noted on the Blake Escarpment and continental rise. Drilling problems also are compounded by the excessive water depths in the survey area that range between 200 and 1,000 m.

INTRODUCTION

The purpose of this report is to describe the nature and disposition of features that may pose a risk to drilling operations on the Blake Plateau. The distribution of these potential geologic hazards as interpreted from about 4,700 km of high-resolution seismic-reflection profiles (ISELIN cruise 78-3 and FAY cruise 025) is depicted on the accompanying map (fig. 8-1). Because Ball and others (1980) and McCarthy and others (1980) succinctly review the general drilling difficulties likely to be associated with each of the geologic hazards identified by this survey, no elaboration is required in this report. Field methodology, instrumentation, and data processing are detailed in chapter 7 of this volume.

POTENTIAL GEOLOGIC HAZARDS OF THE BLAKE PLATEAU

A variety of geologic features that pose potential problems for drilling operations over the Blake Plateau are classified conveniently into one of five categories. These include 1) structural features, such as faults, diapirs, and slump blocks; 2) frozen gas hydrates and shallow trapped gas; 3) stratigraphic features including cut-and-fill structures and cavernous limestones; 4) Gulf Stream-generated features, such as surface scour and channeling; and 5) biogenic features, mainly deepwater reef banks. Pertinent characteristics of each feature are described below and their distributions in the survey area are shown on figure 8-1. Plate 8-1 (in pocket in back cover) is a larger version of this map.

STRUCTURAL FEATURES

Faults

A fault of regional extent was mapped across the northern end of

Figure 8-1. Geologic hazards map of the central and northern Blake Plateau showing location of features and figures discussed in the text. A large version of this map is included as a plate in the pocket at the back of the volume.

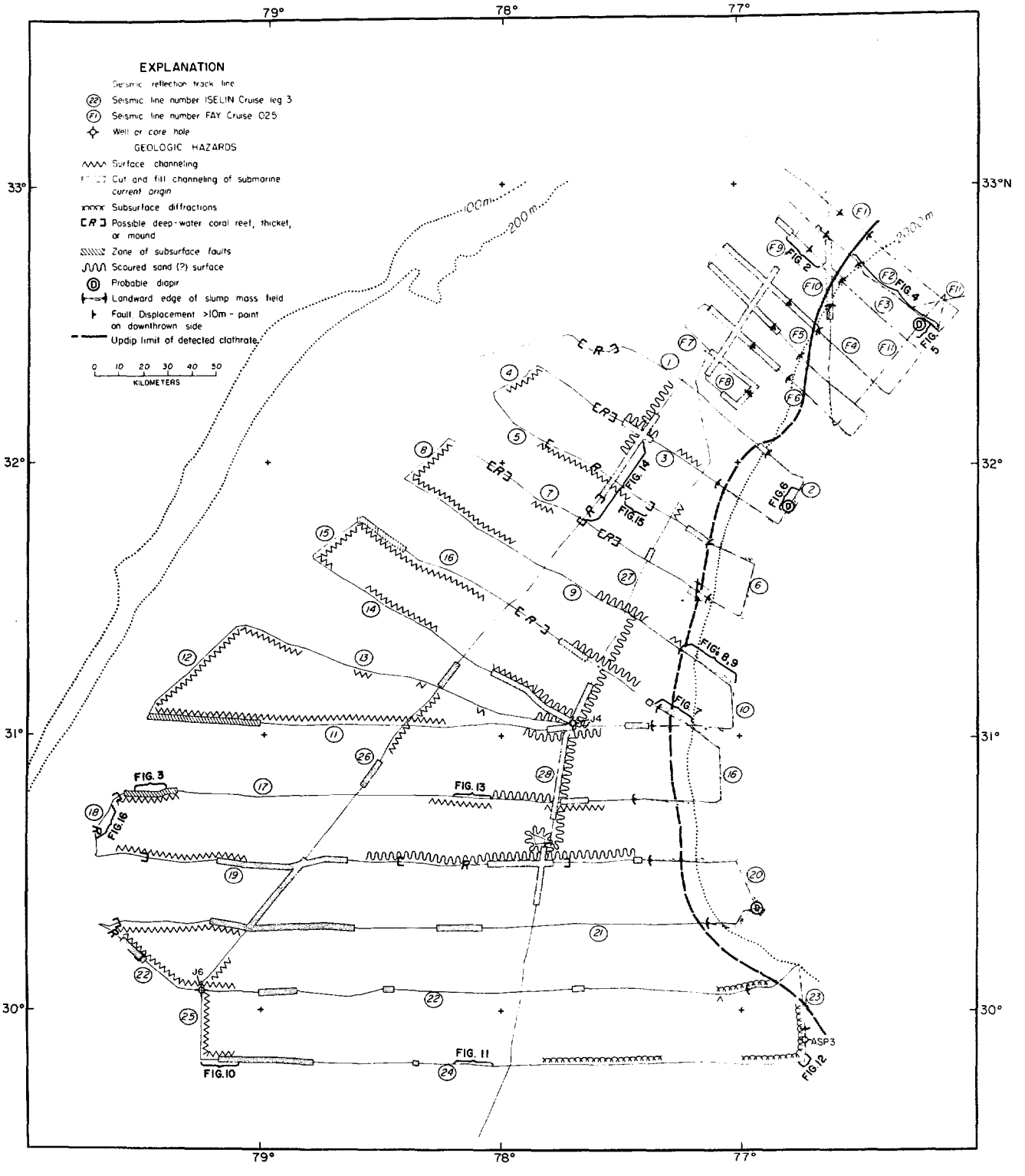
EXPLANATION
Seismic reflection track line
Seismic line number ISELIN Cruise leg 3
Seismic line number FAY Cruise 025
Well or core hole
GEOLOGIC HAZARDS
Surface channeling
Cut and fill channeling of submarine current origin
Subsurface diffractions
Possible deep-water coral reef, thicket, or mound
Zone of subsurface faults
Scoured sand (?) surface
Probable diapir
Landward edge of slump mass field
Fault Displacement >10m - point on downthrown side
Updip limit of detected clathrate
0 10 20 30 40 50
KILOMETERS
79°
78°
77°
33°
33°N
32°
31°
30°
100m
200m
2000m
FIG. 2
FIG. 4
FIG. 5
FIG. 6
FIG. 7
FIG. 8,9
FIG. 10
FIG. 11
FIG. 12
FIG. 13
FIG. 14
FIG. 15
FIG. 16
FIG. 3
J4
J6
ASP3

the Blake Plateau using FAY 025 seismic data. The fault which was identified reliably on four dip lines (F3, F4, F5, F6) extends north-northeast to south-southwest for over 50 km along the plateau (fig. 8-1) and appears in the seismic profiles as a narrow, steeply dipping zone of disrupted and offset reflectors (fig. 8-2). No displacement of the seafloor was noted on any seismic crossing of this fault, however, high-resolution data indicates a displacement of about 1 m at 10 m depth along several crossings, and common-depth-point deep seismic data (Sylwester and others, 1979) indicate that displacement of beds across the fault increases with depth to at least 200 and possibly 400 m at 4 km. The fault, which is the largest to displace Tertiary sediments on the Atlantic coast is believed to result from subsidence caused by the removal of salt during diapirism (Sylwester and others, 1979).

Along the eastern portions of ISELIN line 7 (fig. 8-1), a high-angle fault has severed Paleocene and older reflectors. This fault is described as a gravity fault by Dillon and Paull (1978) on common-depth-point line FC-7. Short transects to either side of the main trackline indicate the fault trends essentially north-south and has a minimum length of 8 km. The reflector configuration near the inferred fault indicates that the eastern block has been downthrown relative to the western block. A thin blanket of undisturbed post-Oligocene sediment covers the fault, attesting to the absence of fault activity during the recent past.

Complex zones of numerous subsurface faults disrupt Upper Cretaceous beds along the inshore portions of dip lines 11, 16, and 17 (figs. 8-1, 8-3). The best expression of the faults on the seismic records occurs in areas where Upper Cretaceous units subcrop at the

Figure 8-2. Picture of seismic record showing growth fault on dip line F-3. Note that no displacement occurs at the sediment surface. The magnitude of displacement increases with depth with displacement of 1 m at the 10 m depth increasing to possibly 400 m at the 4 km depth. Depths shown on profile are based on the velocity of sound through water.

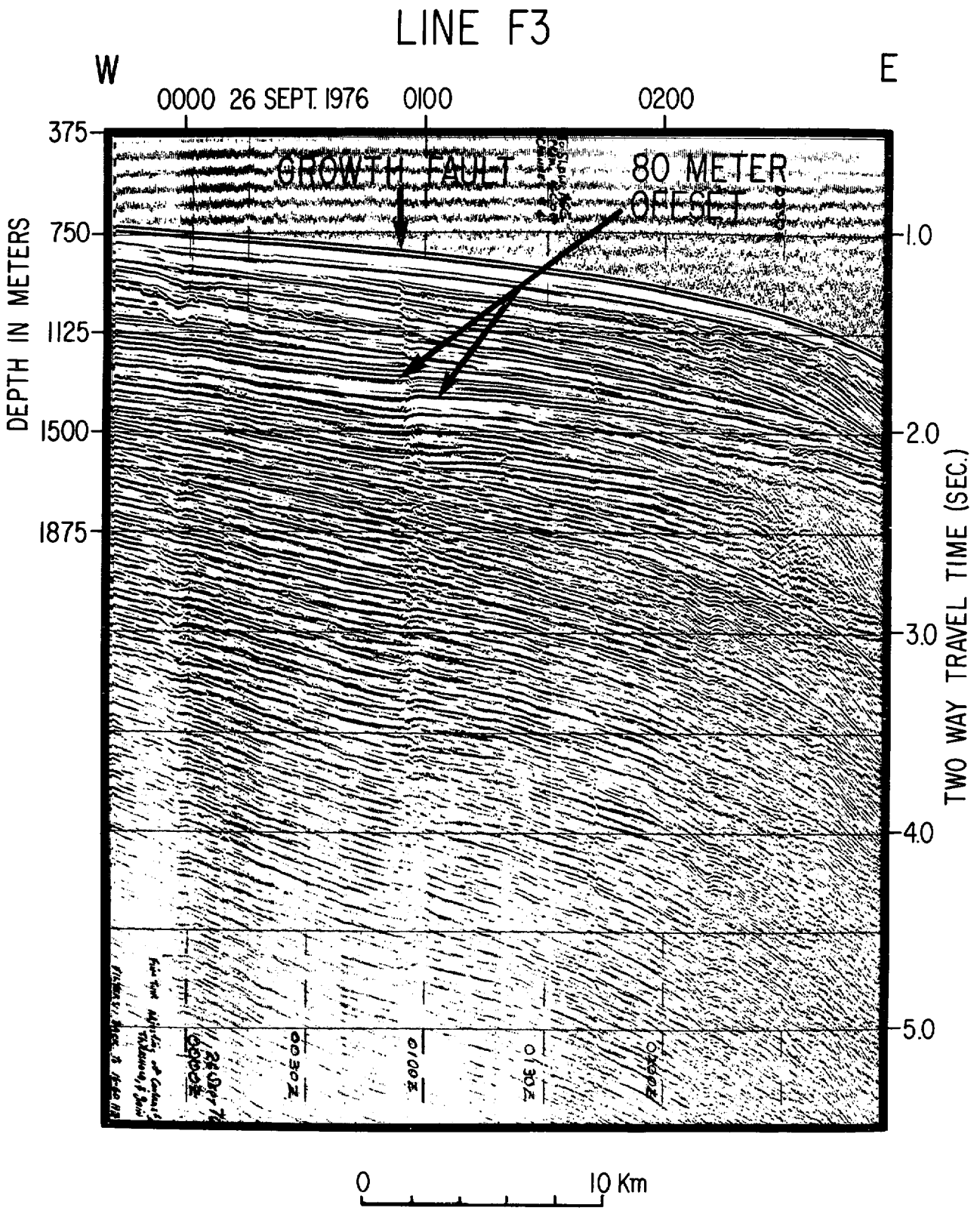
LINE F3
W
E
0000 26 SEPT. 1976
0100
0200
GROWTH FAULT
80 METER
OFFSET
DEPTH IN METERS
375
750
1125
1500
1875
TWO WAY TRAVEL TIME (SEC.)
1.0
2.0
3.0
4.0
5.0
0
10 Km

Figure 8-3. Picture of seismic record from line 17 showing subsurface faults in rocks of Upper Cretaceous age. Paull and Dillon (1979) attribute these faults to postdepositional compaction. Depths shown on profile are based on the velocity of sound through water.

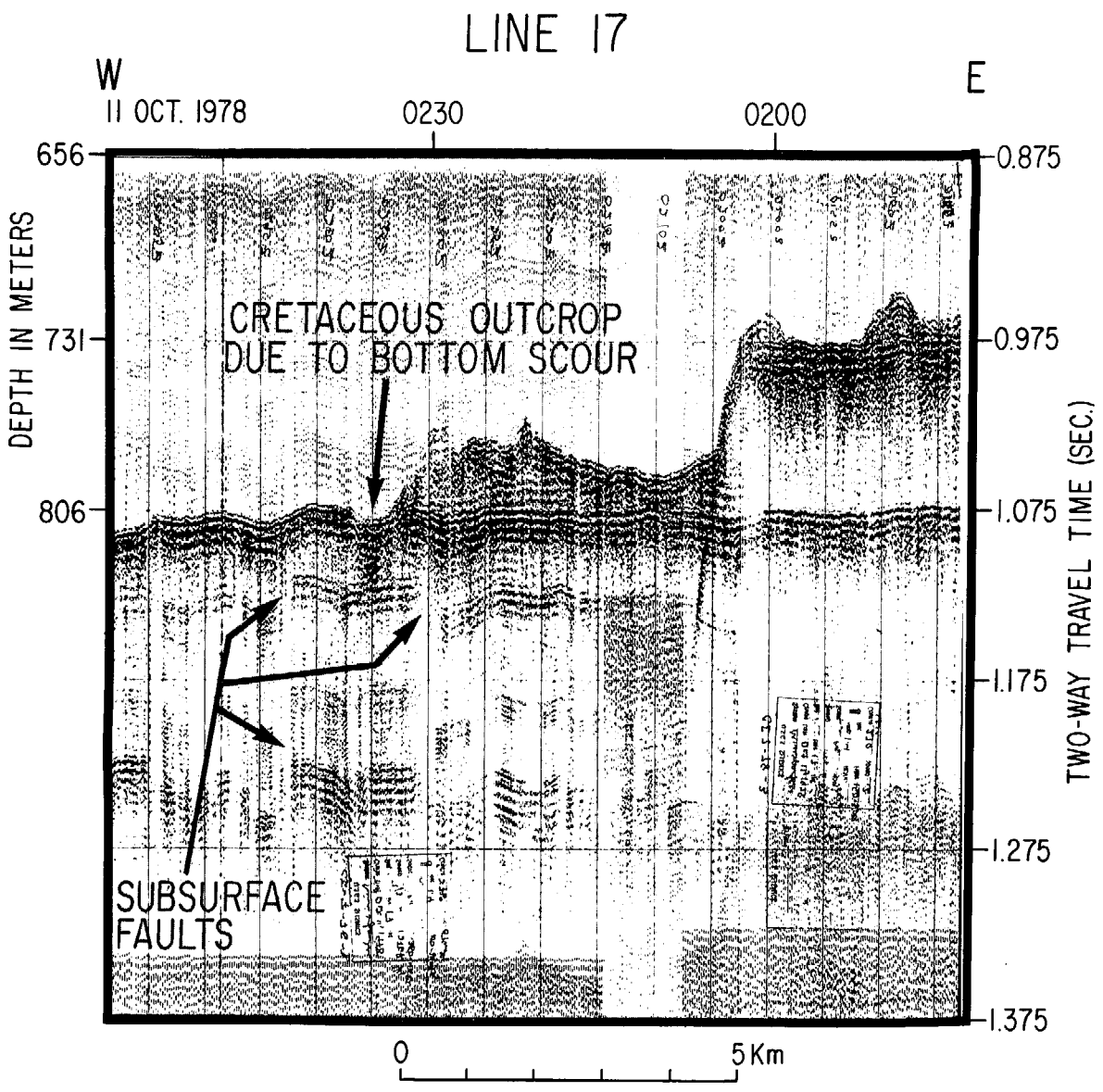
LINE 17
W
E
11 OCT. 1978
0230
0200
656
731
806
DEPTH IN METERS
0.875
0.975
1.075
1.175
1.275
1.375
TWO-WAY TRAVEL TIME (SEC.)
CRETACEOUS OUTCROP
DUE TO BOTTOM SCOUR
SUBSURFACE
FAULTS
0
5 Km

Figure 8-3

bottom of large channels eroded by the Gulf Stream. The faults within these zones are numerous, but small. For example, a conservative estimate indicates that 19 individual faults are clustered along a 15-km stretch of profile 17; many more undoubtedly are present. Maximum observable offset is estimated at 20 m. Line spacing did not permit determination of fault orientation. Paull and Dillon (1979) first noted clusters of small faults in Upper Cretaceous sediments of the inner Blake Plateau and attributed them to the effect of postdepositional compaction.

Clathrates and Accompanying Trapped Gas

A bottom simulating, seismic reflector believed to arise from the impedence contrast between the lower boundary of a frozen gas hydrate layer in the shallow subsurface (clathrate) and unfrozen sediment has been described as occurring beneath the slope and upper rise on the eastern edge of the Blake Plateau (Shipley and others, 1979; Dillon and others, 1980; Paull and Dillon, 1980). Gas hydrates can form and be stable in the marine environment at temperatures of up to 27°C if pressures are sufficiently high (Tucholke and others, 1977). The gas hydrate or clathrate is an icelike crystalline lattice of water molecules in which gas molecules become trapped. On the Blake Outer Ridge and on the upper rise in the area of our data, the lower phase boundary of the clathrate generally occurs about 0.4 to 0.6 seconds subbottom where the gas hydrate becomes unstable due to the geothermal gradient. This boundary will follow a pressure temperature surface, thus it may be recognized easily on some seismic records where it cuts across reflections arising from bedding planes or stratigraphic units (figs. 8-4, 8-5), but is less recognized where it parallels the bedding. Generally bedding reflections within the clathrate layer may be subdued

Figure 8-4. Line drawing of a portion of FAY 025 line 2 showing the location and expression of the bottom simulating reflector marked C on the drawing. This reflector is believed to mark the bottom of a clathrate horizon in the shallow subsurface which may trap shallow gas. Beneath the arrow marking the cross line FAY 025 line 11 is the diapir shown in figure 8-5. Also shown near the arrow marking FAY 025 line 10 is the extension of the growth fault shown on figure 8-2. The strong subhorizontal reflectors shown at about 3.0 s depth on the west end of the profile mark the Lower Cretaceous shelf edge.

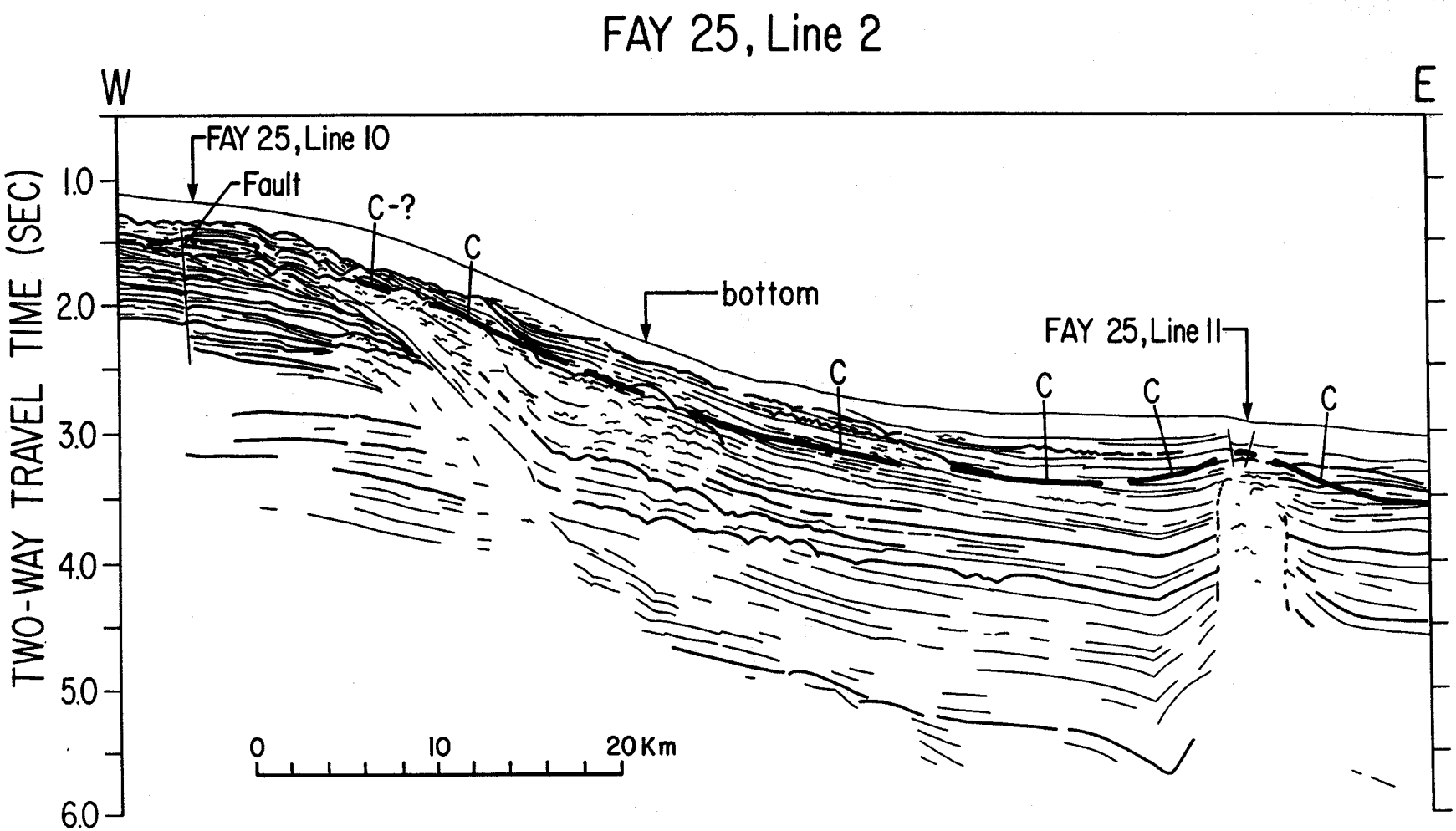
FAY 25, Line 2
W
E
FAY 25, Line 10
Fault
C-?
C
bottom
FAY 25, Line 11
C
C
C
C
TWO-WAY TRAVEL TIME (SEC)
1.0
2.0
3.0
4.0
5.0
6.0
0
10
20 Km

Figure 8-4

Figure 8-5. Picture of seismic record showing a well-developed diapir with associated trapped gas beneath the clathrate layer on tie line F11. The clathrate is evident as a strong reflector crosscutting bedding planes. Depths shown on profile are based on the velocity of sound through water.

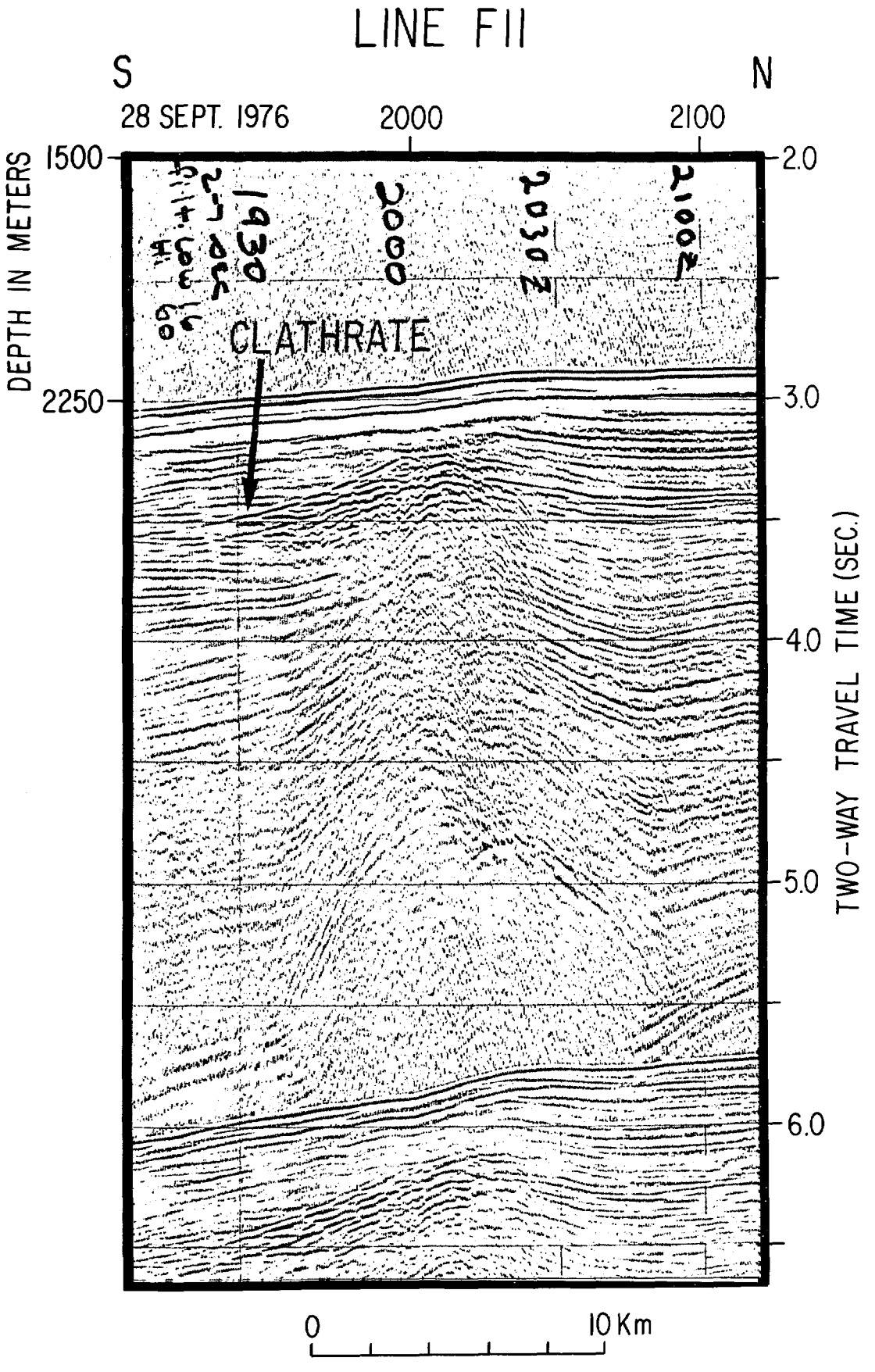
LINE F11
S
N
28 SEPT. 1976
2000
2100
1500
2250
DEPTH IN METERS
2.0
3.0
4.0
5.0
6.0
TWO-WAY TRAVEL TIME (SEC.)
1930
2000
2030
2100
CLATHRATE
0
10 Km

relative to the stronger reflections of subclathrate horizons, which may contain gas saturated water or free gas. The presence of the gas-hydrate layer is most easily seen where it terminates "bright spots" or amplitude anomalies (Savit, 1974) caused by gas-water, gas-oil, or oil-water contacts within the sedimentary section.

The gas-hydrate boundary is the most obvious in seismic reflection data that has been processed with automatic gain control (AGC) to approximately true amplitude. This is not possible for most single-channel seismic records that are not digitally recorded. Amplitude records can be approximated on single-channel seismic-reflection records by delaying or slowing down the AGC, however, in this process a certain amount of the shallow data is lost and this is normally not done unless clathrates are the specific target of the investigation. As the boundary occurs at greater than 0.5 seconds subbottom, the amplitude of seismic signal (air-gun size) is also an important factor in producing records where clathrates can be recognized. Strong clathrate layers are clearly visible on reflection data obtained from the FAY 025 (fig. 8-4) and GILLISS 5 cruises where large air guns and a delayed AGC were used, and are less obvious in the seismic data from the ISELIN, leg 3 cruise where smaller air guns and normal AGC were used. Because of the widespread distribution of the clathrate layer recognized in the FAY 025, FAY 019, and GILLISS 5 data (Dillon and others, 1980; Paull and Dillon, 1980) in water depths ranging from about 800 m to over 3,000 m on the Blake Escarpment and continental rise, clathrates should be expected in any drilling in these water depths even though clathrates were not specifically recognized in the ISELIN 3 data.

Drilling into clathrates should not pose a threat to operations

unless shallow gas is trapped beneath the frozen layer (methane, ethane, carbon dioxide, hydrogen sulfide, etc.). The penetration of shallow gas pockets beneath permafrost off Mackenzie Delta, Alaska has led to the loss of several drill rigs (Peter Day, Phillips Petroleum Company, personal communication, 1980) and this danger probably also exists associated with gas trapped beneath clathrates. Very little is known of the hazards associated with clathrates because these layers occur in water depths that are at the frontier of exploration or production technology at the present time. As exploration proceeds into greater water depths, shallow gas trapped beneath clathrates may prove to be a primary hazard.

Diapirs

Two well developed diapirs (figs. 8-5, 8-6) believed to originate from a Jurassic salt layer at depth (Grow and others, 1979) and one less developed diapir were detected beneath the continental rise east of the Blake Escarpment. Although diapirs are not considered a hazard to petroleum exploration, indeed they are a primary exploration target, their association with shallow gas trapped beneath the clathrate layer may pose a threat to exploration (fig. 8-6). Well developed diapirs that uplift the seafloor were crossed at the north end of line F11 (figs. 8-1, 8-5), and near the center of ISELIN line 2 (fig. 8-6). A possible diapir occurs along the southern end of line 20. In seismic section the features have a body diameter of 4 to 6 km, although the true three-dimensional geometry is indeterminate with a single line crossing.

Slump Masses

Slumps or slides are not evident over the Blake Plateau proper except along its eastern edge near the Blake Escarpment where bottom

Figure 8-6. Picture of seismic record from line 2 showing a diapir located at the base of the Blake Escarpment. Step in record is a scale change. Note that the diapir slightly uplifts the seafloor. Near the left margin of the profile the deeper reflectors define a subsidence moat around the feature which is typical of diapirs.

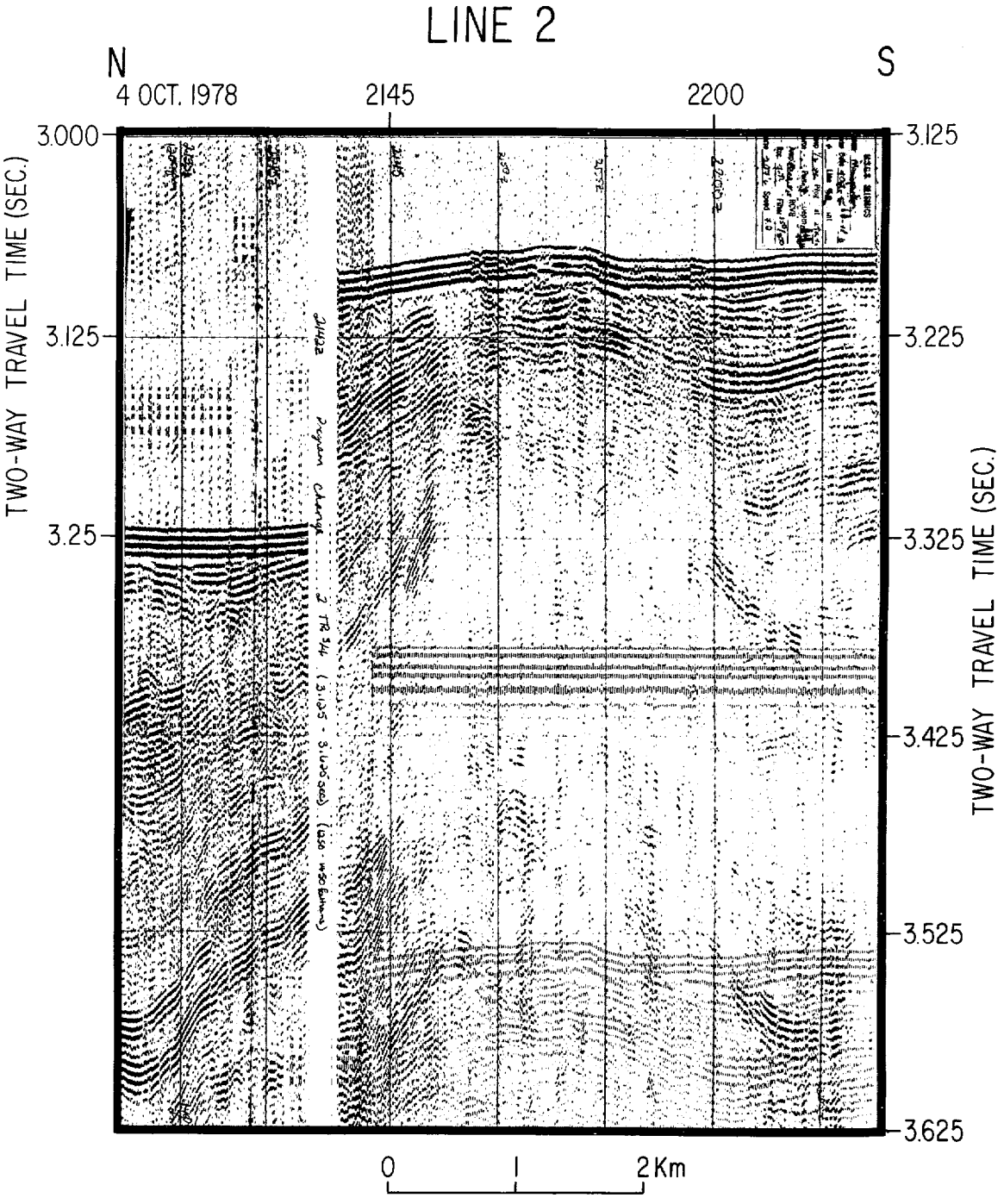
LINE 2
N
S
4 OCT. 1978
2145
2200
3.000
3.125
3.25
3.125
3.225
3.325
3.425
3.525
3.625
TWO-WAY TRAVEL TIME (SEC.)
TWO-WAY TRAVEL TIME (SEC.)
0
1
2 Km

slopes become precipitous. Although interpretations are difficult and in some cases impossible, because of the steep declivity of the escarpment and limited acoustical penetration, discrete seismic intervals display reflector configurations that can be construed as originating by slumping. Our interpretations of seismic units as slumps are liberal by intent, and many slump masses plotted on the hazards map (fig. 8-1) may turn out not to be so when more detailed information is available for analysis. We justify our liberal interpretations on the basis of slope instability known to be associated with the steep bottom gradients that typify the Blake Escarpment.

An accurate assessment of submarine slides requires knowledge about the three-dimensional geometry of the bodies. As this was not possible because of the broad line spacing, we relied on indirect evidence of former slump activity, including topography, a chaotic or a jumbled reflector pattern (figs. 8-7, 8-8, 8-9), and outcropping of older rocks not mantled by recent sedimentary accumulations.

Along most tracklines, the landward limit of inferred slump-mass fields coincides with a distinct break in bottom slope (figs. 8-7, 8-8, 8-9) that marks the top of the Blake Escarpment. Seismic units in this region display chaotic reflectors that suggest sliding. Some of these disturbed masses are surface blocks while others are subsurface, having been buried by younger sedimentary deposits following emplacement by slumping (figs. 8-7, 8-8). Also, Tertiary and Cretaceous units outcrop at the escarpment, suggesting that younger sedimentary units have slid downslope to greater depths. It was not possible to delineate the seaward limit of the slump fields along the survey lines, because of limited acoustical penetration and poor resolution and definition of reflectors over the steep escarpment.

Figure 8-7. Picture of seismic profile showing inferred slump mass on line 16. Note the disturbed bottom at the bend of the slope in the area marked creep and the chaotic reflectors within the sediments. A second slump fault has dimpled the bottom just below the scale changes at 0200. The surface slump appears to have covered over several additional slump scars at depth.

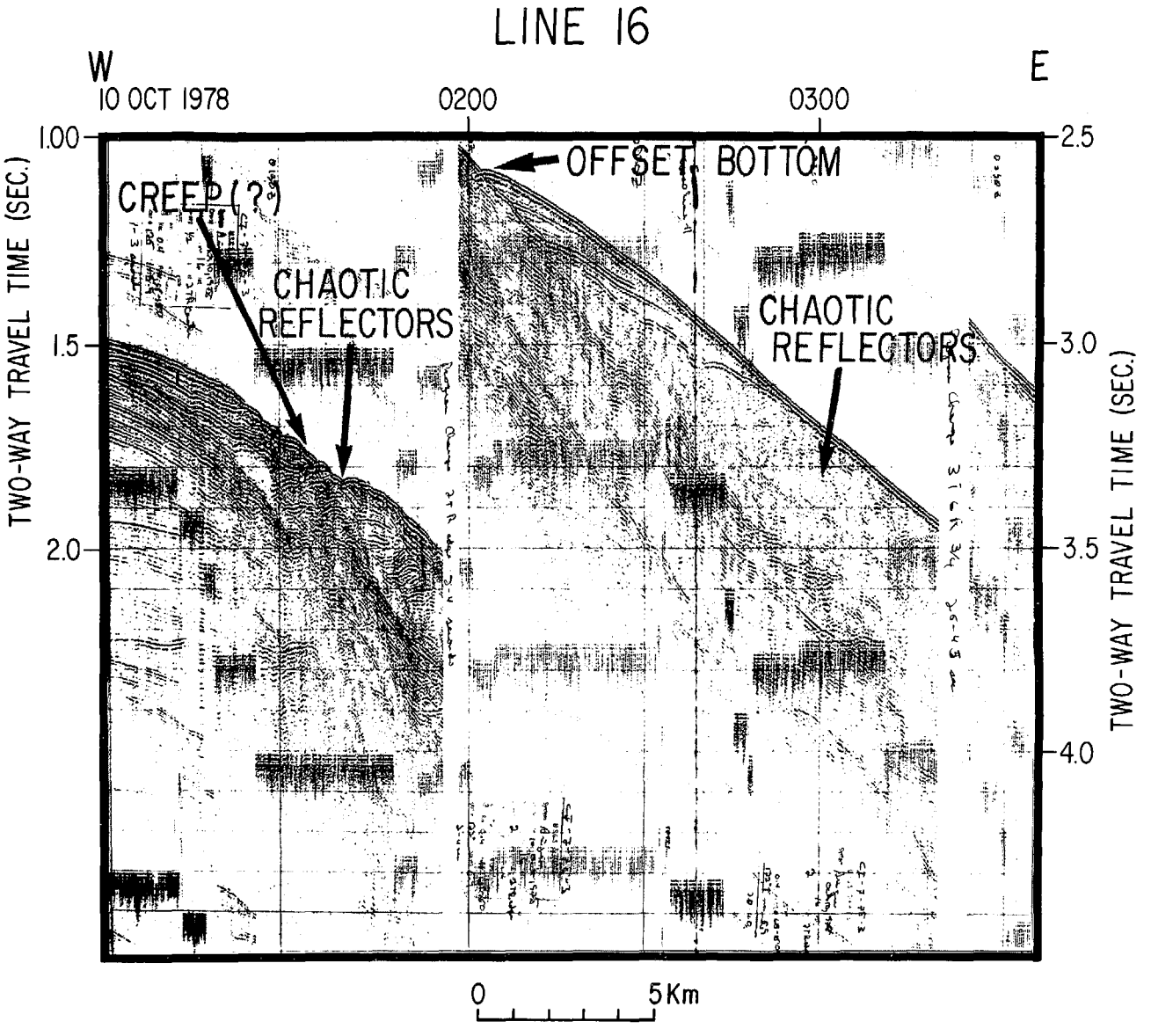
LINE 16
W
E
10 OCT 1978
0200
0300
1.00
1.5
2.0
2.5
3.0
3.5
4.0
TWO-WAY TRAVEL TIME (SEC.)
TWO-WAY TRAVEL TIME (SEC.)
CREEP (?)
CHAOTIC REFLECTORS
OFFSET BOTTOM
CHAOTIC REFLECTORS
0
5 Km

Figure 8-7

Figure 8-8. Picture of seismic profile showing an inferred slump mass on Blake Escarpment from line 9. Note the dimpled bottom at the head of the slump feature and the chaotic beds below the bottom near the center of the picture. The termination of horizontal reflectors below the dimpled bottom on the west side of the picture suggests that the dimpled bottom may also reflect a high-angle normal fault at depth.

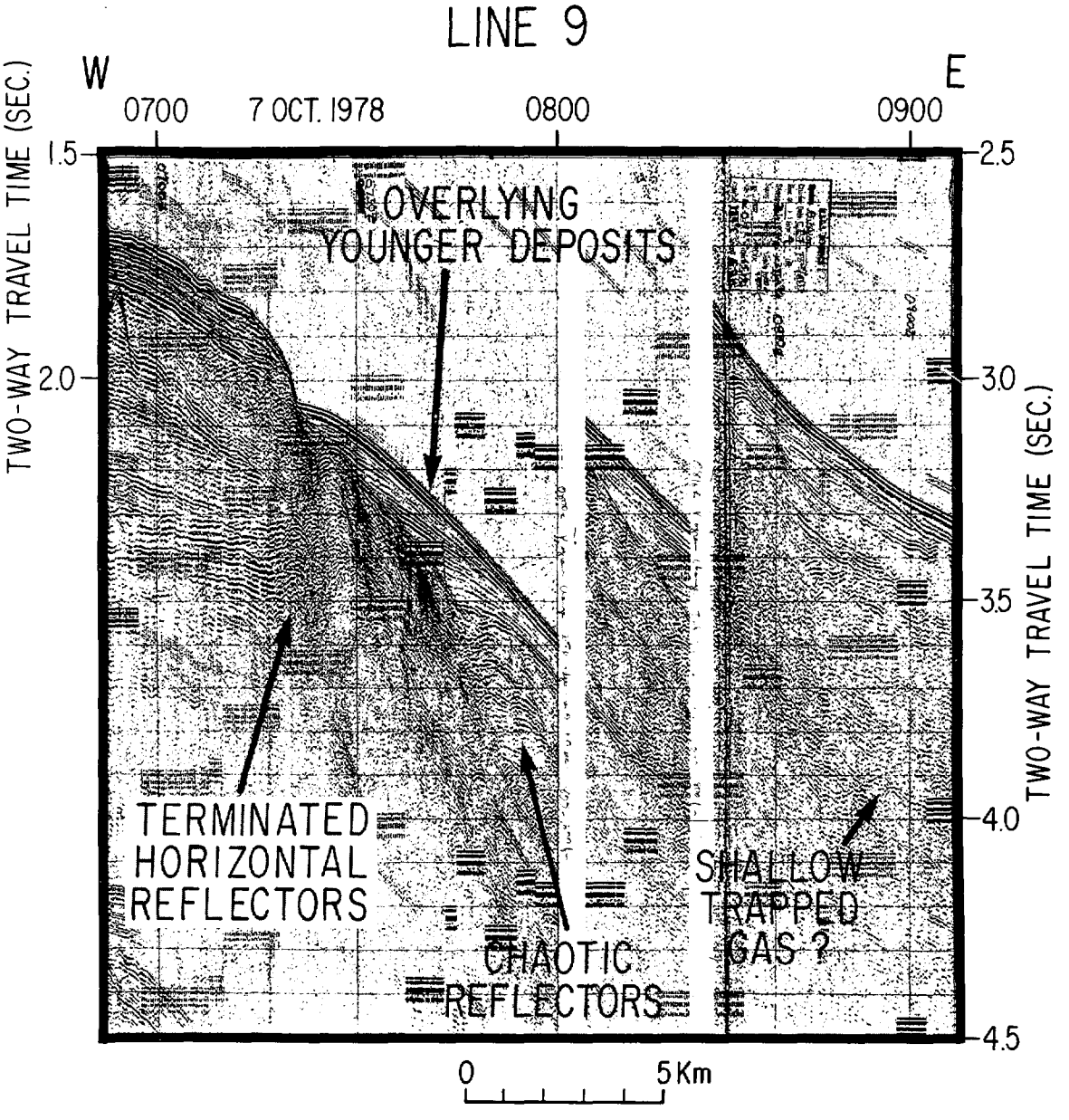
LINE 9
W
E
0700
7 OCT. 1978
0800
0900
TWO-WAY TRAVEL TIME (SEC.)
1.5
2.0
2.5
3.0
3.5
4.0
4.5
OVERLYING
YOUNGER DEPOSITS
TERMINATED
HORIZONTAL
REFLECTORS
CHAOTIC
REFLECTORS
SHALLOW
TRAPPED
GAS ?
0
5 Km

Figure 8-9. Picture of seismic profile showing the inferred slump mass of figure 8-8 without scale changes but with less detail. The linear blotches covering the record are cross-talk between the sparker and air-gun systems. Cross-talk is caused by differing firing rates of the two systems and is unavoidable if the two systems are operated simultaneously. The sparker fires every one to two seconds and the air gun every 10 seconds. Therefore, there are 5 to 10 sparker firings which are picked up during each sweep of the air-gun record. The steps in the cross-talk are phase changes in the firing rate manually done by the operator to avoid obliterating the record in one spot for any period of time.

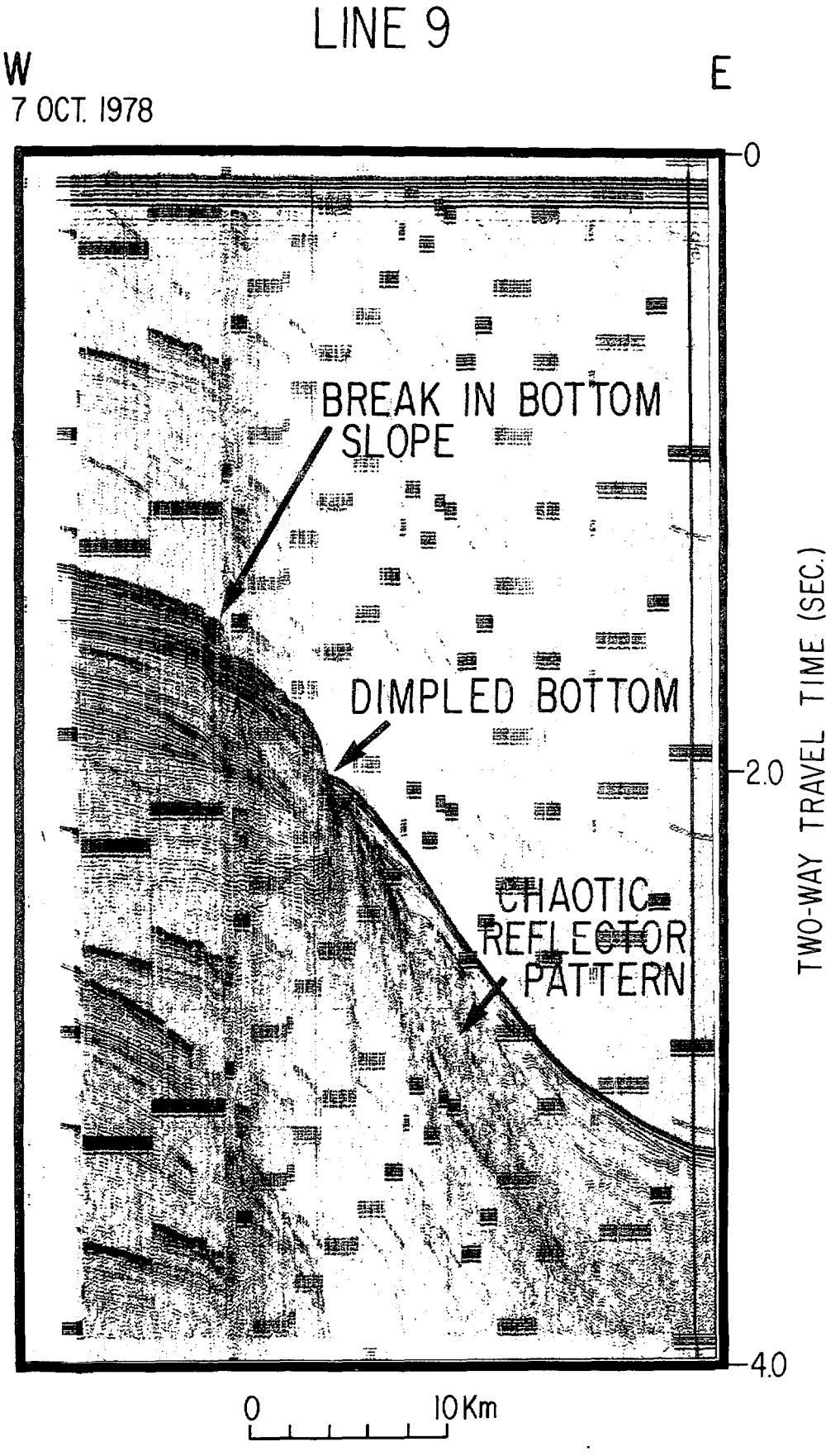
LINE 9
W
E
7 OCT. 1978
0
2.0
4.0
TWO-WAY TRAVEL TIME (SEC.)
BREAK IN BOTTOM SLOPE
DIMPLED BOTTOM
CHAOTIC REFLECTOR PATTERN
0
10 Km

STRATIGRAPHIC FEATURES

Cut-and-Fill Structures

Cut-and-fill, as the term denotes, is produced by the infilling of channels that have been incised into an erosional surface (fig. 8-10). Conspicuous cut-and-fill structures are associated with a regional Paleocene unconformity that is the most distinctive reflector surface within the Cenozoic section of the Blake Plateau. At the northern end of the survey area, this erosion surface is typically smooth but undulating and is covered by post-Oligocene sediments. In contrast, the nature of the Paleocene unconformity to the south consists of rugged, deeply eroded topography buried by Eocene-Oligocene deposits. Intense erosion locally has extended the bottom of a few channels downward into Upper Cretaceous strata. Lithological information obtained at drill site J4 (Charm and others, 1969; Schlee, 1977) indicates a major compositional and, hence, velocity-density contrast across the unconformity, Paleocene limestones and clays underlying Eocene-Oligocene carbonate ooze and sand. Based on channel dimensions and morphology that are similar to those of the present-day surface of the inner Blake Plateau (Pratt and Heezen, 1964; Uchupi and Emery, 1967), the irregular topography of the Paleocene unconformity is attributed to scouring by the ancient counterpart of the Gulf Stream. Supporting evidence and details regarding this interpretation are discussed in chapter 7 of this volume.

Cavernous Limestone

Differential solution of carbonate rock can produce caverns that can adversely affect drilling because of potential losses of circulating mud or drill strings (McCarthy and others, 1980). Solution features in

Figure 8-10. Picture of seismic profile showing cut-and-fill structures on line 24. Depths shown on profile are based on the velocity of sound through water.

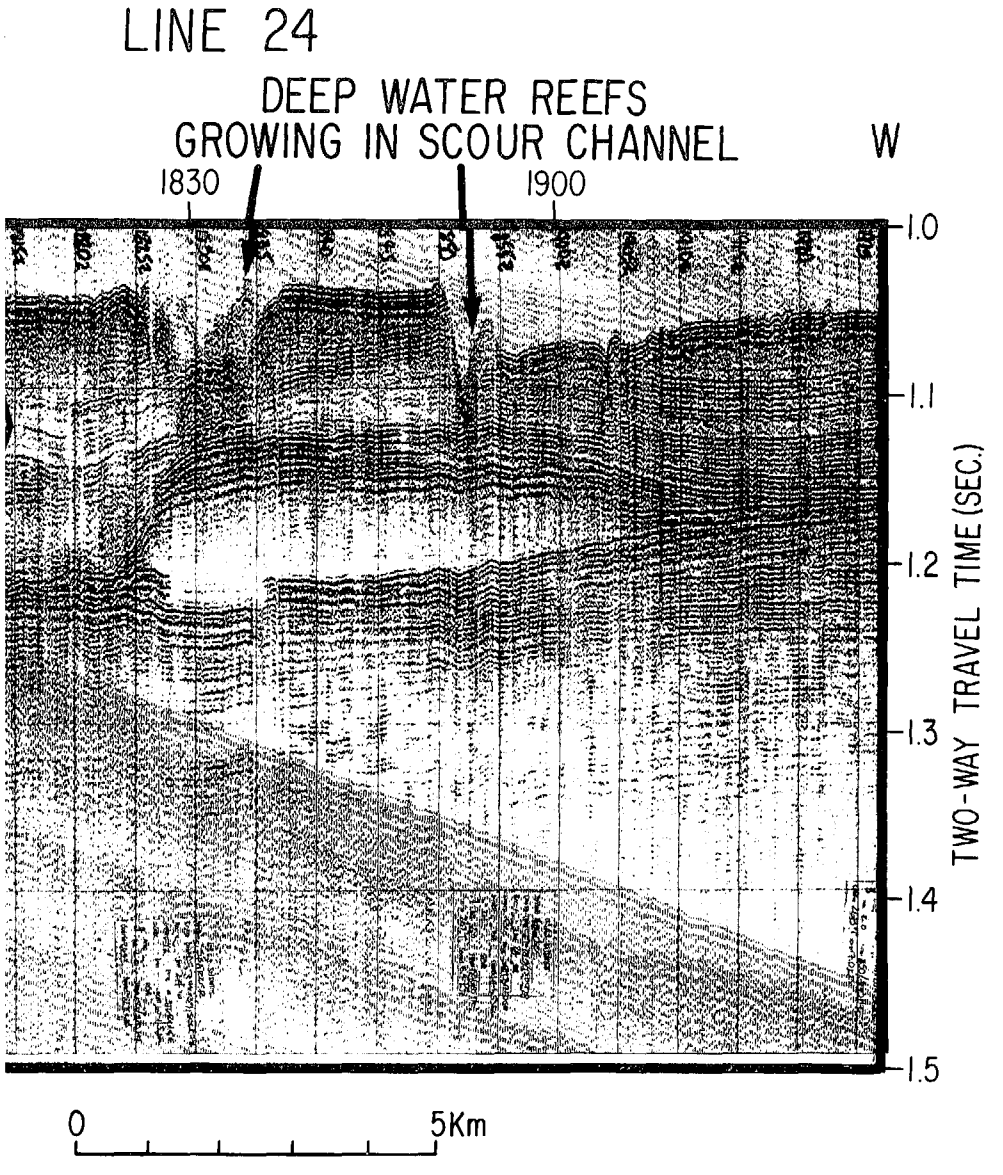
LINE 24
DEEP WATER REEFS
GROWING IN SCOUR CHANNEL
W
1830
1900
1.0
1.1
1.2
1.3
1.4
1.5
TWO-WAY TRAVEL TIME (SEC.)
0
5Km

Figure 8-10

limestone are common in coastal plain sediments and continental margin deposits of the southeastern United States. For example, the Ocala Group of Eocene age in southeastern Georgia and Florida is partly cavernous (Herrick and Vorhis, 1963), as well as a carbonate sequence penetrated in several wells that adjoin the South Atlantic Outer Continental Shelf (OCS) Lease Sale 43 (Dillon and others, 1975). Extensive cavernous porosities were encountered in Cretaceous carbonates in the Bahamas on Andros Island well (Meyerhoff and Hatten, 1974). Finally, karst topography marks the Miami Terrace of the Florida Straits (Jordan, 1954; Malloy and Hurley, 1970; Mullins and Newman, 1979). Hence, it is not unreasonable to suspect that limestones farther offshore beneath the Blake Plateau also may be interlaced with large solution features.

A widespread seismic unit that is bounded above and below by regional unconformities displays numerous strong, continuous reflectors having a parallel, even-to-wavy configuration (figs. 8-1, 8-11). Drill data at well J4, J6, and ASP 3 establish that the unit consists dominantly of Paleocene limestones (Charm and others, 1969; Schlee, 1977). At the southeast corner of the survey area along the eastern ends of dip lines 22 and 24 (figs. 8-1, 8-12) the Paleocene interval is thin and displays a peculiar, but distinctive reflector pattern. Internal reflectors here are not parallel and continuous as elsewhere, but consist of a complex arrangement of overlapping hyperbolas that have strong definition on the seismic profiles. Although problematical, the reflector configuration tentatively is interpreted as arising from large solution features within the limestones. A somewhat similar, but not as prominent, reflector pattern characterizes Eocene-Oligocene deposits along the eastern half of dip line 24 that likewise may be related to

Figure 8-11. Picture of seismic record showing the Paleocene limestone unit characterized by wavy reflectors, tentatively interpreted as cavernous limestone. Depths shown on profile are based on the velocity of sound through water.

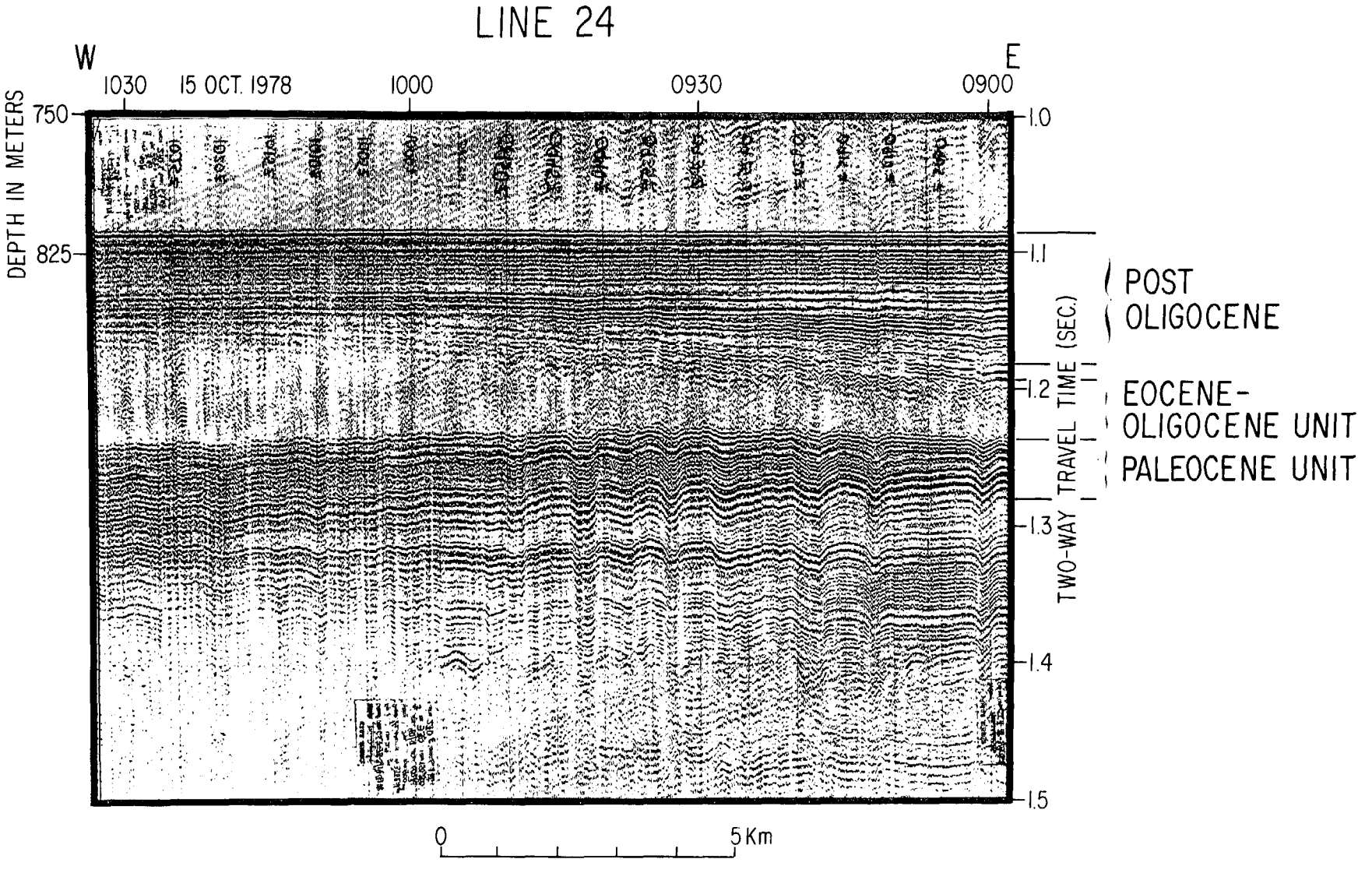
LINE 24
W
E
1030
15 OCT. 1978
1000
0930
0900
DEPTH IN METERS
750
825
1.0
1.1
1.2
1.3
1.4
1.5
TWO-WAY TRAVEL TIME (SEC.)
POST OLIGOCENE
EOCENE-OLIGOCENE UNIT
PALEOCENE UNIT
0
5 Km

Figure 8-11

Figure 8-12. Picture of seismic record showing the overlapping hyperbolas characteristic of Paleocene unit on eastern end of line 24. Depths shown on profile are based on the velocity of sound through water.

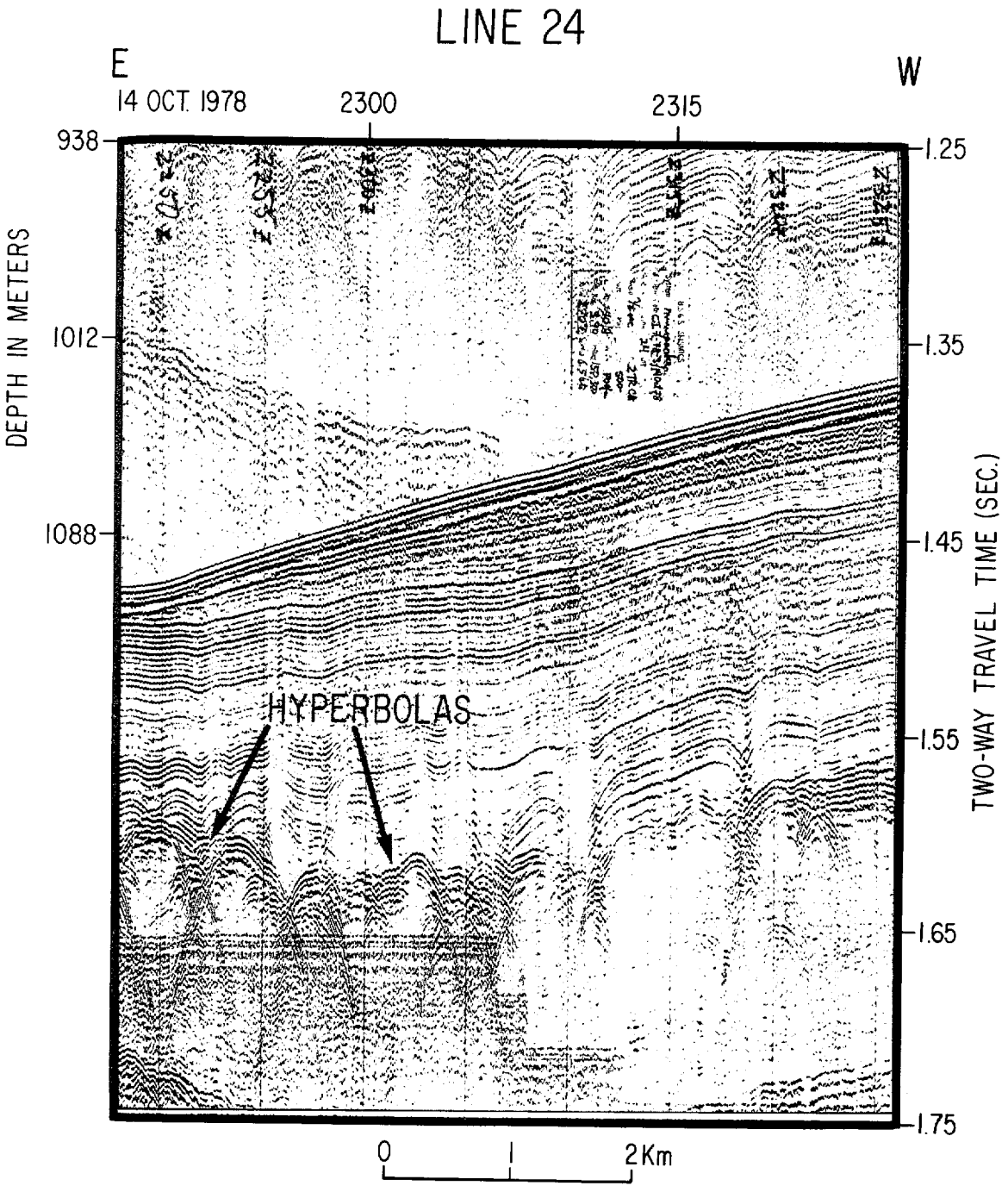
LINE 24
E
W
14 OCT. 1978
2300
2315
938
1012
1088
DEPTH IN METERS
1.25
1.35
1.45
1.55
1.65
1.75
TWO-WAY TRAVEL TIME (SEC.)
HYPERBOLAS
0
1
2 Km

reflections from solution cavities that permeate carbonate rocks.

GULF STREAM-GENERATED FEATURES

The persistent northerly flow of the Gulf Stream across the Blake Plateau is vigorous and has been instrumental in shaping the surface character of the plateau in addition to controlling the late Tertiary and Quaternary position of the Florida-Hatteras Continental Slope (Emery and Zarudski, 1967). Although surface velocities in the Gulf Stream can exceed 250 $cm.s^{-1}$, bottom velocities are weaker, but still capable of scour as determined by current-meter measurements (Pratt, 1966). The nature and disposition of sediment, the ubiquity of manganese pavement, and the erosional topography of the Blake Plateau indicate clearly that the bottom has been and continues to be affected by strong current activity.

Surface Scour

Bottom scour prevails in two main areas of the Blake Plateau. Beginning at dip line 19, an irregular band of bottom scour can be traced northward for about 120 km to dip line 9 (figs. 8-1, 8-13). The width of the scour band generally is less than 30 km, except at its southern terminus where it broadens to 100 km. Bottom sediment at well J4 drilled within the scour band is composed of carbonate sand (Charm and others, 1969). The second region of scour is centered at the intersection of lines 3 and 26 and has a more modest extent, having a length of 30 km and a width of 15 km (fig. 8-1). The textural and compositional nature of the bottom sediment in this second scour zone is not known.

Figure 8-13. Picture of seismic record showing bottom scour, channeling, and cut-and-fill along line 17. Depths shown on profile are based on the velocity of sound through water.

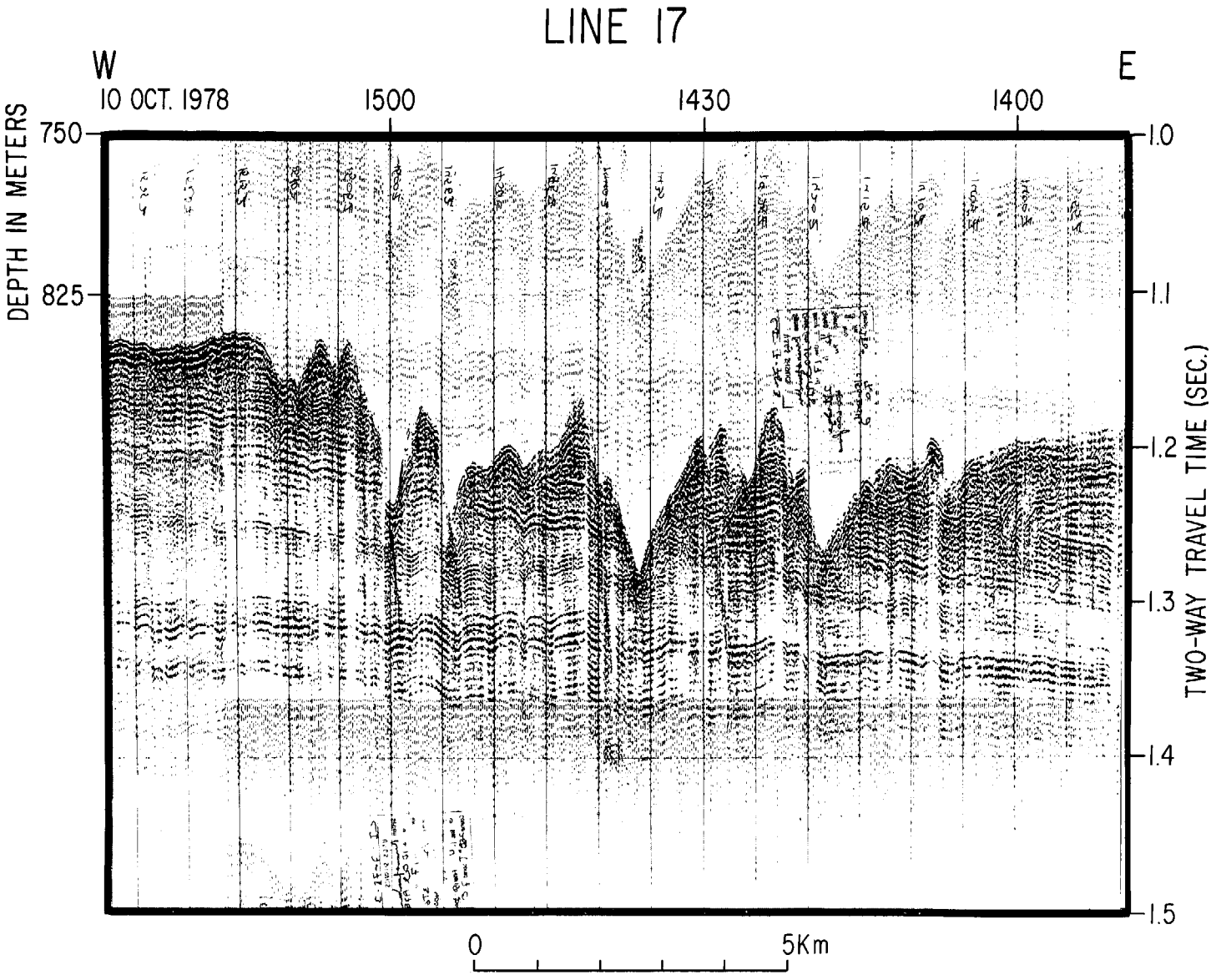
LINE 17
W
E
10 OCT. 1978
1500
1430
1400
DEPTH IN METERS
750
825
1.0
1.1
1.2
1.3
1.4
1.5
TWO-WAY TRAVEL TIME (SEC.)
0
5Km

Figure 8-13

Channeling

The bottom of the inner Blake Plateau is channeled to a much greater degree than elsewhere on the plateau (fig. 8-1). This zone of channeled topography lies beneath the main axis of the Gulf Stream and has been produced by the erosional activity of this powerful northerly flowing current, although probably most of this scouring occurred during lower stands of sea level. Considerable relief, sometimes exceeding 200 m, is evident. Narrow channels typically display a V-shaped bottom, broad channels flat bottoms. The latter result from the fact that erosion has exhumed a resistant horizon that has precluded deepening of the channel until such time when this hard layer of rock is penetrated (fig. 8-4). Scattered among the channels are hummocks that represent loci of carbonate buildup produced by thriving deepwater coral (fig. 8-14). These biogenic features are discussed in the following section. Channels occur elsewhere on the Blake Plateau (fig. 8-1), but they are isolated and less imposing than those along its western fringe.

BIOGENIC FEATURES

Irregular topography on the Blake Plateau is both erosional and depositional in character. The former is produced by the scouring action of strong bottom currents, whereas the latter reflects carbonate buildup by deepwater coral. Bottom photographs and dredge samples reveal that chiefly two species of branching coral produce the reef banks on the Blake Plateau: *Lophelia prolifera* and *Dendrophyllia profunda* (Stetson and others, 1962), although as many as 20 species may be present (Ayers and Pilkey, chapter 5 of this report). Individual reef masses are composed of two distinct facies: living coral organisms abound near the top of the bank, whereas flanks are covered by coral

Figure 8-14. Picture of seismic record showing the Charleston Valley, a prominent scoured channel along line 26. The pinnacles on the plateau are reflections from deepwater coral reefs. Reefs are particularly abundant near scour channels and other features that cause turbulence in the currents. Depths shown on profile are based on the velocity of sound through water.

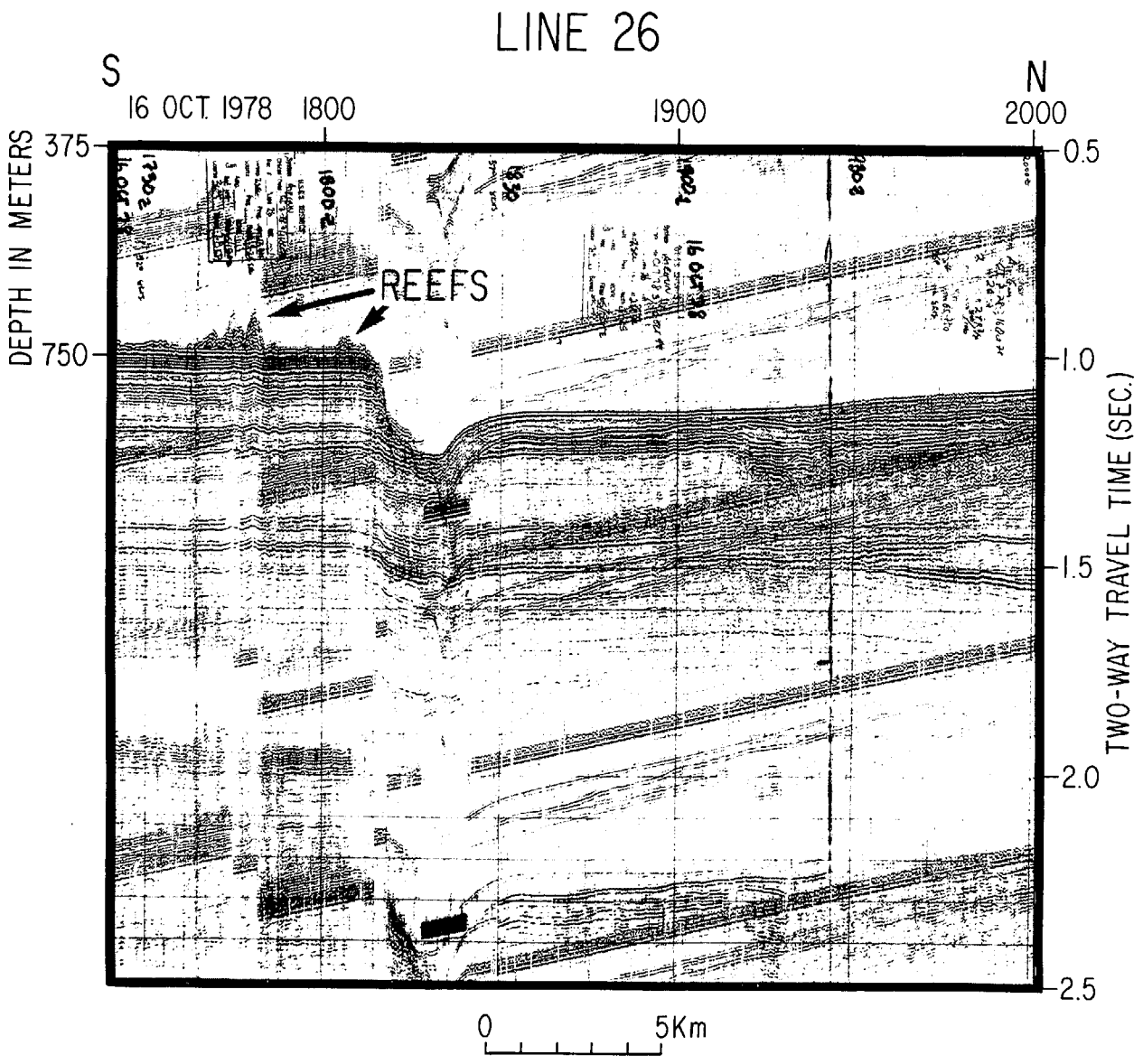
LINE 26
S
N
16 OCT. 1978
1800
1900
2000
DEPTH IN METERS
375
750
0.5
1.0
1.5
2.0
2.5
TWO-WAY TRAVEL TIME (SEC.)
REEFS
0
5Km

Figure 8-14

skeletal debris and mud (Stetson and others, 1962; Ayers and Pilkey, chapter 5 of this report).

Recognition of the coral banks on seismic records is based on their morphology and seismic signature. Typically they appear as prominent topographic highs that are sharp crested and that, in many cases, display secondary peaks. In profile view, they are either pinnaclelike (fig. 8-15) or moundlike (fig. 8-16) in appearance, the latter being much broader for a given height than the former. Topographic relief is quite variable, ranging from less than 10 m to over 100 m. Reflections from the coral banks are distinctive, consisting of numerous overlapping hyperbolas of different sizes that produce a chaotic pattern (figs. 8-15, 8-16). Reflectors within the sedimentary deposits that underlie the reef banks can be traced beneath the features with no evidence of "fade-outs" as reported by Stetson and others (1962).

There are three areas on the Blake Plateau where carbonate buildup is common (fig. 8-1). The main area is crossed by the middle and western ends of seismic lines 1, 3, 4, and 7. A second less expansive zone of reef mounds occurs in the southwest corner of the survey area along lines 18, 19, 21, and 22. Finally, the middle segment of dip line 19 displays a series of small corallike structures having a maximum relief of 25 m. These small features are not apparent on contiguous lines, indicating that they are of very limited extent.

CONCLUSIONS

Few features revealed by the high-resolution seismic-reflection survey with the exception of shallow gas trapped beneath the clathrate layer, represent real hazards to drilling on the Blake Plateau, because they are well within the experience, expertise, and design capability of

Figure 8-15. Picture of seismic record showing pinnaclelike coral banks found on line 5. Depths shown on profile are based on the velocity of sound through water.

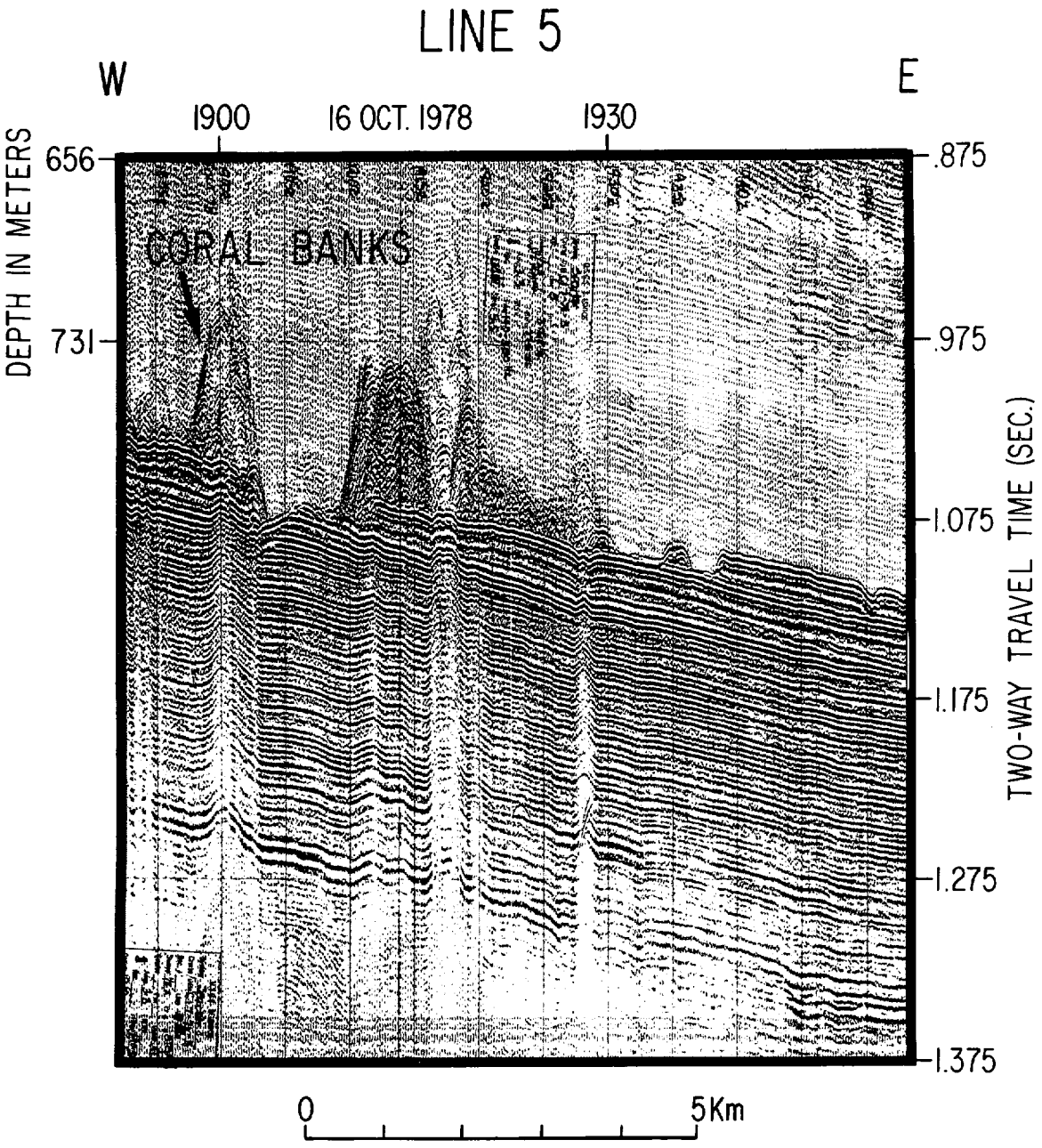
LINE 5
W
E
1900
16 OCT. 1978
1930
DEPTH IN METERS
656
731
CORAL BANKS
.875
.975
1.075
1.175
1.275
1.375
TWO-WAY TRAVEL TIME (SEC.)
0
5Km

Figure 8-16. Picture of seismic profile showing moundlike coral reefs on line 18. Depths shown on profile are based on the velocity of sound through water.

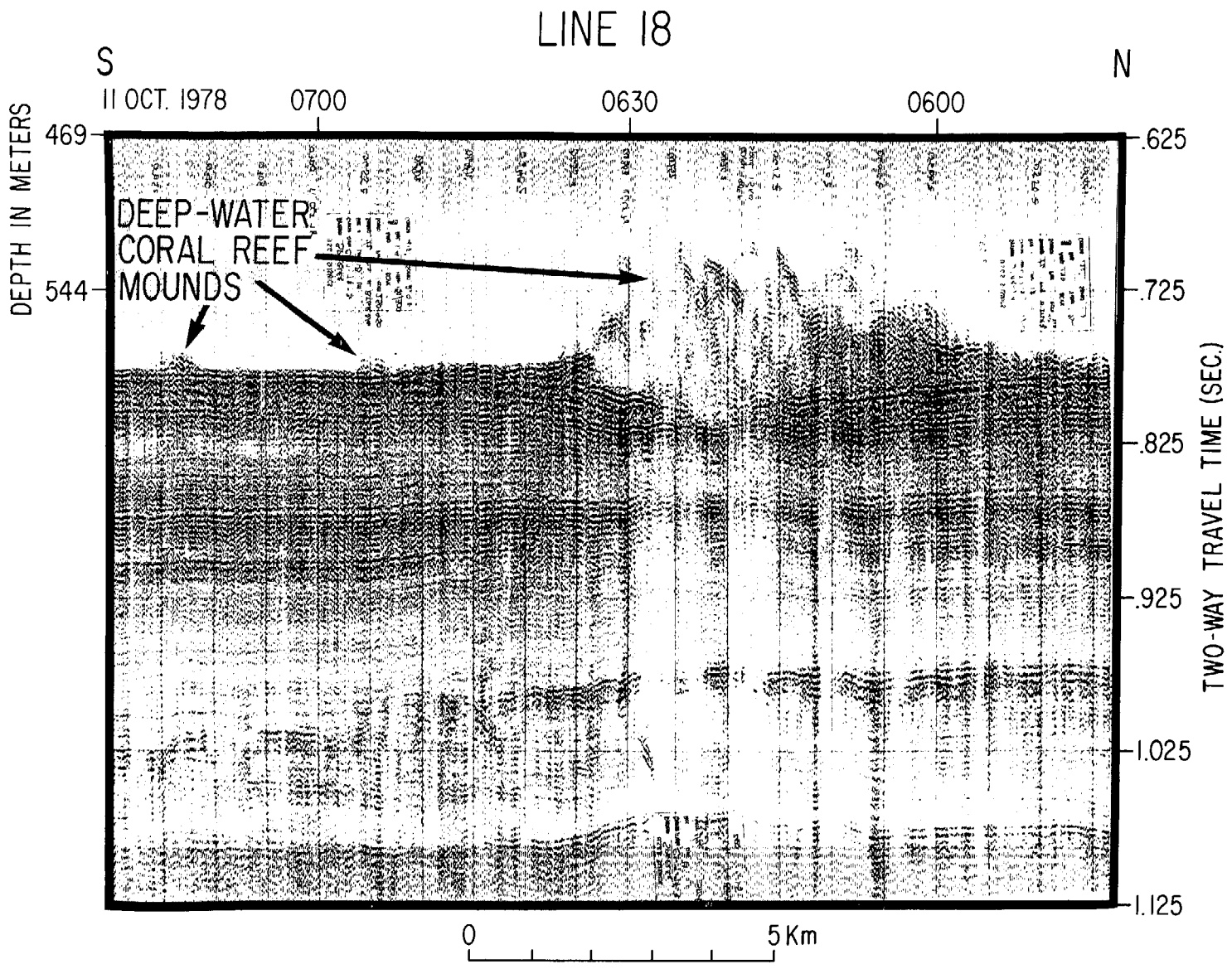
LINE 18
S
N
11 OCT. 1978
0700
0630
0600
DEPTH IN METERS
469
544
DEEP-WATER
CORAL REEF
MOUNDS
.625
.725
.825
.925
1.025
1.125
TWO-WAY TRAVEL TIME (SEC.)
0
5 Km

Figure 8-16

modern offshore-drilling technology. Slumps and slides are absent from the plateau region, except at the head of the precipitous Blake Escarpment. Faults are distributed sparsely in the survey area and most show no evidence of recent activity. Problems related to the presence of cavernous limestones, cut-and-fill structures, and deepwater reef banks can be averted by incorporating specific design measures into the drilling plans. The most pressing concern from the engineering standpoint pertains to the activity of the Gulf Stream which sweeps across the plateau's surface. Ample topographic, sedimentologic, and stratigraphic data point to a long and continuing history of Gulf Stream interaction with the floor of the Blake Plateau. Additionally, this problem is compounded by the plateau's excessive water depths that range between 200 and 800 m. At water depths of 800 to 2,000 m a clathrate layer which may trap shallow high-pressure gas should be expected.

REFERENCES CITED

Ball, M.M., Popenoe, P., Vazzana, M.E., Coward, E., Dillon, W.P., Durden, T., Hampson, J., and Paull, C.K., 1979, South Atlantic outer continental shelf hazards map, in Environmental studies of the southeastern U.S. Atlantic outer continental shelf, Geology, 1977: U.S. Geological Survey Open-File Report 80-146, Ch. 11, p. 11.1-11.16.

Charm, W.B., Nesteroff, W.D., and Valdes, S., 1969, Detailed stratigraphic description of the JOIDES cores on the continental margin off Florida: U.S. Geological Survey Professional Paper 581-D, p. D1-D13.

Dillon, W.P., Gerard, O., Weed, E., Sheridan, R., Dalton, G., Sable, E., Irivoy, H., Grim, M., Robbins, E., and Rhodehamel, E., 1975,

Sediments, structural framework, petroleum potential, environmental conditions, and operations considerations of the United States outer continental shelf: U.S. Geological Survey Open-File Report 75-411, 202 p.

Dillon, W.P., Grow, J.A., and Paull, C.K., 1980, Unconventional gas hydrate seals may trap gas off southeast United States: Oil and Gas Journal 78, v. 1, p. 124-130.

Dillon, W.P., and Paull, C.K., 1978, Interpretation of multichannel seismic reflection profiles of the Atlantic continental margin off the coasts of South Carolina and Georgia: U.S. Geological Survey Map MF-936.

Emery, K.O., and Zarudski, E.F.K., 1967, Seismic reflection profiles along the drill holes on the continental margin off Florida: U.S. Geological Survey Professional Paper 581-A, p. A1-A8.

Ewing, J., Ewing, M., and Leyden, R., 1966, Seismic-profiler survey of Blake Plateau: American Association Petroleum Geologists Bull. 50, v. 9, p. 1948-1971.

Grow, J.A., Dillon, W.P., and Popenoe, P., 1979, Diapirs along the continental slope southeast of Cape Hatteras (abs.): Geological Society of America Abstracts with Program, v. 11, no. 4, p. 181.

Herrick, W.M., and Vorhis, R.C., 1963, Subsurface geology of the Georgian coastal plain: Georgia State Division of Conservation, Geological Survey Information Circular 25, 78 p.

Jordan, C.F., 1954, Large sinkholes in the Straits of Florida: American Association Petroleum Geologists Bull. 38, p. 1810-1817.

Malloy, R.J., and Hurley, R.J., 1970, Geomorphology and geologic structure: Straits of Florida: Geological Society of America Bull. 81, p. 1947-1972.

McCarthy, J.C., Clingan, R.S., and Roberts, J.W., 1980, Potential geologic hazards and constraints for blocks in South Atlantic OCS Oil and Gas Lease Sale 43: U.S. Geological Survey Open-File Report 80-866a, 41 p.

Meyerhoff, A.A, and Hatten, C.W., 1974, Bahamas salient of North America: tectonic framework, stratigraphy, and petroleum potential: American Association Petroleum Geologists Bull. 58, p. 1201-1239.

Mullins, H.T., and Newmann, A.C., 1979, Geology of the Miami Terrace and its paleooceanographic implications: Marine Geology, v. 30, p. 205-232.

Paull, C.K., and Dillon, W.P., 1979, The subsurface geology of the Florida-Hatteras shelf, slope, and inner Blake Plateau: U.S. Geological Survey Open-File Report 79-448, 94 p.

Paull, C.K., and Dillon, W.P., 1980, The appearance and distribution of the gas-hydrate reflector off the southwestern United States: U.S. Geological Survey Open-File Report 80-88, 8 p.

Pratt, R.M., 1966, The Gulf Stream as a graded river: Limnology and Oceanography, v. 11, no. 1, p. 60-67.

Pratt, R.M., and Heezen, B.C., 1964, Topography of the Blake Plateau: Deep-Sea Research, v. 11, p. 721-728.

Savit, C.H., 1974, Bright spot in the energy picture: Ocean Industry, v. 9, p. 60-65.

Schlee, J.S., 1977, Stratigraphy and Tertiary development of the continental margin east of Florida: U.S. Geological Survey Professional Paper 581-F, p. F1-F25.

Shipley, T.H., Houston, M.H., Buffler, R.T., Shaub, F.J., McMillen, K.J., Ladd, J.W., Worzel, J.L., 1979, Seismic evidence for widespread possible gas hydrate horizons on continental slopes and

rises: American Association Petroleum Geologists Bull. 63, no. 12, p. 2204-2213.

Stetson, T.R., Squires, D.F., and Pratt, R.M., 1962, Coral banks occurring in deep water on the Blake Plateau: American Museum Novitates, no. 2114, p. 1-39.

Sylwester, R.E., Dillon, W.P., and Grow, J.A., 1979, Active growth fault on seaward edge of Blake Plateau, in Gill, O., Merriam, O.F., eds., Geomathematical and Petrophysical Studies in Sedimentology: New York, Pergamon Press, p. 197-209.

Tucholke, B.E., Bryon, G.M., and Ewing, J.I., 1977, Gas hydrate horizons detected in seismic profiler data from the western North Atlantic: American Association Petroleum Geologists Bull. 61, no. 5, p. 698-707.

Uchupi, E., and Emery, K.O., 1967, Structure of continental margins off Atlantic coast of United States: American Association Petroleum Geologists Bull. 51, p. 223-234.

OVERSIZED PAGE,
NOT IMAGED

51 OVERSIZED NOT IMAGED